UNIVERSITY OF SOUTHAMPTON

FACULTY OF ENGINEERING, SCIENCE AND MATHEMATICS

School of Ocean and Earth Science

Organically bound tritium in sediments from the Severn estuary, UK.

by

Jennifer Ellen Morris,

BSc (Hons.), ARSM, FGS

Thesis for the degree of Doctor of Philosophy

February 2006

UNIVERSITY OF SOUTHAMPTON

ABSTRACT

FACULTY OF ENGINEERING, SCIENCE AND MATHEMATICS
SCHOOL OF OCEAN AND EARTH SCIENCE

Doctor of Philosophy

ORGANICALLY BOUND TRITIUM IN SEDIMENTS FROM THE SEVERN ESTUARY, UK.

by Jennifer Ellen Morris

Amersham plc, now GE Healthcare, has discharged both organically bound tritium (OBT) and tritiated water (HTO) into the Severn estuary since 1981. The OBT component of these discharges results in elevated tritium (^{3}H) activities in the sediments and biota of the estuary. A monthly sampling programme, covering February 2000 to May 2004, has provided the first detailed description of the spatial and temporal distribution of ^{3}H activities in surface sediments from the estuary. Four sediment cores were also collected from salt marshes on the northern shore, to obtain longer term records of tritium accumulation. The spatial distribution of sediment ^{3}H activities correlates well with predicted patterns of suspended sediment circulation, with higher activities (up to 3 Bq/g dry weight) in sediments from sites within 10 km of the Amersham plc discharge point and at a greater distance to the east. Temporal variations in the ^{3}H activities of both surface and core sediments are predominantly controlled by the magnitude, composition and pre-discharge treatment of organic ^{3}H discharges from Amersham plc, with secondary sediment composition effects; lower ^{3}H activities are generally measured in sandy/gravelly sediments than in muddy sediments. The dated sediment ^{3}H activity profile in one of the salt marsh cores corresponds to the Amersham plc OBT discharge record, indicating that ^{3}H is persistent in sediments over a period of 25 years. Up to 60 % of the OBT in sediments could only be extracted with strong acids and bases, indicating that it may be composed of large, complex and hydrophobic compounds that are only extractable when lysed, such as humic compounds and/or large biomolecules. The sediment-bound fraction of OBT is predicted to be less than 2 % of the total organic tritium discharged from Amersham plc, however, these molecules do have the potential to remain in salt marsh and subtidal mud patch sediments for decades, unless the sediments are eroded and resuspended, until tritium activities decline by radioactive decay.

Contents

List of Figures

List of Tables

Graduate School of the National Oceanography Centre, Southampton

This PhD. dissertation by

Jennifer Ellen Morris

has been produced under the supervision of the following people:

Supervisors
Dr Ian Croudace
Dr Phil Warwick
Dr Alan Howard

Chairs of Advisory Panel
Professor Bill Jenkins
Professor Chris German

Declaration

The work presented in this thesis was predominantly carried out by myself and was done wholly whilst in candidature for a research degree at this University. Some data were produced by other researchers in the Geosciences Advisory Unit at the National Oceanography Centre, Southampton, in which case this is indicated in the text. Where I have consulted or quoted from the published work of others, the source is always clearly attributed. None of this work has been published prior to submission.

Signed:

Date:

Acknowledgements

This study was funded by the Food Standards Agency. The Ordnance Survey granted me an academic data licence to use their Mastermap data, and Julie Williams from Amersham plc provided data on the Amersham plc discharges. Krista Doucette began this project, did a lot of validation of the tritium method and ran the sampling programme for the first year.

I would like to thank my supervisors Phil, Ian and Alan for being so generous with their time and expertise throughout, and especially while I was writing up. I am grateful to Fran for all the great sampling trips, for answering all my stupid questions and loads of help in the lab too. Wink, Jon, Phill T, Jung Suk, Daryll, Belinda, Ross, Tina, Bob, John and Daphne helped me out whenever I asked and always had time for a chat. I could not have wished for a friendlier bunch of people to work with. I'd also like to thank Tammy, Nikki, Georgia, Nancy, Robbie and Uyen at Crabtree and Evelyn for making my 'free' time so enjoyable.

Thanks to Chris for proof-reading this for me, as well as being the best 'tech support', and for all the sanity-restoring chocolate and Shakeaway breaks. The experience wouldn't have been much fun without Roz, Jude, Jules and Simon, Sarah, Adam, Nev and Cheryl, Andy and Chris, and Jacqui. Southampton wouldn't have been the same without Mark, Kerry and Ollie, so its a good job we're leaving too! Thanks to Millie, Sali, Sarah and Nick for all the emails and get-togethers whenever we were all in the same country, and of course to Clare, Nicky, Jo, Bob, Cindy and Carolyn, I'm looking forward to seeing you more often!

Most of all, thanks to Mum, Dad, Karen and Grampy for their unstinting support, I couldn't have done it without you all! This is for Clive, who has put up with me through everything and helped me with lots of the figures too, you're a star!

Las cosas claras y el chocolate espeso

Ideas should be clear and chocolate thick

A Spanish proverb

Abbreviations

$^3H_{ext}$	Water-extractable tritium
$^3H_{total}$	Total tritium
Bq	Bequerels, the SI unit of radioactivity
Ci	Curies, the pre-SI unit of radioactivity
EA	Environment Agency
FSA	Food Standards Agency
HAT	Highest astronomical tide
HTO	Tritiated water
IC	Inorganic carbon
ICRP	International Commision on Radiological Protection
LSC	Liquid Scintillation Counting
MAFF	Ministry for Agriculture, Fisheries and Foods
MHWN	Mean high water at neap tides
MHWS	Mean high water at spring tides
MLW	Mean low water
NCRP	National Council on Radiation Protection and Measurement
OBT	Organically bound tritium
PM	Photomultiplier tube
SQP(E)	Spectral Quench Parameter of the Internal Standard
Sv	Sieverts, SI unit of dose
T	Tritium
TC	Total carbon
TOC	Total organic carbon
TU	Tritium Units
UNSCEAR	United Nations Scientific Committee on the Effects of Atomic Radiation
USGS	United States Geological Survey
WWTW	Waste water treatment works
XRD	X-ray diffraction
XRF	X-ray fluorescence

Chapter 1

Introduction

1.1 Introduction

Tritium, the radioactive isotope of hydrogen, is discharged into the Severn estuary, in southwest Britain, by three nuclear power stations and Amersham plc, a company based in Cardiff who produce radiolabelled organic molecules for medical and research applications (Figure 1.1). Tritium activities in biota in the Severn estuary are over 2 orders of magnitude higher than those at other monitoring sites around the UK coastline (McCubbin *et al*, 2001). Notably, a significant proportion of the total tritium activity released by Amersham plc is organically bound tritium (OBT), whereas only tritiated water (HTO) is discharged by nuclear power stations and nuclear fuel reprocessing plants (Kirchmann *et al*, 1979). OBT generally has a higher dose coefficient than HTO, although this is variable, depending on the composition of OBT.

Bioaccumulated tritium in the Severn estuary is predominantly found in benthic fauna and demersal (bottom-dwelling) fish, implying that sediments or sediment-dwelling microbes may be incorporating tritiated organic molecules and passing them up the food chain (McCubbin *et al*, 2001). The Severn estuary is large and macrotidal, with strong tidal currents that regularly suspend sediment particles up to sand size, transporting them around the estuary and depositing them on intertidal mud/sand flats and salt marshes, and subtidal mud patches and sand banks (Collins, 1987; Kirby and Parker, 1983). It is therefore likely that tritiated sediments are widely dispersed from the Amersham plc discharge point, and trapped in intertidal or subtidal sediment deposits, from which they may be released in the future.

Previous work in this region has focused on sediment dynamics (Collins, 1987; Dyer, 1984; Kirby, 1994; Parker and Kirby, 1982), the magnitude and the mechanisms of bioaccumulation of organically bound tritium (McCubbin *et al*, 2001; Williams *et al*, 2001), and the likely dose the general public is exposed to through consumption of tritiated biota (Hodgson *et al*, 2005). This project builds on earlier research, aiming to answer the following questions:

- How far is the tritiated sediment transported?
- How variable are the tritium activities in sediments over time?
- What factors affect the tritium activities of sediments?
- Which tritiated species are present in the sediments?

This will increase our understanding of the mechanisms by which tritium is dispersed around the estuary and transferred up the food chain, and allow the future implications of the discharges to be assessed.

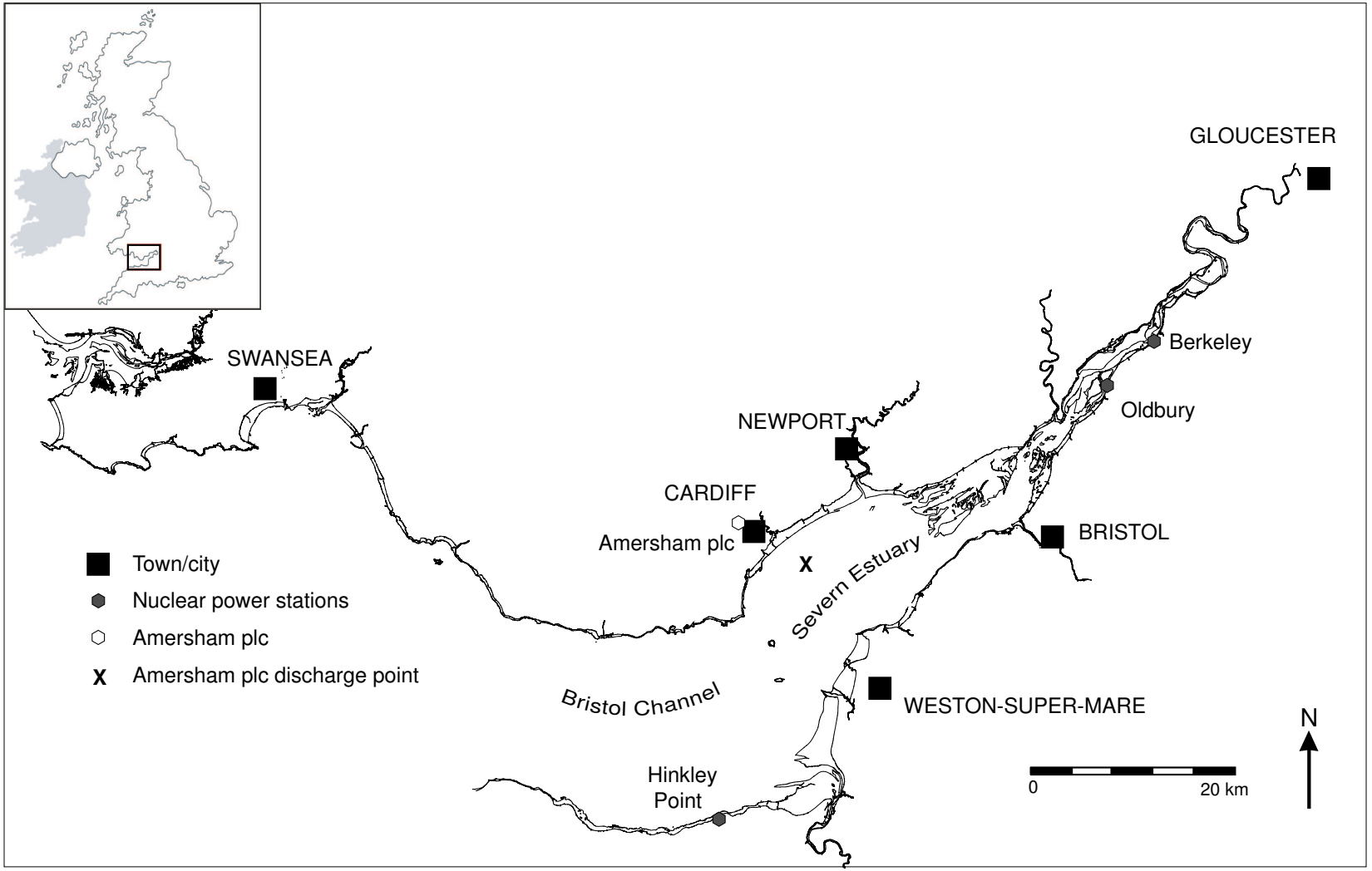

Figure 1.1: Location of the Severn estuary in SW Britain, and sources of tritium discharges into the estuary: Hinkley Point, Berkeley and Oldbury nuclear power stations, and Amersham plc, a company based in Cardiff who produce radiolabelled organic molecules for medical and research applications.

1.2 Tritium

Tritium (^{3}H or T) is a β-emitting radioisotope of hydrogen with a half-life of 12.32 years (Lucas and Unterweger, 2000). Tritium decays to ^{3}He, emitting an electron (e^-) from the nucleus with a mean energy of 5.7 keV and a maximum energy of 18.6 keV (NCRP, 1985).

Tritium is ubiquitous in the environment and can occur as $T_{2(g)}$, $HTO_{(l)}$, and as exchangeably or non-exchangeably bound organic tritium. In the marine environment, it most commonly occurs as $HTO_{(l)}$ (NCRP, 1985).

1.2.1 Organically bound tritium

Organically bound tritium (OBT) is theoretically defined as a tritium atom that is bound to a carbon atom in an organic molecule by an exchange or enzymatically catalysed reaction (Diabeté and Strack, 1993). This tritium atom is non-exchangeably bound because C – ^{3}H bonds are stable except in the presence of strong acids, strong bases or catalysts (Diabeté and Strack, 1993). However, a tritium atom bound to a nitrogen, oxygen or sulphur atom in an organic molecule can theoretically be exchanged with hydrogen isotopes in other molecules (Krishnamurthy *et al*, 1995), and so is not defined as OBT, although they can be shielded from exchange by the 3-dimensional structure of molecules (Sessions *et al*, 2004).

1.2.2 Analytical determination of organically bound tritium

In practice, it is difficult to isolate and measure the theoretically defined OBT fractions. The choice of technique depends on the form of tritium to be determined; it is also influenced by the type and activity of the sample. Tritiated water (HTO) is extracted from liquids by distillation, and in solids by freeze-drying or azeotropic distillation. Total tritium or OBT can be measured in liquid samples by direct counting on a liquid scintillation counter or by extraction of the organic fraction using chromatographic extraction columns. However, the accuracy of the extractions depends on their effectiveness at isolating the types of OBT present in the sample (Williams, 2001); using another method, or analysing a different type of OBT, can produce incompatible OBT results (Ware and Allot, 1999).

For solid samples, the most reproducible analytical methods operationally define OBT as the tritium activity remaining in the sample once tritiated water has been removed (e.g. McCubbin *et al*, 2001; Ware and Allott, 1999), this is usually achieved by oven-drying or freeze-drying prior to analysis (Bogen *et al*, 1973; Kim *et al*, 1992; Pointurier *et al*, 2003). OBT is then extracted by wet oxidation (Ware and Allott, 1999) or combustion in a conventional or modified furnace, or a plasma source (Bogen *et al*, 1973; Momoshima *et al*, 1994; Strack and Koenig, 1981); these methods oxidise all organic matter to CO_2 and either H_2O or HTO, which is collected by condensation of the combustion water and can be measured using liquid scintillation counting. Pointurier *et al* (2000) also removed exchangeably bound tritium from dried, ground vegetation samples containing very low

tritium activities by mixing them with large volumes of tritium free water, before determining the non-exchangeably bound OBT content by combustion. The range of methods for OBT and HTO analysis are discussed in more detail in Chapter 2. The speciation, or chemical form, of tritium affects its radiological significance; for example, both the exchangeably and non-exchangeably bound tritium fractions have longer residence times in biota than tritiated water, and both therefore potentially impart higher doses of radiation, so it is appropriate to combine them for the purpose of radiological dose assessments (Ware and Allot, 1999).

1.2.3 Significance of chemical form

The speciation, or chemical form, of OBT is a significant factor that affects its fate in the environment, bioavailability and radiological significance. Tritiated water is diluted and dispersed on its release into the marine environment and has been used as a radiotracer for large-scale ocean circulation (Jenkins and Rhines, 1980; Jenkins, 2001). However, the fate of OBT depends upon its composition: hydrophilic OBT may remain in solution, whilst hydrophobic OBT (e.g. hydrocarbons and lipids) is more likely to be adsorbed onto colloids or suspended sediment and consumed by biota, where it can be incorporated into biomass or excreted (Blaylock *et al*, 1986). The radiological significance of tritium is also dependent on the chemical form of the tritium molecule; HTO has a shorter average residence time in biota than OBT and a lower dose coefficient, as discussed below. Tritium in general is a low energy β-emitter, so there is no external radiation hazard, but tritium gas or tritiated molecules can be absorbed through the skin, inhaled or ingested (Hill and Johnson, 1993). After consumption of HTO, tritium is excreted by humans as two or three components with half-times of around 10 days, 21 to 76 days and 280 to 550 days (Harrison *et al*, 2002; NCRP, 1979). In an experiment where rats were fed HTO, 97 % of the activity was excreted with a half-time of 3 days and the remaining 3 % with a half-time of 10 days (the biological half-life is also dependent on the mass of biota, as this is related to the size of the body water pool; Hill and Johnson, 1993; Hodgson *et al*, 2005). Tritium in HTO rapidly reaches equilibrium with hydrogen in the body water pool, imparting a uniform dose on soft tissues; however, a small fraction is incorporated into organic molecules. Therefore, while the first component represents water retention, the second (and third, if present) component represent excretion of tritium following the degradation of organic molecules into metabolites that enter the body water pool, indicating that OBT is more radiotoxic than HTO (Harrison *et al*, 2002; NCRP, 1979).

After consumption of OBT from Cardiff Bay flounder, rats excreted 70 % of the ingested activity with a half-time of 3 days and 30 % with a half-time of 25 days (Hodgson *et al*, 2005). The second component excreted probably represents tritium that was exchangeably bound to organic molecules or is present in fast turnover body compartments, while the third component, if present (this was not included in the experimental design of the study by Hodgson *et al* (2005)), may represent tritium atoms that were non-exchangeably bound to organic molecules, or that were present in slow turnover organs or molecules, such as collagen, nerve cell phospholipids and lipids in fat deposits (Hill and Johnson,

1993). As tritium emits relatively low energy β particles, radiation damage is restricted to the cell or organ containing the tritiated organic molecules. Tritiated thymidine and other DNA precursors are of particular concern because they tend to be concentrated in the nucleus of cells, therefore the β particles can potentially produce DNA mutations (Hill and Johnson, 1993).

The radiological dose (measured in Sieverts) received by biota ingesting tritium therefore depends on the form of the tritium, and the molecules or organs that tritium is incorporated into in the body. The dose is calculated by multiplying the activity (expressed in Becquerels) absorbed by the organ or body by a dose coefficient (Sv Bq^{-1}), which is calculated by modelling or experimental studies and accounts for differences introduced by the type and energy of radiation, as well as for differences in the size of the organ or biota receiving the dose. ICRP (1993) have calculated a higher dose coefficient for OBT (4.2 x 10^{-11} Sv Bq^{-1}) than HTO (1.8 x 10^{-11} Sv Bq^{-1}), assuming the subject is an adult human and the activity is excreted in two components of 10 days and 40 days half-time respectively (a ratio of the total tritium activity in each component of 97:3 and 50:50 were assumed for HTO and OBT respectively). These assumptions are not considered to be valid for the critical group in the Severn estuary; Hodgson *et al* (2005) have calculated a dose coefficient of 6.1 x 10^{-11} Sv Bq^{-1} for adults consuming Cardiff Bay flounder, extrapolating half-times of 10 and 100 days for the two components from experimental data and assuming a ratio of activities of 70:30. This dose coefficient is used to estimate an annual dose to the critical group of seafood consumers of $\sim$60 μSv, compared with 43 μSv using the ICRP (1993) OBT dose coefficient; this indicates that distinguishing not only between HTO and OBT, but also between different forms of OBT, is important to allow the calculation of accurate radiological dose assessments (Hodgson *et al*, 2005; Lambert, 2001).

1.2.4 Sources of tritium

Global sources

Tritium is produced both naturally, by spallation reactions in the stratosphere, and anthropogenically, from atmospheric nuclear weapons testing, nuclear power stations and industry.

The naturally-produced tritium inventory is $\sim$1 x 10^{18} Bq (UNSCEAR, 1977); cosmic ray-induced spallation reactions produce 7.4 x 10^{16} Bq of ^{3}H per year (Kaufman and Libby, 1954; Okada and Momoshima, 1993)):

$$^{14}\mathrm{N} + \mathrm{n} \rightarrow {}^{3}\mathrm{H} + {}^{12}\mathrm{C} \text{ and } {}^{14}\mathrm{N} + \mathrm{p} \rightarrow {}^{3}\mathrm{H} + \text{products}$$
$$^{16}\mathrm{O} + \mathrm{n} \rightarrow {}^{3}\mathrm{H} + {}^{14}\mathrm{N} \text{ and } {}^{16}\mathrm{O} + \mathrm{p} \rightarrow {}^{3}\mathrm{H} + \text{products},$$

where n = neutron and p = proton

Tritium then combines with itself to form tritium gas ($^{3}H_{2(g)}$), or with oxygen to form tritiated water, which is predominantly transferred to the surface by precipitation (NCRP, 1979). Tritium is also produced in the Earth's crust, when ^{6}Li in rocks is bombarded by neutrons from the spontaneous fission of uranium (Craig and Lal, 1961; Kaufman

and Libby, 1954). The naturally-produced tritium inventory was swamped by ~2.4 x 10^{20} Bq of 'bomb tritium', released into the environment, predominantly in the northern hemisphere (Begemann and Libby, 1957), during atmospheric nuclear weapons testing between 1945 and 1980 (UNSCEAR, 1993; 2000). Other anthropogenic sources of ^{3}H include discharges from nuclear power plants, nuclear fuel reprocessing plants, tritium production and radiolabelling facilities, pharmaceutical and medical establishments, and the disposal of consumer products containing ^{3}H (NCRP, 1979). These sources are smaller in magnitude, but can have significant local effects.

Sources in the Severn estuary

Tritium has been discharged directly into the Severn estuary from three nuclear power stations (Berkeley, Oldbury and Hinkley Point (A and B sites), although Hinkley Point 'A' and Berkeley are currently being decommissioned; FSA and SEPA, 2001) and Amersham plc (Figure 1.2). The nuclear power stations discharge tritium as HTO, the majority from Hinkley Point 'B' station (Kirchmann *et al*, 1979; Lambert, 2001; Verrall and Odell, 2002), but Amersham plc discharges tritium as both HTO and OBT. Discharges from Amersham plc are similar in magnitude to the combined discharges from the nuclear power stations, but significantly lower than the tritium discharges from the nuclear fuel reprocessing plants in Sellafield, Cumbria and La Hague, France (Figure 1.2). Tritium in the form of tritiated water could potentially be transported into the Severn estuary from Sellafield, via the Irish Sea (Figure 1.3); however, elevated ^{3}H activities are not detected during routine monitoring of sediments and biota around the British coastline (FSA and SEPA, 1994-2002; EA, EHS, FSA and SEPA, 2003-2004). The accumulation of tritium in Severn estuary sediments and biota is probably the result of OBT discharges from Amersham plc.

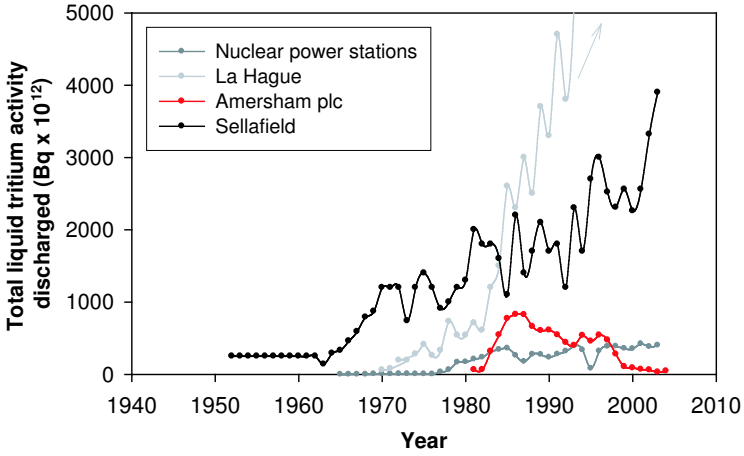

Figure 1.2: Comparison of total ^{3}H discharges from Amersham plc, Hinkley Point, Berkeley and Oldbury nuclear power stations and Sellafield and La Hague nuclear fuel reprocessing plants (Camplin, 1992-1995; COGEMA, 2004; EA, EHS, FSA and SEPA, 2003-2005; FSA and SEPA, 1996-2002; Hunt, 1977-1989; Mitchell, 1968-1978).

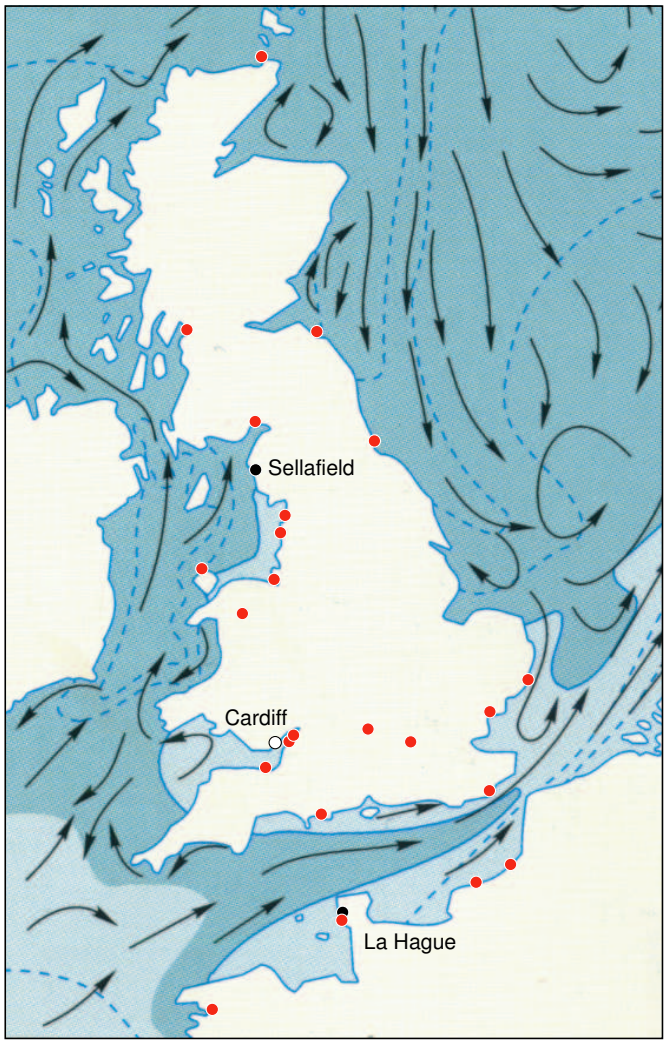

Figure 1.3: Sources of tritium that are potential inputs into the Severn estuary, including nuclear power stations and nuclear fuel reprocessing plants (EA, EHS, FSA and SEPA, 2004), with the predominant direction of currents in UK coastal waters and the North Sea (Pernetta, 1994). This circulation pattern varies on local and seasonal scales, especially in the English Channel and Irish Sea (Cooper, 1966; Howarth, 2001; GAU, 2005; Pernetta, 1994).

Amersham plc

Amersham plc, who were renamed GE Healthcare in May 2004, produce radiolabelled organic molecules for pharmaceutical applications and life science research at their site in Cardiff (Figure 1.1). They discharge a range of liquid byproducts and waste products of these processes into the Severn estuary (Williams, 2001); these discharges have undergone a number of significant changes in magnitude (Figure 1.4), composition and treatment since the plant opened in 1980 (Table 1.1). Monitoring of OBT activities in the waste products prior to their release into the sewer system reveals considerable temporal variation in the composition of discharges from the site (Rowe *et al*, 2001), although Table 1.1 gives an estimated discharge composition. The introduction of the waste water treatment works (WWTW) in March 2002 may have had a significant impact on ^{3}H activities in sediments and biota in the estuary; 12 % of the total tritium, probably including the majority of the 'high impact' fraction of hydrophobic, highly bioavailable tritiated organic molecules (e.g. hydrocarbons, amino acids and proteins, nucleotides, fatty acids, lipids and purine/pyrimidines), is now retained in the sewage sludge and no longer released into the estuary (Williams, 2005; Table 1.1). A tritium recovery plant (Project Paragon) is due for completion in 2007; this will reclaim and recycle the majority of tritium from the Amersham plc discharges (EA, 2003). Although this gradual decrease, and eventual cessation, in discharges should lead to decreasing ^{3}H activities in biota and sediments in the future, the large number of variables controlling tritium accumulation in the Severn estuary mean that the rate of this decrease cannot currently be predicted.

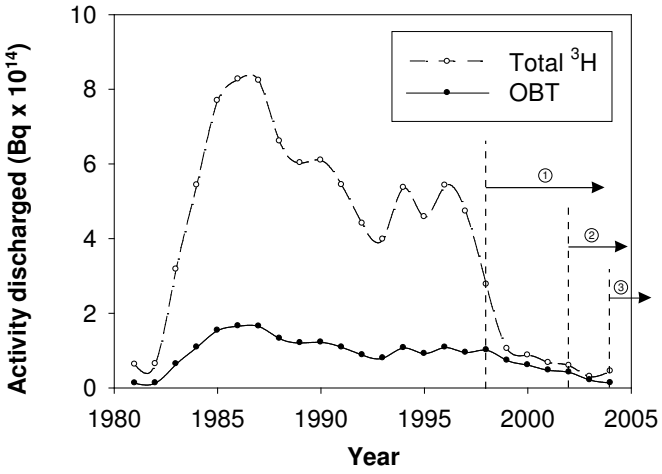

Figure 1.4: Historical discharges of total ^{3}H and estimated OBT from Amersham plc, showing changes in magnitude, composition and treatment (Williams, 2003; 2005). The vertical dotted lines highlight significant changes in the magnitude or treatment of either total ^{3}H or OBT discharges, as described in Table 1.1.

Table 1.1: Changes in the magnitude, composition and treatment of liquid discharges from Amersham plc into the Severn estuary.

Date	**Magnitude**[1]	**Estimated composition**[2]	**Treatment**[3]
October 1986	Maximum ^{3}H discharged	20 % OBT, 80 % HTO (since discharges began in 1981).	Released into the sewer system and discharged untreated into the estuary.
May 1998 (1)	Significant reduction in discharges.	OBT component of discharges increased to 70 % due to storage of HTO and tritiated methanolic wastes.	Untreated.
Jan/Feb 2002	^{3}H discharges dramatically reduced for operational reasons	70 % OBT, 30 % HTO.	Some treatment, as waste water treatment works (WWTW) gradually became operational.
March 2002 (2)	Treated waste water and ∼6 tonnes sewage sludge per day released from the WWTW. 12 % of ^{3}H associated with the sludge, not released into the estuary.	The OBT fractions associated with the sewage sludge may have included the 'high impact'[4] organic fraction	Cardiff East WWTW became fully operational. The WWTW, which employs a series of activated sludge batch reactors, converts 12 % of the tritiated effluent to sludge, with the remainder discharged into the estuary as HTO.
April 2003		70 % OBT, but 80 % of the 'high-impact'[4] organic fraction removed.	
Jan 2004 (3)		Change in discharge composition to 30 % OBT, 70 % HTO	

[1] Williams (2001; 2003)
[2] Williams (2005)
[3] Williams (2003), Dwr Cymru (2002)
[4] Hydrophobic, highly bioavailable tritiated organic molecules, including lipids, proteins, nucleotides and hydrocarbons (Williams, 2001)

1.3 Accumulation of tritium in sediments and biota in the Severn estuary

Tritium activities in biota and sediments have been monitored by Amersham plc since 1980 (Lambert, 2001) and by the Ministry for Agriculture, Fisheries and Food (MAFF), now the Food Standards Agency (FSA), since 1997. This monitoring has recorded high levels of OBT in flounder and other biota from the Severn estuary since 1988 (Figure 1.5; Williams, 2001). Food chain studies, where vegetation, grazing and predatory species were incubated with HTO in an enclosed pool, concluded that the highest proportion of ^{3}H was incorporated as OBT in algae, and that there was no bioaccumulation of tritium through the food chain (Blaylock *et al*, 1986; Harrison and Loranda, 1971; Harrison *et al*, 1973), however, in these studies ^{3}H was initially present as HTO. Biota consuming OBT contain a higher proportion of tritium with a longer biological half-life, resulting in bioaccumulation (Blaylock *et al*, 1986; Harrison and Koranda, 1971; Rodgers, 1986).

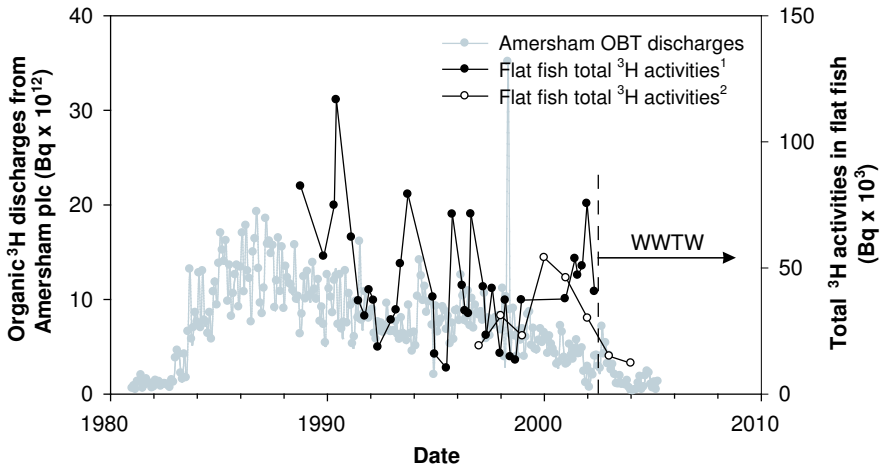

Figure 1.5: Comparison between total ^{3}H activities in flat fish (^{1} Williams, 2002, and ^{2} FSA and SEPA, 1998 - 2002; EA, EHS, FSA and SEPA, 2003 - 2005) and monthly OBT discharges from Amersham plc (Williams, 2005).

1.3.1 Potential mechanisms for the incorporation of tritium into biota

Both HTO and OBT can be assimilated into vegetation and biota during photosynthesis, by exchange with tritiated water or by the consumption and incorporation of OBT. Tritium is also excreted by biota, with the overall residence time depending on the size of the organism and the composition of the tritiated molecule (Diabeté and Strack, 1993). Experimental studies of the rates of incorporation and excretion of ^{3}H in plants and animals provide further insights into these processes; however most studies have used ^{3}H in the form of HTO.

Photosynthesis in green plants can transfer ^{3}H from HTO to OBT (Rudran, 1988); tritiated water is split into ^{3}H, H and O atoms, using light as a catalyst, and ^{3}H can be non-exchangeably bound to a C atom in an organic molecule (Diabeté and Strack, 1993). However, crops grown in tritiated water contain non-exchangeable OBT primarily

as 'buried' ^{3}H bound to O and N atoms in macromolecules, not carbon-bound ^{3}H as was previously thought (Baumgartner and Donhaerl, 2004). In an estuarine environment, however, salinity changes, ligand activity or the presence of enzymes may cause coiling or folding of the 3-dimensional structure of the molecules, significantly altering ^{3}H exchange rates at these buried sites (Krishnan *et al*, 2000; Mareque-Rivas *et al*, 2004; Sessions *et al*, 2004).

Tritium atoms from tritiated water can also exchange with hydrogen atoms in biological molecules; heavier ^{3}H atoms preferentially accumulate in the weaker bonds of the organic molecule, while H atoms are attracted to the stronger hydrogen bonds in water (Vre and Binet 1984; Baumgartner and Donhaerl, 2004). The rate of isotopic exchange between an organic molecule and tritiated water (HTO) is affected by the type of molecule, the presence of a catalyst (such as a mineral surface; Alexander *et al*, 1982; 1984), temperature and isotopic effects and the position of hydrogen in the molecule. Exchange reactions are faster at higher temperatures: the exchange rate of isocane on a mineral substrate has a half-time of 100 000 years at 7 °C, but only 10 000 years at 60 °C (Sessions *et al*, 2004). The position of a tritium or hydrogen atom in a molecule also affects its exchange rate: for example, hydrogen atoms in aromatic groups exchange significantly faster than hydrogen atoms in aliphatic molecules (Alexander *et al*, 1984; Sessions *et al*, 2004). Hydrogen atoms bound to nitrogen or oxygen atoms inside the coiled structure of large biomolecules, such as proteins and carbohydrates, are inaccessible to cell or pore waters, which may dramatically reduce exchange half-times from seconds to days, months or even years, compared to hydrogen atoms bound at more accessible sites (Baumgartner and Donhaerl, 2004).

If HTO is ingested, or tritiated gas is inhaled, by biota, ^{3}H can be incorporated into organic molecules using the processes described above. The consumption of OBT can also lead to its incorporation into biota (Diabeté and Strack, 1993); the ingestion of OBT from Severn estuary flounder resulted in longer T_bs in rats (70 % excreted with a half-time of 3 days and 30 % with a half-time of 25 days) than when equivalent doses of HTO were administered (97 % in first component and just 3 % with a half-time of 10 days; Hodgson *et al*, 2005). High tritium activities are predominantly found in benthic fauna and demersal (bottom-dwelling) fish, implying that sediments or sediment-dwelling microbes may be incorporating tritiated organic molecules and passing them up the food chain (McCubbin *et al*, 2001), with the result that the circulation and accumulation of sediments in the Severn estuary may affect the distribution of tritium, and therefore its bioaccumulation.

1.4 Sediment sources, transport mechanisms and sinks in the Severn estuary

1.4.1 Sources of sediments

Approximately half of the suspended sediment in the Severn estuary comes from streams and rivers (Severn Estuary Survey and Systems Panel, 1977; Figure 1.6). Rivers transport sediments, soils, nutrients and both dissolved and particulate organic matter into the estuary. The mineral composition of this sediment reflects the geology of the catchment area, which includes Silurian andesites and mudstones, Devonian Old Red Sandstone, Carboniferous limestones and Coal Measures, Triassic marls, mudstones and dolomites, Jurassic Lias (interbedded limestones and shales) and Oolites (limestones), as well as more recent alluvial deposits and peats (Green and Welch, 1965; Kellaway and Welch, 1993; Welch and Trotter, 1961), as sediments are eroded from the base and sides of rivers and streams and soils are washed into the rivers after heavy rainfall. Inputs from the rivers that feed the estuary, in particular the Severn, Avon, Usk and Parrett, also contain domestic sewage and agriculturally-derived pesticides and nutrients (Figure 1.8; Langston *et al*, 2003). The urban areas of Cardiff, Newport, Gloucester, Bristol and Avonmouth also discharge sewage and industrial wastes directly into the estuary. Rivers contribute ∼60 % of the particulate organic matter in the estuary, compared to ∼15 % from sewage and ∼25 % from industrial effluents, including paper mills (Langston *et al*, 2003).

Anthropogenic inputs into the Severn estuary have been significant since the onset of the industrial revolution in the 1850s, which led to the exploitation of the extensive Carboniferous coal deposits in South Wales and the Forest of Dean. The catchment became heavily industrialised, with numerous factories engaged in Zn smelting and the production of steel, Sn, Ni and Co. Leachate from coal-mining wastes (containing Fe, Zn and Cu) into rivers, and both aqueous and gaseous discharges from the factories, led to increasing metal concentrations in estuary sediments from the 1850s (Allen and Rae, 1986); concentrations of coal and ash also increased (Allen, 1987a). There are natural mineral deposits of Sr, Cu, Pb, Zn and Ba in the upper estuary, where Pb was mined from the 1850s until 1918 (Langston *et al*, 2003). After World War II, the area experienced a decline in coal mining, driven by falling demand, complex geology and cheaper imports. This, together with increased environmental legislation, led to decreasing sediment metal concentrations from 1950 onwards (French, 1996; French *et al*, 1994). The Corus plants at Ebbw Vale and Llanwern also stopped production of steel and coke in 2001 and 2002 respectively (Langston *et al*, 2003). However, there are still significant inputs of other pollutants, such as hydrocarbons, from fossil fuel combustion, shipping and chemical production; and radionuclides, from Amersham plc and the nuclear power stations, as discussed previously.

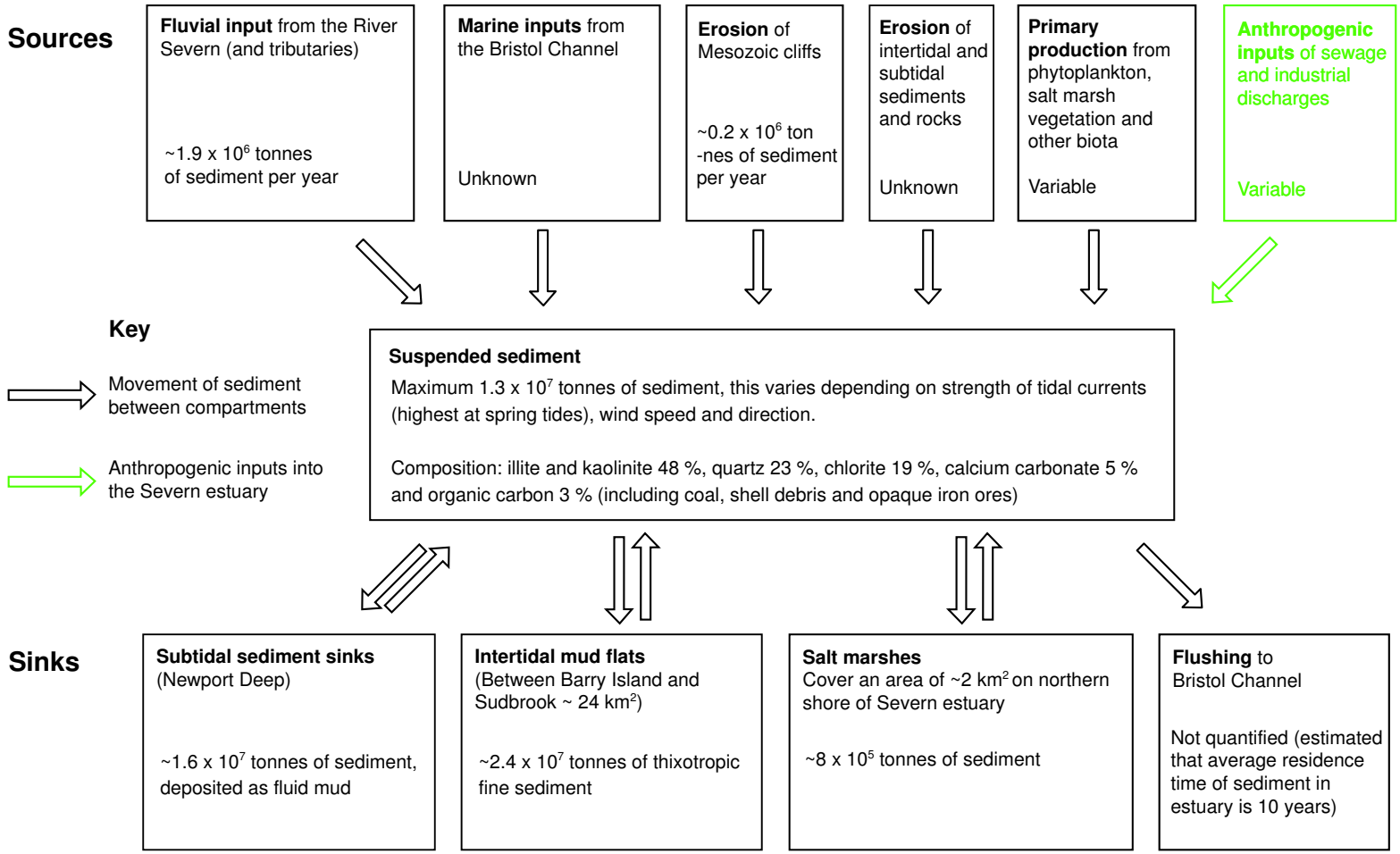

Figure 1.6: Sources and sinks of fine sediment in the Severn estuary (data from Allen, 1987, 1990, 1992; Bryant and Williams, 1983; Collins, 1987; Hamilton *et al*, 1979; Kirby, 1994; Parker, 1972; Parker and Kirby, 1982).

The remaining sediments come from marine inputs, primary production within the estuary, and the erosion of cliffs, exisiting intertidal and subtidal sediments, and exposed rocks on the estuary bed (Figure 1.6). Marine inputs have been identified by the presence of marine foraminifera in mud flat and salt marsh sediments (Murray and Hawkins, 1976; Sollas, 1883), but the magnitude of these inputs have not been quantified (Parker and Kirby, 1982). Primary production within the estuary includes phytoplankton, *Zostera* beds (Langston *et al*, 2003), diatom biofilms on mud flats (Allen and Duffy, 1998a), *Spartina* salt marshes and vegetated tide-washed pastures (Allen, 2000); the rate of these processes are expected to vary seasonally (Allen and Duffy, 1998b). The magnitude of erosive inputs of sediment from cliffs and banks have been estimated by the rates of erosion, and are minor in comparison to inputs from rivers and anthropogenic activities (Figure 1.6; Allen, 1990). The erosion of intertidal and subtidal rocks and sediments has not been quantified; however, sediments are frequently resuspended following deposition (Parker and Kirby, 1982). Mechanisms for the resuspension, circulation and deposition of these sediments are discussed further in the following sections.

1.4.2 Circulation of sediments

The Severn estuary is funnel-shaped, dynamic and well-mixed, with an extremely high tidal range (14.8 m mean spring tide at Avonmouth; Allen, 2000; Hydrographer of the Navy, 1981). Tidal currents, predominantly oriented parallel to the channel axis, are asymmetric, with a shorter but stronger flood tide. These currents, with speeds greater than 1.5 m s^{-1} at springs and 0.75 m s^{-1} at neaps (Uncles, 1984), can suspend particles up to sand size and produce a 10 - 15 km excursion of water at spring tides (Dyer, 1984). Coarser sediments tend to be predominantly transported by tidal currents in a seaward direction from a bed-load parting zone located between Barry and Hinkley Point (Figure 1.8; Culver, 1980; Parker and Kirby, 1982).

Fine sediment is predominantly transported in suspension by wind and tidal currents, with the mobile sediment population at any time equal to 3 to 8 years of riverine supply (Collins, 1983). During spring tides, the instantaneous mobile fine sediment load in the Severn estuary exceeds 30 million tonnes (Kirby, 1986); as tidal energy falls to a minimum at neap tides, it is estimated that 50 % of this sediment settles to the bed forming stationary suspensions (Kirby and Parker, 1983). Storms and strong winds can increase erosive wave action (Allen and Duffy, 1998a) and the turbidity of the water column, also resulting in high suspended sediment loads. Parker and Kirby (1982) estimated the fine sediment circulation regime for the Inner Bristol Channel and Severn estuary using a combination of salinity distribution data, suspended sediment concentration data, sediment flux measurements and identification of source and sink areas (Figure 1.8). A suspended sediment front (Figure 1.8) separates the more turbid southern water mass from a region with lower suspended sediment concentrations to the north (<0.5 g l^{-1} as opposed to 0.5 - 1 g l^{-1}); therefore, most suspended sediment transport occurs on the English side of the estuary, with little cross-channel flow (Parker and Kirby, 1982).

Within this dynamic estuarine circulation system, fine, cohesive sediment frequently

moves between the three states of mobile suspensions, stationary suspensions (fluid mud) and settled mud (Figure 1.7; Kirby and Parker, 1983). This settling process is not simple; a linear progression from a mobile dispersed suspension to a mobile layered suspension, then to a stationary suspension and finally settled mud, occurs only if, as tidal energy rises over the neap to spring cycle, erosive processes do not resuspend it (Dyer, 1984; Parker and Kirby, 1982).

There are a variety of sources of fine sediment into the Severn estuary, both natural and anthropogenic, including radionuclides from nuclear power stations and Amersham plc. Fine sediment circulation is tidally driven and predominantly rectilinear with only minor cross-channel flow. Therefore, if ^{3}H is transported with fine sediments in suspension, they should also be deposited together.

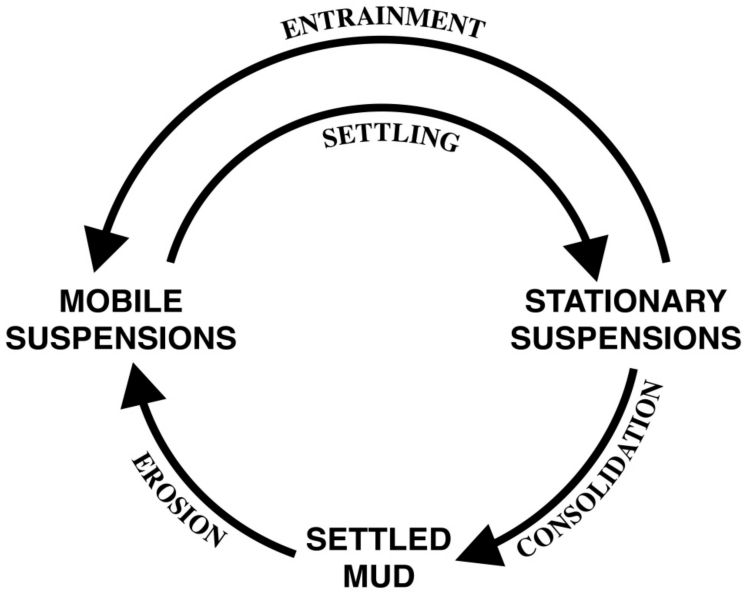

Figure 1.7: A simple model showing the modes of occurence of fine sediment in the Severn estuary, and mechanisms for transferring sediment between the three modes (Kirby and Parker, 1983).

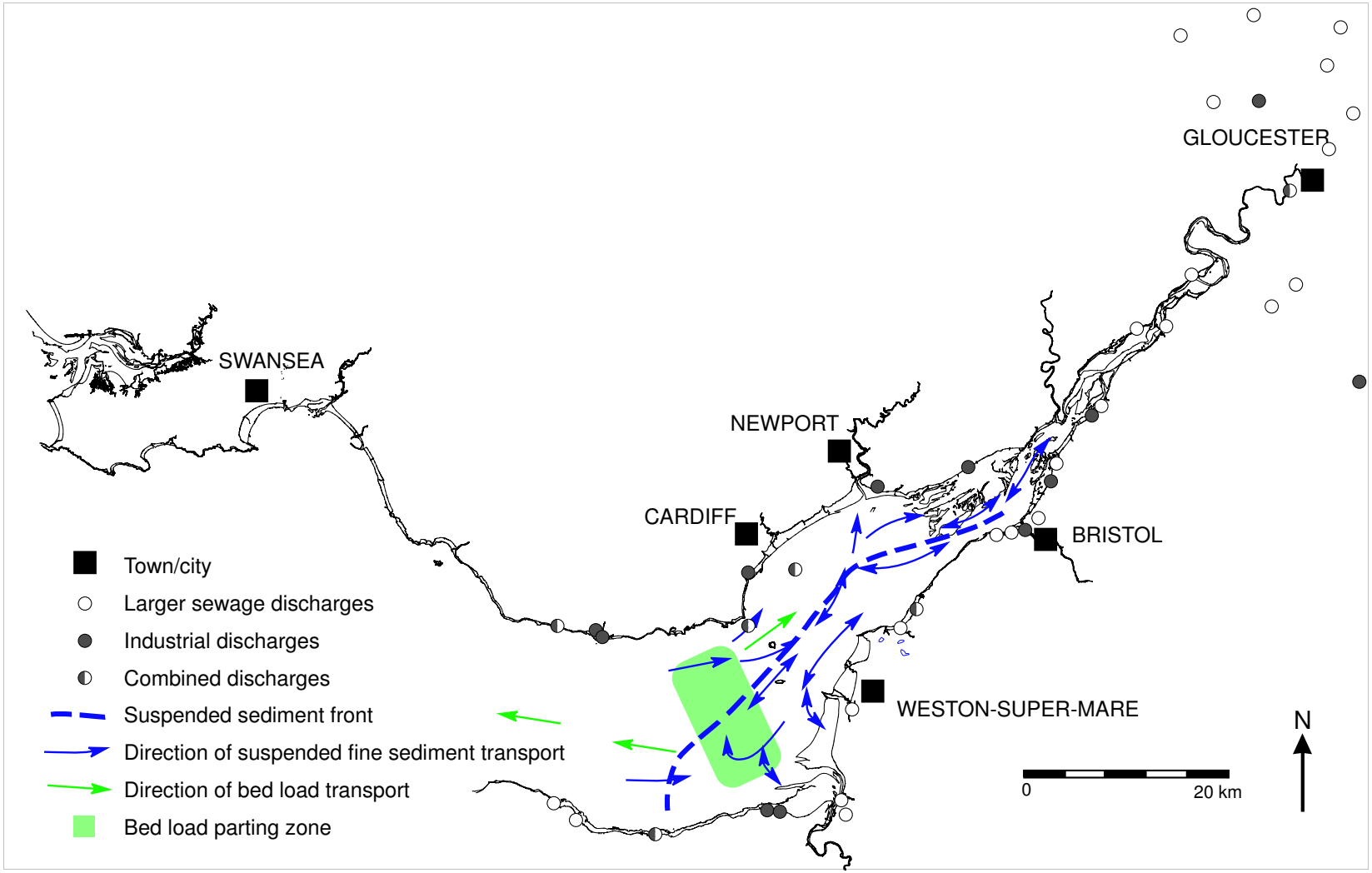

Figure 1.8: Major sources of anthropogenic sewage (>1000 m^3/day) and industrial discharges (>500 m^3/day) into the Severn estuary (after Langston *et al*, 2003), with the estimated tidally driven circulation of fine sediments (Parker and Kirby, 1982) and bedload transport pathways of coarse sediments (Culver, 1980).

1.4.3 Sediment sinks

As coarse and fine sediments are circulated separately in the Severn estuary, they also tend to be deposited separately (Figure 1.9). Fine sediments are accreted in subtidal mud patches at Newport Deep (Kirby, 1994), Bridgwater Bay and Kings Road (Parker, 1972), and intertidal mud flats and salt marshes (Allen, 1988; 1990), while sands and gravels are sorted by tidal currents and deposited as sand waves and banks on the channel floor (Culver, 1980).

Subtidal mud patches and intertidal mud flats

Although approximately half of the suspended fine sediment load settles out of suspension during neap tides, there are only three subtidal areas that consistently accrete fine sediment. These areas are located in topographic lows, which are sheltered from erosive currents, although the Bridgwater Bay mud patches are layered and overspill the topographic hollows (Parker, 1972).

There are large thixotropic intertidal to subtidal mud flats along the northern shore of the Severn estuary, and to the south in Bridgwater Bay. Due to the high tidal range, large expanses of these mud flats are exposed at low tide. Mud flats accrete fine sediment in favourable tidal and meteorological conditions, however they are easily eroded at spring tides or when high winds increase wave energy (Allen and Duffy, 1998a).

Salt marshes

Salt marshes are areas of mainly halophytic vegetation, located between the low and high-water marks, that are regularly flooded by the sea (Allen and Pye, 1992; Beeftink and Rozema, 1998). The Severn estuary is fringed by extensive cyclic salt marshes which have accreted over the past 2000 years (French, 1996). There are four marsh units, named (from oldest to youngest) the Wentlooge, Rumney, Awre and Northwick formations after their type localities (Allen and Rae, 1987 and references therein; Figure 1.10). The Wentlooge formation began accreting in the pre-RomanoBritish period (Allen and Rae, 1986), and the three later formations have been dated to the 17th century (French, 1996). Extensive reclamations, which began in Roman times, have enclosed 840 km^2 of marsh, leaving just 14 km^2 of active marsh in the Severn estuary (Burd, 1984).

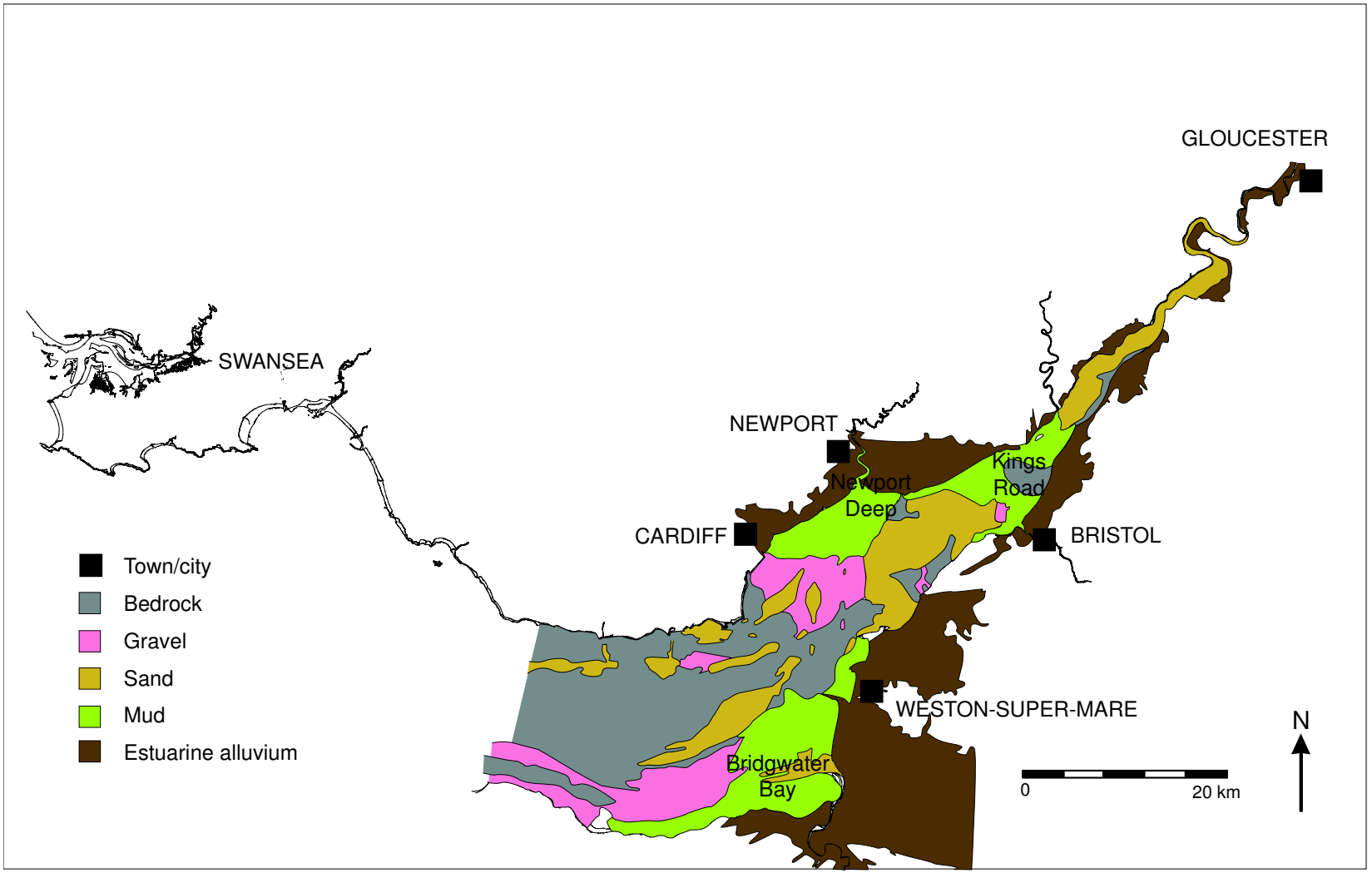

Figure 1.9: The distribution of depositional environments on the estuary bed and estuarine alluvial deposits (after Allen, 1988; 1990).

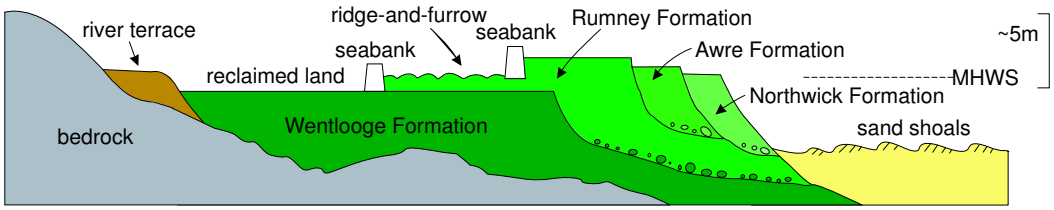

Figure 1.10: Schematic stratigraphy of the Severn estuary salt marshes (after Allen, 1988; Allen and Rae, 1987).

Salt marshes evolve from mud flats in response to relative sea level rise (Figure 1.11; Allen, 2000). When the mud flat accretes to a level above mean high water at neap tides (MHWN) and becomes partially vegetated, halophytic plants (usually *Salicornia*, *Spartina* and *Puccinellia*) help to trap and bind mineral sediment with roots and biofilms, which assists further accretion (Figure 1.11; Beeftink and Rozema, 1998). The plants also supply organic material to the marsh by growth above and below ground (Allen, 2000). As the marsh grows higher in the tidal frame, the surface topography becomes more irregular, other plant species become established and a deeper drainage network of creeks develops (Figure 1.11; Beeftink and Rozema, 1998). The mature marsh, with its surface above mean high water springs (MHWS), accretes more slowly, and usually grades into a mud or sand flat at its seaward edge; the two environments are normally separated by a ramp or cliff (Allen and Pye, 1992). A repeating cycle of erosion and accretion on a decadel to century timescale can therefore produce a series of stepped marshes, as observed in the Severn estuary (Allen *et al*, 1993; Figure 1.10).

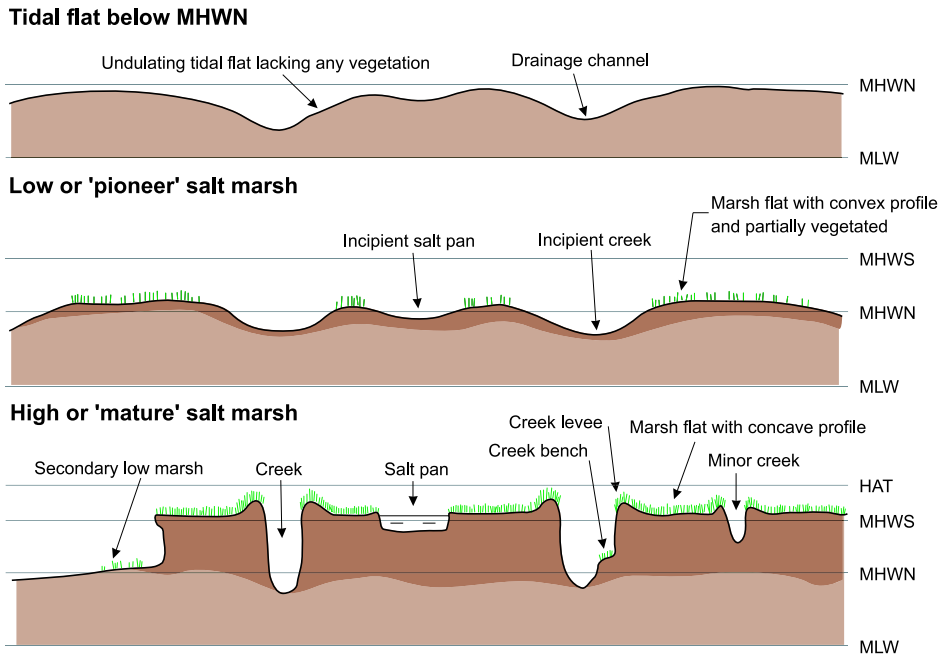

Figure 1.11: A series of cross-sections showing the evolution from a mud flat to a 'pioneer' and 'mature' salt marsh (after Allen, 2000; Beeftink and Rozema, 1998). MLW = mean low water, MHWN = mean high water neaps, MHWS = mean high water springs, HAT = highest astronomical tide

Salt marsh sediments are sorted by grain size and density, with finer grained sediments deposited on platforms and coarser silts and sands deposited in the drainage channels (Allen, 2000). There is a landward decline in grain size across river-dominated salt marshes in the Inner Severn estuary (Allen, 2000), but this trend is much weaker in the Middle and Outer estuary where the marshes are tidally-dominated. Discrete layers of coarser, well sorted, sediments can also be deposited on the marsh platform by storms (referred to as storm-overwash deposits by Allen and Pye (1992)).

Salt marshes have the potential to trap and store fine sediment and associated pollutants over long periods. Sediment cores from Severn estuary salt marshes have previously been used to produce historical records of pollutant inputs, including trace metals and coal dust (Allen, 1987; Allen, 1988; Allen and Rae, 1986; Allen *et al*, 1990; French, 1998; French *et al*, 1994). For a core to be suitable, the sediment record must not be mixed by bioturbation or grazing, and the elements of interest must not have been remobilised, due to changes in the oxidation state of pore waters and sediments (Jickells and Rae, 1997) or the degradation of organic matter (Allen *et al*, 1990; Rae and Allen, 1993). The core must also be dateable; a range of techniques have been used to date Severn estuary salt marsh deposits, including radiometric dating (Allen *et al*, 1993; French *et al*, 1994), archaeological remains (Allen, 1991), historical aerial photographs and maps (Allen, 1991; Allen *et al*, 1993) and counting of sediment layers (Allen *et al*, 1993). It may therefore be possible to study the historical accumulation of OBT in Severn estuary sediments using salt marsh cores.

1.5 Objectives

The present study aims to establish the spatial distribution and temporal variation of ^{3}H activities in surface sediments from the Severn estuary, using results from a four year sampling programme (Chapter 3). The historical (decadel) accumulation of ^{3}H activities in salt marshes (Section 1.4.3) on the northern shore of the Severn estuary is then investigated by analysing shallow sediment cores (Chapter 4). The factors controlling these ^{3}H activities, which include the sources of ^{3}H into the estuary and their characteristics (Section 1.2.4), and sediment composition, transport and depositional processes (Section 1.4), are identified (Chapters 3 and 4). An attempt to characterise the OBT present in Severn estuary sediments provides some insights into its composition (Chapter 5). Finally, the potential implications of these findings, for both the Severn estuary and other sites, are evaluated (Chapter 6). The methods used to achieve these objectives are discussed in Chapter 2.

Chapter 2

Experimental methods

2.1 Introduction

The methods used for the analysis of surface and core sediment samples in the present study were:

- Total and aqueous tritium analysis.
- X-ray fluorescence analysis, to determine the major and trace element concentrations of the sediment.
- Gamma-ray spectrometry, to measure ^{137}Cs and ^{210}Pb activity concentrations of the sediment.
- Organic carbon analysis, obtained by the difference between total and inorganic carbon content, using coulometric methods.
- X-ray diffraction analysis, to identify the minerals present in the sediment.

2.2 Tritium analysis

A range of methods have been used to extract tritium (^{3}H) from environmental samples, depending on the form of tritium to be determined and the type and activity of the samples (Table 2.1). Distillation or freeze-drying is used to extract tritiated water (HTO) from aqueous samples or solids with a high water content, such as vegetation and fruits. Sub-boiling distillation (at $40 - 80\,^{\circ}$C) has the advantage that a lower proportion of the volatile organically bound tritium (OBT) compounds are distilled over than in conventional distillation at $100\,^{\circ}$C; the apparatus can also be left unattended overnight (Warwick *et al*, 1999). If samples are likely to be contaminated, they can either be distilled with $KMnO_4$ and Na_2O_2 to oxidise organic residues and remove trace contaminants, or hold back carriers can be incorporated into a conventional distillation rig to trap other radionuclides (Ware and Allott, 1999).

Freeze-drying is used, both to analyse the condensate for tritiated water (Wickenden, 1993), and to obtain a dry residue for organically bound tritium extraction (e.g. Bogen *et al*, 1973; Kim *et al*, 1992). However, the removal of water from samples disrupts the HTO/OBT equilibrium, introducing isotopic effects that distort the results (Kim and Baumgartner, 1991). Azeotropic distillation using aromatic solvents such as benzene allows the sample to be distilled at a lower temperature than conventional distillation (69°C compared to 100°C) and reduces the isotopic effects that can be produced by the incomplete removal of water (Moghissi *et al*, 1973); however, there are significant health risks associated with benzene.

Sediment samples can be oxidised by either wet chemical digestion or combustion, using a conventional furnace, plasma source or oxygen bomb, to extract either the total or organically bound tritium fraction, depending on the pretreatment of samples (Table 2.1). For example, Bogen *et al* (1973) collected the tritiated water produced by combustion of a freeze-dried sample, so the measured fraction was organically bound tritium. These

methods all assume that any tritium present in the sample, in any form (e.g. as OBT or HTO), will be oxidised to HTO, collected and counted (Ware and Allot, 1999). For organic samples (such as wood, milk or vegetables), all tritium remaining once HTO has been removed will probably be OBT; however, this may not be the case with mixed inorganic/organic samples such as sediments, where HTO could be trapped in flocs or the interlayer spaces of clays, and only released by reactions which divide these flocs or combustion to higher temperatures than 100 °C.

The combustion furnace method reduces the loss of activity through evaporation and can fully combust larger sample sizes than the wet chemical oxidation method. However, in a national intercomparison exercise, Ware and Allot (1999) found that, although the wet chemical oxidation method produced lower activity concentrations than the furnace combustion method, results from both methods were within 95 % uncertainty of the mean result. The furnace combustion method is more effective and efficient than the plasma combustion method, which took 23 hours (compared with ∼2 hours for the furnace combustion) and did not always completely combust the organic matter in the sample (Momoshima *et al*, 1994). The oxygen bomb method has similar yields to the furnace combustion method (Bogen *et al*, 1973; Moghissi *et al*, 1975), and takes a similar length of time (1.5 and ∼ 2 hours respectively) but the sample size for the oxygen bomb method is restricted to 10 g for safety reasons.

In the present study, sediment samples were analysed using a modified version of the combustion furnace method, which was first used by Bogen *et al* (1973). This method is cheap, rapid (8 to 12 samples per day were analysed), reproducible and easily verifiable.

Table 2.1: Methods of analysis for tritiated water and organically bound tritium.

Method	Type of sample	Level of activity	Details of method	Reference
Tritiated water				
Conventional distillation	Aqueous samples	Low/ high	Sample placed in bottom of distillation rig and heated to 100 °C. Water vapour, which will include HTO, is condensed and collected for analysis.	Ware and Allott, 1999
Sub-boiling distillation	Aqueous samples	Low	Water in the outer ring of an annular distillation unit is covered with a watch glass and gently warmed (40 − 80 °C). Tritiated water evaporates onto the watch glass and runs into the centre, where it is collected for analysis.	Warwick *et al*, 1999
Freeze-drying	Milk and pureed foodstuffs	Low	Known mass of sample is weighed into round-bottom flask, frozen in liquid nitrogen and evacuated using a high vacuum pump. The receiving vessel is then cooled and the sample allowed to reach room temperature. An aliquot of the collected water is analysed.	Wickenden, 1993
Azeotropic distillation with benzene	Biological, environmental and soil	High/ labelled	Samples were covered with dry thiopene-free benzene and distilled at 69 °C for 2-4 hours.	Moghissi *et al*, 1973
Tritiated water and organically bound tritium (OBT)				
Freeze-drying and combustion	Environmental and biological	Low	Freeze-dried sample was placed in low pressure chamber with CuO catalyst in O_2-Ar flow. Combustion water was collected in a dry ice-cooled trap.	Bogen *et al*, 1973
Freeze-drying, conventional and plasma combustion	Environmental (leaf litter and humus)	Low	Free water is removed by freeze-drying in a vacuum, distilled and electrolytically enriched. Thin layer of freeze-dried sample is spread across glass plates in a glass chamber and oxygen plasma induced. Pt-alumina catalyst in combustion tube is held at 450 °C,and the sample is heated with a gas burner for 2 hours. Resulting water vapour is trapped in dry-ice cooled trap and distilled with $KMnO_4$ and Na_2O_2.	Momoshima *et al*, 1994
Split combustion	Environmental and effluent	Low/ high	Dual-zone combustion furnace with Pt-alumina catalyst at 750 °C. Sample is initially held at 100 °C for 2 hours in mixed N_2/O_2 flow and combustion water is trapped in cooled distilled water bubblers. Then bubblers are changed and the sample is heated to 700 °C, gas is changed to O_2 only at 450 °C.	Verrall and Odell, 2002

Method	Type of sample	Level of activity	Details of method	Reference
Freeze-drying and combustion	Environmental	Low	Free water is removed by freeze-drying. Freeze-dried samples are combusted in mixed N_2/O_2 flow and combustion water collected. Purified by double-distillation after adding $KMnO_4$ and Na_2O_2.	Kim *et al*, 1992; Kim and Han, 1999
Combustion	Vegetation	Low/ background	Pre-treatment by drying at 40 °C and grinding. Dry samples are mixed with tritium-free water for 2 days to remove exchangeable OBT, then filtered and freeze-dried. Dual zone furnace with CoO catalyst and quartz beads at 850 °C. Samples are gradually combusted to ash by a mobile heating unit at 450 °C in a pure oxygen flow. The combustion water is collected in a cold trap and distilled after pH adjustment with Na_2O_2.	Pointurier *et al*, 2003
Oxygen bomb combustion	Environmental	Low	Up to 10 g of sample was placed into a vessel, which was sealed and pressurised to 250 psi with oxygen, which was then ignited with two electrodes joined by a Ni-Cr wire. Combustion gases were subsequently passed through a dry ice and alcohol cooled trap, collecting tritiated water, which was counted by liquid scintillation counting.	Moghissi *et al*, 1975
Wet chemical digestion	Filtered effluent	High	Tritiated water is determined separately by direct distillation of the sample under alkaline conditions at 100 °C. Total tritium is then extracted by refluxing the sample with chromium trioxide and sulphuric acid to oxidise the organic fraction to HTO, followed by alkaline distillation at 100 °C.	Ware and Allott, 1999

2.2.1 Total tritium method

Total tritium ($^3H_{total}$) was extracted from the fresh sediment samples using a combustion furnace method. The purpose-built furnace consisted of four silica glass tubes that passed through two independent furnaces: the 'sample' and 'catalyst' zones (Figure 2.1). A silica or ceramic boat containing an accurately weighed aliquot of fresh sediment (usually ~5 g) was placed in a tube in the centre of the sample zone. The tube end cap was replaced and this zone was heated from 50 °C to 500 °C at a rate of 5 °C/minute, with holding stages at 200 °C, 300 °C and 500 °C. Oxygen was added to the air flowing through the system when the sample zone reached 500 °C. The catalyst zone contained around 10 g of a Pt-coated alumina catalyst, held at a constant 800 °C, which oxidises organic compounds in the combustion products to CO_2 and H_2O. The combustion gases were bubbled through a tube containing 20 ml of 0.1 M HNO_3 to trap the combustion water, which contained all of the tritium activity in the sample in the form of tritiated water.

This method has been developed and validated by a group of researchers in the Geosciences Advisory Unit at the University of Southampton: Dr I.W. Croudace, K. Doucette, Dr F.M. Dyer, J.E. Morris, Dr J. Oh, Dr P. Teasdale and Dr P.E. Warwick.

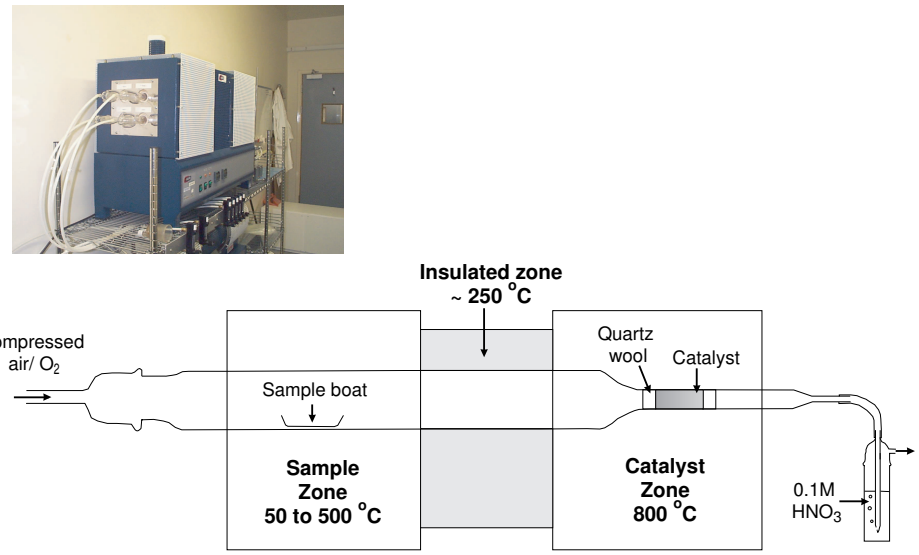

Figure 2.1: Design of the purpose-built four tube combustion furnace used for tritium analysis. Inset: Photograph of the combustion furnace used in the present study

Method validation

Reproducibility The method reproducibility was assessed by replicate analysis of a homogeneous in-house reference sediment (Figure 2.2). All results were within 2σ uncertainty of the mean $^3H_{total}$ activity (ca. 0.2 Bq/g dry weight). Two or more sub-samples of 60 fresh bulk sediment samples were also analysed for $^3H_{total}$ (Figure 2.3). 90 % of the results were reproducible to within 2σ uncertainty. The remaining 10 % of samples may have been affected by changes in the wet/dry ratio of the samples during storage because the replicate analyses were normally performed at a later date, following repeated freezing and defrosting of the samples, which occasionally resulted in sample bags splitting and

leaking. This is unlikely to have affected samples that were routinely analysed because they were only frozen and defrosted once, then homogenised and analysed immediately, reducing the chance of leaking.

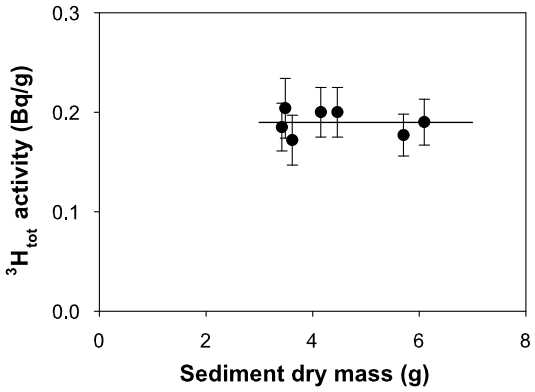

Figure 2.2: Assessment of method reproducibility by analysing 9 replicates of the freeze-dried, ground and homogeneous in-house reference sediment for $^3H_{total}$ activities using the combustion furnace method. Total method uncertainties were propagated to the 95 % confidence interval (2σ) and plotted as error bars. The mean$^3H_{total}$ activity of the sediment is shown as a horizontal line.

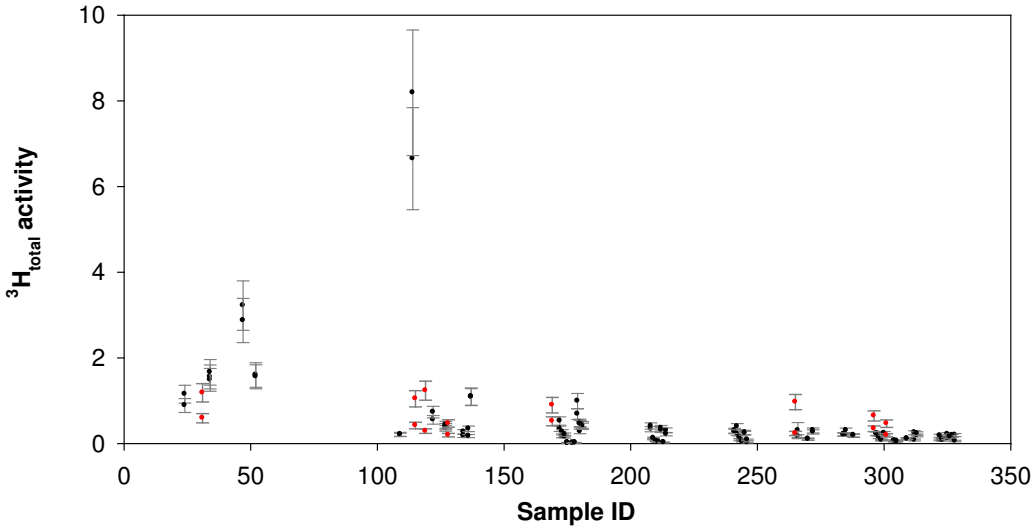

Figure 2.3: Replicate analyses of 60 fresh surface sediments for $^3H_{total}$ (in Bq/g dry weight) using the combustion furnace method. Total method uncertainties were propagated to the 95 % confidence interval (2σ) and plotted as error bars. Samples that were not reproducible to within 2σ are shown in red, and reproducible samples are shown in black.

A total tritium intercomparison exercise in 1999, which was funded by the Environment Agency (Toole, 2001; Warwick *et al*, 2003), used dried sediments labelled with a range of tritiated species; this allowed the combustion furnace method to be rigorously tested against a range of other methods and laboratories. Results were close to the intercomparison mean for the higher activity sample, and low, but still within the range of

data, for the lower activity sample (Table 2.2).

Table 2.2: Total tritium intercomparison exercise results (after Toole, 2001; Warwick *et al*, 2003)

Sample	Result from SOC	Reference result	Intercomparison mean	Intercomparison range
A8318sp	8450 ± 90	9786	8763	7103 - 10093
A8320	614 ± 43		436	202 - 707
A8318	< 50		155	< 50 - 272

Background measurement Blank filter papers were regularly analysed in each silica glass furnace tube after every standard analysis (Figure 2.4). Contamination, when detected, was usually attributed to the deposition of tritiated organic compounds onto the inside of the tubes, which was easily removed by heating to 600 °C. Results were only acceptable if their associated blanks had tritium activities that were below the limit of detection of the liquid scintillation counter (0.005 Bq/g fresh sample), otherwise further blanks were analysed until background tritium activities dropped to below the limit of detection.

Furnace recovery Pt-alumina catalysts were used in the combustion furnace because they convert a higher proportion of a wide range of tritiated compounds to tritiated water than a CuO catalyst (Figure 2.5). The speciation of the tritiated compounds also affects the furnace recoveries; volatile compounds are released at lower temperatures and are more effectively oxidised by the catalyst, so they have higher recoveries than more refractory compounds that only decompose at higher temperatures (Figure 2.6). The speciation of tritium in the sediments is unknown, but as the majority of the tritium in the in-house reference sediment is only released above 300 °C, it is probably present in refractory compounds.

A ^{3}H-sucrose (prior to August 2003) or ^{3}H-thymidine standard (Amersham plc, Cardiff) was analysed after every fifth sample to monitor the catalyst efficiency. Thymidine is a more refractory compound than sucrose; therefore thymidine was preferred because it could be assumed that other tritiated compounds had similar or higher recoveries. Catalyst recoveries tended to decrease over time, therefore it was routinely changed after 20 runs, or earlier if the standard recoveries fell below 80 %. Results were only accepted if their associated measured standard recoveries were between 80 % and 110 %, and sample activities were corrected for a mean furnace recovery of 92 % (Figure 2.7).

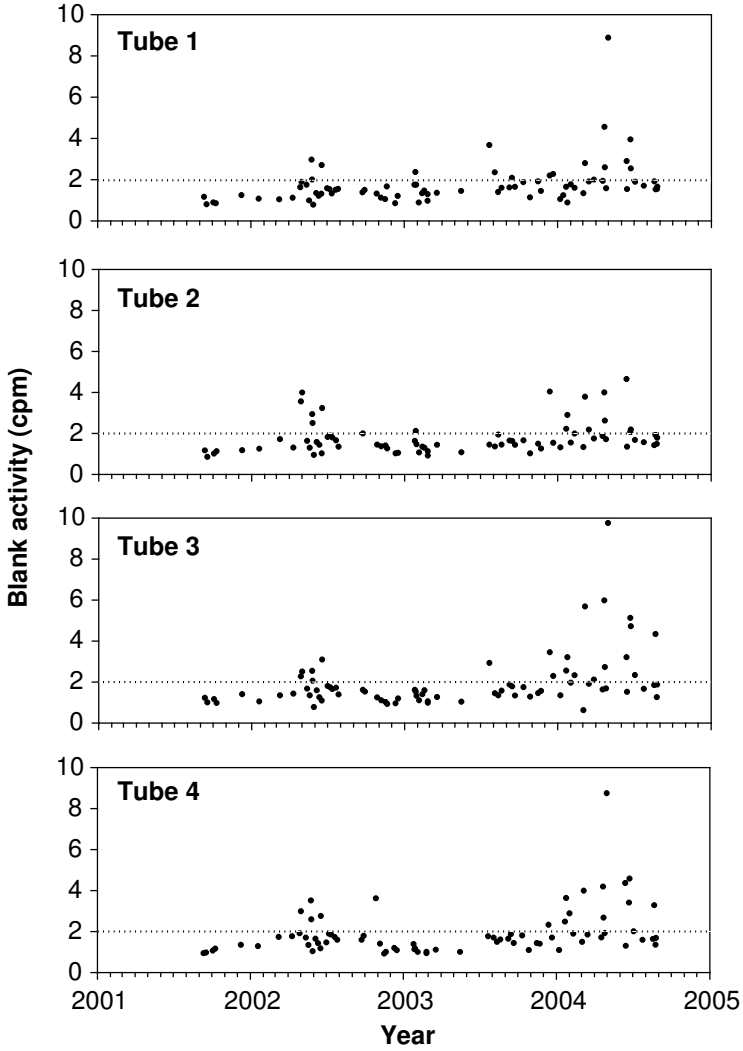

Figure 2.4: Control charts showing blank activities (in counts per minute or cpm) for the four tube furnace throughout the present study. The acceptable upper limit for blank activities is shown as a dotted line (outliers are discussed on page 43). These data were compiled from measurements by K. Doucette, J.E. Morris, Dr F.M. Dyer, Dr P. Teasdale and Dr J. Oh.

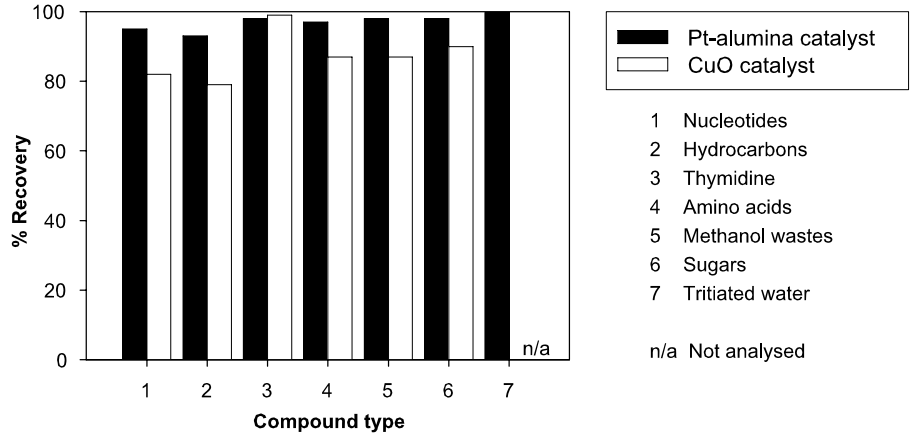

Figure 2.5: Comparison of furnace recoveries with Pt-alumina or CuO catalysts. These data were produced by K. Doucette.

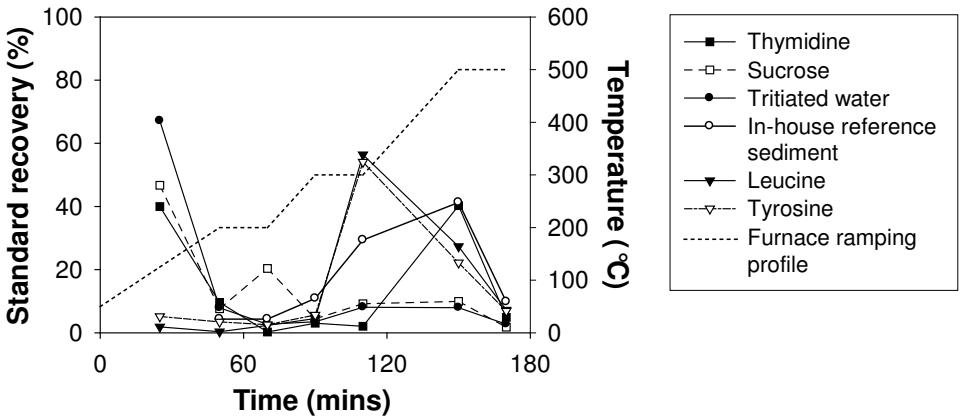

Figure 2.6: The evolution of tritium activities with time and furnace temperature, and the effect of speciation on furnace recovery. A range of tritiated standards and the in-house reference sediment were analysed in the combustion furnace, with the 0.1 M HNO_3 traps changed at intervals during the analysis. These data were compiled from measurements by Dr J. Oh, Dr P.E. Warwick and J.E. Morris.

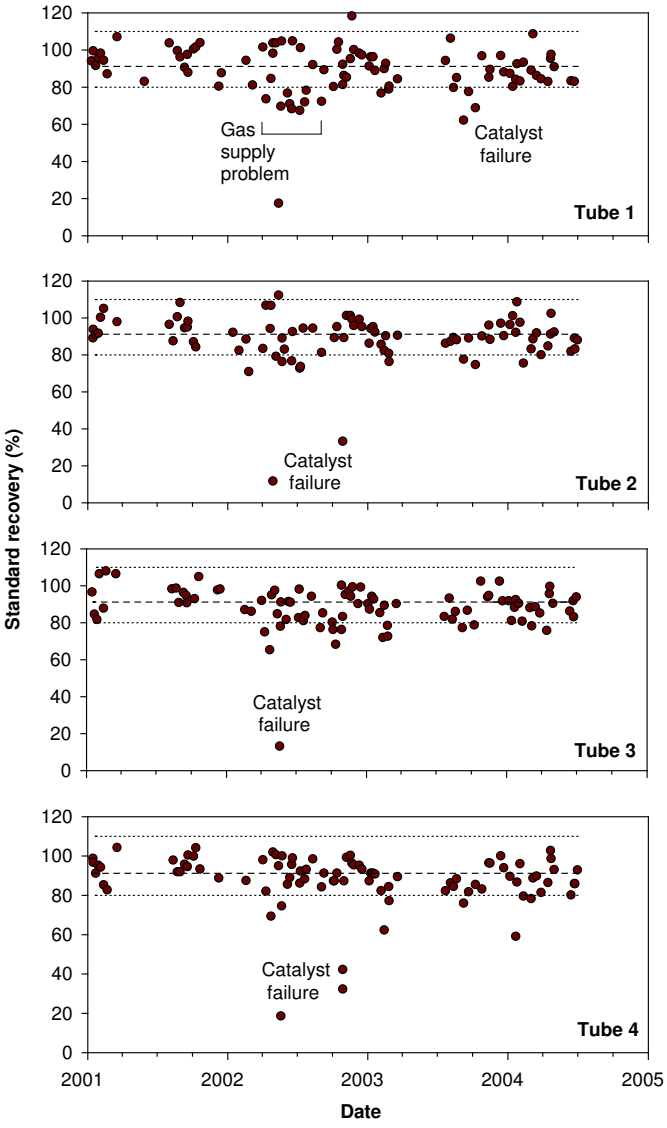

Figure 2.7: Control charts showing standard recoveries for the four tube furnace throughout the present study. Either tritiated thymidine or sucrose standards were used. Data are presented as the percentage of the standard recovered by the furnace and measured in the LSC. The mean furnace recovery (92 %) is shown as a dashed line and the upper and lower limits as dotted lines. These data were compiled from measurements by K. Doucette, J.E. Morris, Dr F.M. Dyer, Dr P. Teasdale and Dr J. Oh.

2.2.2 Water-extractable tritium method

Water-extractable tritium ($^3H_{ext}$) was determined by mixing 8 ml of MilliQ pure water (with blanks below the measurement limit of detection) with 5 g of fresh sediment on a mixing wheel for 1 hour to allow the exchange of interstitial and free water. The $^3H_{ext}$ fraction includes HTO, soluble and slightly soluble tritiated organic molecules (such as ^{3}H-methanol), and ^{3}H exchanged from hydrophilic groups (e.g. -OH, =NH) on large hydrophobic molecules, if they are not trapped by molecular structures. The liquid and solid phases were separated by centrifuging at 3000 rpm for 5 minutes, then the supernatant was filtered through a 0.45 μm cellulose nitrate filter and mixed with Goldstar scintillation cocktail.

Method validation

To confirm that tritiated water and water-soluble tritiated organic compounds were extracted from the sediment, aliquots of the in-house reference sediment were:

- Extracted after being spiked with a range of tritiated standards.
- Equilibrated with a tritiated water standard for different lengths of time (Figure 2.8).

The in-house reference sediment was spiked with 0.1 g of the ^{3}H-water, ^{3}H-thymidine or ^{3}H-sucrose standards using a pipette. The spiked sediment was then mixed with water for 1 hour, centrifuged at 2500 rpm and filtered through a GF/A filter. Both the supernatant and sediment were analysed for tritium, to assess the extent of re-adsorption of the tritiated organic molecules onto the sediment. Recoveries were < 80 % for all of the samples, despite acceptable combustion furnace standard and blank activities. There are a number of possible reasons for this:

- It is assumed that all of the water removed after centrifuging will contain the extracted activity; however, the sample is then dried before the solid is analysed. The remaining activity could have been contained in the pore waters and subsequently lost during this drying step.
- The spike added was not mixed homogeneously with the sediment but adsorbed to the plastic centrifuge tubes used. This is unlikely for the ^{3}H-water but possible for the ^{3}H-thymidine or ^{3}H-sucrose standards.
- The ^{3}H-thymidine was adsorbed onto the sediment, and was subsequently insoluble in the water used to extract the added activity.
- A proportion of the ^{3}H activity may have been adsorbed onto fine sediment, which was trapped on the filter paper and not analysed, again this is more likely for ^{3}H-thymidine or ^{3}H-sucrose than for ^{3}H-water.

As a range of potential problems have been identified with the experimental setup, it appears unlikely that tritiated water is absorbed in the sediment. However, further work is necessary to confirm this.

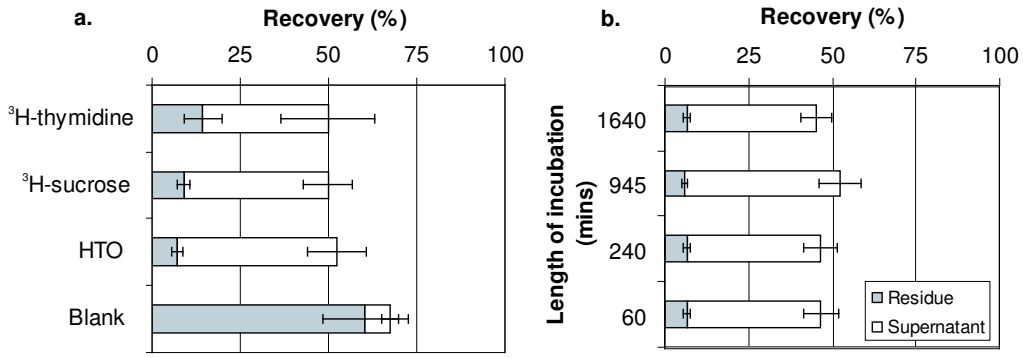

Figure 2.8: Validation of the water-extractable tritium method. a. Aliqouts of the in-house reference sediment were spiked with a range of tritiated standards at activities ∼10 x the measured activity of this sample. A blank (unspiked in-house reference sediment) was also analysed. b. Aliqouts of the in-house reference sediment were incubated with tritiated water on a mixing wheel for a range of lengths of time.

2.2.3 Tritium measurement

The ^{3}H activity present in a sample can be measured using several methods, depending on the type of samples and the tritium activities present (Table 2.3). Tritium activities are expressed in tritium units (TUs), Bequerels (Bq) (the SI unit of radioactivity) or Curies (Ci)(a pre-SI unit of radioactivity), where 1 TU = 1 ^{3}H atom per 10^{18} H atoms (Okada and Momoshima, 1993), which is equivalent to 0.118 Bq HTO per litre of H_2O, and 1 Ci = 3.7 x 10^{10} Bq (NCRP, 1979). Liquid scintillation counting is a common method for the quantitative analysis of radioactivity, including β particles (Table 2.3). It has appropriate limits of detection for the samples in the present study, and it is rapid and cost-effective. The ^{3}He ingrowth method can also be used to determine ^{3}H activities in extremely low level samples (<0.1 TU; Clarke *et al*, 1976); however, the lengthy ingrowth period of ∼6 months is a major disadvantage to this method.

Table 2.3: Methods of tritium measurement

Method	**Type of sample**	**Limit of detection**	**Brief details of method**	**Advantages**	**Disadvantages**	**References**
Liquid scintillation counting	Colourless liquids	∼0.005 Bq/g	Sample and solvent are mixed with scintillators, which release energy as light in response to an α or β decay event. This light is measured by photomultiplier tubes.	Low background (∼1 cpm). Relatively efficient detection of low energy β-emitters such as tritium.	Interference by other radionuclides if present. Chemiluminescence. Quenching (self-absorption) can prevent tritium detection.	Kallman, 1950; Reynolds *et al*, 1950; Dyer, 1974; L'Annunziata, 2003a
^{3}He ingrowth	Water samples	0.1 TU (for water samples (∼40g) sealed for 6 months to 1 year)	Degassed water sample is sealed in a (low He permeability) glass bulb for a length of time. The ^{3}He/^{4}He ratio of the water is measured using a noble gas mass spectrometer. This allows the amount of ^{3}He attributed to tritium decay to be calculated.	Very low detection limit. Simple analytical procedure.	Length of time for ingrowth of ^{3}He (∼6 months).	Clarke *et al*, 1976

Liquid Scintillation counting

Theory and development The development of liquid scintillation counting is attributed to Kallman (1950) and Reynolds *et al* (1950), who reported that homogeneous solutions of samples with organic scintillators or 'fluors' emit light photons, which can be measured, on interaction with α and β-particles (Figure 2.9; Dyer, 1974). Improvements to the technique have focused on:

- Increasing the efficiency and miscibility with water of scintillation cocktails, and reducing their impact on health and the environment (Dyer, 1974).
- Reducing noise in the electronics by using two photomultiplier (PM) tubes and the coincidence counting technique, which reduces background counts significantly by eliminating thermal and electrical noise (L'Annunziata, 2003a).

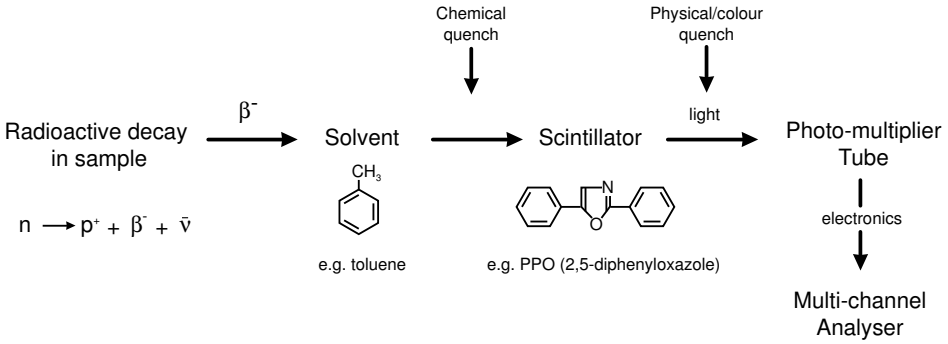

Figure 2.9: The basic mechanism of liquid scintillation counting (after Dyer, 1974).

The transfer of energy from a β particle (electron or positron) to the solvent, the fluor and finally detection by the photomultiplier tubes can be substantially reduced by quenching. Quenching most strongly affects weak β-emitters such as ^{3}H and ^{14}C because it can result in photons from a particular decay event not being detected by the PM tubes (L'Annunziata, 2003a). There are three main types of quenching; physical, chemical and colour quench, which occur at different stages in this energy transfer (Figure 2.9). Physical quenching occurs when energy is not transferred from the radioactive particle to the scintillator solution, or when photons of light are physically absorbed within the vial. For example, a heterogeneous counting mixture may prevent the maximum interaction between the β particles and the solvent/scintillant mixture. Chemical quench occurs when non-fluorescent molecules absorb the energy of the solvent molecules instead of the scintillant molecules, and the energy is lost as heat instead of light. Any compound without an aromatic structure will produce quench, but the strongest quenching agents are halogenated compounds; salts, bases, acids, alcohols and water have less quenching effect and are described as diluters (L'Annunziata, 2003a). Chemical quench cannot generally be avoided, so it must be accurately corrected for. There are a wide range of methods for doing this but the most accurate methods use either an internal or external standard of known activity to allow the efficiency of the energy transfer process to be calculated for

each individual sample:

$$Efficiency \; = \; amount \; out \; (CPM)/amount \; in \; (DPM)$$

, where CPM = counts per minute and DPM = disintegrations per minute.

The Quantulus 1220 Liquid Scintillation Counter, used in the present study, applies the Spectral Quench Parameter of the External Standard (SQP(E)) method to correct for quenching effects. A γ-ray source (37 000 Bq of ^{152}Eu), placed next to the vial, irradiates the sample, producing Compton electrons with a constant spectrum of energies. This allows the effect of quench (measured as the position of 99.5 % of the endpoint of the external standard spectrum) to be quantified (L'Annunziata, 2003a).

Colour quenching, when coloured compounds absorb light, occurs after the fluorescence stage, reducing the number of photons leaving the vial. Colour can be produced either by reactions between the scintillator solution and the sample, or by the introduction of a coloured sample (Dyer, 1974). The SQP(E) method is not as accurate at correcting for colour quench as for chemical quench (L'Annunziata, 2003a), so the analysis of coloured samples has been avoided in the present study.

Measurement and calibration To measure the tritium activity of an aqueous sample, an aliquot (normally 8 ml) was pipetted into a 22 ml polythene scintillation vial, to which 12 ml of Goldstar scintillation cocktail was added. The vial was labelled, shaken to homogenise the phases, and dark-adapted overnight. It was then counted for 2 hours (10 x 12 minutes) on the Wallac 1220 ultra-low-level liquid scintillation counter. Only 5 ml of supernatant from the water-extractable tritium procedure was usually analysed. The total tritium activity (Bq/g) was then calculated using the equation:

$$A = \frac{CPM}{60} \cdot \frac{100}{E} \cdot \frac{V_t}{V_m} \cdot \frac{1000}{M} \cdot \frac{100}{R_s}$$

, where CPM = counts per minute (output of LSC); E = efficiency; V_t = Total volume of bubbler; V_m = Measured volume; M = Sample mass; and R_s = Standard recovery.

MilliQ pure water blanks were also used to determine the instrument background. This was subtracted from the measured cpm to produce the actual count used in the calculation (CPM). The efficiency was calculated using an empirically-defined calibration curve, which corrected for the amount of quench in the samples. The standard calibration curve used was for 4 to 10 ml of MilliQ pure water spiked with a certified tritiated water source (supplied by Amersham plc, Cardiff), mixed with the appropriate volume of Goldstar Scintillation cocktail to make up 20 ml in a 22 ml polythene scintillation vial and counted for 1 hour (Figure 2.10). The limit of detection for this technique was 0.02 Bq/g of fresh sediment, based on 1.3 cpm background and 120 minutes count time.

Interferences The combustion furnace method was used because most matrix elements and radionuclides remain in the sample residue after combustion. However, ^{14}C is a potential interference because it can also dissolve in water and the tail of the ^{14}C energy

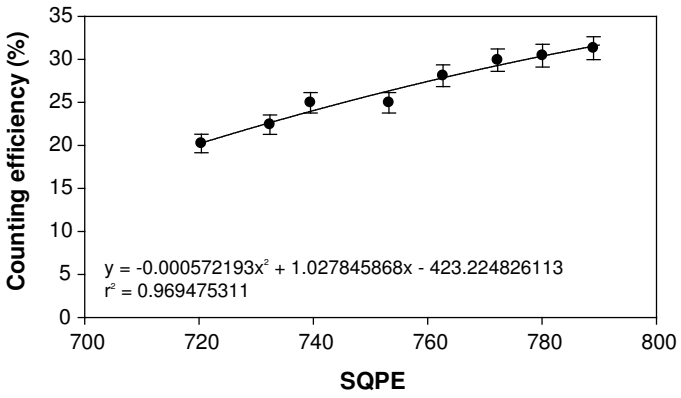

Figure 2.10: The standard calibration curve for ^{3}H measurement on the Quantulus 1220 liquid scintillation counter (instrument Q1), calculated by Dr J. Oh on 23/06/04. Aqueous samples, ranging in volume from 3 to 10 ml, were spiked with a tritiated water standard (from Amersham plc, Cardiff), then made up to 20 ml in a 22 ml polythene scintillation vial, dark adapted and counted for 1 hour.

spectrum overlaps with the ^{3}H energy spectrum (Figure 2.11). To counteract this, a solution of 0.1 M HNO_3 was used instead of water because the acid reduced the solubility of CO_2.

Chemiluminescence, or the emission of light from chemical reactions, is a major interference for tritium because it produces peaks with similar energies to the ^{3}H energy spectrum (Figure 2.11). It is often produced by exposure of the scintillation cocktail to UV light, which is short-lived, or by reaction with basic samples (pH 8 to 14), which is usually more persistent. To prevent chemiluminescence, samples can either be acidified or stored in a cool dark place overnight (L'Annunziata, 2003a); in the present study samples were dark adapted overnight before counting.

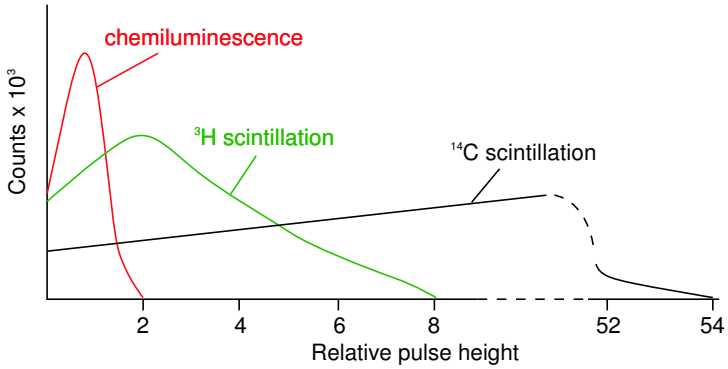

Figure 2.11: Schematic diagram showing the potential interferences with the measurement of tritium activities by liquid scintillation counting, including chemiluminescence and the presence of ^{14}C activity (redrawn from L'Annunziata, 2003a).

2.2.4 Method uncertainty

The method uncertainty was calculated by propagating the uncertainties associated with both sub-sampling and analysis of the sediments (Table 2.4). The analysis of fresh sediment for total tritium involved a number of systematic uncertainties. Weighing of samples, standards and water bubblers and pipetting solutions into vials, introduced quantitative uncertainties in the final result. The variability in furnace recovery introduced the largest uncertainty, with a spread from 80 to 110 % of the measured standard activity (results associated with recoveries outside this range were discarded). Counting statistical uncertainties are incorporated into the total method uncertainty, but were not included in the propagated method uncertainty (Table 2.4) as they varied between samples.

Table 2.4: Calculation of a propagated uncertainty for the total tritium method.

Measurement	**Uncertainty (%)**	**Relative standard deviation (1σ)**
Weighing	0.1	0.001
Pipetting	0.3	0.003
Furnace recovery	8.5	0.085
Speciation	2.5	0.025
LSC calibration	1	0.01
Standard activity (non-certified)	1	0.01
Total (1σ)	9	0.09
Total (2σ)	18	0.18

2.3 X-Ray fluorescence (XRF) analysis

X-ray fluorescence (XRF) analysis is a well-established, fast and economical method for determining the concentration of both major and trace elements in sediments. Concentrations of major element oxides (e.g. SiO_2, Al_2O_3 and CaO) can be used to indicate variability in the proportion of different sediments in a sample (e.g. sand, mud and limestone). The concentration of redox-sensitive elements (Fe, Mn and S) can also be measured to identify redox-potential changes in a core profile.

X-ray fluorescence is produced by irradiating a sample with X-rays. When X-rays collide with atoms in the sample, they eject electrons from the inner shells of these atoms. These electrons are replaced by electrons from an outer shell, which release fluorescent X-rays as they 'fall' into a lower energy shell. Each of the transitions produces an X-ray photon with a characteristic energy (Figure 2.12), named firstly after the shell of the displaced electron (the 'K' and 'L' series are the most important for analytical measurement), and secondly after the length of the transition (such as Kα or Lβ (Figure 2.12; Tertian and Claisse, 1982). Auger electrons can also be produced when the fluorescence X-ray displaces an electron from one of the outer shells. The energy of the fluorescence lines increases with atomic number, so elements below Na in the periodic table cannot be detected by this technique (Potts, 1993).

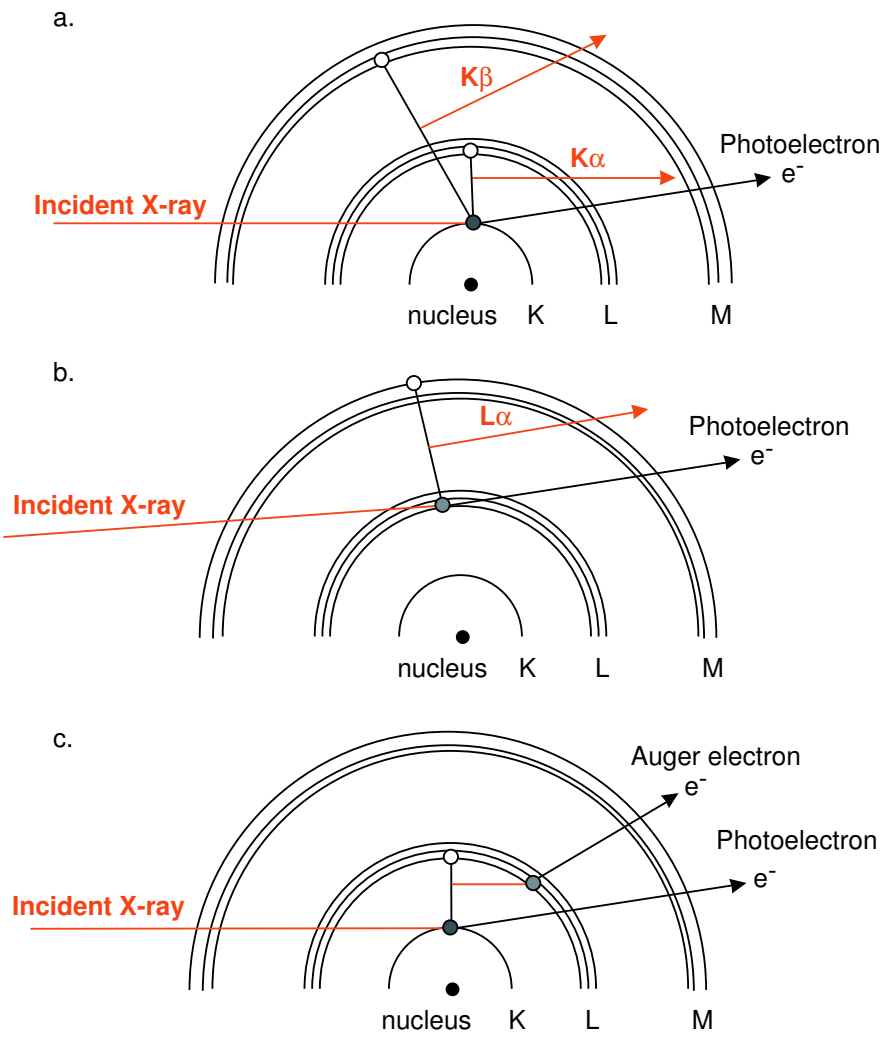

Figure 2.12: Mechanisms of production of X-ray fluorescence: a. K_α and K_β X-rays; b. L_α X-rays; and c. Auger electrons (a competing mechanism). The paths of X-rays are shown in red and photoelectrons in black. (after Moore and Reynolds, 1997 and Potts, 1993).

Sample preparation Sediment samples were initially freeze-dried and finely ground using a TEMA mechanical grinding unit with tungsten carbide pots. Then, approximately 10 g of the ground sediment was placed into an aluminium cup and pressed into a powder pellet (40 mm diameter) using an automatic hydraulic press. Clay-rich samples were cohesive and formed smooth pellets; however, sandy samples required a binder to prevent cracking. In the present study, boric acid, a dry binder, was used as a binder; 2 g was ground with 8 g of sediment. Boric acid was used instead of the more common wet binder PVA to prevent the mobilisation of soluble components such as salts, which are present in relatively high concentrations in these recent estuarine sediments.

For selected samples, fused beads were also produced. The ground sediment was oven-dried, then heated to 650 °C in a furnace overnight. Exactly 4 g of an lithium tetraborate flux (Spectroflux 100B) and 0.8 g of the ignited powder were weighed into a platinum crucible and melted at 1150 °C in a furnace. The melt was then transferred to a Pt-Au casting dish, where it solified into a flat glass bead (Tertian and Claisse, 1982).

Beads v pellets To minimise particle size and mineralogical effects, samples must be homogeneous, representative and have a smooth, flat surface (Tertian and Claisse, 1982). Dissolving the sediment powder in a flux to produce a glass bead entirely removes these matrix effects, and at the lower end of the periodic table, the X-rays from major elements are more susceptible to attenuation by the sample. However, because the sample is diluted by the flux, trace elements cannot be measured on beads; they are more energetic and therefore less affected by matrix effects. Sediments were not ignited when making pellets, which prevents the loss of volatiles such as S, I, Br and Cl. Pellets provided adequate major element data (Figure 2.13) and were simpler to produce; it was also more cost-effective to just analyse pellets.

Sample measurement and calibration The major and trace elements were measured with a Philips MagiX PRO wavelength dispersive X-ray fluorescence spectrometer. Incident X-rays are produced using an X-ray tube, which produces X-rays characteristic of the Rhodium anode (as discussed above) and bremsstrahlung or 'braking' radiation - a broad continuous spectrum of wavelengths (Moore and Reynolds, 2003). These X-rays are collimated before striking the sample (a glass bead or powder pellet). The fluorescence X-rays emitted are collimated and different wavelengths are diffracted with a rotating crystal into the detector (Figure 2.14). The crystal and detector are mechanically coupled to maintain the correct angle (θ) between the diffracting crystal and the detector using a goniometer mechanism (Potts, 1993). If θ is gradually increased from 5 ° to 75 °, the spectrometer will detect the characteristic X-rays of different elements as lines on the spectra above a recognisable background (Tertian and Claisse, 1982). Three detectors are used: a gas-proportional detector to measure low energy X-rays, and a Xe sealed proportional counter and NaI scintillation counter to detect higher energy X-rays.

The spectrometer was calibrated using pressed powder pellets of certified reference materials, including rocks and sediments, with a range of elemental concentrations. The

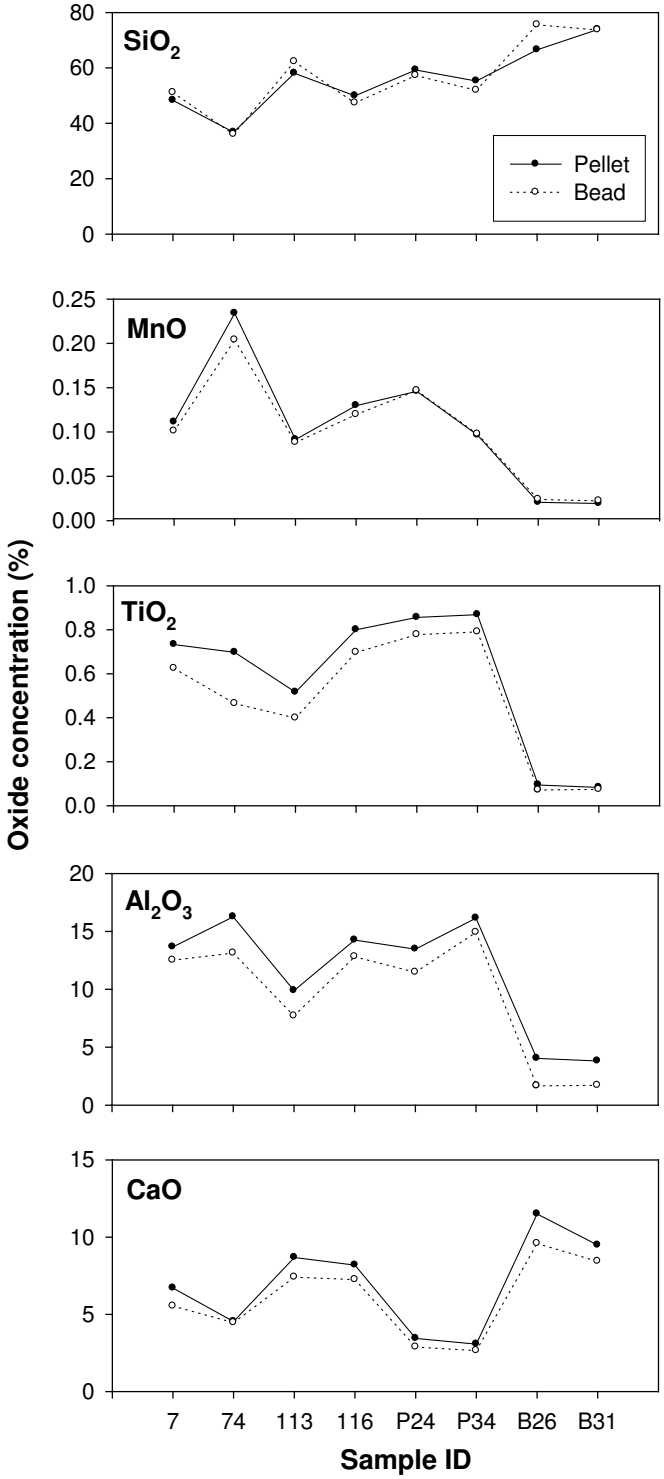

Figure 2.13: Comparison between major element concentrations measured on pressed powder pellets and fused glass beads.

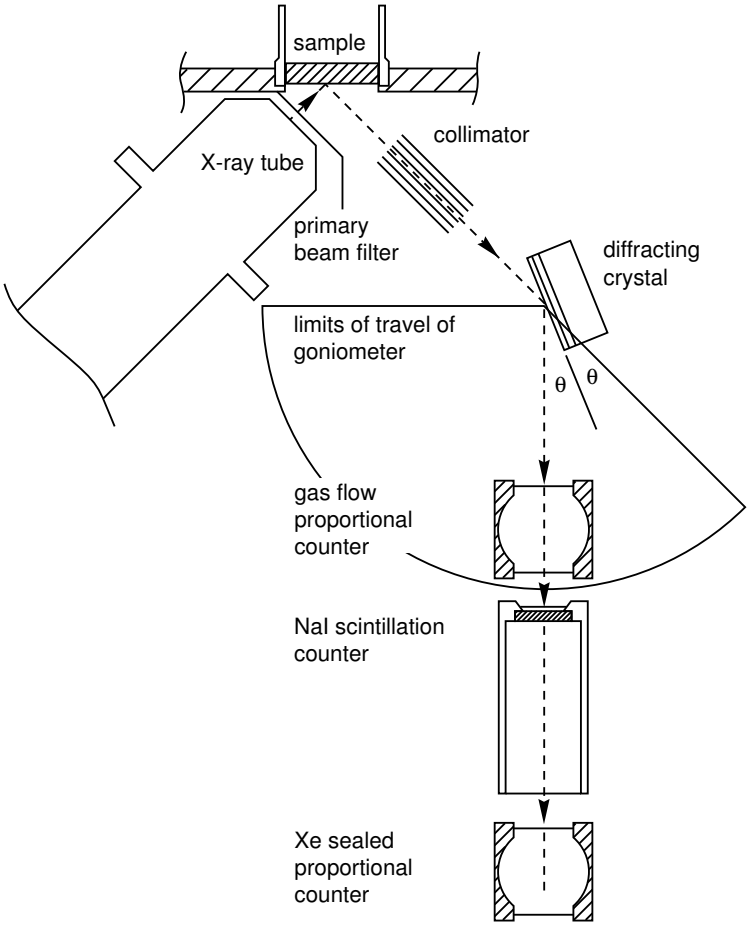

Figure 2.14: The design of an X-ray fluorescence spectrometer (redrawn from Potts, 1993; Tertian and Claisse, 1982).

accuracy of the pellets was also determined by analysing a certified reference sample MAG-1 (a marine mud supplied by USGS); accuracy varies between the elements but most had a standard deviation better than 10 % to 2σ. However, the standard deviations of Na, Cl, I, Br, S, Cr, V and Ba were worse than 30 % to 2σ; this was probably the result of analysing an old pellet in which soluble components had moved and S had oxidised, in which case regrinding the pellet may have improved the precision for these elements. A range of standard pellets with boric acid as a binding agent were also analysed to calibrate for sandy samples.

The random error associated with the measurement of background activities determines the detection limit, the size of the smallest peak that can be distinguished from the background (Fitton, 1997). The detector response to X-rays is dependent on their energy, so both the limit of detection and the precision of measurements varies across the X-ray spectrum (Potts, 1993). Variations observed during measurement of a peak intensity, which affect the precision of the analysis (Fitton, 1997) are produced by random fluctuations in X-ray intensity, changes in the voltage and current of the X-ray detectors and electronic drift (Hamilton *et al*, 1979). The precision of a range of element concentrations was also assessed by repeated analysis of a Severn estuary sediment sample (Table 2.5).

Table 2.5: X-ray fluorescence analysis limits of determination and precision for a range of trace elements. [1,2] From Croudace, 1998 [3] - calculated from repeated analysis (n=12) of sample MT 39.

Element	**Possible interferences**[1]	**Limit of detection (ppm)**[2]	**Precision (2σ)**[3]
As		3	2
Ba	Ce, high As	8	3
Bi	W	3	< LD
Br		2	1
Ce		8	23
Cl		30	3
Cr	V	3	2
Cu	Cu from tube	2	2
Ga		1	7
I		2	19
La		5	19
Mo		3	< LD
Ni		1	1
Nb	Y	1	3
P		20	6
Pb	Bi	1	1
Rb	High U	1	1
S		20	4
Sb		4	< LD
Sn		3	13
Sr		1	1
Th	High Pb	2	< LD
U	High Rb	2	< LD
V		3	2
Y	Rb	1	2
Zn		1	1
Zr	Sr	1	1

2.4 Gamma-ray spectrometry

Gamma rays are released during the radioactive decay of many natural and anthropogenic radionuclides, including ^{210}Pb, ^{137}Cs and ^{241}Am. Gamma-radiation is produced during the de-excitation of the daughter nucleus, usually following β-decay of the parent nuclide (Knoll, 1979). Therefore γ-rays have a half-life that is characteristic of the parent nuclide; however, the γ-ray energies, which are related to the transition between energy states in the daughter nucleus, are almost monoenergetic for a specific transition (Figure 2.15; Knoll, 1979).

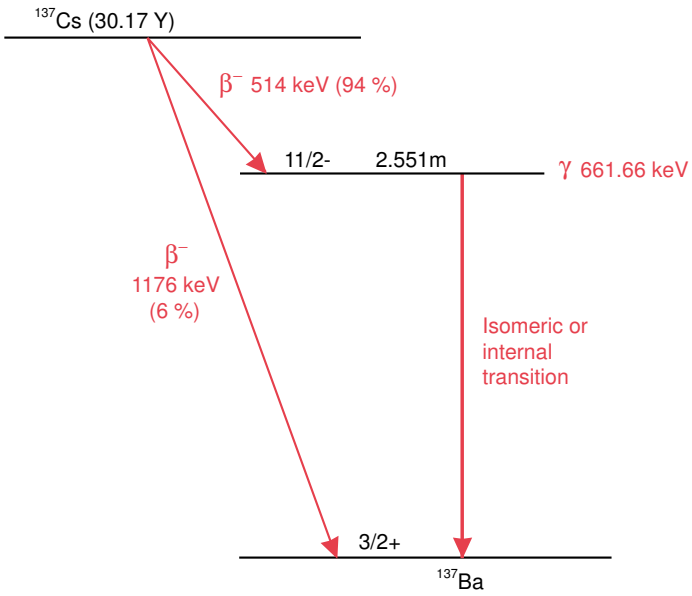

Figure 2.15: A single γ-ray emission following the β-decay of ^{137}Cs to ^{137}Ba. The 514 keV β-particle excites a 2.55 minute isomeric level of ^{137}Ba, which de-excites by emitting a single γ-ray with an energy of 661.66 keV (from Fettweis *et al*, 2003)

There are three mechanisms by which gamma rays interact with matter (Figure 2.16; L'Annunziata, 2003b):

- Photoelectric effect, where the energy of the photon is completely absorbed by an atom.
- Compton effect, where the photon transfers some of its kinetic energy to an electron.
- Pair production, where the photon interacts with the nucleus of an atom, producing two particles, a negatron and a positron, with opposite charges. Only γ-rays with energies > 1.02 MeV interact in this way because only they have sufficient energy to convert to mass.

Modern γ-detectors are normally made of high-purity germanium (HPGe), a dense semiconductor material (Fettweis *et al*, 2003). The charge carriers in these detectors are usually electrons, which are collected by an applied bias (voltage) across the detector (Knoll, 1979). This charge is electronically preamplified, converted to a digital signal and

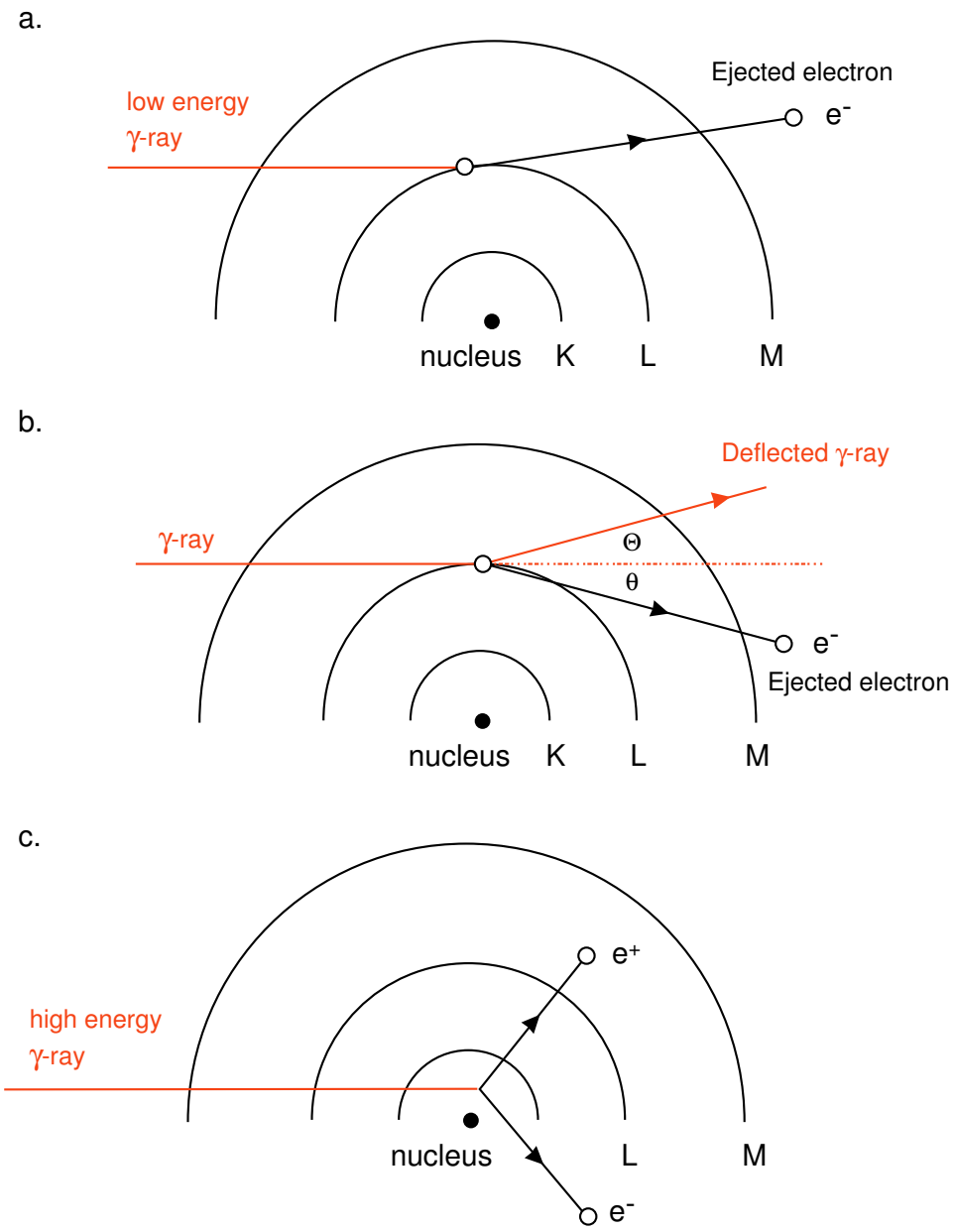

Figure 2.16: The interaction of γ-rays with matter by three mechanisms: a. the photoelectric effect; b. the Compton effect; and c. pair production (after L'Annunziata, 2003b)

collected by a multichannel analyser. The pulse heights obtained are proportional to the energy of the γ-rays (Fettweis *et al*, 2003).

A co-axial Canberra 45 % N-type HPGe well detector was used in the present study; this type of detector almost completely surrounds the sample (almost 4π counting geometry), which increases the detection efficiency (Canberra, 2002). The detector was calibrated for energy, peak shape parameters and efficiency over γ-ray energies ranging from 60 to $\sim$ 2000 keV, using QCYK8163 (a mixed gamma calibration standard, supplied by AEA Technology, Isotrack, UK), which contained all the major nuclides of interest for peak shape calibration by comparison with a peak reference library. This reference sample was prepared with a similar matrix to the samples, using a 22 ml scintillation vial geometry. The detector is most efficient for γ-ray energies of 60 keV; the efficiency decrease at low γ-ray energies due to self-absorption and at high γ-ray energies because the probability of the γ-ray interacting with the active volume of the detector decreases (Figure 2.17. Resolution also varies with γ-ray energy; at 122 keV the resolution is 1.6 keV and at 1332 keV it is better than 2.3 keV. The calibrations were checked weekly using samples IAEA-373 or IAEA-135 (supplied by the International Atomic Energy Agency, Vienna, Austria). The detector background was also determined weekly by counting a blank sample.

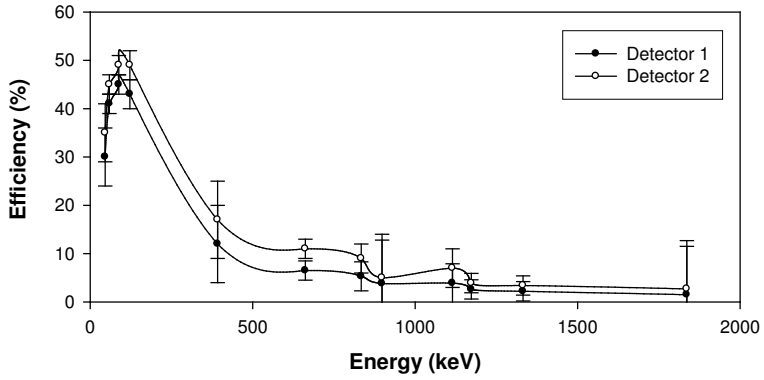

Figure 2.17: Variations in the efficiency of the two γ-ray detectors (co-axial Canberra HPGe well detectors) with γ-ray energy, from the analysis of the mixed gamma calibration standard QCYK8163. Error bars show 2σ uncertainties.

Samples were prepared to resemble the standard as closely as possible, with similar dimensions and distribution of radionuclides (Fettweis *et al*, 2003); sediments were freeze-dried and then weighed into 22 ml polythene scintillation vials. Between 15 and 25 g of sample was required, this variation in density was unavoidable due to the natural variability of the samples but no density correction was applied. However, a height correction was applied if the sample vials were not filled to the rim; this correction did not vary with sample composition.

All samples were counted for >25 000 seconds to achieve the required degree of precision. The γ-ray spectrum obtained was analysed using Fitzpeaks software (www.jimfitz.co.uk),

which identifies peaks in the spectra by spectral deconvolution, enabling peaks to be differentiated from other spectral features. The peak areas were then calculated using function fitting (this can also be used to deconvolute multiplets) and corrected for detector background. The efficiency of the detector at the γ-ray energy of the peak was also determined, following which the activity of the radionuclide can be quantified and the decay correction for the counting period applied, which can be significant for short-lived radionuclides or over long count times (Fettweis *et al*, 2003). Both the activities and their associated uncertainties, including counting uncertainties and those associated with sample and calibration source preparation, are also calculated by the Fitzpeaks software.

The precision of the γ-ray spectrometry method varied between radionuclides, depending on their γ-ray energies and the sample count times, but for ^{137}Cs and ^{210}Pb results were typically within 10 % and 30 % uncertainty respectively, to the 95 % confidence interval (2σ) The accuracy of the γ-ray spectrometry method was determined by taking part in the 2003 NPL γ-spectrometry intercomparison exercise; the laboratory result for ^{137}Cs was 2.88 $\pm$ 0.40 Bq/kg, compared with 2.522 $\pm$ 0.021 Bq/kg recommended activity (GAU, 2005).

2.5 Organic carbon analysis

In the Severn estuary, the organic carbon content of the sediments may represent inputs from primary productivity and sewage and industrial discharges, as well as terrestrial organic detritus and coal dust (Allen, 1987a; Langston *et al*, 2003). The organic carbon content of sediments can be determined using a range of methods (Froelich, 1980):

- Thermal decomposition of organic carbon by ashing at between 450 °C and 600 °C.
- Leaching of the carbonate fraction with phosphoric acid, followed by analysis of the residue (and sometimes the excess acid) for total carbon (or measuring the carbonate and total carbon fractions separately and subtracting one from the other).
- Wet oxidation of the organic carbon by strong acid, followed by either back-titration of the excess oxidant or direct measurement of the evolved CO_2.

The thermal decomposition method separates organic carbon from inorganic carbon by combusting the sample at a temperature, between 450 °C and 600 °C, where organic carbon is oxidised to CO_2 but carbonate is apparently stable, and analysing the evolved CO_2. However, the fractions cannot be reliably separated because their degradation temperatures overlap: high-Mg calcite begins to decompose at or below 500 °C, whilst some refractory organic matter does not decompose completely until $<$ 1000 °C (Froelich, 1980). This can result in serious errors (King *et al*, 1998).

The organic carbon content can also be determined by measuring the total carbon content of the sediment and the inorganic fraction separately, and subtracting one from the other. Inorganic carbon in the sediments is decomposed to CO_2 using a non-oxidising acid, phosphoric acid, because this limits the oxidation of organic carbon to CO_2 (Froelich,

1980; King *et al*, 1998). Froelich (1980) measured the dissolved organic carbon in the acid (up to 15 % of the organic carbon in carbonate-poor sediments) and the organic carbon of the residue after acidification, having added acid in excess to remove all of the carbonate fraction. The determination of organic carbon is not straightforward and there are a large number of potential errors: the hydrolysis of organic matter by acidification can result in organic carbon being either discarded or counted as inorganic carbon; the incomplete removal of carbonate can increase the apparent organic carbon fraction; and uncertainties may be large if there is little organic carbon present when organic carbon is calculated by subtraction of the total and inorganic carbon (King *et al*, 1998). Therefore, King *et al* (1998) recommended that standard reference materials should be analysed if possible, to verify the accuracy of measurements.

The organic carbon fraction can also be extracted directly by wet oxidation with a strong oxidant. Sediment samples are initially acidified with phosphoric acid to remove carbonates, then oxidised with potassium persulphate in a sealed ampoule at 110 °C for 3 hours (Mills and Quinn, 1979). The accuracy of wet oxidation methods can be affected by the presence of chloride ions and the potential inability of the chemical oxidant to completely oxidise refractory organic matter (Froelich, 1980). A similar method was developed by Gaudette *et al* (1974) to analyse organic carbon with the exception of coal particles: the sediment is heated with potassium dichromate and concentrated sulphuric acid, and the excess dichromate is measured by titration with 0.5 N $Fe(NH_4)_2(SO_4)_2{\cdot}6H_2O$.

The evolved CO_2 can also be measured by coulometric methods (discussed in detail below) or by commercially-available total carbon or elemental analysers that separate and quantify gaseous products, such as a total carbon analyser with a non-dispersive infra-red detector to measure the evolved CO_2 (Mills and Quinn, 1979).

2.5.1 Total and inorganic carbon methods

Sediment samples were initially freeze-dried and finely ground using a TEMA mechanical grinding unit. Total organic carbon was extracted from the sediment by combustion at 900 °C, which decomposed all but the most refractory organic matter (Froelich, 1980), and inorganic carbon was extracted using phosphoric acid. The CO_2 released was measured using a CM 5012 UIC, Inc. CO_2 coulometer. Approximately 25 mg of sample was required for both the total and inorganic carbon analyses. For total carbon determination, the sample was weighed into a small Ni boat with a small amount of tungsten trioxide and placed into the furnace at 900 °C. The combustion gases were passed through tubes containing magnesium perchlorate, acid dichromate and manganese dichromate to remove other gases (such as water vapour, sulphur oxides, nitrogen oxides and acid halides (UIC, Inc., 2005)) and into the coulometer cell (Figure 2.18). For inorganic carbon determination, the sample was weighed into an aluminium foil cup and placed in a pear-shaped flask. About 5 ml of 10 % phosphoric acid was added to decompose the carbonate fraction, producing CO_2 gas which was bubbled through a KI scrubber and into the coulometer cell (Figure 2.18).

The coulometer cell consists of silver electrodes in proprietary anode and cathode

solutions (containing dimethyl sulphoxide and ethanol amine (UIC, Inc., 2005); potassium iodide acts as a salt bridge (Figure 2.18). The cathode solution quantitatively adsorbs CO_2 and reacts with it to form an acid, which causes a colorimetric indicator to fade and the intensity of light passing through the cell to increase. This initiates a current in the cell, which produces a base until the solution is titrated back to its original colour. The magnitude of this current is quantitatively related to the amount of CO_2 released by the sample. The current was measured by the coulometer for six minutes after the introduction of the sample

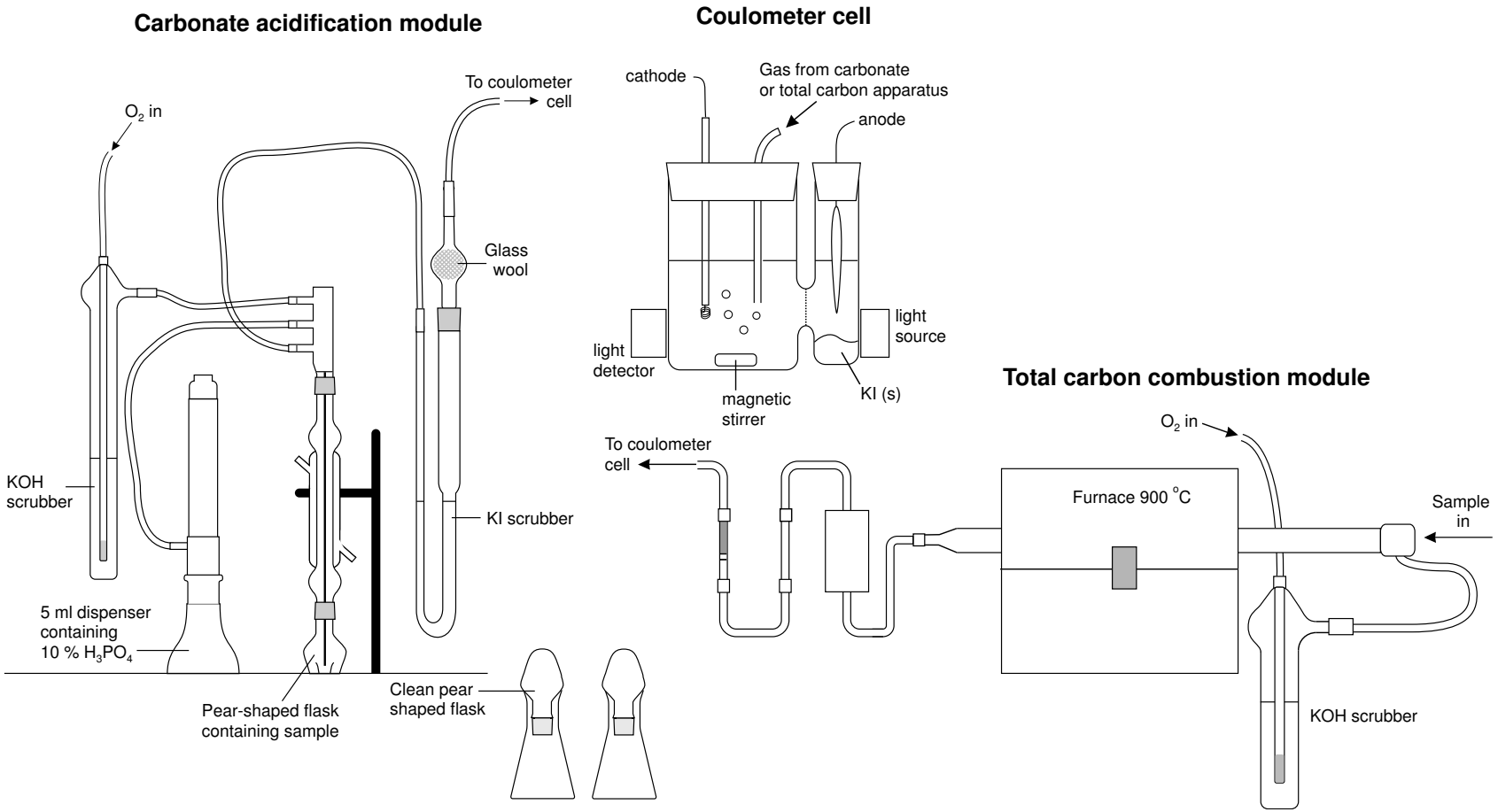

Figure 2.18: Apparatus used to extract total carbon and carbonate fraction from 25 mg of sediment sample as CO_2, and coulometer cell used to measure CO_2, allowing the amount of TC or IC in the sample to be quantified.

into the furnace or the phosphoric acid. The sample size was then adjusted, if necessary, to ensure that all of the CO_2 was released during this period. The total or inorganic carbon content (%) of the sediment was calculated by:

$$TC\ or\ IC = (CR - BL) \cdot \frac{25}{M} \cdot \frac{1}{250}$$

, where $TC\ or\ IC$ = Total or inorganic carbon, CR = Coulometer reading, BL = Blank and M = mass of sample in mg. The total organic carbon (TOC) content of the sediments can be determined by subtracting IC from TC.

Approximately 10 mg of pure dried $CaCO_3$ and a well-characterised bulk sediment were used as standards; these were initially analysed repeatedly until results were within 10 % of the theoretical result, and then after every 10 to 15 samples. Blank samples were run by analysing an empty tin boat or aluminium cup, and were run every two hours as the background tended to decrease with time. Reproducibility was assessed by repeat analysis of the in-house reference sediment (Figure 2.19); TC and IC measurements had relative standard deviations of 1.1 and 55.4 respectively, to 2σ.

2.5.2 Elemental carbon methods

Selected sediments were also analysed for elemental carbon because particulate coal is ubiquitous in Severn estuary sediments (Allen, 1987). The elemental carbon fraction was separated from a 2 g sediment sample by sequentially digesting it in aqua regia, hydrofluoric acid (followed by saturated boric acid to remove any fluoride complexes) and aqua regia; at each stage the samples were left overnight on a hot-plate at 60 °C. The remaining organic carbon was filtered into a sintered glass funnel, air dried and weighed. The percentage of elemental carbon in the sediments was calculated by:

$$EC\ =\ (M_f/M_i) \cdot 100$$

, where EC = elemental carbon, M_f = final mass and M_i = initial mass.

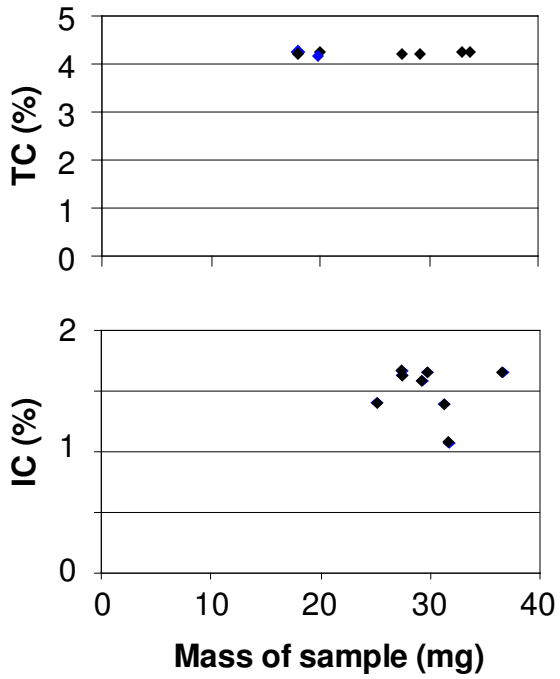

Figure 2.19: Assessment of the reproducibility of total organic carbon measurements by repeat analysis of an in-house reference sediment.

2.6 X-ray diffraction (XRD) analysis

X-ray diffraction can be used to identify minerals in sediments and clay minerals in clay separates. X-rays produced by an X-ray tube are used to irradiate a sample, producing secondary or fluorescent X-rays (as described in Section 2.3). These are collimated and diffracted by a crystal into the X-ray detectors. The crystal and detectors are mounted on a goniometer to maintain a constant angle between them (see Figure 2.14). The angle of diffraction of an X-ray photon is dependent on its wavelength (as described by the Bragg equation (Moore and Reynolds, 1997):

$$n\lambda = 2d \sin\theta$$

, where n = 1, λ = wavelength, d = spacing between planes in the diffracting crystal and θ = angle of incidence (Figure 2.14)). Minerals are identified by the position of lines on the spectrometer.

In the present study a Philips X'Pert X-ray diffraction spectrometer, with a Co X-ray tube and a Xe sealed proportional detector, was used. Approximately 10 g of sediment was finely ground using a TEMA mechanical grinding unit and pressed into a loose powder pellet, in an aluminium holder. Carbonates were dissolved from a 10 g sediment sample with 10 % acetic acid, then washed several times with dissolved water. Around 5 ml of sodium hexametaphosphate (Calgon) was added to disperse the clay minerals, and this mixture was ultrasounded for 15 minutes. The sample was allowed to settle for 3 hours, before the top 4 cm of the mixture (the <2 μm fraction) was decanted. Around 5 ml of 10 % $MgCl_2$ was added to saturate the clays with cations and the mixture centrifuged at 2000 rpm. The residue was rinsed with fresh water and centrifuged three more times. The supernatant was discarded and the clays were smeared onto a glass slide and left to dry overnight.

The pressed powder was run through the angle θ from 2 to 74 °. Non-clay minerals were identified by the position of the peaks in the spectra using X'Pert Graphics and Identify and XRD8, a specialist software program designed by T. Clayton (Figure 2.20). As all clay minerals diffract at about the same Bragg angle, their peaks were superimposed and they could not be distinguished using this method.

Separate clay smears were run: from 2 to 17 ° of θ air dried; from 2 to 40 ° of θ glycolated in ethylene glycol (EGL) vapour for 6 hours; after heating to 375 °C overnight; and after heating to 550 °C. Clay minerals can be identified by the movement of peaks between treatments (Figure 2.21). The proportion of each type of clay in the <2 μm fraction was determined using this method.

Although this method has not been used quantitatively, the information on the mineral phases present in the sediments was useful in interpreting the elemental composition data obtained by X-ray fluorescence analysis. As the fine sediments in the Severn estuary were relatively homogenous, only a small number of the total samples collected were analysed using this method.

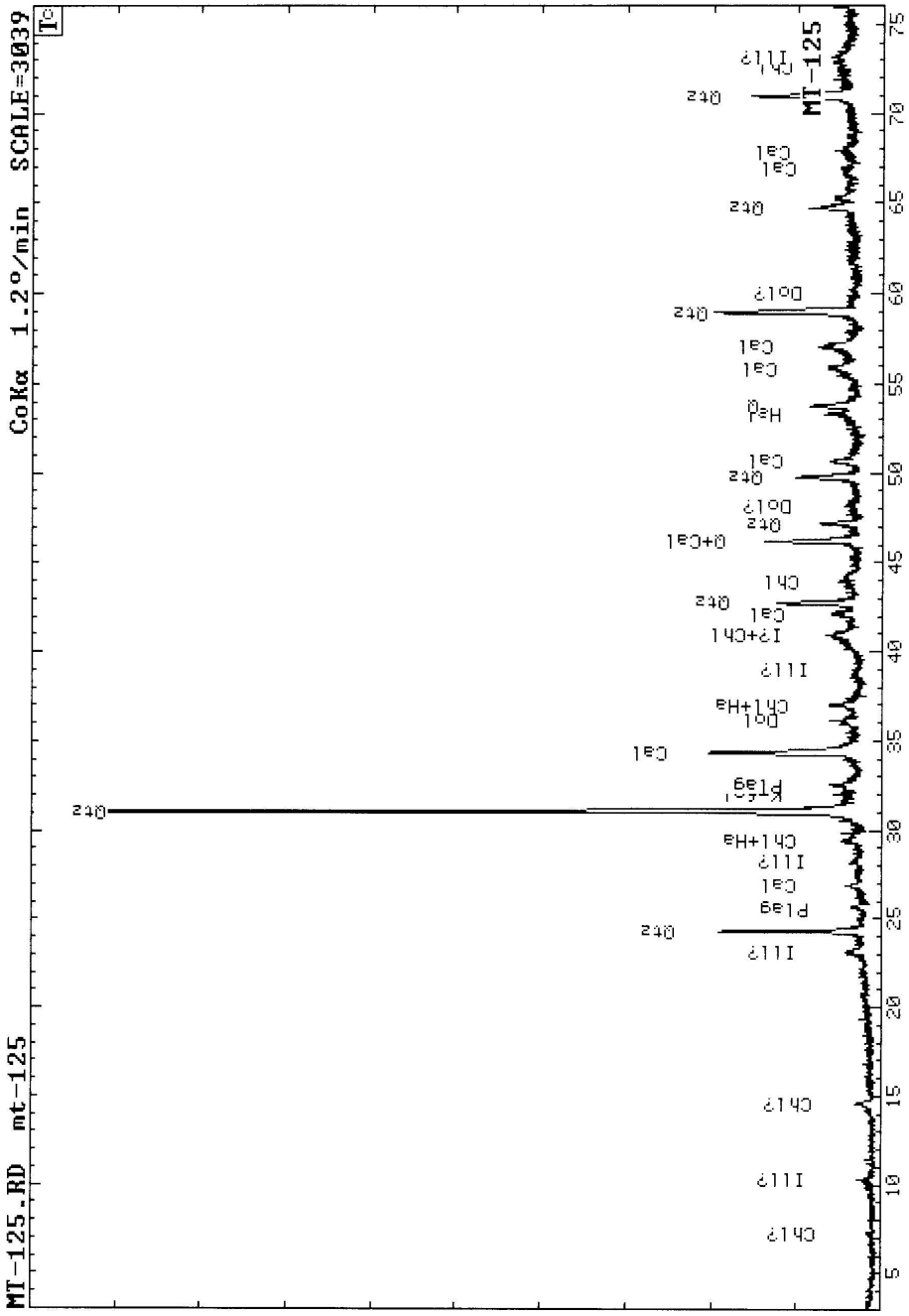

Figure 2.20: X-ray diffraction spectra of a dried and ground powdered bulk sediment sample with identified peaks.

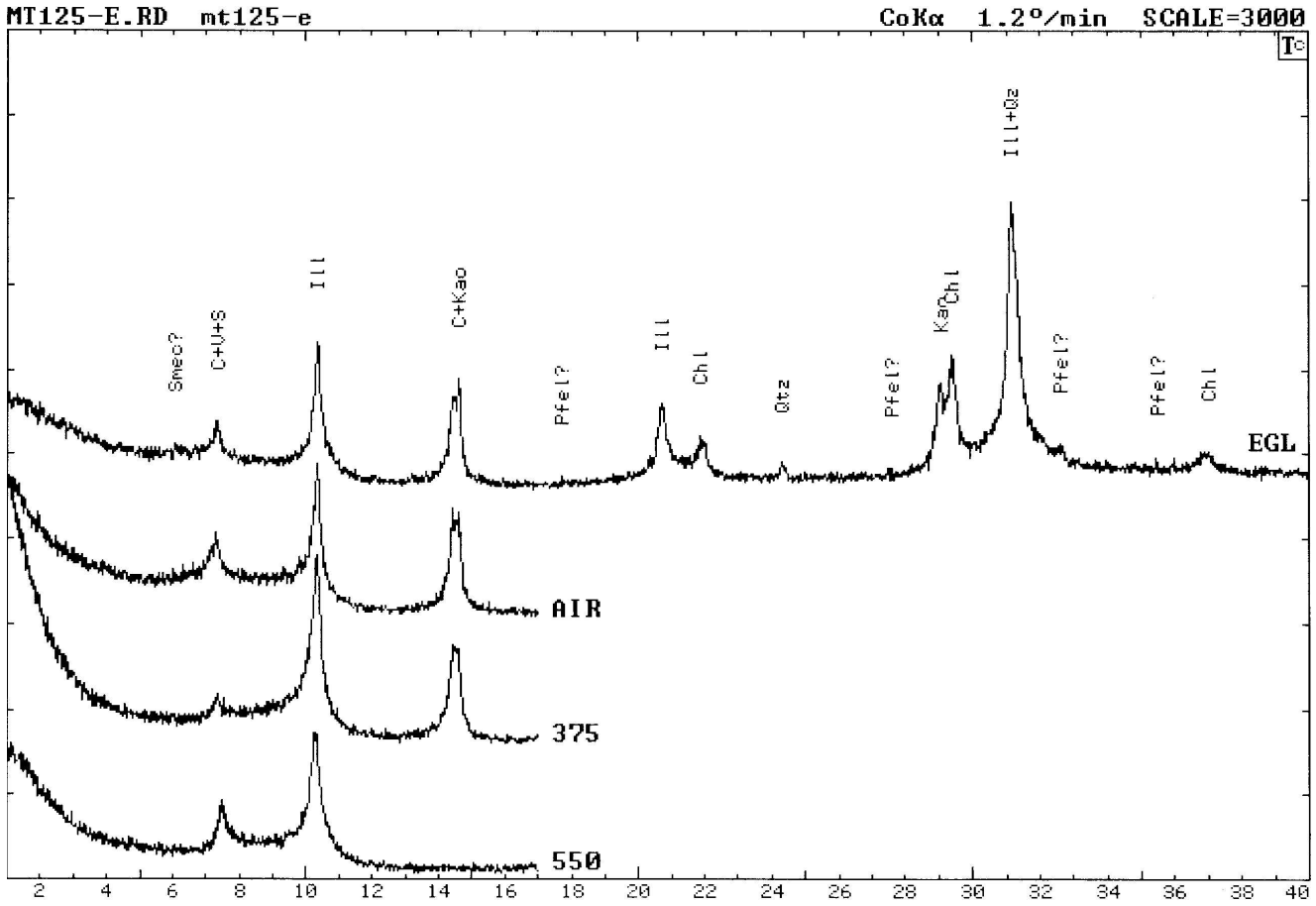

Figure 2.21: X-ray diffraction spectra of a separated clay (< 2 μm) fraction from the same sample as Figure 2.20, which was run 4 times: 1. glycolated with ethylene glycol (EGL); 2. air dried; 3. heated to 375 °C; and 4. heated to 550 °C.

Chapter 3

Spatial and temporal variability of tritium in intertidal surface sediments from the Severn estuary

3.1 Introduction

The Severn estuary, in southwest Britain (Figure 3.1), is a large, well-mixed, macro-tidal estuary. It is fringed by salt marshes and tide washed pastures, although the majority of these wetlands have been reclaimed since Roman times (Allen, 1988). Muddy, sandy and gravelly sediments are both circulated (Kirby, 1994) and deposited separately within the estuary (Allen, 1988; Allen, 1990; Kirby, 1994; Figure 3.1). Sand is transported as bed load and deposited on the channel floor, while fine sediment is transported in suspension and deposited on salt marshes, mud flats and in isolated patches on the channel floor, such as Bridgwater Bay and Newport Deep (Allen, 1988; Kirby and Parker, 1983). The estuary generally has a high suspended sediment load, although it is more turbid on the southern side, and a suspended sediment front is located parallel to the channel axis. This partitioning is produced by the tidally dominated rectilinear flow regime in the estuary, which results in little cross-channel flow (Dyer, 1984; Dyer, 1997; Parker and Kirby, 1982).

Tritium is discharged under licence into the Severn estuary as tritiated water (HTO) by the nuclear power stations at Hinkley Point, Berkeley and Oldbury, and as both tritiated water and organically bound tritium (OBT) by Amersham plc, a company based in Cardiff that produces radiolabelled compounds for life science research. This chapter examines the spatial distribution and temporal variation of tritium (specifically non-aqueous tritium) activity concentrations in sediments from the Severn estuary and identifies the secondary controls that may affect tritium activities in sediments.

3.2 Sampling

The temporal variation and spatial distribution of tritium in surface sediments was studied using three methods:

- A single large-scale survey of tritium activities at specific sites around the estuary (Figure 3.1), undertaken in May 2003.
- Monthly sediment samples from seven mud flat sites on the northern shore of the estuary, within 25 km of the Amersham plc discharge point (Figure 3.1), collected between February 2000 and May 2004.
- Sediment traps deployed at five sites for 6 months, to study tritium activities in sediment that had settled out of suspension.

From February 2000 to October 2001, the monthly sediment surveys were conducted by K. Doucette, Dr A.B. Cundy and Dr P.E. Warwick. From October 2001 samples were collected by J.E. Morris with the assistance of Dr F.M. Dyer, Dr P. Teasdale, L. Janes or J. Burnett.

Sampling sites Sampling sites were selected using the following criteria:

- Distance from the Amersham plc. discharge point.

- Presence of fine sediment
- Ease of access to the intertidal zone via roads and public rights of way.

Seven mud flat sites were selected on the northern shore of the Severn estuary, within 25 km of the discharge point (Figure 3.1; Table 3.1), for the monthly sampling programme. Fifteen other sites located further from the discharge point were also sampled to assess the spatial distribution of tritium on a larger scale.

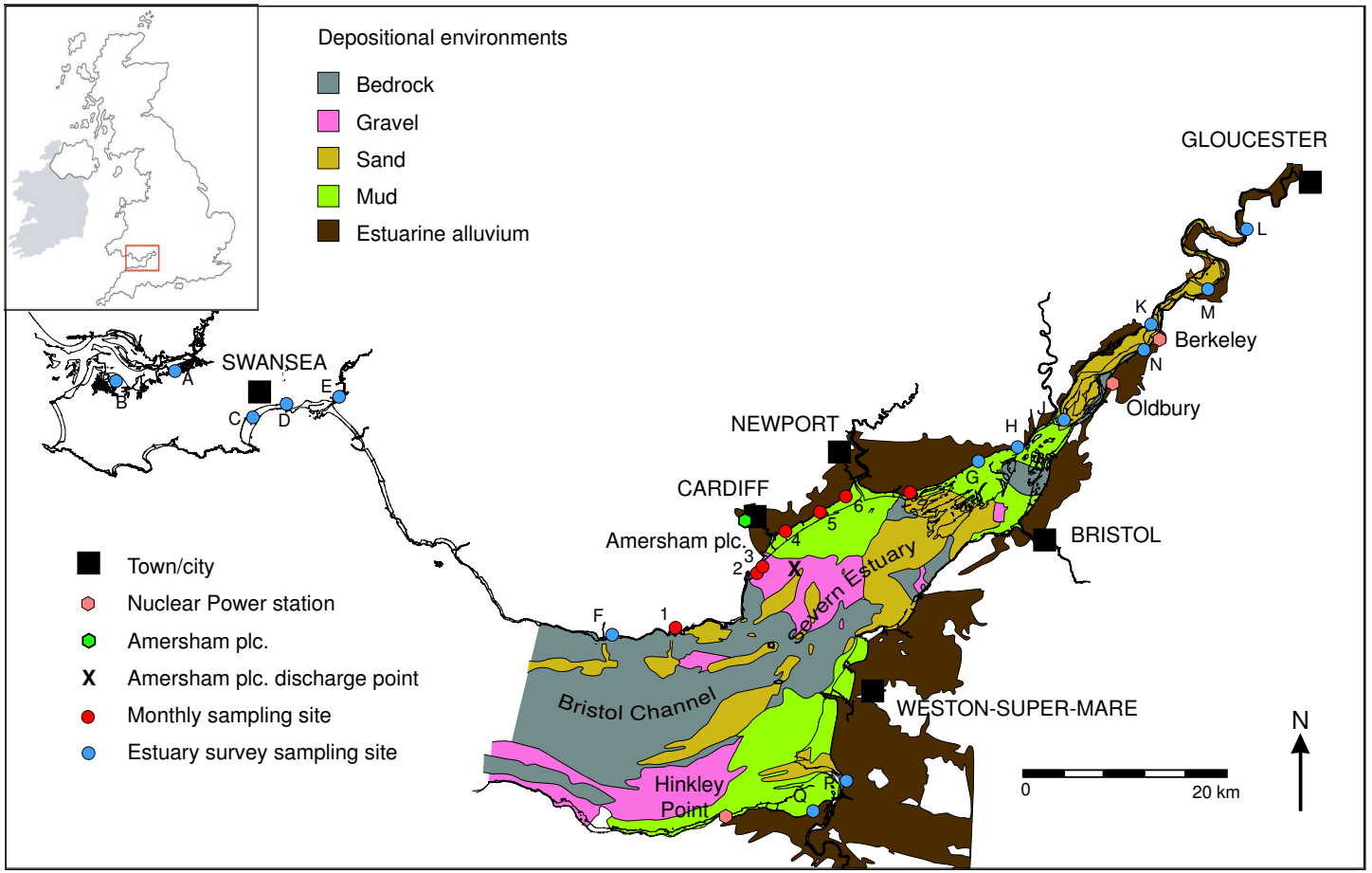

Figure 3.1: The location of sampling sites, sources of tritium and the distribution of estuarine depositional environments and alluvium (after Allen, 1988; 1990) in the Severn estuary. Inset: Location of the Severn estuary in SW Britain.

Table 3.1: Location and description of sampling sites

Site number	Site name	Grid reference	Number of times sampled	Site description	Sediment description	Special features
1	Barry Island	ST 10834 66525	36	Mud flat in small harbour. Patches of *Spartina* salt marsh (Fig. 3.2)	Surface to 2 cm: light brown oxic silty mud, 2 to 10 cm: dark grey anoxic sediment, sandy substrate	Near sewage outfall
2	Orchard Ledges SW	ST 20018 73418	35	At western end of 2.5 km of exposed beach (Fig. 3.2)	Gravelly sands containing particulate coal and anthropogenic debris, mud drapes in the lee of ripples	Within ABP Cardiff docks, regularly scoured of fine sediments by tidal currents or waves
3	Orchard Ledges NE	ST 20730 74177	34	At eastern end of 2.5 km of exposed beach (Fig. 3.2)	Surface to variable depth: semi-consolidated patches of muddy deposits. Sandy gravel substrate with boulders and large blocks of building debris	Within ABP Cardiff Docks, regularly scoured of fine sediments by tidal currents or waves
4	Maerdy Farm	ST 23170 77635	36	Mud flat overlying relict salt marsh in inlet (Fig. 3.2)	Light brown silty fluid mud layer of variable thickness overlaying light grey, well consolidated substrate	Scoured of fine sediments 5 times during sampling, probably by storms
5	Peterstone	ST 27016 79755	34	Mud flat on seaward edge of eroding *Spartina* salt marsh (Fig. 3.2)	Unconsolidated light brown silty mud of variable thickness overlying light grey, well consolidated substrate	Scoured of fine sediments 5 times during sampling, probably by storms
6	St Brides	ST 30083 81537	38	Mud flat in front of seawall	Silty mud layer of variable thickness, overlying an irregular substrate of gravelly sand, pebbles and boulders	Scoured of fine sediment 4 times during sampling, probably by storms
7	Goldcliff	ST 37504 82123	28	Mud flat in front of seawall	Silty mud layer of variable thickness overlying an irregular substrate of pebbles with some boulders	
A	Pen-clawdd	SS 53545 95961	2	Bank of small creek (Fig. 3.2)	Mud	
B	Llanrhidian Marsh	SS 47110 94546	1	Small creek that drains salt marsh	Surface: light brown oxic mud. Below 5 mm: dark grey anoxic mud	
C	Swansea West	SS 62210 90700	1	Eastern side of a stream on the beach (Fig. 3.2)	Thin veneer of fresh mud overlying a sandy substrate	
D	Swansea East	SS 65965 92215	1	100 m from marina steps (Fig. 3.2)	Thin veneer of fresh mud overlying a sandy substrate	

Site number	Site name	Grid reference	Number of times sampled	Site description	Sediment description	Special features
E	Neath	SS 72056 93104	1	Bank of muddy creek, surrounded by sand dunes (Fig. 3.2)	Mud overlying a sandy substrate	Opposite oil refinery
F	East Aberthaw	ST 30398 16595	2	Edge of eroding salt marsh, surrounded by sand dunes on the west side of an inlet. (Fig. 3.3)	Thin veneer of fresh mud overlying a sandy substrate	
G	Collister Pill	ST 45450 85670	2	Mud flat overlying relict salt marsh	Surface: unconsolidated light brown sediment. Irregular light grey consolidated substrate	
H	Sudbrook	ST 50156 87245	2	Beach (Fig. 3.3)	Unconsolidated fresh brown mud overlying a rocky substrate	
J	Beachley	ST 54965 90250	2	Mud flat on beach	Unconsolidated sediment overlying a shingle substrate	Under old Severn Bridge
K	Lydney	SO 64750 01215	1	Mud flat on rocks (Fig. 3.3)	Surface: unconsolidated light brown sediment. Substrate of consolidated dark brown mud and rocks	
L	Longney	SO 75491 12448	1	Muddy sand flats between reed beds and small stream (Fig. 3.3)	Thin layer of mud overlying a sandy substrate	
M	Slimbridge	SO 71450 05160	1	Phragmites and Spartina salt marsh, adjacent to mud flats at edge of estuary (Fig. 3.3)	Top 1 cm of core from *Spartina* marsh	Salt marsh sediment
N	Severn House Farm	ST 64342 98290	1	Mud flat in front of sea wall	Mud overlying a rocky substrate	
P	Burnham on Sea	ST 30135 48567	1	Beach	Muddy sand	
Q	Steart	ST 26460 45740	1	Beach in front of salt marsh (Fig. 3.3)	Consolidated mud overlying a sandy substrate	

Site 1 - Barry Island

Site 4 - Maerdy Farm

Site C - Swansea West

Site 2 - Orchard Ledges SW

Site 5 - Peterstone

Site D - Swansea East

Site 3 - Orchard Ledges NE

Site A - Pen-clawdd

Site E - Neath

Figure 3.2: Photographs of selected sampling sites.

Site F - East Aberthaw

Site K - Lydney

Site M - Slimbridge

Site H - Sudbrook

Site L - Longney

Site Q - Steart

Figure 3.3: Photographs of selected sampling sites (cont.).

Sampling methods Surface sediments were usually collected from an area of approximately 25 x 25 cm to a depth of between 0.5 and 2 cm (typically 1 cm), using a spade or a plastic dustpan. The resulting fresh sediment sample weighed ∼500 g. At some sites, samples obtained by this method tended to contain a mixture of sediment types, e.g. mud and sand. When a very thin veneer of mud overlay a sandy substrate, a similar volume of sample was sometimes collected over a larger surface area, to maximise the amount of mud collected. Occasionally samples could not be collected because high tides prevented access to sampling sites or scouring had removed the surface fine sediment layer.

Samples were homogenised, sub-sampled, and frozen at − 40 °C within 48 hours of collection. Cross-contamination was avoided by wrapping collected samples in a second sealed plastic bag and then freezing sub-samples in sealed plastic bags. When required for analysis, samples were thawed, homogenised and an aliquot of fresh sediment removed for analysis. About half of each sample (∼200 g) was freeze-dried for γ-spectrometry and X-ray fluorescence analysis.

Sediment traps were constructed from sections of plastic drainpipe (0.4 to 0.6 m in length) and inserted vertically into the sediment, leaving the top about 20 cm from the sediment surface, although this height varied over time as a result of mud flat mobility. A plastic bag was fixed inside the top of the drainpipe to collect sediment deposited vertically out of suspension, as the trap limited the effect of the lateral scouring of fine sediment. These traps were deployed at Sites 2, 4, 5, 6 and 7 for six months.

Analytical methods All samples were analysed for total tritium ($^3H_{total}$) and selected samples for exchangeable tritium ($^3H_{ext}$), using the methods described in Chapter 2. The $^3H_{total}$ and $^3H_{ext}$ data discussed in this chapter were collated from measurements predominantly made by J.E. Morris, but also by K. Doucette, Dr F.M. Dyer, Dr P. Teasdale and Dr J. Oh. All ^{3}H activities are reported in Bq/g dry weight. For compositional analysis, samples were selected from those collected from a range of sampling sites and dates, in addition to their sediment composition (from visual inspection). These samples were freeze-dried and analysed for:

- Elemental composition using X-ray fluorescence (XRF) analysis.
- Mineralogical composition using X-ray (XRD) diffractometry.
- Gamma-emitting radionuclides using γ-spectrometry.
- Total organic carbon (TOC) using coulometry.
- Elemental carbon content using an aqua regia and HF acid digestion.

These methods are described in Chapter 2. Analytical support was provided by Dr I.W. Croudace, R. Williams, Dr F.M. Dyer, D. Green and Dr P.E. Warwick.

3.3 Results

3.3.1 Spatial distribution of ^{3}H in surface sediments from the Severn estuary

The highest $^3H_{total}$ activities in the whole estuary survey were measured in sediments from the northern coast between Cardiff and Newport (Sites 2 to 7; Figure 3.4). The maximum activity was measured at Site 4, the closest sampling site to the Amersham plc discharge point. At more distant sites, activities decrease to <0.15 Bq/g; this includes sites located close to Berkeley, Oldbury and Hinkley Point nuclear power stations.

Activities vary in the monthly sampling surveys, so no site has consistently higher $^3H_{total}$ activities (Figure 3.5). In general, however, the highest sediment $^3H_{total}$ activities were present at Site 4 and the lowest at Site 2. There is an asymmetric bell-shaped spatial distribution of average $^3H_{total}$ activities around the peak at Site 4, with lower average $^3H_{total}$ activities at Sites 1 and 2 than at Sites 6 and 7.

Ninety samples, selected from a range of sites throughout the sampling period, were measured for water-extractable tritium ($^3H_{ext}$), however, measured activities for all samples were $\leq$0.12 Bq/g dry weight equivalent (the limit of detection is $\sim$ 0.02 Bq/g dry weight), indicating that over 90 % of the $^3H_{total}$ activity measured in sediments is not water-extractable, and may therefore be present as non-aqueous tritium or NAT. However, some problems were identified with this method (Section 2.2.2), so further work is required to confirm this.

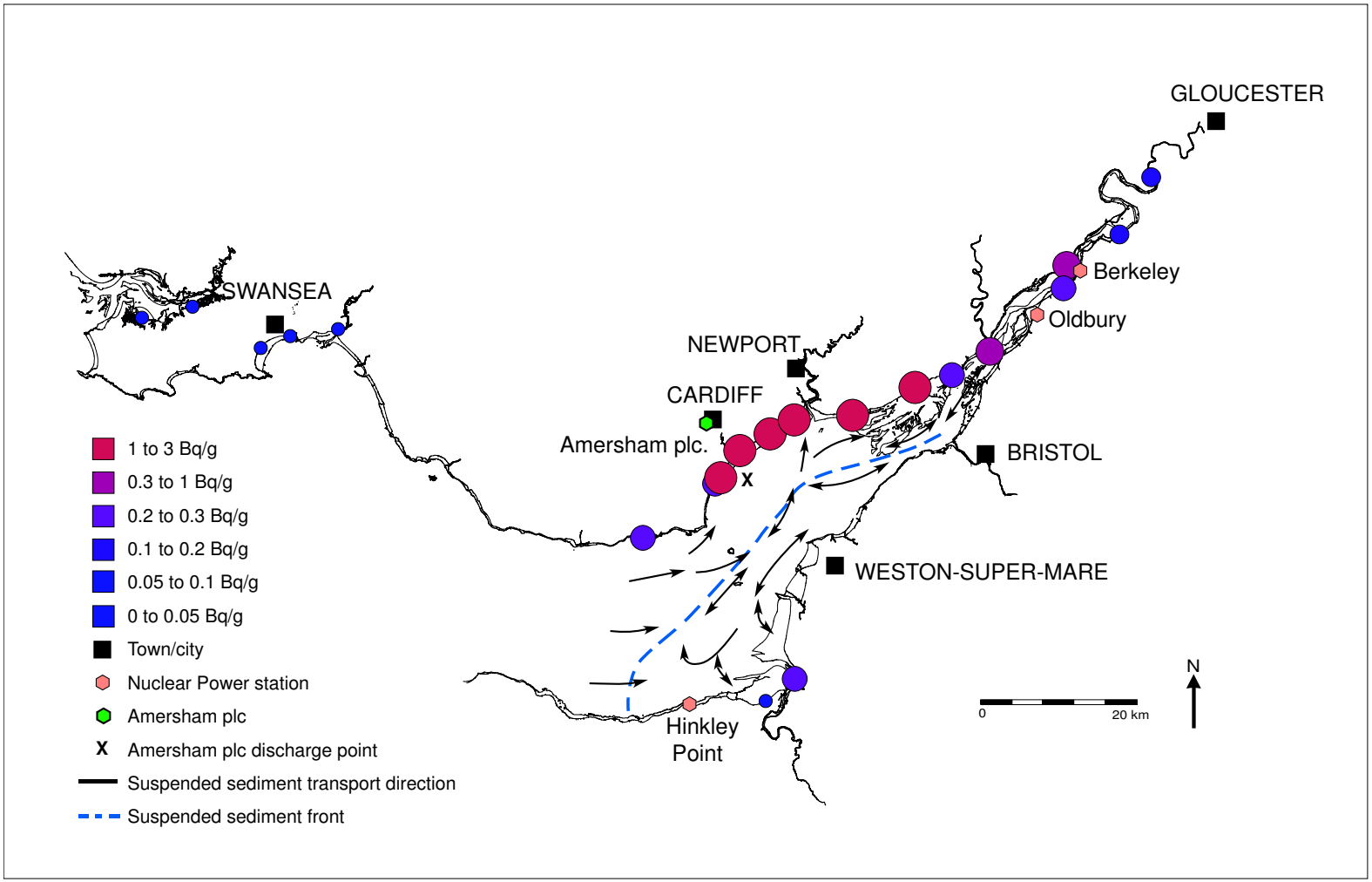

Figure 3.4: $^{3}H_{total}$ activities (Bq/g dry weight) in surface sediments collected in March 2003 (except from sites M (July 2003) and P (November 2001)), compared with a suspended sediment transport model for the Severn estuary (from Parker and Kirby, 1982). The sources of tritium discharges into the Severn estuary are also shown.

3.3.2 Temporal variation of ^{3}H in surface sediments from the Severn estuary

There is a general decline in $^3H_{total}$ activities at all of the sampling sites over the period from February 2000 to May 2004; two discrete downward steps are apparent in February 2002 and mid 2003 (Figure 3.6). Although activities do vary over time, peaks are not well correlated between the sampling sites.

3.3.3 Grain size

Sediments from all sites are composed of a mixture of mud and sand sized grains. The coarsest sediment is present at Site 2; two replicates contain 93 % and 98 % of the >250 μm (coarse sand and gravel) fraction, respectively (Figure 3.7). Sediment from Sites 1 and 5 have comparable grain size distributions, while the proportion of clays and silts (<63 μm fraction) in the sediment increases eastwards from Sites 5 to 7.

The $^3H_{total}$ activity of each grain size fraction was determined for a different sample from Site 2, where the dominant >250 μm fraction contains only 36 % of the total activity (Table 3.2). More activity was measured in the finer fractions that together comprise just 8 % of the sediment, indicating that the ^{3}H activity is preferentially, but not exclusively, associated with the fine sediment fraction.

Table 3.2: Proportion of of $^3H_{total}$ activity associated with each grain size fraction for a bulk surface sediment sample from Site 2, collected in August 2001.

Grain size fraction (μm)	**Sediment fraction**	**Proportion of sediment (%)**	**$^3H_{total}$ activity (%)**
<63	Clay and silt	2.1	42
63 - 125	Fine sand	0.2	5
125 - 250	Medium sand	5.5	17
>250	Coarse sand and gravel	92.1	36

3.3.4 Mineralogical composition

The mineralogy of bulk powdered sediments and clay separates were determined by non-quantitative X-ray diffraction (XRD) analysis. Quartz, calcite, plagioclase and potassium feldspars and clay minerals are present in samples from all of the sites (Table 3.3), and dolomite was identified in samples from Sites 1 to 5. These minerals reflect the composition of source rocks, soils and sediments in the Severn estuary catchment (Hamilton *et al*, 1979). Halite is present in samples from Sites 1, 3, 4, 5 and 6 due to the entrainment of seawater. Magnetite is only detected in sediments from Site 3 and pyrite is possibly present in sediments from Site 4. These dense minerals would not have been transported far from their respective sources, which may be anthropogenic, such as spilt ballast or ore cargoes from the dockyards or waste from the steel works (now disused) in Cardiff.

The clay fraction (<2 μm) was separated from the bulk sediment and analysed separately in order to identify the clay minerals. The proportions of clay minerals are similar

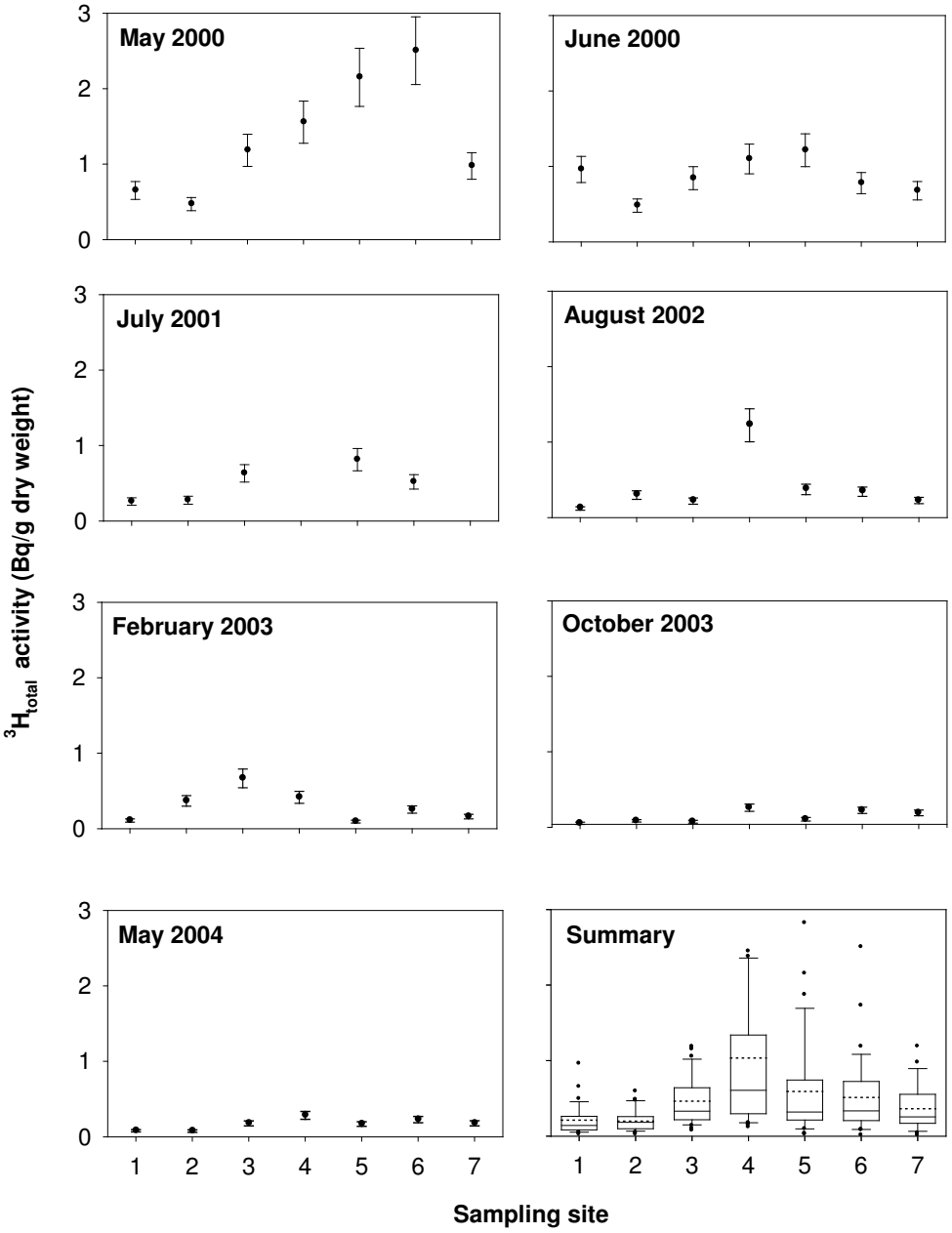

Figure 3.5: $^3H_{total}$ activities (Bq/g dry weight) for selected representative months from the monthly sampling of surface sediments from 7 sites in the Severn estuary, with a summary of $^3H_{total}$ activities measured at each site from February 2000 to May 2004. The mean $^3H_{total}$ activity is shown as a dotted line and the median as a solid line, while the box encloses the 25th to 75th percentiles of the data and the lines show the 5th and 95th percentiles. Outliers are represented by black circles, although two outliers measured at Site 4 could not be included on this scale. Data were compiled from measurements performed by J.E. Morris, K. Doucette, Dr F.M. Dyer, Dr P. Teasdale and Dr J. Oh.

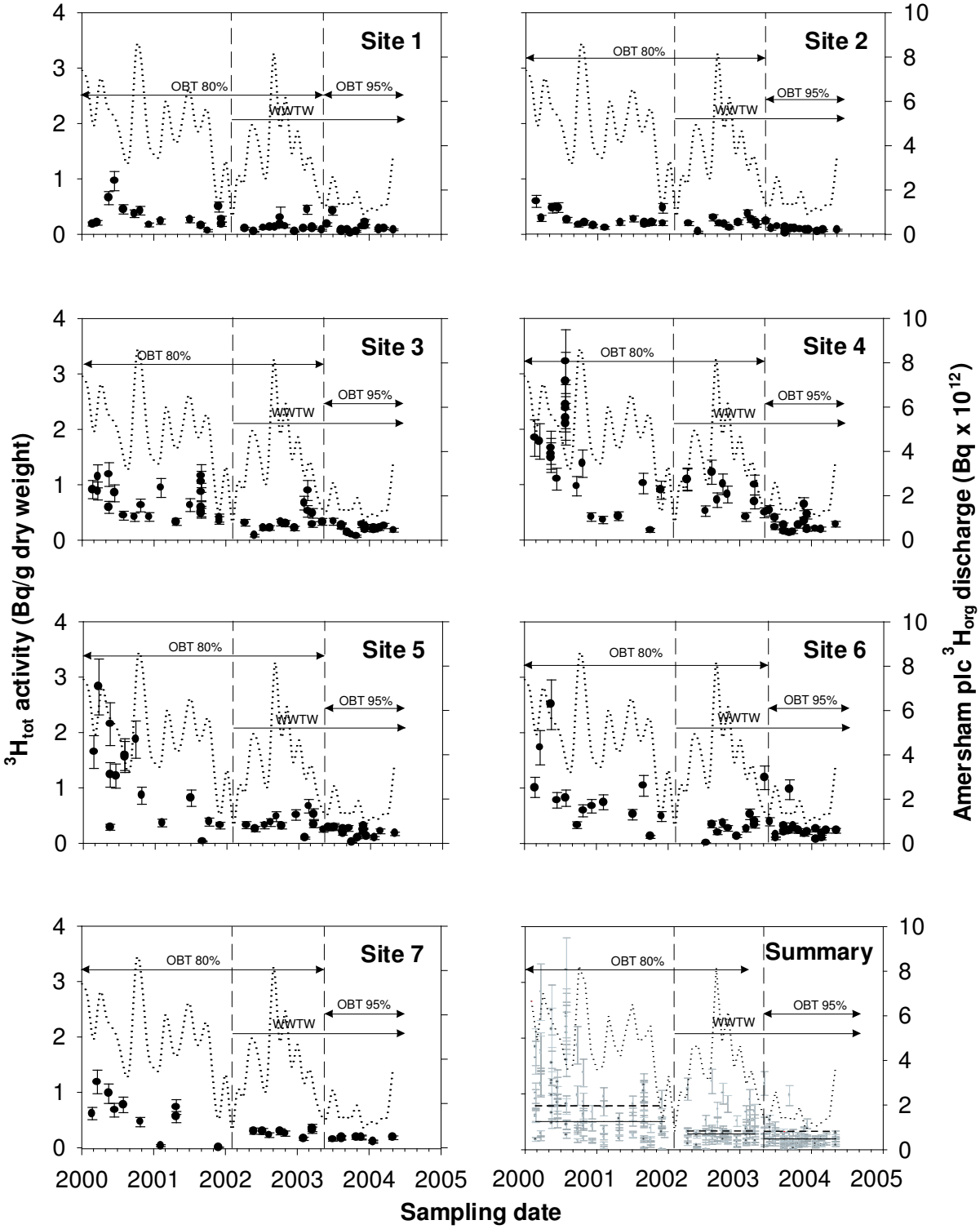

Figure 3.6: Temporal variation of $^3H_{total}$ activities in sediments from 7 sites in the Severn estuary, compared with changes in the magnitude, treatment and composition of organic ^3H discharges from Amersham plc. Sediment $^3H_{total}$ activities are represented by black circles and the magnitude of organic ^3H discharges from Amersham plc (from Williams, 2003; 2004; 2005) is shown as a dotted line. The introduction of a waste water treatment works (WWTW) and the change in composition of total ^3H discharges from 80 % OBT to 95 % OBT are indicated by vertical dashed lines. In summary, the mean (thick dashed horizontal line) and median (thin solid horizontal line) activities are plotted for the data set. Data are compiled from measurements performed by J.E. Morris, K. Doucette, Dr F.M. Dyer, Dr P. Teasdale and Dr J. Oh.

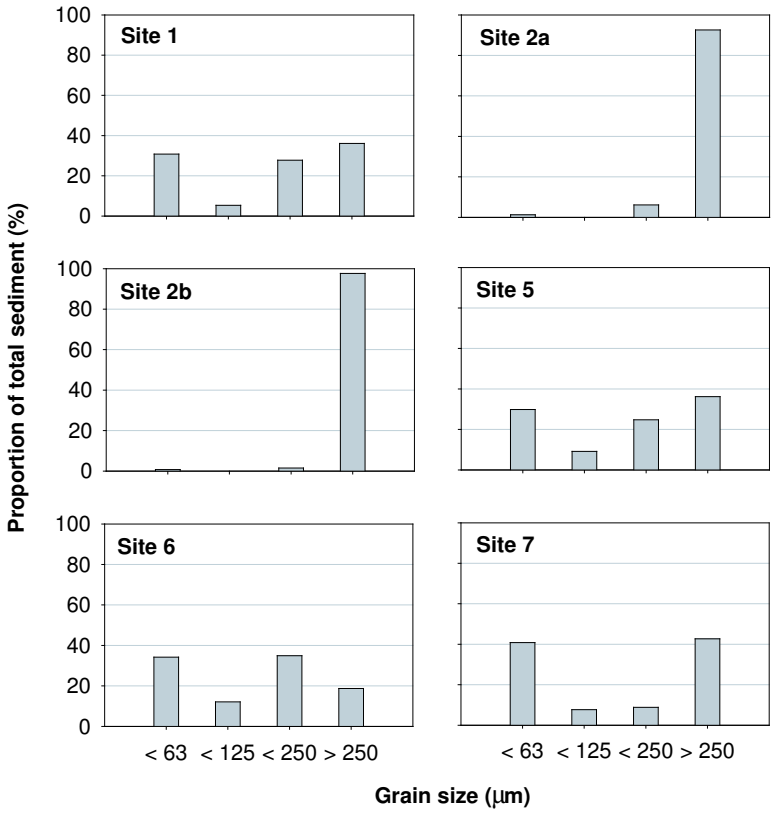

Figure 3.7: Proportion of total sediment in each grain size fraction for bulk surface sediments collected from Sites 1, 2 (duplicate samples), 5, 6 and 7 in August 2003.

in sediments from Sites 1 to 6 (Figure 3.8). Illite comprises 50 to 54 % of the clay fraction, chlorite and kaolinite 16 to 18 %, and expanding clays, such as smectite and vermiculite, make up 28 to 33 %.

Table 3.3: Mineralogy of bulk powdered sediments measured by XRD analysis.

Sampling site	Date sampled	Mineralogy of bulk powders (P - present, U - undecided, A - absent)											
		Qtz	Cal	Dol	Plag	K-fel	Hal	Mag	Pyr	Chl	Ill	Kaol	Smec
1	29/11/01	P	P	P	P	P	P	A	A	U	U	A	A
2	29/11/01	P	P	P	P	P	A	A	A	U	U	A	A
3	17/05/00	P	P	U	P	P	P	P	A	U	U	A	A
3	08/12/00	P	P	A	P	P	A	P	A	P	U	A	A
3	30/08/01	P	P	P	P	A	P	A	A	U	U	A	A
3	21/02/03	P	P	P	P	P	P	A	A	U	U	A	A
4	31/07/00	P	P	P	P	P	P	A	U	P	U	A	A
4	26/04/01	P	P	A	P	P	P	A	A	U	U	A	A
4	29/11/01	P	P	A	P	P	P	A	U	U	U	U	A
5	25/09/00	P	P	U	P	P	P	A	A	U	U	A	A
5	06/02/01	P	P	P	P	U	A	A	A	U	U	A	U
6	03/10/01	P	P	A	P	P	P	A	A	U	U	A	A

Qtz - Quartz, K-fel - Potassium feldspar, Chl - Chlorite, Cal - Calcite, Hal - Halite, Ill - Illite, Dol - Dolomite, Mag - Magnetite, Kaol - Kaolinite, Plag - Plagioclase feldspar, Pyr - Pyrite, Smec - Smectite

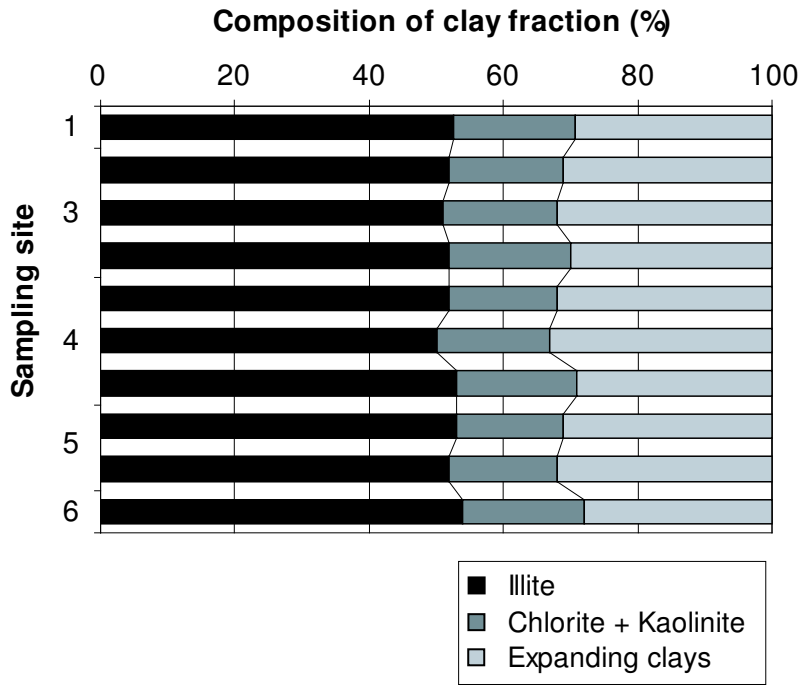

Figure 3.8: The composition of the separated clay fraction from surface sediments collected from Sites 1 to 6, analysed using X-ray diffraction. Insufficient clay was obtained from a sample from Site 2 for successful analysis.

3.3.5 Elemental composition

X-ray fluorescence (XRF) analysis was used to determine the elemental composition of 100 surface sediment samples. The concentrations of Si, Ca, Al, S, Pb and Zn are enriched in the surface sediments relative to the element/Rb ratio of the standard shale, because the sediments contain quartz sands, calcite and feldspars in addition to the clay minerals that comprise the standard shale (Turekian and Wederpohl, 1961; Figure 3.9). Sediments from different sites have contrasting compositions; at Sites 2 and 3 sediments are more enriched in Cu, Ni, Al, Fe and S than the standard shale or other sites, indicating that these sediments are influenced by anthropogenic metal inputs. Spatial and temporal variation of the proportion of clay minerals in sediments may also affect sediment ^{3}H concentrations.

Fine sediment indicators

Rb, Al, Fe and K have been used in other studies of estuarine sediments as proxies for fine sediment (e.g. Allen and Rae, 1986; Zwolsman *et al*, 1993). Although iron oxides occur naturally in clay rich sediments, Fe is enriched relative to the standard shale at Sites 2 and 3 (Figure 3.9) and magnetite is also detected in sediments from Site 3 (Table 3.3), indicating that Fe concentrations are anthropogenically influenced. Al is an essential constituent of clays and feldspars but Al concentrations are also enriched by anthropogenic activities, such as steelworks, dockyards and other industry in the vicinity of Sites 2 and

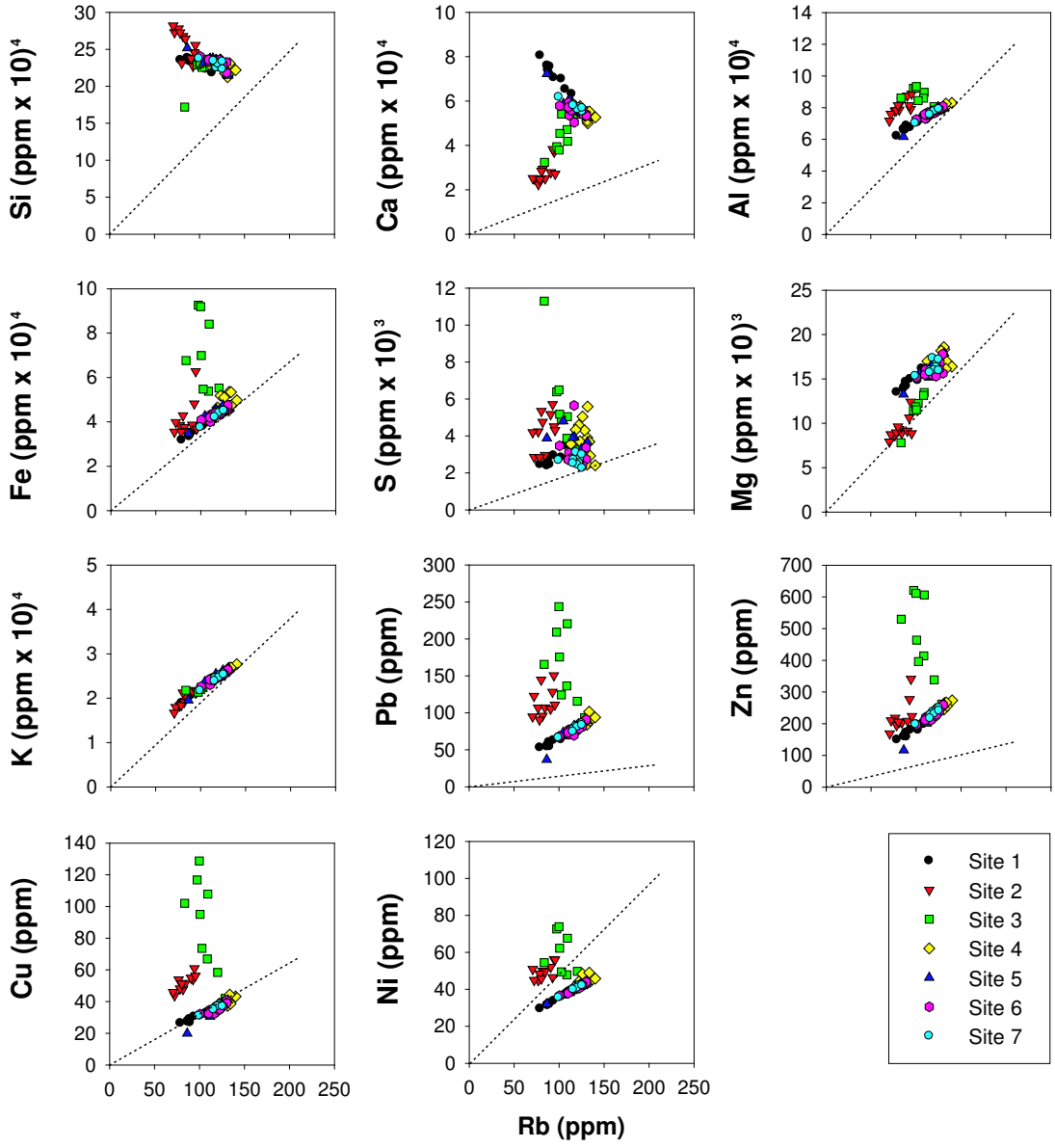

Figure 3.9: Correlation between selected element concentrations and Rb for surface sediments from 7 sites in the Severn estuary. These are compared to the Element/Rb ratio of the standard shale (Turekian and Wederpohl, 1961), represented by a dotted line.

3 (Figure 3.9). K is a constituent of both clays and potassium feldspar, and correlates well with Rb and the standard shale (Figure 3.9), indicating that neither element is anthropogenically influenced. Rb is also a constituent of clays and has low concentrations in sandy sediments (32 ppm, Hamilton *et al*, 1979). Reliable measurements of Rb can be obtained by XRF analysis. Allen (1987) found a strong linear correlation between the proportion of sediment with a grain size <10 μm and Rb concentrations in Severn estuary sediments, indicating that it was a dependable grain size proxy, therefore it has been used in the present study. Rb concentrations do not vary significantly across the sites (Figure 3.10). They varied over time at Sites 2 and 3 but were relatively constant at the other five sites (Figure 3.11).

Although analysis of separate grain size fractions shows that a disproportionate amount of sediment $^3H_{total}$ activity is associated with the clay and silt fractions (Table 3.2), Rb and K do not correlate well with sediment $^3H_{total}$ activities (Figure 3.12). The magnitude of OBT inputs has varied with time independently of the sediment composition; however, because significant activity remains associated with the coarser sediment fractions, tritium may also be associated with another component of the sediments, such as organic matter.

Carbonate indicators

CaO concentrations can be used to indicate variations in carbonate content of the sediments. The highest CaO concentrations were generally found in sediments from Site 1 and the lowest from Site 2 (Figure 3.13), with steady concentrations at Sites 4 to 7. The trace element Sr also associates with carbonates, however Sr concentrations were relatively uniform at all sites except Site 2. It is likely that the proportion of shells and shell fragments observed in the sediments at Site 2 varied over time, producing erratic Sr and CaO concentrations. However, Sr and CaO concentrations do not tend to co-vary with time (Figure 3.14).

Trace metals

The highest Cu, Pb and Zn concentrations were found at Site 3 (Figure 3.15). The concentrations of these elements decrease westwards from this peak towards Site 1, and remain relatively constant across Sites 5, 6 and 7. Ni and Sn concentrations were generally constant at all sites, while Cu, Pb and Zn concentrations are more variable at Sites 2, 3 and 5; the trace metals co-varied over time (Figure 3.16). The trace metals Pb and Zn were enriched at all sites with respect to the standard shale; this indicates that their inputs are either widespread or well mixed, possibly from a natural source such as the Carboniferous Pb-Zn mineralisation associated with the large South Wales coal field (Allen and Rae, 1986; Allen, 1987a), or anthropogenic inputs (Hamilton *et al*, 1979). There are strong correlations between Rb and Pb, Zn, Ni and Cu concentrations (Figure 3.9), indicating that trace metals are predominantly associated with finer grained sediments. However, at Sites 2 and 3 it is likely that local inputs of anthropogenic debris produced the poor

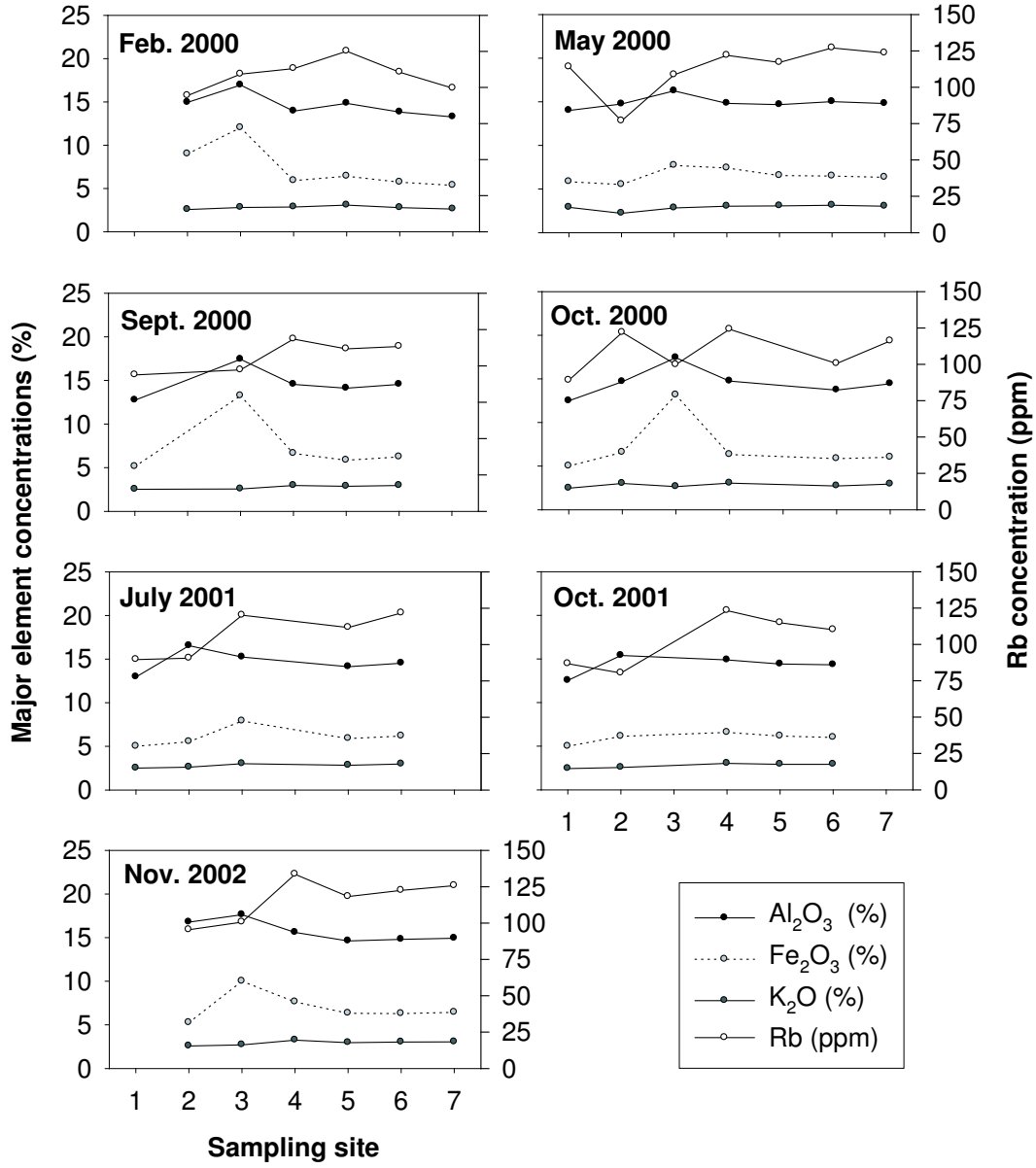

Figure 3.10: Spatial variation in the concentrations of potential proxies for fine sediment content (Al_2O_3, Fe_2O_3, K_2O and Rb) for selected months at 7 sites in the Severn estuary.

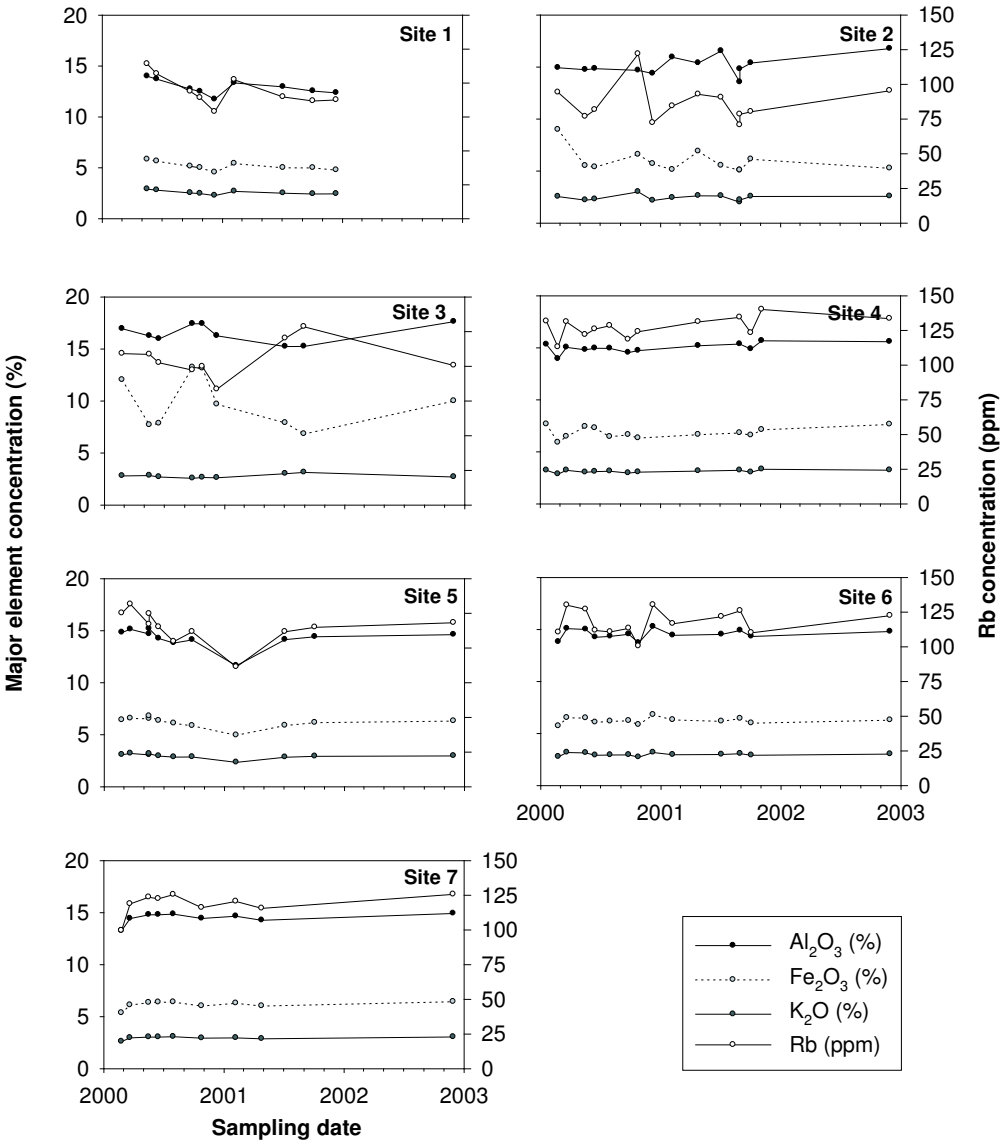

Figure 3.11: Temporal variation in the concentrations of four potential proxies for fine sediment content (Al_2O_3, Fe_2O_3, K_2O and Rb) at 7 sites in the Severn estuary.

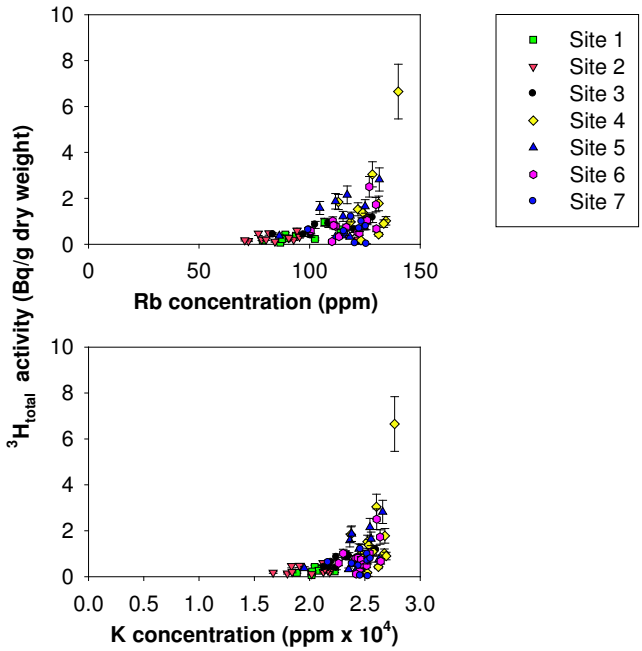

Figure 3.12: Correlation between Rb and K concentrations, measured by XRF analysis, and sediment $^3H_{total}$ activities for surface sediments at 7 sites in the Severn estuary.

correlations with Rb, and the observed enrichment in Cu and Ni concentrations.

Organic, inorganic and elemental carbon

The total organic carbon (TOC) content (calculated by subtracting inorganic carbon from total carbon) of the sediments range from 0.3 to 6 %, apart from one anomalous sample from Site 3 which contains 18 % organic carbon (Figure 3.17).

Particulate coal is ubiquitous in Severn estuary sediments (Allen, 1987a). The elemental carbon contents of ten samples (nine core sediments from Site 5 and one surface sample from Site 3), determined by mass difference after aqua regia and HF acid digestion, vary from 4 to 22 % (Appendix 3). The highest coal content was found in the surface sediment sample from Site 3, probably because this site is more anthropogenically influenced than Site 5.

The TOC fraction includes elemental carbon, vegetation and algae, benthic organisms, detritus (decomposing plant or animal matter) and particulate organic matter. Allen and Rae (1986) measured a TOC content of 2 % in surface sediments from a salt marsh in the Severn estuary, however their method (from Gaudette, 1976) did not include particulate coal, which could account for the higher values obtained in the present study. The observed variability of TOC in the sediments may be produced by natural variation in any of the components listed above. There is no correlation between TOC content and Rb concentration, which implies that the organic fraction associates with a range of particle size fractions.

The inorganic carbon (IC) content of the sediments ranges from 0.5 to 1.8 %; it did not

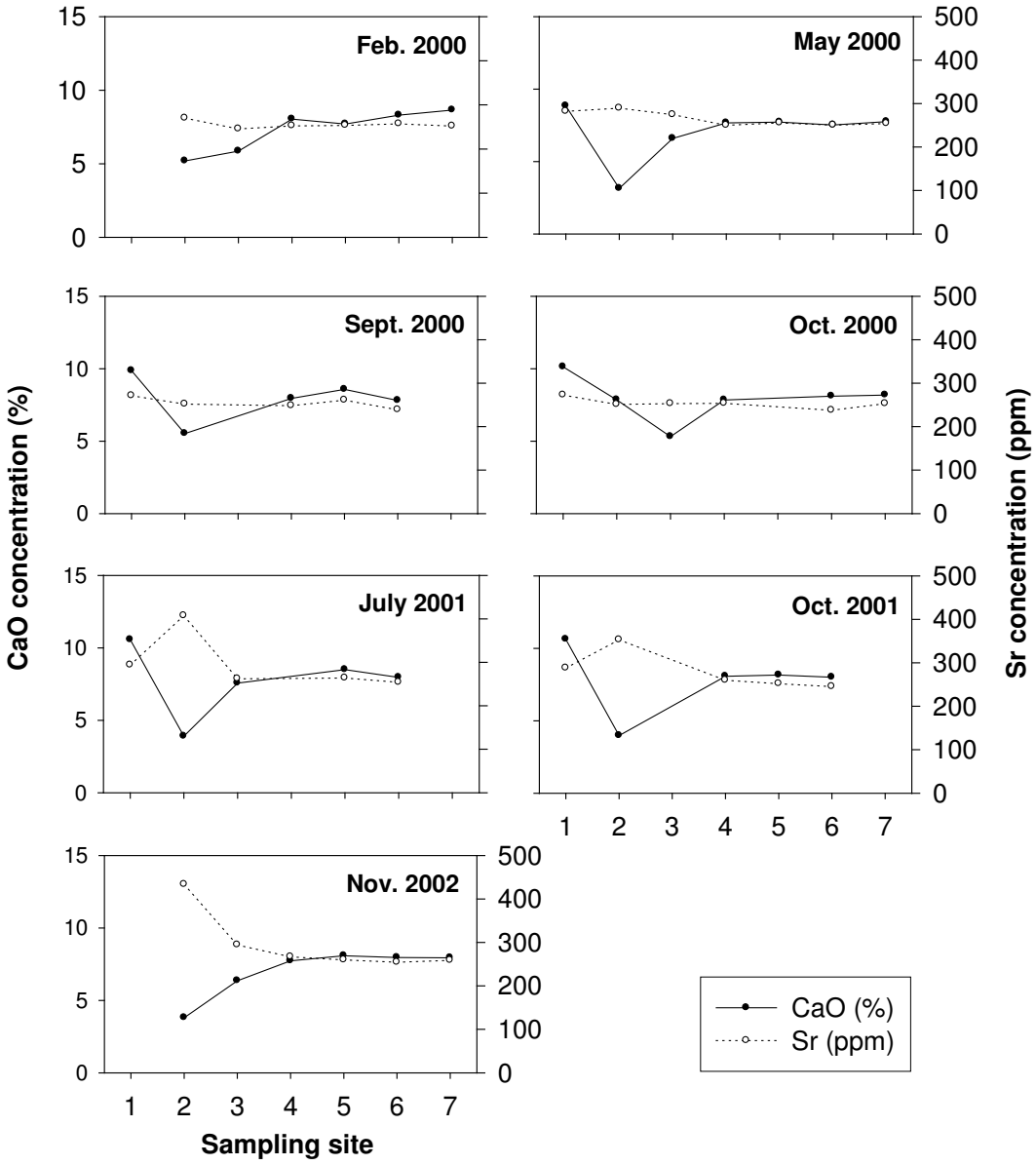

Figure 3.13: Spatial variation of CaO and Sr concentrations in surface sediments at 7 sites in the Severn estuary for selected months, measured by X-ray fluorescence analysis.

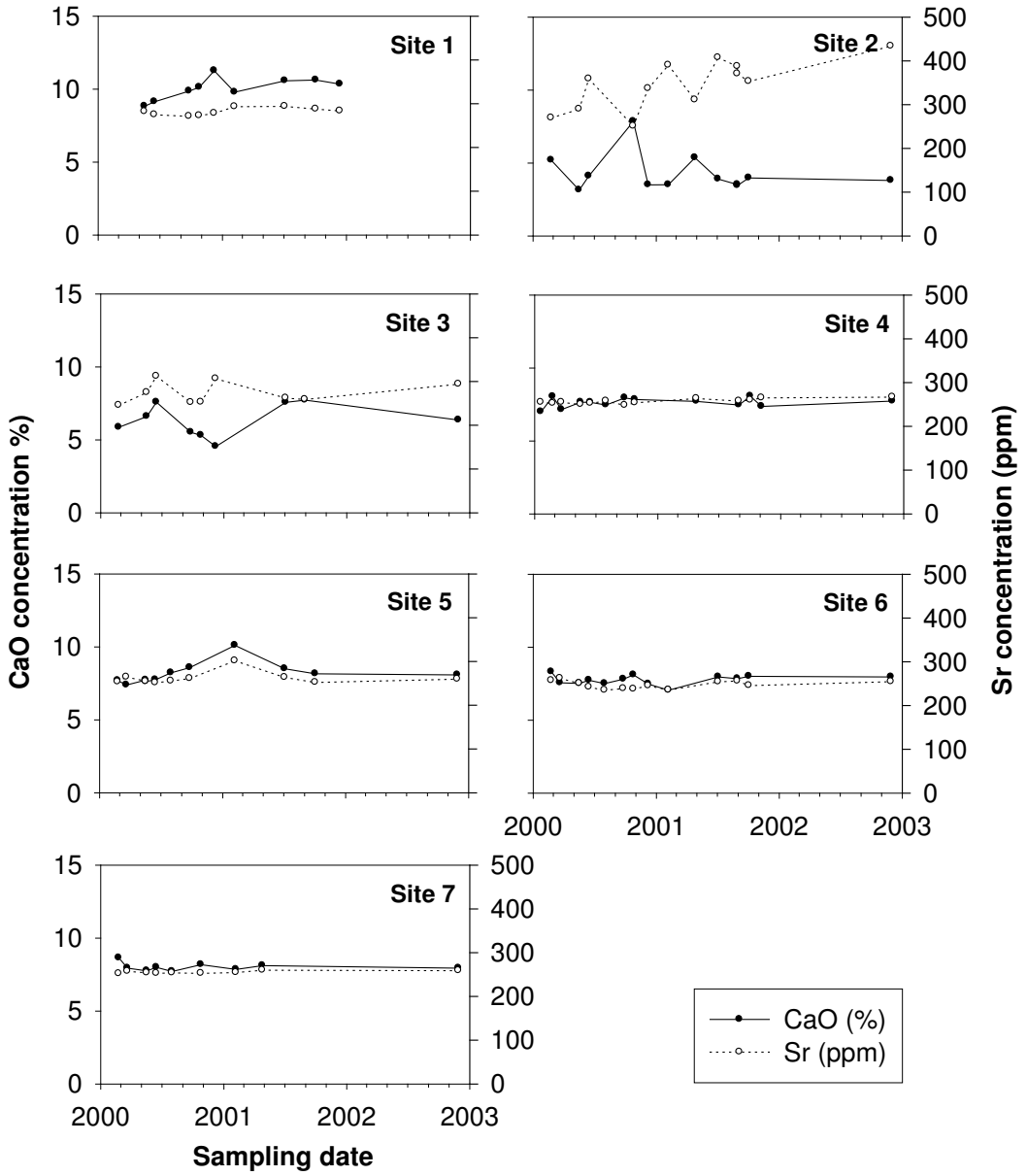

Figure 3.14: Temporal variation of CaO and Sr concentrations in surface sediments at 7 sites in the Severn estuary, measured by X-ray fluorescence analysis.

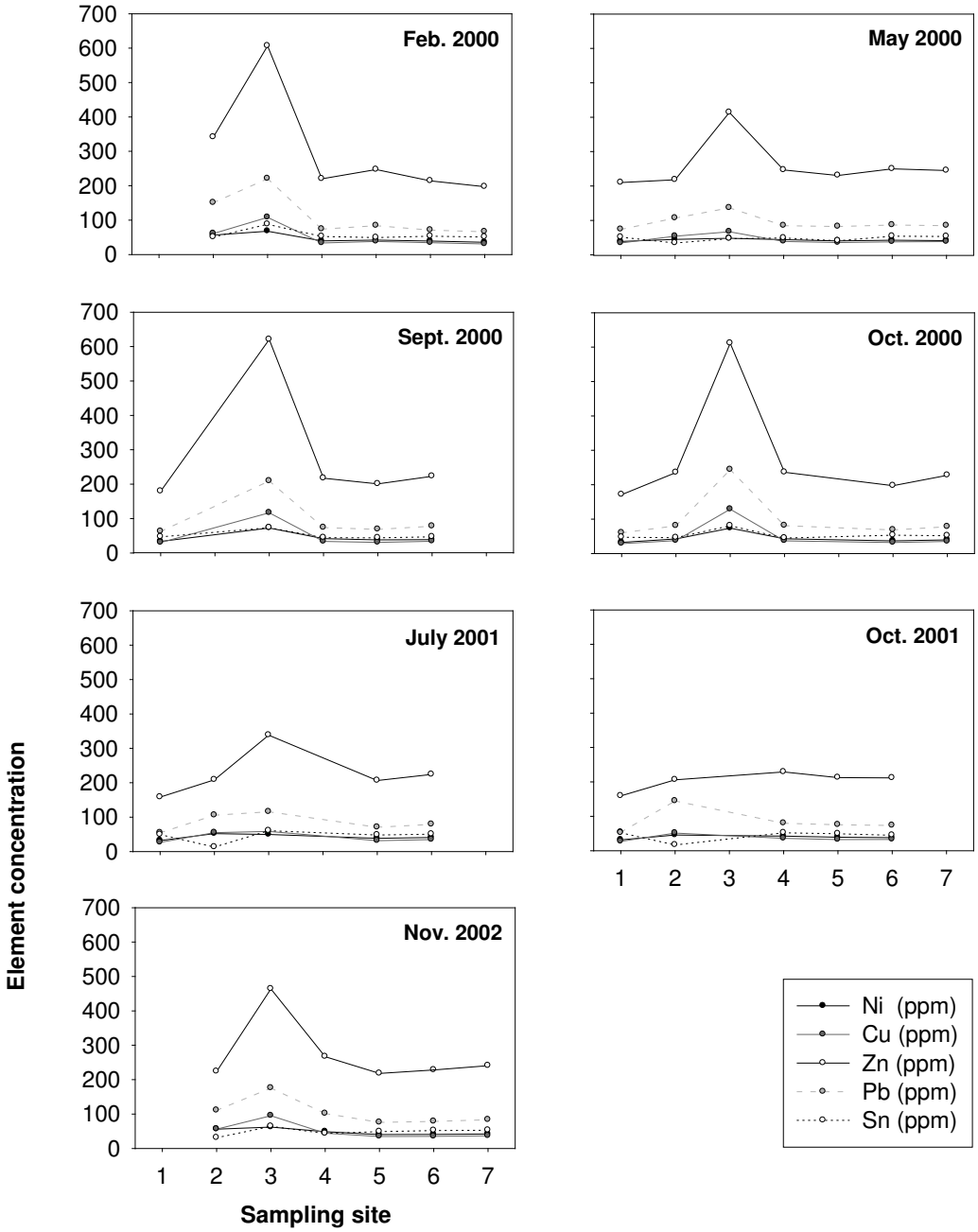

Figure 3.15: Spatial variation of trace metal concentrations (Ni, Cu, Zn, Pb and Sn) in surface sediments at 7 sites in the Severn estuary for selected months, measured by X-ray fluorescence analysis.

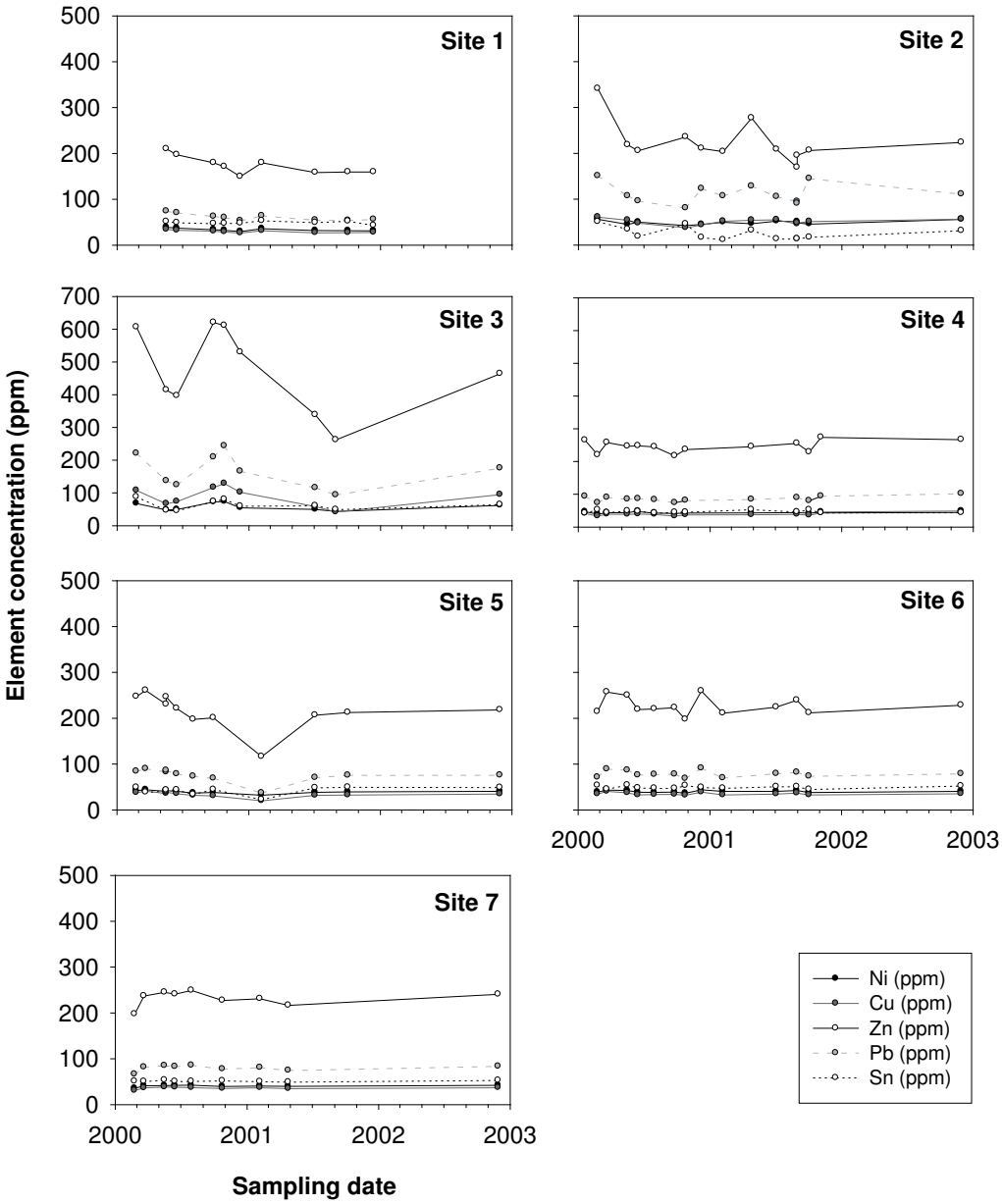

Figure 3.16: Temporal variation of trace metal concentrations (Ni, Cu, Zn, Pb and Sn) in surface sediments at 7 sites in the Severn estuary, measured by X-ray fluorescence analysis.

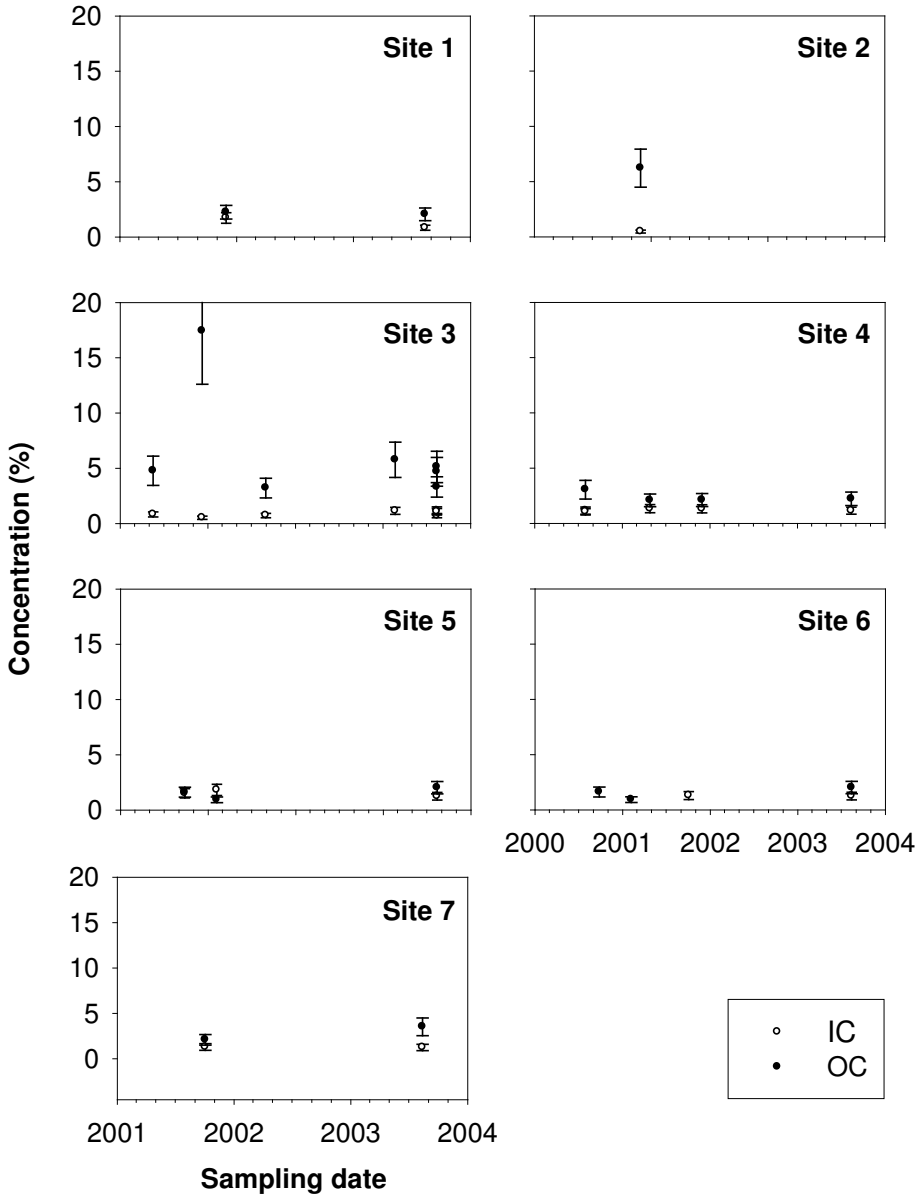

Figure 3.17: Total organic (TOC) and inorganic (IC) carbon contents of surface sediments at 7 sites in the Severn estuary.

vary over time, but correlated well with Ca concentrations. This indicates that most of the Ca in the sediment is present in carbonates (Figure 3.18), although in contrast there was a weaker correlation between IC and Sr. Carboniferous limestones are common in the Severn estuary catchment (Langston *et al*, 2003) and were observed in sediments using optical microscopy by Hamilton *et al* (1979). Shells and shell fragments are also observed in surface sediments collected from Site 2 and salt marsh sediments from Site 5 (Appendix 1). It is therefore likely that limestones and shells are both sources of carbonates to the sediments.

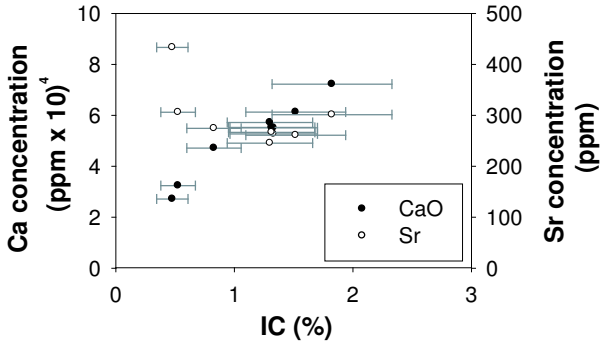

Figure 3.18: Correlation between inorganic carbon content (IC), measured by coulometry, and Ca/Sr concentrations, measured by XRF analysis.

Sediment trap study

Tritium activity There are no consistent trends between the $^3H_{total}$ activities of sediment trap and surface sediment samples (Figure 3.19). At Site 2 the sediment trap sediments had higher $^3H_{total}$ activities, whereas at Sites 4, 5, 6 and 7 they had lower $^3H_{total}$ activities on at least two occasions. However, due to the higher water content of sediment trap samples compared to surface scrapes, they may have been more vulnerable to leakage when repeatedly frozen and defrosted, altering the wet/dry ratio of the samples between replicate analyses and leading to incompatible results.

Elemental composition Sediment trap samples collected in February 2004 (Site 7 was collected in January 2004), were analysed for elemental composition using XRF. Concentrations of Al_2O_3, Fe_2O_3, K_2O, CaO and Sr remain relatively constant across the sampling sites, apart from a slight decrease in concentrations at Site 6 (Figure 3.20). Rb concentrations are highest at Site 4 and lowest at Site 6.

The elemental composition of sediment trap and surface sediment samples was compared at each site (Figure 3.21). At Sites 2 and 7 sediment trap samples have higher Rb concentrations and are therefore finer grained. However, at Sites 4, 5 and 6 the sediment trap samples have lower Rb concentrations and are coarser grained than the surface sediments. This variability does not explain the differences in $^3H_{total}$ activity between sediment trap and surface sediment samples at all of the sites (Figure 3.20).

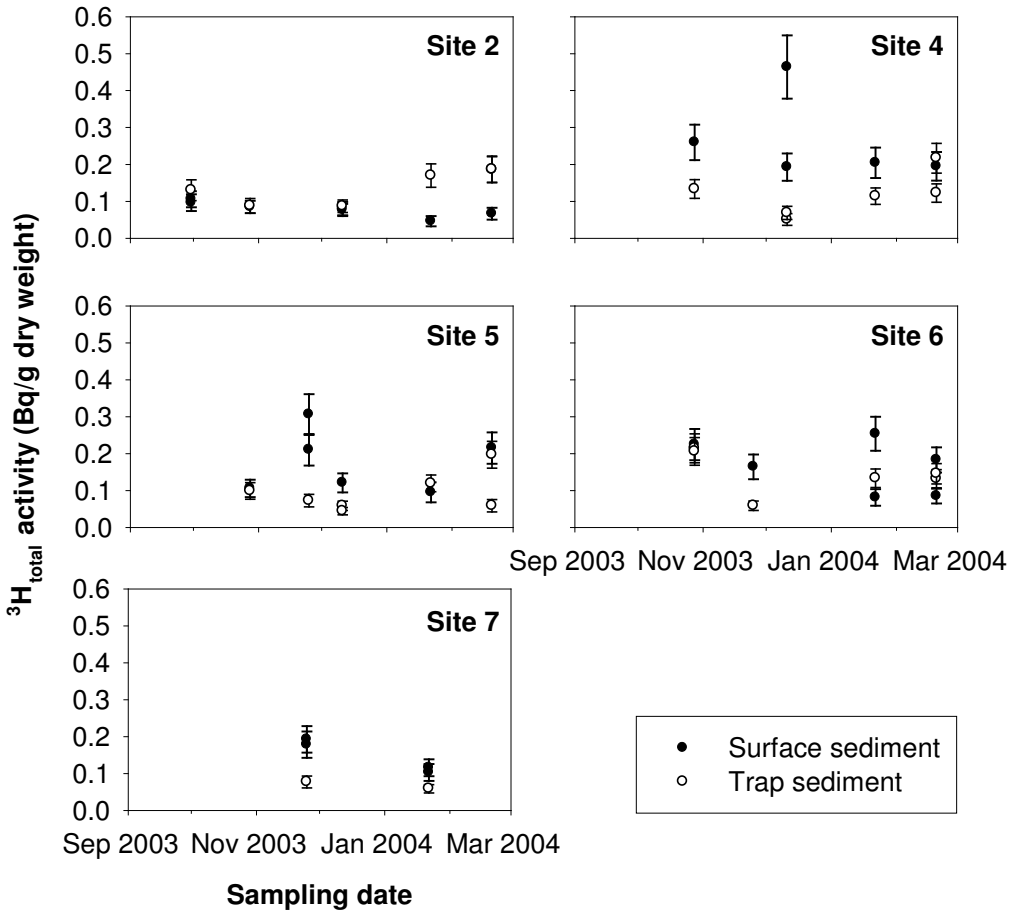

Figure 3.19: Comparison between $^3H_{total}$ activities from sediment trap and surface sediment samples collected simultaneously from 5 sites in the Severn estuary.

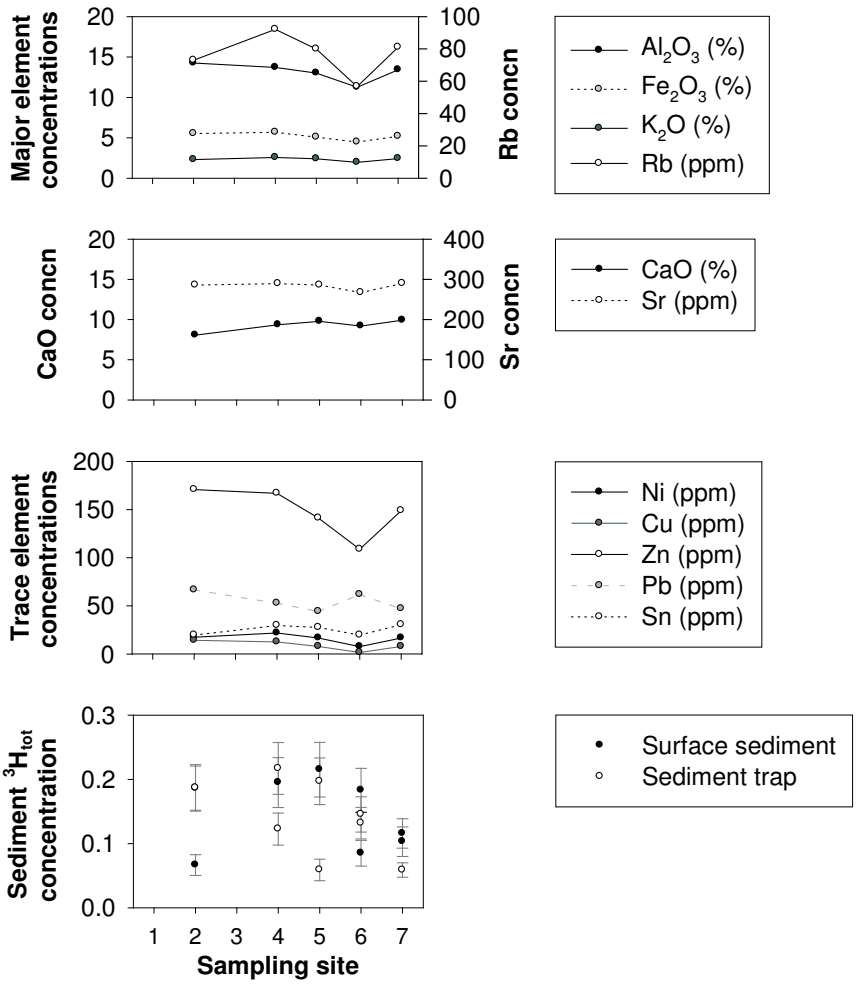

Figure 3.20: Elemental composition of sediment trap samples collected from 5 sites in the Severn estuary (Sites 2, 4, 5 and 6 in February 2004 and Site 7 in January 2004).

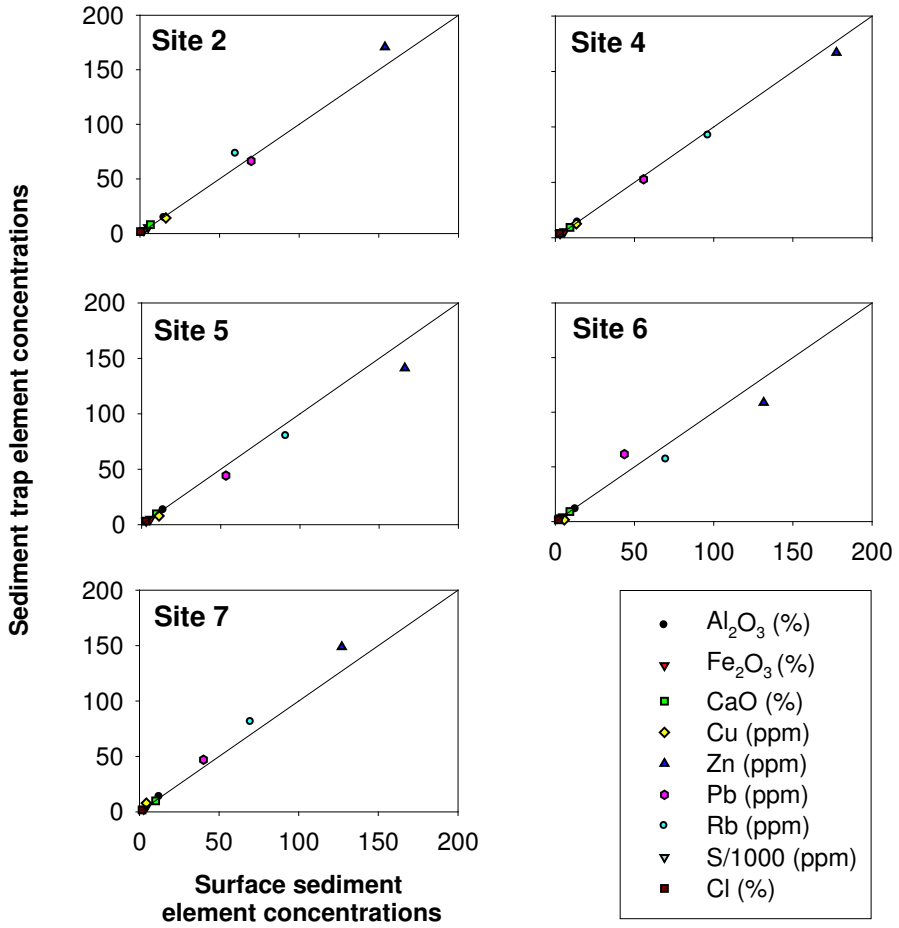

Figure 3.21: Comparison between the composition of sediment trap and surface sediment samples collected from 5 sites in the Severn estuary (Sites 2, 4, 5 and 6 in February 2004 and Site 7 in January 2004). S concentrations were divided by 1000 to plot on the same scale as the other elements.

Organic and inorganic carbon There are no significant differences between total, organic and inorganic carbon measurements on the sediment trap and surface sediment samples discussed above (Figure 3.22).

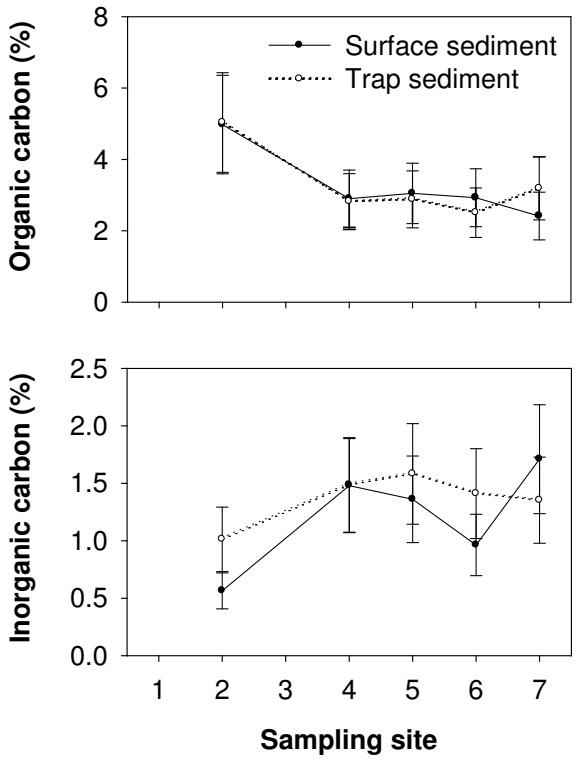

Figure 3.22: Comparison between the total organic carbon (TOC) and inorganic carbon (IC) contents of the sediment trap and surface sediment samples collected from 5 sites in the Severn estuary (Sites 2, 4, 5 and 6 in February 2004 and Site 7 in January 2004).

3.4 Discussion

3.4.1 Comparison with results from other studies

Sediment samples were also collected from Orchard Ledges (Site 3) and analysed for tritium as part of a national environmental monitoring programme around sites that release radionuclides into the environment. These data, from the annual Radioactivity in Food and the Environment (RIFE) reports, are compared with mean annual ^{3}H activities from the present study (Table 3.4). In 2000 and 2001 the average activities in sediments from Site 3 are comparable for both studies, but in 2002 and 2003 the RIFE measurements are lower. These differences may be produced by temporal variability in activities at the sampling sites, as the average results from the RIFE reports are based on fewer measurements (Table 3.4). However, these data agree to within the 95 % confidence level, so the two surveys are comparable.

Table 3.4: Comparison between mean annual $^3H_{total}$ activities at Site 3 from the present study and from the RIFE reports.

Date	$^3H_{total}$ activity in sediment (Bq g^{-1} dry weight)	Number of measure-ments	Source
Mean 2000	0.69 ± 0.1	8	Present study
Mean 2000	0.71	12	RIFE-6[1]
Mean 2001	0.64 ± 0.1	11	Present study
Mean 2001	0.7	2	RIFE-7[2]
Mean 2002	0.22 ± 0.1	10	Present study
Mean 2002	0.11	2	RIFE-8[3]
Mean 2003	0.33 ± 0.2	12	Present study
Mean 2003	0.21	2	RIFE-9[4]

[1] - FSA and SEPA, 2001
[2] - FSA and SEPA, 2002
[3] - EA, EHS, FSA and SEPA, 2003
[4] - EA, EHS, FSA and SEPA, 2004

3.4.2 Effect of variations in the magnitude, composition and treatment of discharges from Amersham plc on sediment ^3H activities

The magnitude, composition and treatment of tritiated discharges from Amersham plc may have affected sediment $^3H_{total}$ activities. When this study began in February 2000, these discharges were composed of 80 % organically bound tritium (OBT) and 20 % tritiated water (HTO), and were released into the estuary through a sewage pipeline with little or no treatment (Williams, 2003). The magnitude of the discharges tended to decrease over the sampling period, as did sediment $^3H_{total}$ activities (Figure 3.6), but there is no correlation between the peaks in monthly organic ^3H discharge and sediment $^3H_{total}$ activity, perhaps because surface sediments are from a range of sources and are cyclically suspended and deposited (Kirby and Parker, 1983). The tritiated wastes are also released in pulses, so the sediment $^3H_{total}$ activity and sediment composition probably vary on a daily basis. Sediments collected from Site 4 in November 2001 contained an anomalously high $^3H_{total}$ activity of 6.7 ± 1.2 Bq/g dry weight, which may have been produced by sampling after the recent release of a high activity pulse. As no changes were made to either the discharge treatment or composition until January 2002, the decline in sediment $^3H_{total}$ activities during this period is attributed to the reduction in magnitude of OBT discharges into the estuary.

In March 2002, a wastewater treatment works (WWTW) was introduced to treat domestic and industrial effluents passing through the Cardiff East sewer system, including discharges from Amersham plc (Table 1.1). The treatment process produces sewage sludge; 12 % of the total ^3H discharged by Amersham plc is associated with this fraction, resulting in activities of 275 Bq/g (Williams, 2005). Most of the sludge is retained; the effluent consists of a liquid phase containing most of the remaining activity, along with no more than 6 tonnes of sludge per day. Average sediment $^3H_{total}$ activities decreased following the introduction of the WWTW, despite a peak in organic ^3H discharges from

Amersham plc in September 2002 (Figure 3.6), implying that the tritiated organic molecules that can become associated with sediments are now largely removed from the effluent before it is released into the estuary.

In April 2003, the proportion of organic ^{3}H in discharges from Amersham plc increased to 95 % of the total tritium released but there was a concurrent decrease in the magnitude of ^{3}H discharges. Median sediment ^{3}H activities also decreased; this may be due to the reduction in the magnitude of discharges, or to the withholding of 80 % of the 'high impact' organic fractions, which were identified, by Amersham plc, as probably responsible for the accumulation of tritium in sediments (Williams, 2001). This fraction includes tritiated hydrocarbons, amino acids, peptides, proteins, nucleotides, fatty acids, lipids and purine/ pyrimidines, which before April 2003 comprised 15 % of the organic ^{3}H fraction (Williams, 2003).

Future changes to the treatment of tritiated effluents from Amersham plc include a tritium recovery plant (Project Paragon), due for completion in 2007. This will completely reclaim tritium from the discharges into the estuary, allowing it to be recycled (EA, 2003).

3.4.3 Effect of variations between sites on sediment ^{3}H activities

The highest sediment $^3H_{total}$ activities were usually found at Site 4, located close to the Amersham plc discharge point on the Wentlooge levels (Figures 3.1 and 3.23). At this site, a thick layer of unconsolidated sediments with high Rb concentrations (113 to 140 ppm) overlies a substrate of consolidated fine grained sediments. However, at Sites 2 and 3, on a gravelly beach less than 4 km from the Amersham plc discharge point, sediment $^3H_{total}$ activities were anomalously low (Figure 3.23). Surface sediments from Site 2 were routinely of coarse sand and gravel composition, with occasional thin mud drapes (Rb concentrations of the bulk samples ranged from 72 to 122 ppm), whereas at Site 3 patches of semi-consolidated fine-grained sediments overlie a similar substrate. The differences in sediment composition between Sites 2 and 4, and the predominantly north-easterly direction of net sediment transport, may contribute to the difference in sediment $^3H_{total}$ activities, as the sites are located at a similar distance from the Amersham plc discharge point.

Spatial variation in sediment sources, seasonal changes in sediment composition and scouring of fine sediments may all contribute to the varying fine sediment content of the sediments. The Severn estuary has a variety of sources of fine sediment, including streams, rivers and ocean currents as well as erosion from cliffs, salt marshes and the bed of the estuary (Section 1.4.1). Anthropogenic sources include sewage, industrial and agricultural discharges. However, despite this wide range of sources, the mineralogy of the clay ($<2\mu$m) fraction is similar at all sites in this study and is also consistent with results reported by Hamilton *et al* (1979) and Allen (1987c). The clay mineralogy is therefore both spatially and temporally invariable, probably because the estuary is well mixed and most of the clay minerals in the estuary are from the River Severn (Allen, 1987b). However, the range of sources of sediment into the estuary may produce spatial variation of other components, such as trace metals.

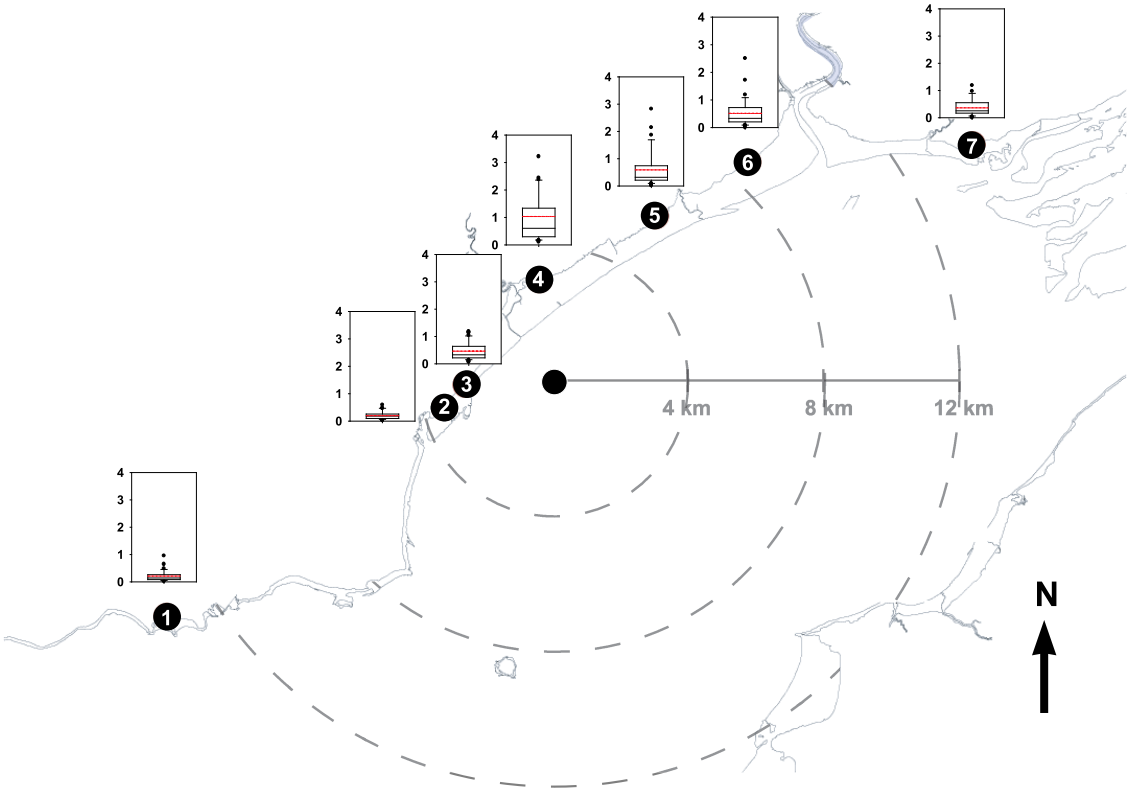

Figure 3.23: Average sediment $^{3}H_{total}$ activities for the monthly sampling sites from February 2000 to May 2004, showing the location of each site relative to the Amersham plc discharge point. The mean $^{3}H_{total}$ activity is shown as a red dotted line and the median as a black solid line, while the box encloses the 25th to 75th percentiles of the data and the lines show the 5th and 95th percentiles. Outliers are represented by black circles, although two outliers measured at Site 4 were not be included. Replicate measurements were also omitted from these calculations. The Amersham discharge point is represented by a black circle. Data were compiled from measurements performed by J.E. Morris, K. Doucette, Dr F.M. Dyer, Dr P. Teasdale and Dr J. Oh.

Seasonal variations are observed in both sedimentation and biological activity by Allen and Duffy (1998b). Coarser sediments are suspended in the water column by increasing water turbulence and viscosity during the winter months (Langston *et al*, 2003). Sedimentation is controlled by wind and tidal regimes (Allen and Duffy, 1998a), which tend to increase the grain size of sediments deposited on mud flats during winter (Allen and Duffy, 1998b). In February 2004, sediment trap samples collected from Sites 4, 5 and 6 were coarser grained than surface sediments, implying that coarse sediments were in suspension during the preceding month. However, at Site 2 the surface sediments were coarser, because the sediment trap retains fine sediments that are removed from the surface sediment by scouring. Seasonal variations in biological activity include a decrease in salt marsh vegetation in the winter, increasing the potential for erosion of consolidated sediments. The growth of microphytobenthos films on mud flat surfaces during sunny days, particularly in the summer, may also increase sediment cohesion and reduce erosion (Underwood and Paterson, 1993). However, during the present study no apparent seasonal trends were observed in the proportion of fine sediment in the surface sediments, and there was no apparent seasonal variation in sediment $^{3}H_{total}$ activities (Figure 3.13).

The susceptibility of sites to the scouring of fine sediments is related to their geographic location and morphology (Figure 3.1; Table 3.1). Site 1 is protected by a harbour breakwater and is therefore never completely scoured, whereas Sites 2 and 3 are situated on an open beach that is regularly scoured of all fine sediment. Sites 4, 5, 6 and 7 are located on the landward edge of large sub-tidal to inter-tidal mud flats (the Wentlooge levels); the gradually shallowing mud flats may attenuate the wave energies and provide some protection, although they are occasionally scoured by storms. Tidal currents may also scour fine sediments from the less sheltered sites, however this effect is likely to be minor compared to the effect of storms.

At Sites 1, 2 and 3, the lowest $^{3}H_{total}$ concentrations correspond with the lowest Rb concentrations, indicating that the sediments are scoured because the substrate had a coarser composition (Figure 3.24). At Sites 4, 5 and 6, there is no correlation between either Rb or wet/dry ratios and sediment $^{3}H_{total}$ activities (Figures 3.24 and 3.25). As consolidation of the substrate produces sediments with lower wet/dry ratios than the non-consolidated surface sediments, this indicates that although the amount of surface sediment is reduced, scoured samples are not composed entirely of the consolidated substrate. Some samples collected from Sites 4, 5 and 6 have low Rb concentrations even though no scouring is apparent at the sampling site, suggesting that processes other than scouring may also affect the grain size of sediments at these sites (Figure 3.20). No scouring is observed at Site 7 and the sediments have unvarying Rb concentrations (Figure 3.12).

3.4.4 Potential mechanisms for the transport of tritiated sediments around the Severn estuary

Because colloidal, particulate and bedload sediments are transported around the Severn estuary by different mechanisms, the predominant association of tritiated organic molecules with one of these fractions would substantially affect its spatial distribution in the

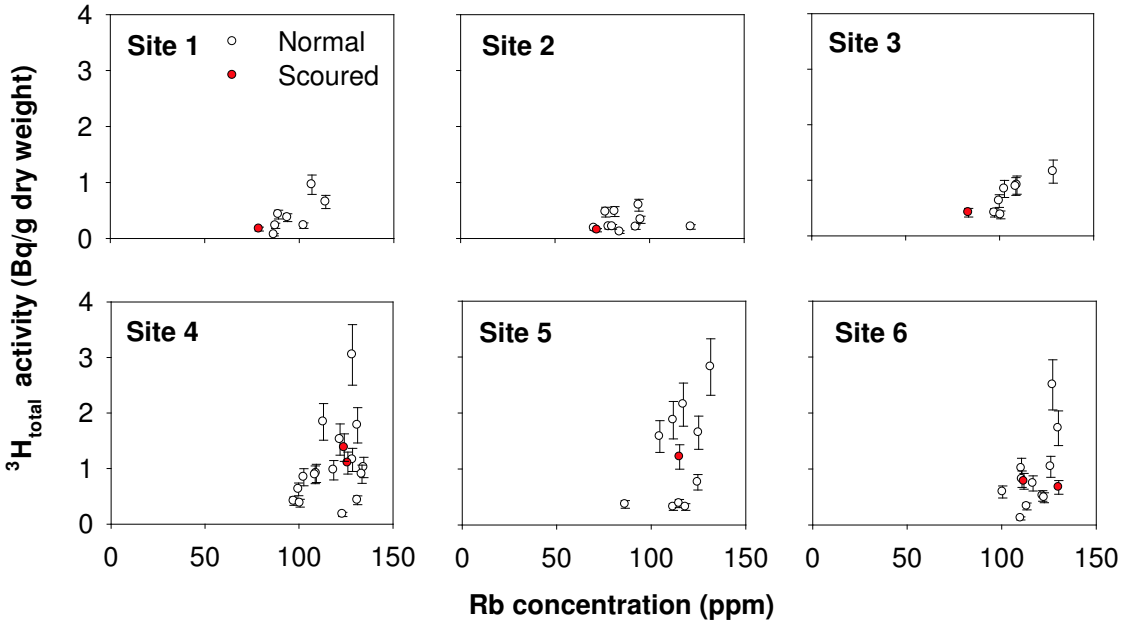

Figure 3.24: The relationship between Rb concentrations and $^3H_{total}$ activities for 'scoured' and normal (unscoured) sediments. Sediments were classified as scoured or unscoured on the basis of field observations (Appendix 1).

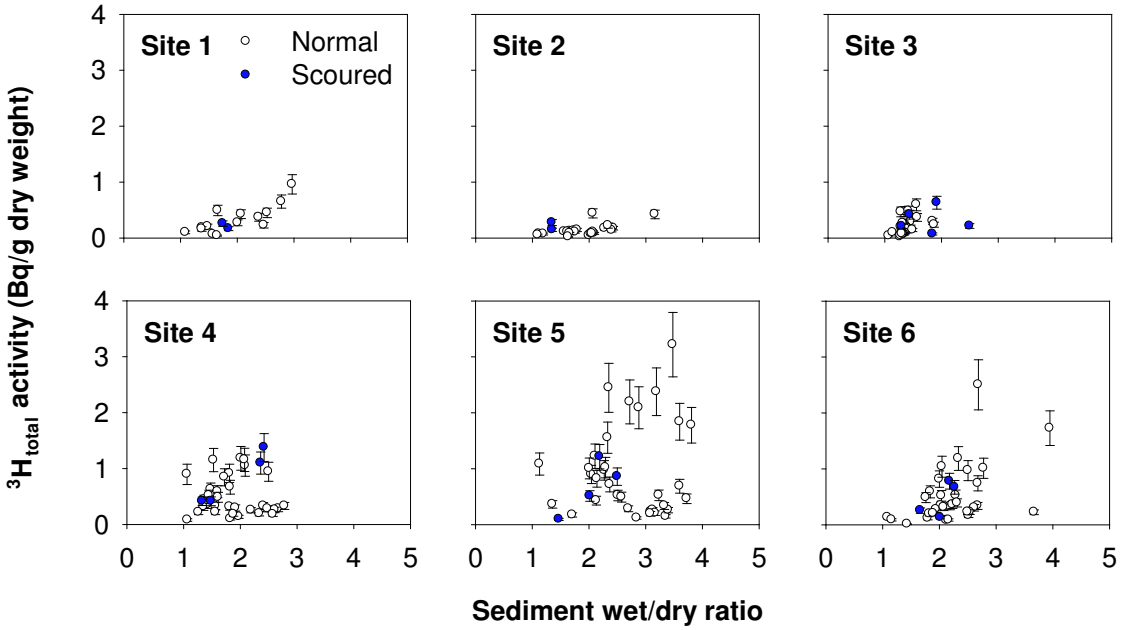

Figure 3.25: The relationship between sediment wet/dry ratios and $^3H_{total}$ activities for 'scoured' and normal (unscoured) sediments. Sediments were classified as scoured or unscoured on the basis of field observations (Appendix 1).

estuary.

Association of tritiated organic molecules with sedimentary particles

The behaviour of organically bound tritium (OBT) is dependent on the chemical form of the carrier molecule (Blaylock *et al*, 1986). In the present study, the tritiated organic molecules are not water-extractable. Although this implies that OBT is not present in solution, colloids are often hydrophobic and can pass through ordinary filter paper (Yariv and Cross, 1979). Filtered water samples from the Severn estuary have low ^{3}H activities (Appendix 5), but hydrophobic colloids could be scavenged onto particles or incorporated into flocs as a result of the high suspended sediment load. This has not been investigated as part of the present study.

Sands and gravels are normally transported as bedload in the Severn estuary, although they can be suspended in turbulent water (Kirby, 1994). Sands have lower $^3H_{total}$ activities than fine sediments (Table 3.2) because they are predominantly quartz, which is chemically inert compared to clays (Yariv and Cross, 1979). Tritium preferentially associates with the finer fractions (Table 3.2), which include clays, silts, carbonates, particulate coal, biota, organic detritus and anthropogenic inputs (Allen and Rae, 1986; Hamilton *et al*, 1979). Particulate fine sediment is transported around the Severn estuary in suspension (Kirby, 1986). Several possible mechanisms exist for the incorporation of OBT into particulate sediments. OBT may bind onto clay minerals, which have platy habits and are layered to produce large surface areas with many potential binding sites (Yariv and Cross, 1979). Clays can also form flocs with other particulate material, which may physically trap tritiated organic molecules (Eisma, 1993; Droppo, 2001). Live biota and microbes feed on tritiated organic matter or sediment, bioaccumulating OBT (McCubbin *et al*, 2001), and abiotic reactions could also occur with organic detritus, forming tritiated humic substances that are resistant to degradation. Coal particles have chemically active surfaces that could also adsorb tritiated organic molecules, and pore spaces, which can hold small organic molecules. Therefore, the incorporation of OBT into the fine particulate fraction is in agreement with the observed results; however, the specific binding mechanisms have not been identified.

Potential mechanism for the transport of tritium around the Severn estuary

As tritiated organic molecules predominantly associate with particulate sediments in the estuary system, they will be transported with the sediment in suspension. Parker and Kirby (1982) produced a model of fine sediment circulation based on residual currents (Figure 3.4), which predicted that fine sediment will predominantly be transported to the northeast from the Amersham plc discharge point, parallel to the axis of the estuary. This is consistent with the observed asymmetric $^3H_{total}$ activity distribution (Figure 3.4). Lower $^3H_{total}$ activities are measured at sampling sites on the southern shore of the estuary, however, any comparison with the model is limited by the irregular distribution of sampling sites on the southern shore of the estuary.

Tidal currents will transport sediment-bound ^{3}H, but as the estuary has a high suspended sediment load (Kirby, 1986), it will also be diluted with unlabelled sediment. An increase in the transport distance of sediment from the Amersham plc discharge point will allow more mixing and dilution of the ^{3}H-labelled sediment with unlabelled sediment, producing the observed decrease in sediment ^{3}H activities with distance from the discharge point. The time taken to transport tritiated sediments from the discharge point to the sampling sites will vary depending on tidal and weather conditions. During spring tides, the high tidal range (12.3 m at Avonmouth) produces a 10 - 15 km excursion of water (Dyer, 1984); this implies a lag time of hours to days, rather than weeks to months, between the release of a discharge pulse and an increase in sediment $^3H_{total}$ activities. In high energy conditions, which occur around spring tides or in windy/stormy weather, currents can reach speeds in excess of 1 m s^{-1} (Uncles, 1984), resulting in increased concentrations of suspended sediment in the water column. This turbulence decreases around neap tides, allowing particles to settle and producing a high density layer of suspended sediment close to the bed - a mobile suspension (Kirby and Parker, 1983). In low energy conditions or sheltered areas such as Newport Deep, this layer can settle onto the bed, producing a stationary suspension. Thixotropic stationary suspensions have also formed on the Wentlooge levels (Kirby, 1994). Over 50 % of the maximum suspended fine sediment load settles out of suspension during neap tides. Although most of this is resuspended during the next spring-neap tidal cycle (Kirby and Parker, 1983), it could provide a mechanism for the deposition of some tritium-labelled fine sediment in the estuary (Figure 3.26).

The proposed model of transport of tritium-labelled sediments by tidally-dominated currents and deposition by settling out of suspension concurs with the observed spatial distribution of sediment-bound tritiated organic molecules, if the modifying effect of sediment compositional variation is included to explain anomalous sediment $^3H_{total}$ activities. However, the large number of variables affecting both sediment composition and $^3H_{total}$ activities mean that it is not currently possible to produce a quantitative model. In particular, sediments would need to be sampled from more sites, and more frequently, especially at the distant sites (some are only visited once during the present study).

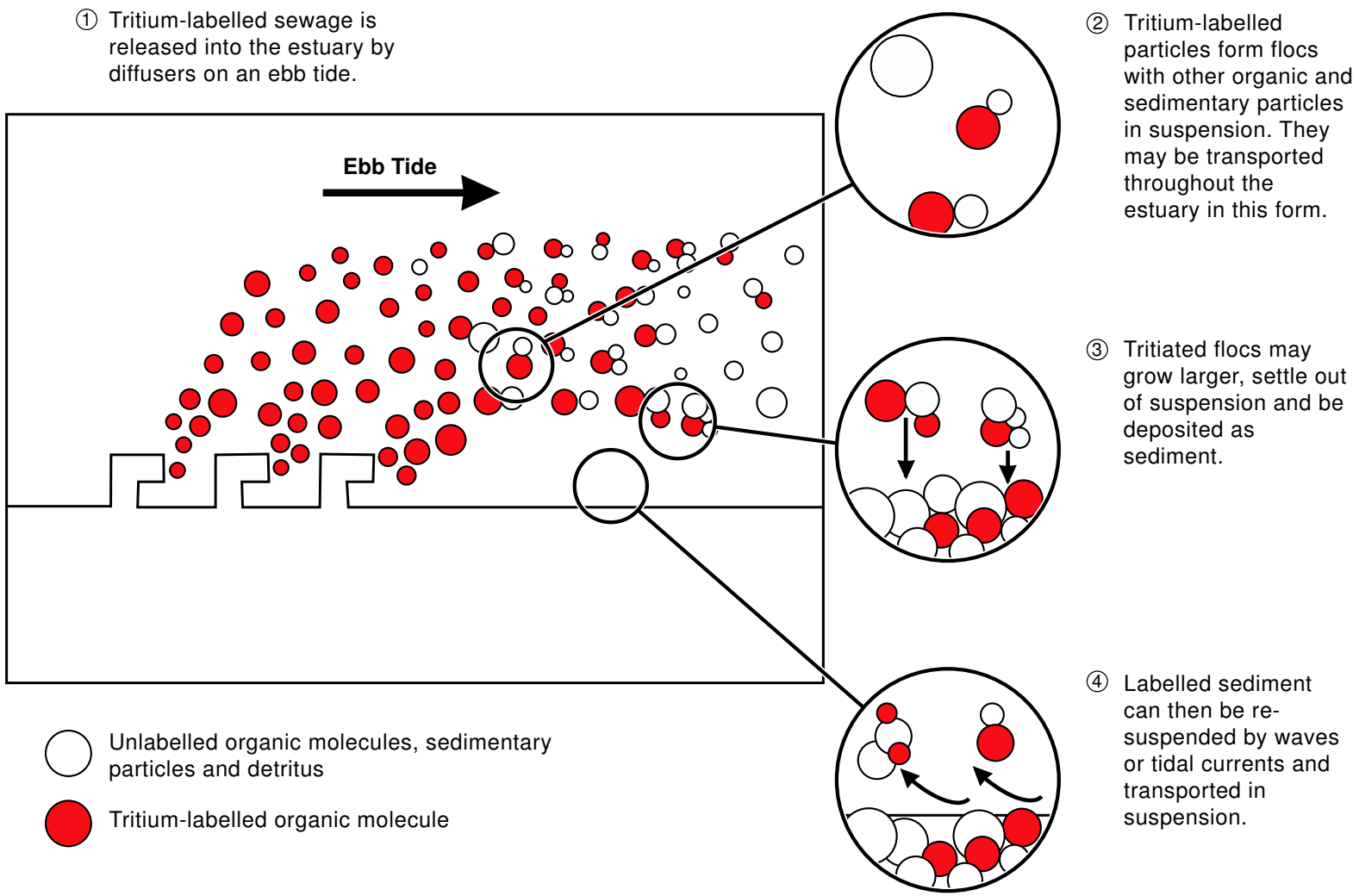

Figure 3.26: Schematic model of the incorporation of tritium into suspended fine sediment, transport around the estuary and deposition. Model constructed with reference to Parker and Kirby (1982) and Hosken (2002).

3.5 Summary

The highest sediment $^{3}H_{total}$ activities are found at sites closest to the Amersham plc discharge point. The spatial and temporal variability is affected by a wide range of variables, including the magnitude, composition and treatment of tritiated discharges from Amersham plc. The decline in the magnitude of organic tritium discharges over the sampling period has resulted in decreasing sediment $^{3}H_{total}$ activities at all sites. The treatment of discharges by a waste water treatment plant from January 2002, and a decrease in the discharge of 'high impact' tritiated organic compounds such as hydrocarbons, proteins, nucleotides and lipids has resulted in further decreases in sediment $^{3}H_{total}$ activities.

As tritiated organic molecules are predominantly but not exclusively associated with fine grained sediments, the composition of the surface sediments at each site has an effect on sediment $^{3}H_{total}$ activities. The deposition or erosion of fine grained sediments is dependent on the geographic location and susceptibility to scouring of the site, which is controlled by the dynamic and macrotidally-driven estuarine circulation. However, there are poor correlations between sediment $^{3}H_{total}$ activities and compositional indicators such as Rb, TOC and CaO. The specific fraction(s) of the sediment that OBT is associated with are not identified by the present study, but do not appear to be well represented by the proxies listed above.

Tritium is transported around the Severn estuary with sediments in suspension. Therefore, it is most likely to be transported to the northeast, with little deposited across the channel. Measured spatial variations in $^{3}H_{total}$ activities agree reasonably well with the proposed model with anomalous results being explained by variations in sediment composition. Therefore, the spatial and temporal variation of sediment $^{3}H_{total}$ activities is predominantly controlled by discharge variability and sediment transport processes; however, sediment composition is an important secondary factor. The longer term accumulation of ^{3}H in salt marsh sediments is discussed in Chapter 4.

Chapter 4

The accumulation of tritium in shallow sediment cores from Severn estuary salt marshes

4.1 Introduction

The Severn estuary in SW Britain is fringed by salt marshes and tide washed pastures, which have developed as the result of repeated cycles of deposition and erosion into a series of stepped terraces (French, 1996; Figure 1.10). Salt marshes evolve from mud or sand flats (Figure 1.11) and their surface sediments are stabilised by surface vegetation and subsurface roots, so they are less well mixed than mud flats and have the potential to accumulate pollutants that associate with fine sediments. In the Severn estuary these pollutants include trace metals and coal dust (Allen, 1987a; Allen and Rae, 1986), and may also include organically bound tritium (OBT).

Significant non-aqueous tritium activities associated with mud flat sediments from the Severn estuary (Chapter 3) are attributed to OBT discharges from Amersham plc (Chapter 1). If OBT also accumulates in salt marshes, it will be stored until tritium activities decline by radioactive decay ($t_{\frac{1}{2}} = 12.3$ years) or the sediments are eroded and resuspended (some Severn estuary salt marshes are currently retreating due to regional sea level rise; Allen, 1987b).

This chapter assesses the historical accumulation of ^{3}H in sediments in three salt marshes on the northern shore of the Severn estuary, and identifies the factors controlling this accumulation.

4.2 Sampling and analysis

Four shallow sediment cores were collected from three salt marshes on the northern coast of the Severn estuary, chosen for their location relative to the Amersham plc discharge point (Figure 4.1; Table 4.1).

Table 4.1: Location of core sampling sites

Site number	Core name	Grid reference	Sampling date	Depth of core	Description of site
5	Peterstone 1 core	ST 27000 79850	4 July 2001	40 cm	Higher level of salt marsh platform
5	Peterstone 2 core	ST 27050 79800	28 October 2003	40 cm	Creek edge on higher level of salt marsh
1	Barry Island core	ST 10834 66525	4 July 2001	32 cm	Isolated mound of salt marsh in harbour
H	Sudbrook core	ST 50156 87245	5 November 2001	28 cm	Middle of salt marsh near new Severn bridge

Shallow sediment cores (11 cm in diameter) were extracted manually using plastic core tubes. The cores were split in half and stored at 4 °C until required for analysis. One half was archived and the other sampled at 1 cm increments; these samples were then weighed and divided, with one aliquot frozen at −40 °C and the other freeze-dried.

The fresh sample was analysed for total tritium ($^3H_{total}$) and the dried sample was finely ground and analysed for:

- Elemental composition using X-ray fluorescence (XRF) analysis.
- Total organic carbon (TOC) and inorganic carbon (IC) using coulometric analysis.
- Gamma emitting radionuclides using γ-spectrometry.
- Elemental carbon content by mass difference, following sediment digestion with aqua regia and HF acid.

These methods are described in more detail in Chapter 2. Sampling and analyses were performed predominantly by J.E. Morris, but also by K. Doucette, Dr F.M. Dyer, Dr P.E. Warwick, Dr I.W. Croudace and Dr A.B. Cundy.

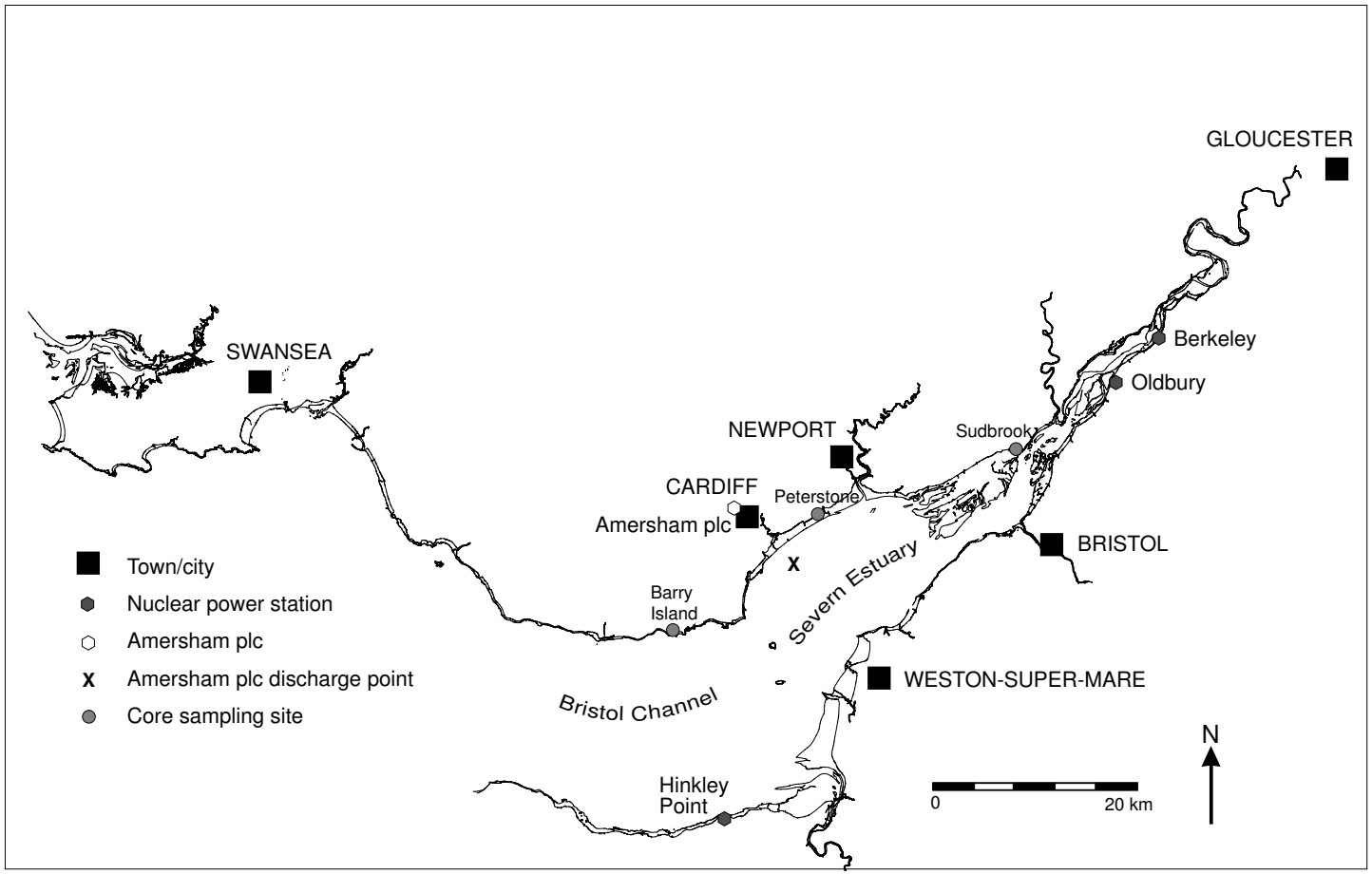

Figure 4.1: The location of core sampling sites relative to sources of tritium (Amersham plc and the nuclear power stations at Hinkley Point, Berkeley and Oldbury) in the Severn estuary.

4.3 Results

4.3.1 Sampling site and core descriptions

Peterstone salt marsh is part of the Wentlooge levels, a large intertidal to subtidal area of muddy deposits on the northern side of the Severn estuary (Figure 4.1). The salt marsh, part of the Northwick Formation (Allen, 1987, Kirby, 1994), began forming before 1947 (from aerial photographs; RAF, 1947; 1950) and accreted rapidly until about 1980 (OS, 1978; 1985). After 1980, the marsh began to retreat, forming sparsely vegetated ridge and furrow erosional topography on the seaward edge (Figure 4.2).

The salt marsh platform has two levels, separated by a break in slope that forms a zone of preferential erosion visible from aerial photographs (OS, 1978; Geonex, 1991). The platform is cut by a number of linear dendritic creeks (Allen, 2000). The Peterstone 1 core was collected from the upper level of the salt marsh, which is populated by vegetation, including *Aster*, *Spartina* and *Puccinelia*, but abundant *Salicornia* on the lower marsh indicates that this level is inundated more frequently (Beeftink and Rozema, 1998). The salt marsh sediments are predominantly silty clays, but layers of shells and small pebbles are observed in the bottoms and banks of creeks.

The Peterstone 2 core was collected from the edge of a creek, also on the upper level of the salt marsh (Table 4.1). At the top of the Peterstone 2 core sediments are red-brown in colour, with a crumbly texture, and contain abundant plant roots and shells. Below an irregular boundary at about 30 cm depth, sediments are grey cohesive muds, containing minor plant roots and some fragmented shells (Figure 4.3). During sampling, the core tubing collapsed, squeezing the sediments in the base of the core, so it was not sub-sampled below 40 cm depth. The core was also compressed vertically by ∼10 % during collection.

The harbour at Barry Island is located on the northern shore of the Severn estuary, approximately 20 km to the west of Peterstone salt marsh (Figure 4.1; Table 4.1). Isolated mounds of pioneer salt marsh, mainly vegetated by *Spartina*, are raised up to half a metre above the surrounding mud flat, which overlies sand (Figure 4.2). The Barry Island core was collected from the centre of one of these isolated salt marsh mounds.

Sudbrook salt marsh is located on the northern shore of the Severn estuary, approximately 20 km to the east of Peterstone salt marsh (Figure 4.1). It is more extensive than Peterstone, and appears to have accreted uniformly, as there is no change in platform height across the marsh (Figure 4.2). Sediments are predominantly silty muds, and the marsh is colonised by a mixture of grasses and succulents. The Sudbrook core was collected from the centre of the salt marsh, midway between the headland and the bridge. The core sediments are dark brown mud with sandy laminations, and contain abundant thin roots as well as a few thick horizontal roots (Figure 4.4). Due to horizontal compression during sampling, the core sediments were squeezed below 24 cm depth. Vertical compaction was less than 10 %.

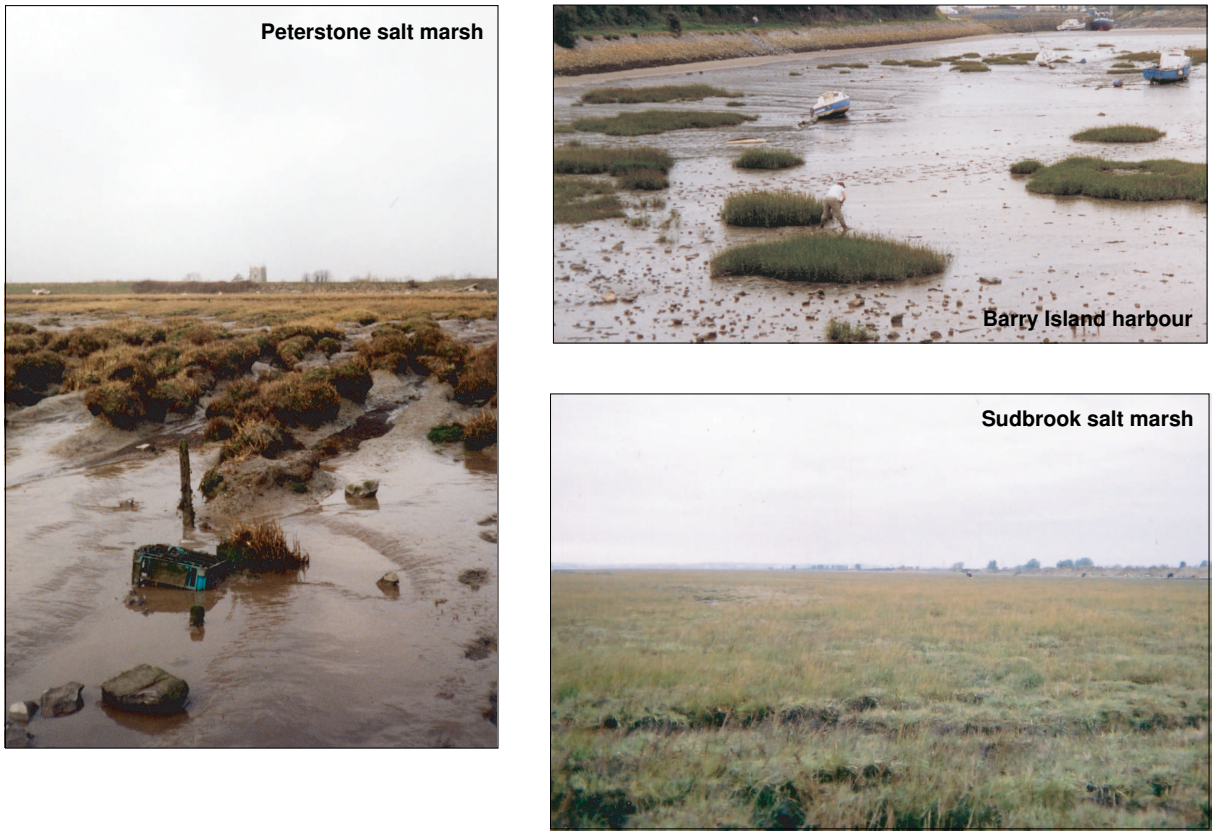

Figure 4.2: Photographs of Peterstone, Barry Island and Sudbrook salt marshes. The Peterstone marsh is linked to the adjoining mud flat by partially vegetated ridges interspersed with erosional furrows. The transition from low marsh to high marsh is also visible, this is marked by a band of increased erosion (Figure **??**). In Barry Island harbour, isolated salt marsh mounds are surrounded by mud flats and the underlying sand flats (visible near the sea defenses). At Sudbrook, the salt marsh is more extensive than at Peterstone, but it has accreted uniformly without any changes in the height of the platform.

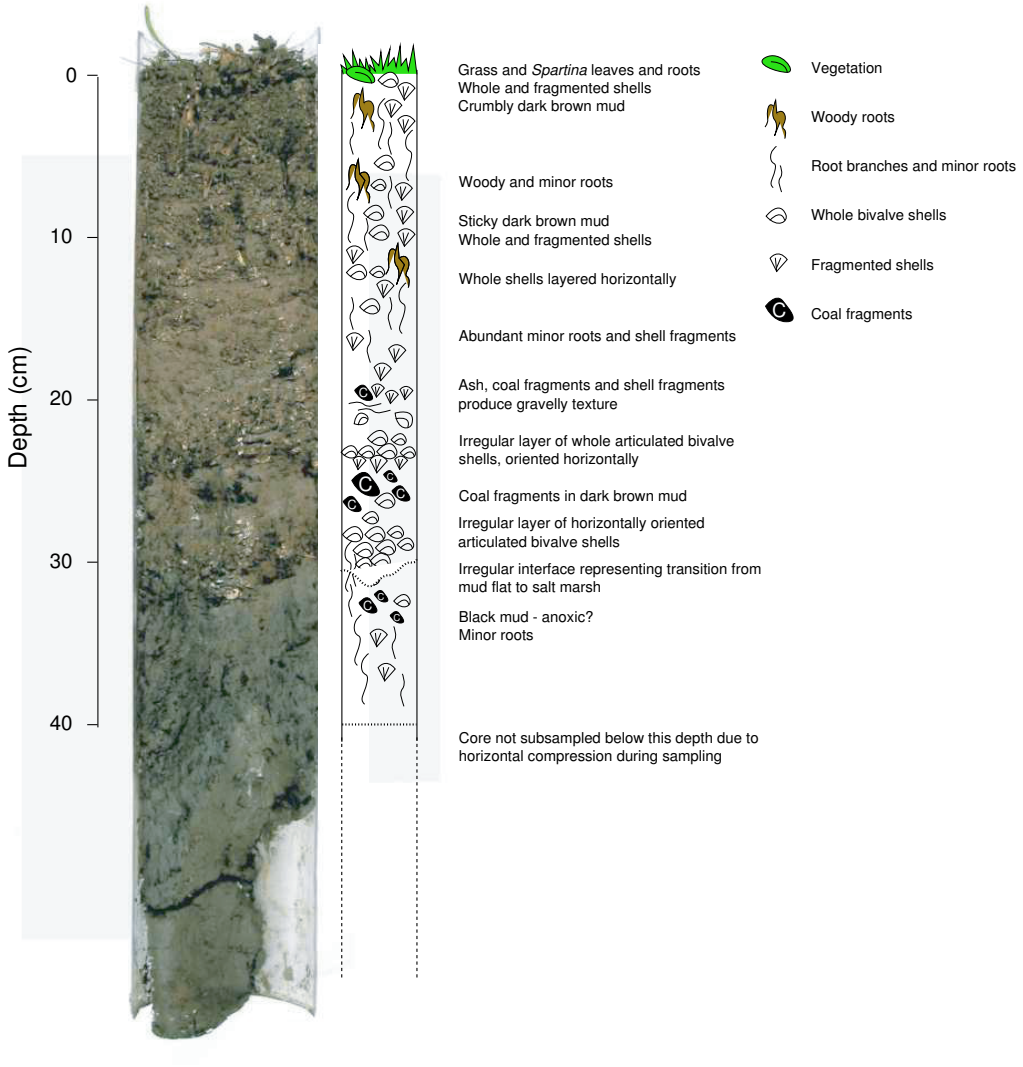

Figure 4.3: Photograph and schematic sedimentary log of the Peterstone 2 salt marsh core.

4.3.2 Sediment composition

Peterstone 1 core

Al_2O_3, K_2O and Rb concentrations increase with depth in the Peterstone 1 core (Figure 4.5). Al and K correlate well with Rb and with the Al/Rb and K/Rb ratios of the standard shale (Turekian and Wederpohl, 1961; Figure 4.6). Concentrations of the redox-sensitive elements Fe_2O_3, MnO and S decrease to a depth of 19 cm, below which they are constant apart from a small peak at 36 cm depth (Figure 4.5). These trends are still observed when the profiles are normalised to Rb to remove any variability produced by changes in grain size (Figure 4.7). Cu, Pb and Zn concentrations also increase with depth, while Ni concentrations remain constant (Figure 4.5). All the trace metals correlate relatively well with Rb; however, Pb/Rb and Zn/Rb ratios are elevated in the core sediments relative to the standard shale (Figure 4.6).

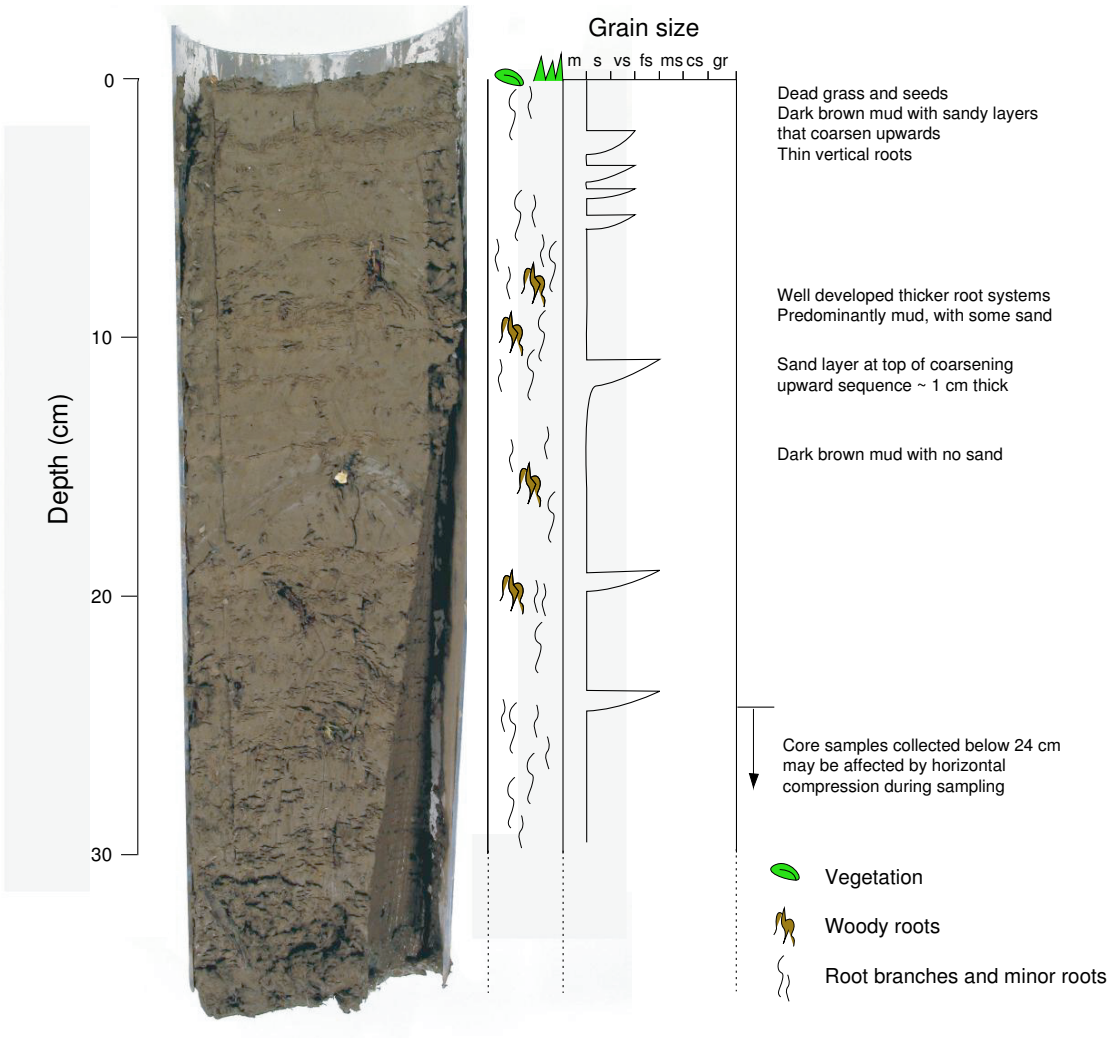

Figure 4.4: Photograph and schematic sedimentary log of the Sudbrook salt marsh core.

CaO and Sr concentrations indicate variations in the carbonate content of sediments, which decrease at 11 cm and 19 cm depth (Figure 4.5). Below this, concentrations remain constant to 38 cm depth, where they increase slightly. The inorganic carbon (IC) content of sediments, measured using coulometry (Section 2.5.1), were generally higher at the top of the core, but decrease sharply at 18 cm depth (Figure 4.9). The total organic carbon (TOC) content of the sediment, calculated by subtracting the IC from the total carbon (TC), which was also measured using coulometry, tends to increase with depth (Figure 4.9). The coal (elemental carbon) contents of three samples, determined by mass difference after digestion with aqua regia and hydrofluoric acid (Section 2.5.2), ranged from 4 - 9 % by mass (Figure 4.9), and also appeared to increase with depth.

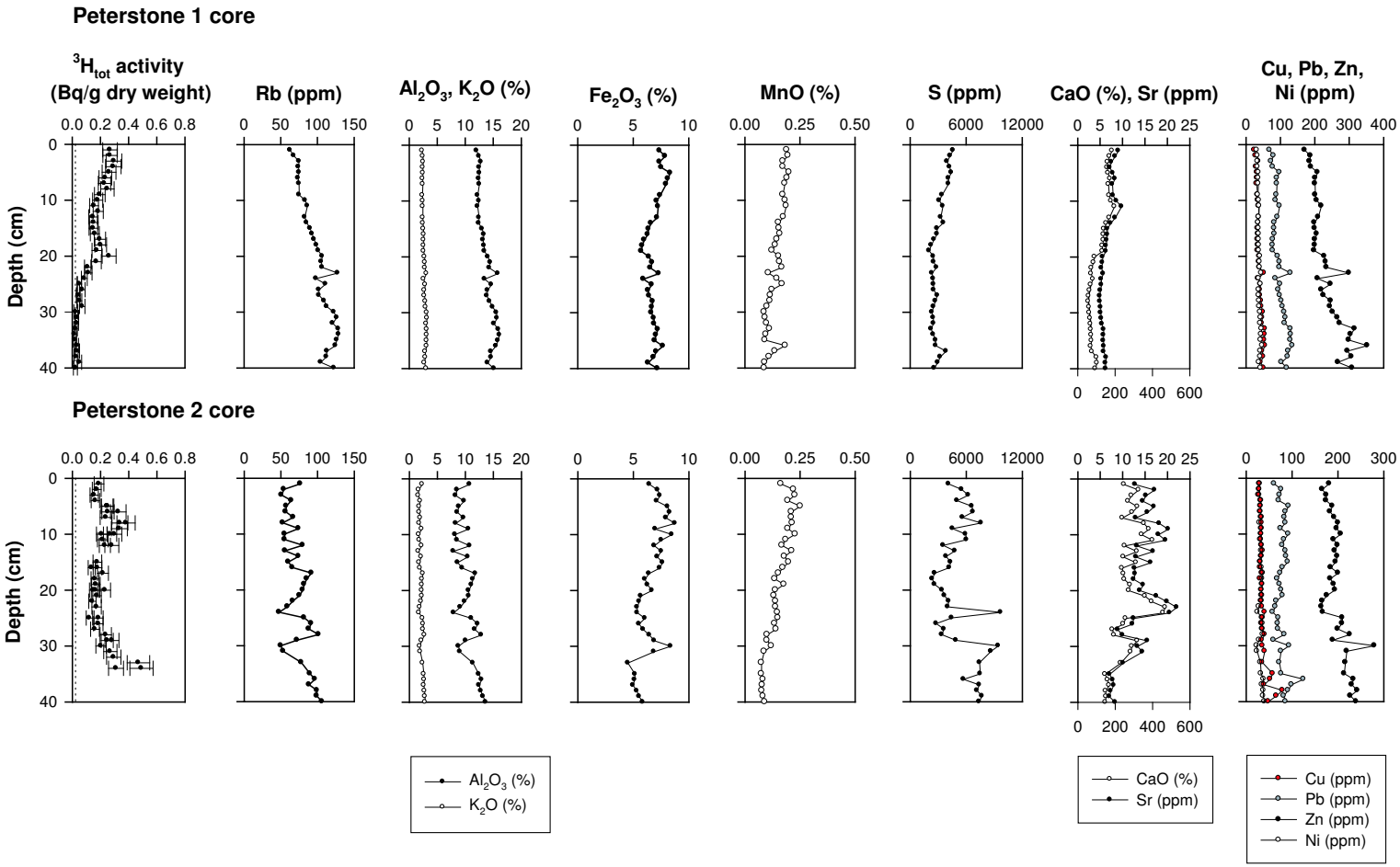

Figure 4.5: Variations in $^3H_{total}$ activities and major and trace element concentrations with depth in the Peterstone 1 and 2 cores. Tritium activities are decay corrected to the date of sampling, total (method and counting statistical) uncertainties have been calculated to the 95 % confidence level and plotted as error bars. The dotted line indicates the limit of detection of the tritium analysis method. Uncertainties for major and trace element concentrations are normally contained within the data point.

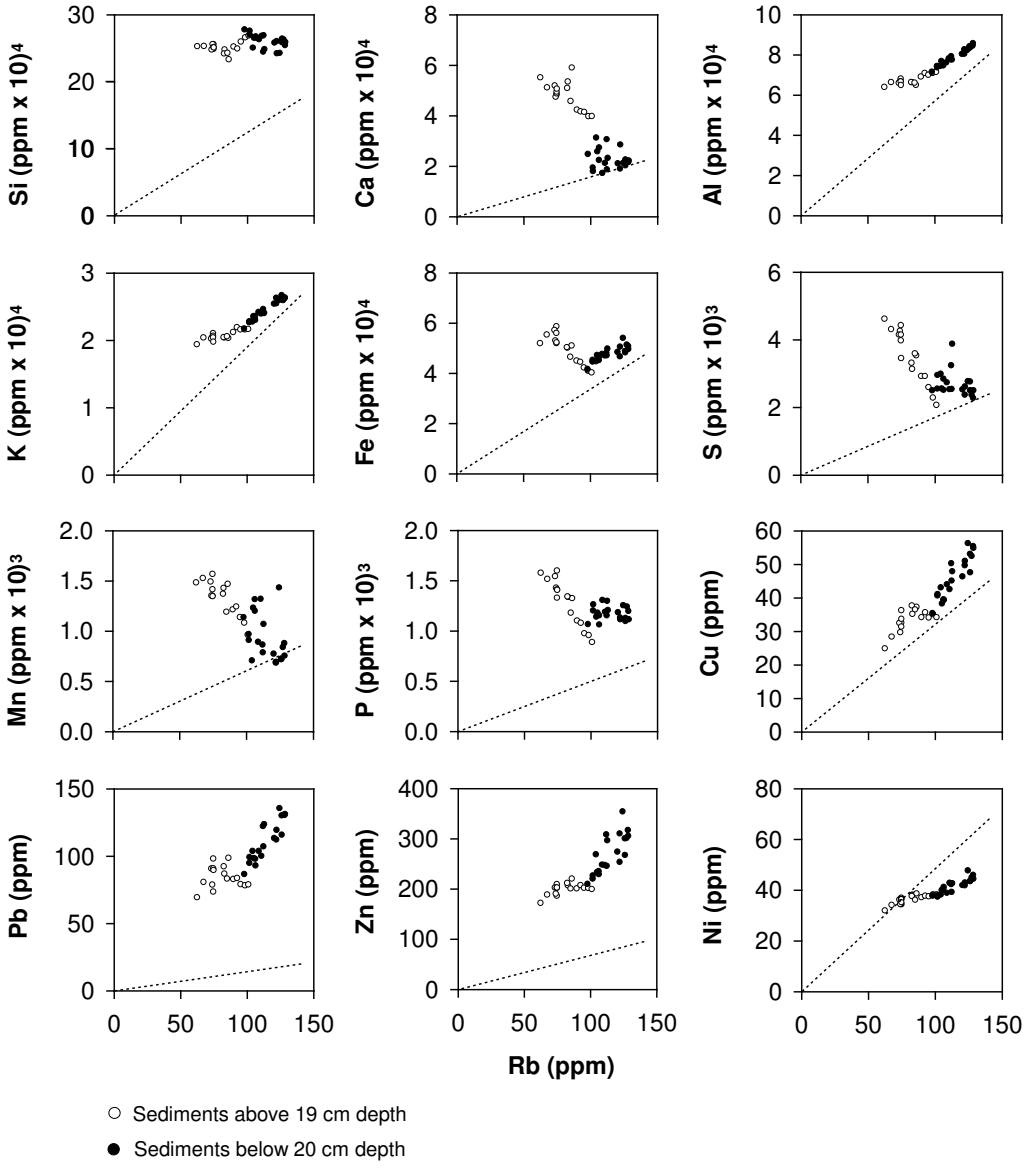

Figure 4.6: Correlation between selected element concentrations and Rb concentrations for sediments from the Peterstone 1 core. The dotted line indicates the Element/Rb ratio of the standard shale (Turekian and Wederpohl, 1961).

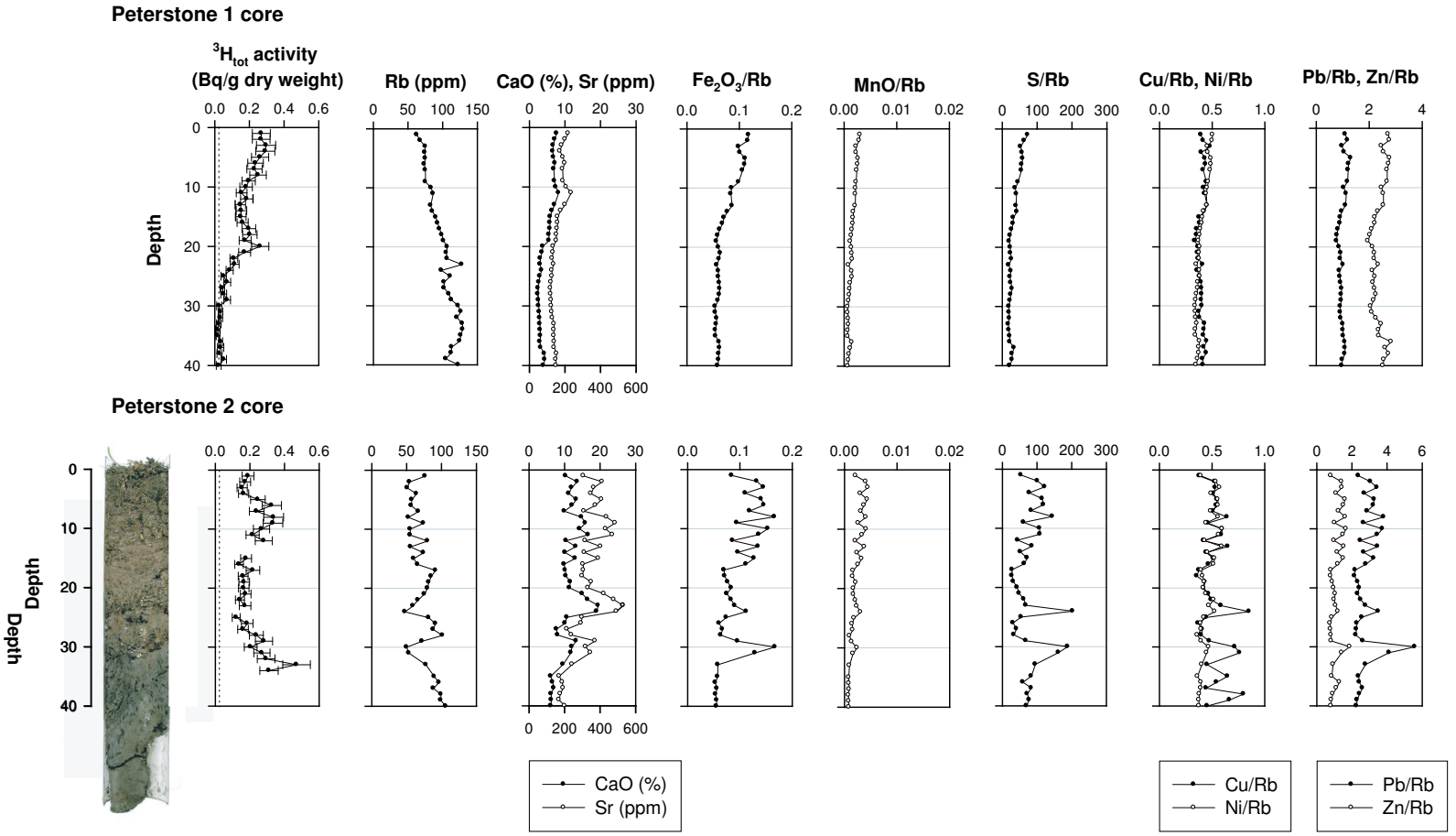

Figure 4.7: Variations in $^3H_{total}$ activities, Rb, CaO and Sr, and normalised Fe_2O_3, MnO, S and trace metals, with depth in the Peterstone 1 and 2 cores. Tritium activities are decay corrected to the date of sampling, total (method and counting statistical) uncertainties have been calculated to the 95 % confidence level and plotted as error bars. The dotted line indicates the limit of detection of the tritium analysis method. Uncertainties for major and trace element concentrations are normally contained within the data point.

Peterstone 2 core

The concentrations of Rb, Al_2O_3 and K_2O vary on a 1 - 2 cm scale to 16 cm depth in the Peterstone 2 core (Figure 4.5), below which they vary more slowly with peaks at 17, 28 and 40 cm depth. Al, K and Rb correlate with each other ($r^2 = 0.96$), and correspond closely to the Al/Rb and K/Rb ratios of the standard shale (Turekian and Wederpohl, 1961; Figure 4.8). The concentrations of the redox-sensitive elements Fe_2O_3 and S concentrations are irregular but tend to decrease with depth, apart from a sharp peak at 30 cm and, for S, another at 24 cm depth. MnO concentrations also tend to decrease with depth. When normalised to Rb to remove grain size effects, Fe_2O_3/Rb, MnO/Rb, S/Rb and P_2O_5/Rb ratios are irregular in the top 16 cm, with significant peaks at 24 and 30 cm depth (Figure 4.7). Concentrations of Cu, Pb and Zn tend to increase with depth, whereas Ni concentrations remain constant (Figure 4.5). However, when normalised to Rb to remove grain size effects, there are peaks in the ratios of trace metals to Rb at 24, 30 and 35 cm depth (Figure 4.7). Cu/Rb also peaks at 38 cm depth, but only Pb/Rb and Zn/Rb ratios are elevated in the core sediments relative to the standard shale (Figure 4.8).

CaO and Sr concentrations vary on a 1 - 2 cm scale in the top 16 cm of the core (Figure 4.5). Below this depth there are peaks at 25 and 31 cm, and concentrations decrease below 35 cm depth. The inorganic carbon (IC) content, measured by coulometry, is relatively constant with depth, apart from a peak at 13 cm depth and a trough at 30 cm depth (Figure 4.9). The total organic carbon (TOC) content peaks at 8, 23 and 30 cm depth (Figure 4.9). Elemental carbon (coal content), which was measured separately (Section 2.5.2), varied from 5 - 22 % (Figure 4.9).

Barry Island core

The concentrations of Rb, Al_2O_3 and K_2O are relatively constant to 17 cm depth in the Barry Island core, where they decrease sharply, then lower, constant concentrations were observed down to 32 cm depth, apart from a small peak at 23 cm depth (Figure 4.10). Al_2O_3 and K_2O concentrations tend to correlate with Rb, and correspond closely to the Al/Rb and K/Rb ratios of the standard shale (Turekian and Wederpohl, 1961; Figure 4.11). Fe_2O_3 and MnO concentrations follow a similar trend to Al_2O_3 and K_2O; in contrast, S concentrations are relatively constant with depth apart from peaks at 11 and 18 cm depth. When normalised to Rb to remove the effects of grain size variations, the Fe_2O_3/Rb, MnO/Rb and S/Rb profiles all contain a trough at 23 cm depth. Otherwise, Fe_2O_3/Rb ratios remain constant with depth whereas MnO/Rb ratios are more variable, with peaks at 4 and 15 cm. The S/Rb profile tends to increase with depth (Figure 4.10), with sharp peaks at 18 cm and 27 cm depth. Concentrations of the trace metals Cu, Pb, Zn and Ni decrease sharply at 17 cm depth, and then remain relatively constant with depth apart from a small peak at 23 cm depth (Figure 4.10). The trace metal concentrations all correlate well with Rb, although sediments above and below 17 cm depth cluster separately (Figure 4.11). Pb and Zn are elevated relative to the Pb/Rb and Zn/Rb ratios

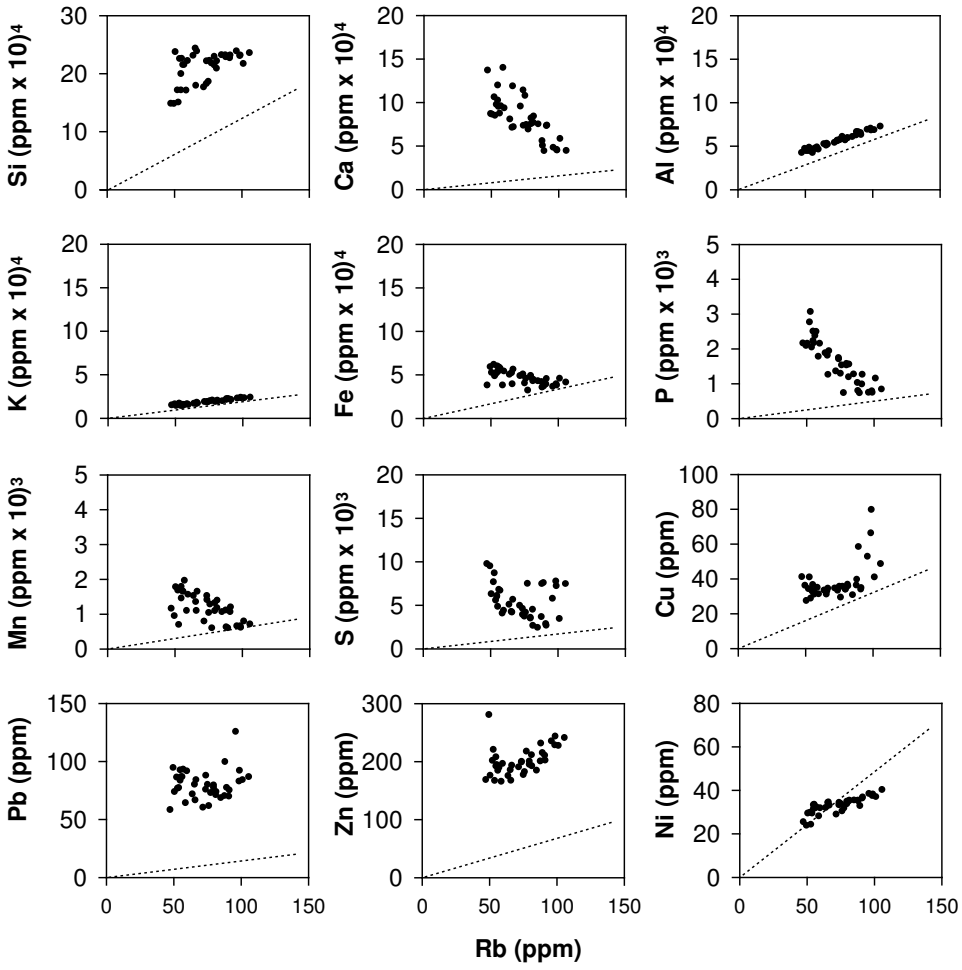

Figure 4.8: Correlation between selected element concentrations and Rb concentrations for sediments from the Peterstone 2 core. The dotted line indicates the Element/Rb ratio of the standard shale (Turekian and Wederpohl, 1961).

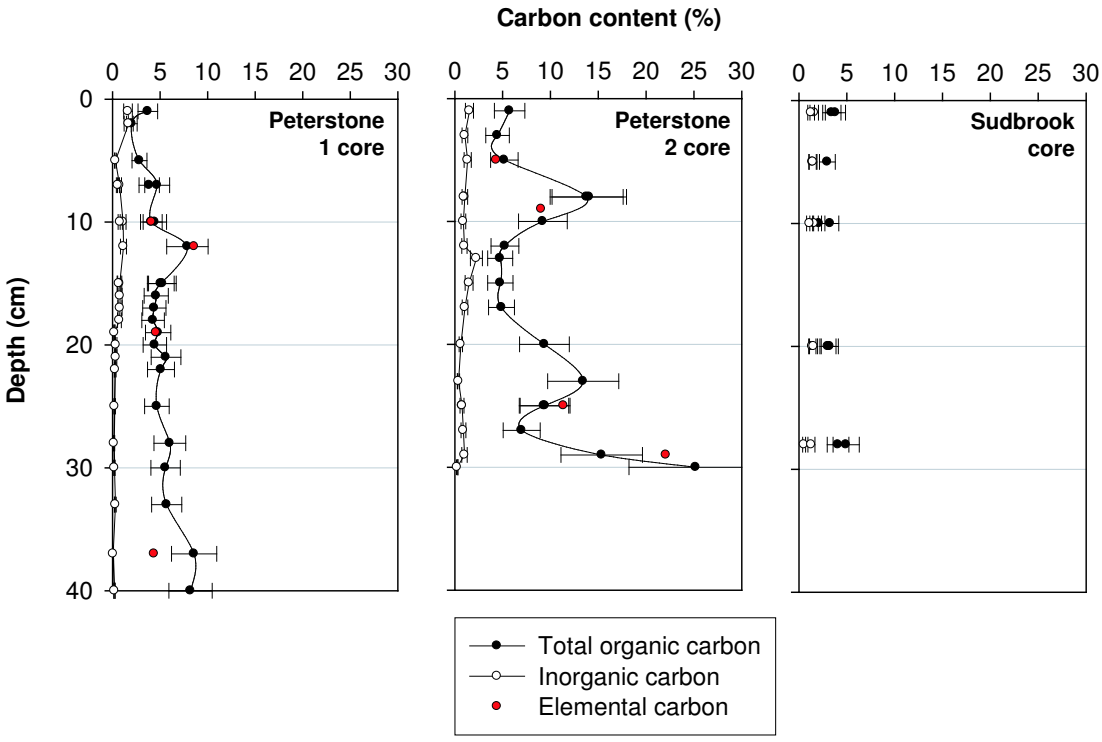

Figure 4.9: Variation in total organic carbon (TOC), inorganic carbon (IC) and elemental carbon (coal) content with depth in the Peterstone 1, Peterstone 2 and Sudbrook cores. TOC and IC were measured using coulometric techniques, and elemental carbon was calculated from the mass difference after aqua regia and hydrofluoric acid digestion. Uncertainties are shown to the 95 % confidence level (2σ).

of the standard shale, as in the Peterstone 1 and 2 cores,

CaO and Sr concentrations are used to indicate variations in the carbonate content of sediments, as IC was not directly measured using coulometry for the Barry Island core. CaO concentrations remain relatively constant with depth, apart from small peaks at 1 cm and 25 cm, and a significant trough at 23 cm depth (Figure 4.10). Sr concentrations are more irregular, and tend to decrease with depth. The second sandy clay layer at 20 - 25 cm depth has a significantly lower carbonate content than the rest of the sediments. In general, there is a significant difference in composition between the sediments above and below 17 cm depth (Figure 4.11).

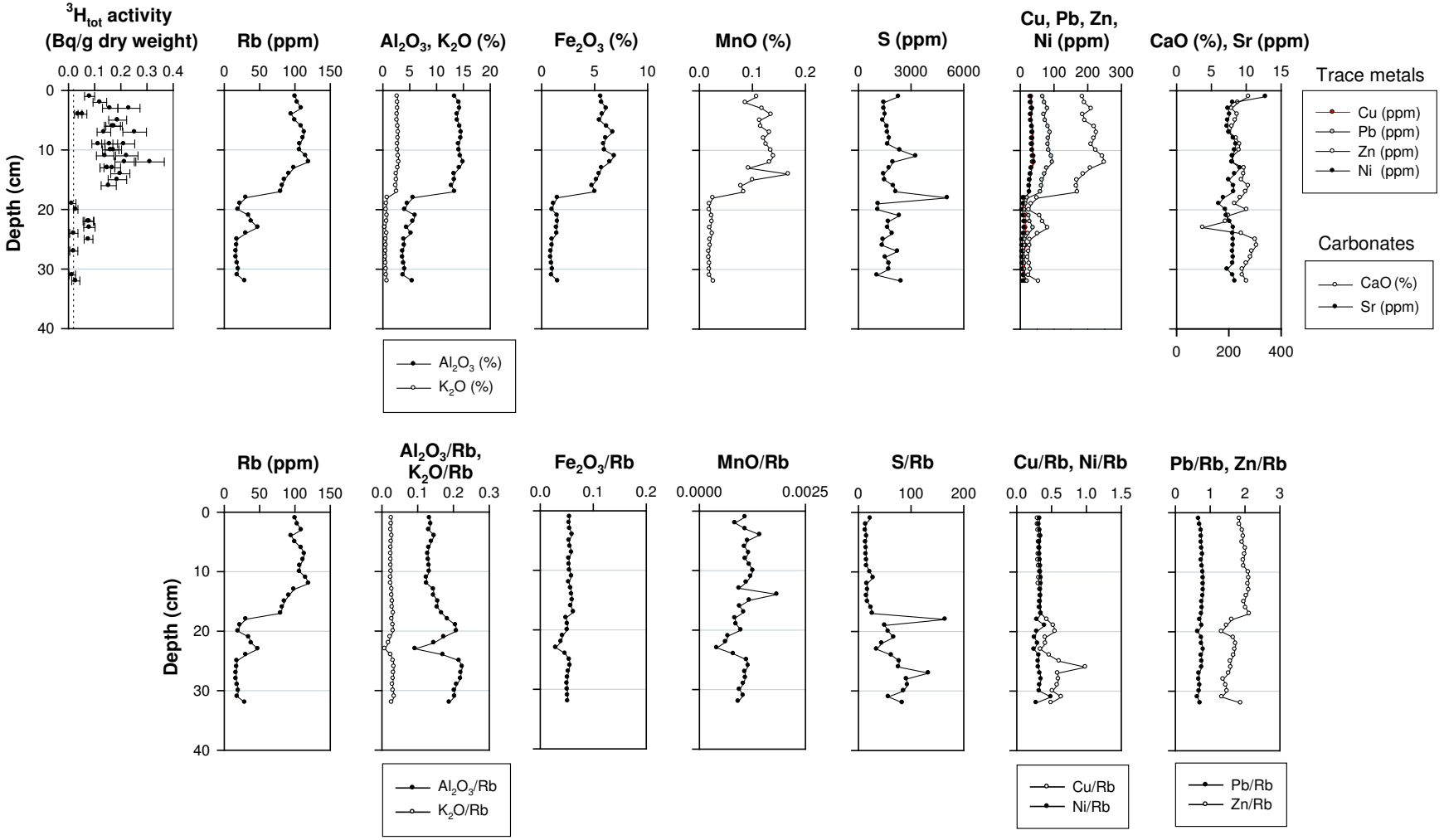

Figure 4.10: Variations in $^3H_{total}$ activities, Rb, CaO and Sr, and normalised Fe_2O_3, MnO, S and trace metals, with depth in the Barry Island core. Tritium activities are decay corrected to the date of sampling, total (method and counting statistical) uncertainties have been calculated to the 95 % confidence level and plotted as error bars. The dotted line indicates the limit of detection of the tritium analysis method. Uncertainties for major and trace element concentrations are normally contained within the data point.

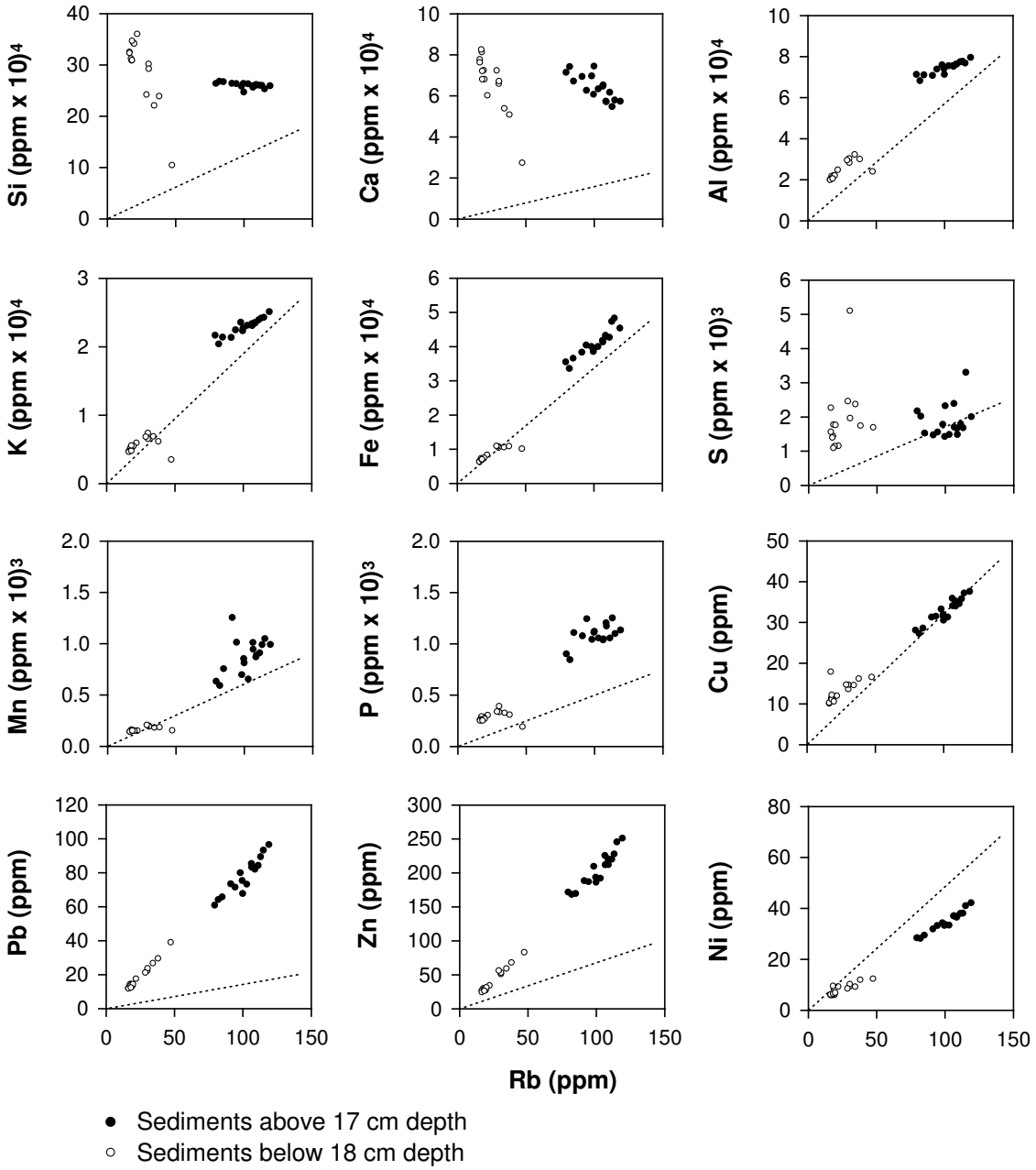

Figure 4.11: Correlation between selected element concentrations and Rb concentrations for sediments from the Barry Island core. The dotted line indicates the Element/Rb ratio of the standard shale (Turekian and Wederpohl, 1961).

Sudbrook core

In Sudbrook core sediments, Al_2O_3 and K_2O concentrations correlate well with Rb, and correspond closely to the Al/Rb and K/Rb ratios of the standard shale (Turekian and Wederpohl, 1961, Figure 4.13). Fe_2O_3, MnO and S concentrations vary with depth, but also correlate well with Rb (Figure 4.12). When normalised to Rb to remove any grain size effects, profiles of these redox-sensitive elements are constant with depth. Trace metal concentrations behave in a similar way (Figures 4.12 and 4.13); however, Pb and Zn are elevated relative to the Pb/Rb and Zn/Rb ratios of the standard shale (Turekian and

Wederpohl, 1961; Figure 4.13).

CaO and Sr concentrations tend to decrease gradually with depth, but the total organic and inorganic carbon contents, determined by coulometry, remain relatively constant with depth (Figures 4.12 and 4.9). However, the coal content of these sediments were not measured.

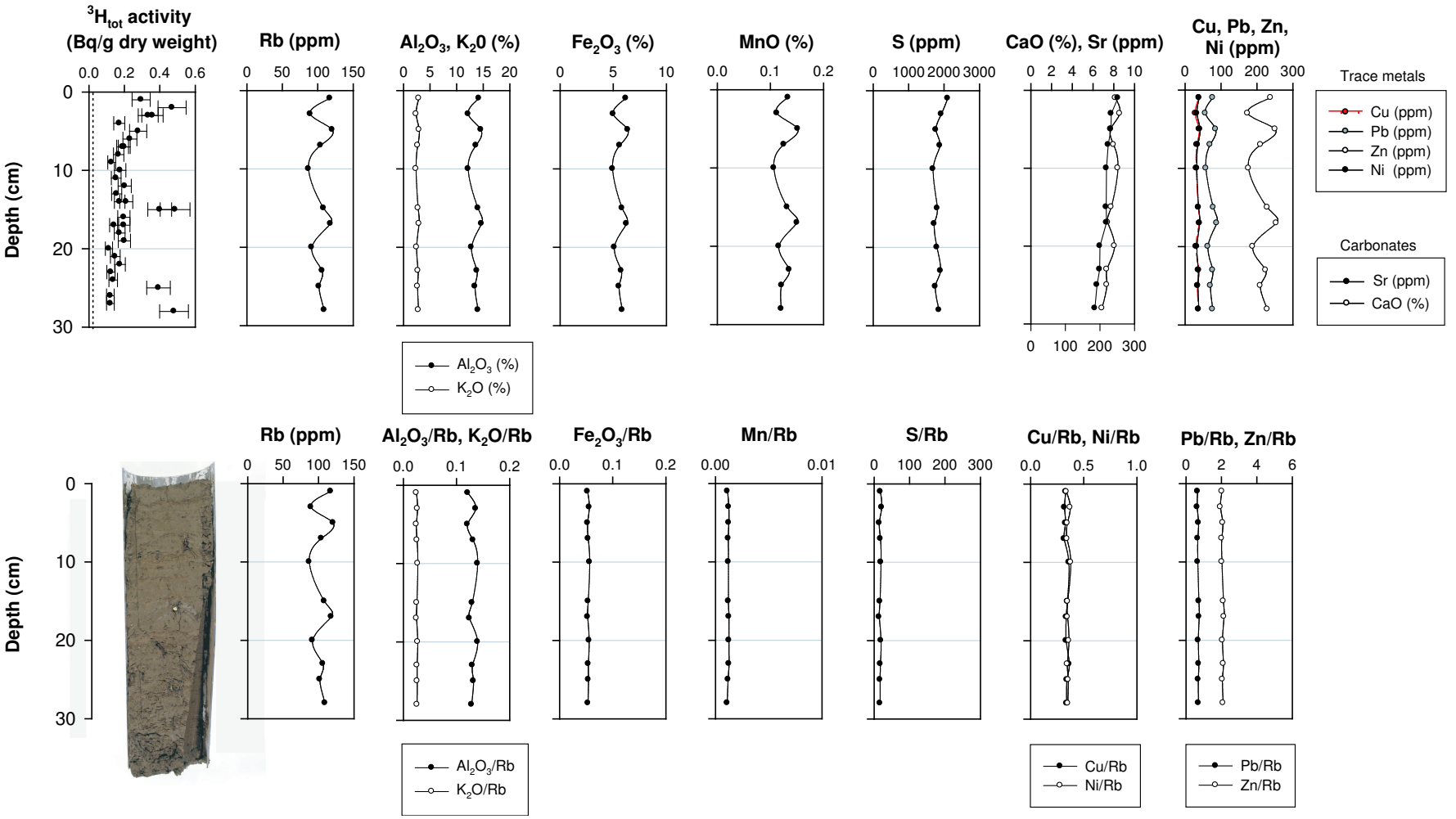

Figure 4.12: Variations in $^3H_{total}$ activities, Rb, CaO and Sr, and normalised Fe_2O_3, MnO, S and trace metals, with depth in the Sudbrook core. Tritium activities are decay corrected to the date of sampling, total (method and counting statistical) uncertainties have been calculated to the 95 % confidence level and plotted as error bars. The dotted line indicates the limit of detection of the tritium analysis method. Uncertainties for major and trace element concentrations are normally contained within the data point.

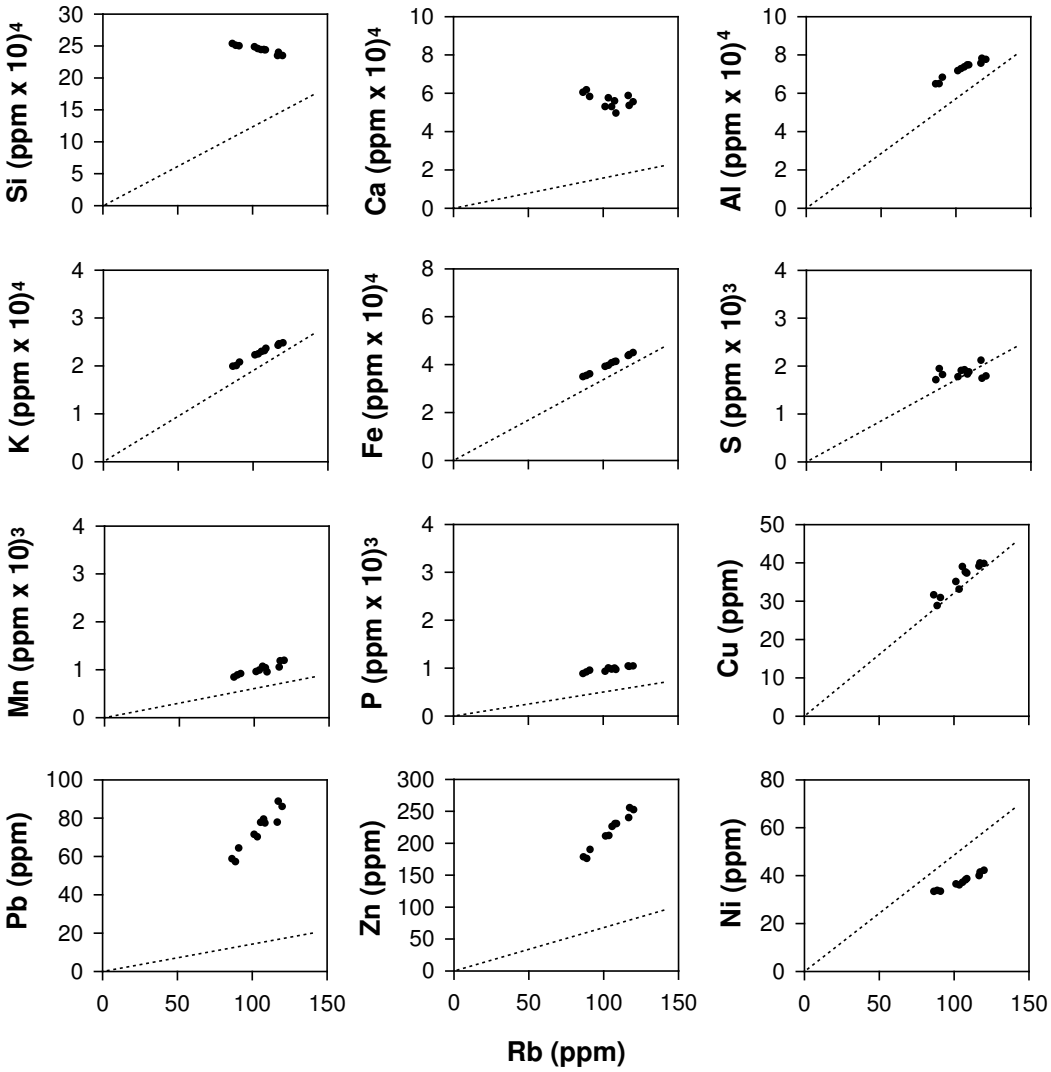

Figure 4.13: Correlation between selected element concentrations and Rb concentrations for sediments from the Sudbrook core. The dotted line indicates the Element/Rb ratio of the standard shale (Turekian and Wederpohl, 1961).

4.3.3 Gamma-emitting radionuclides

The radionuclides ^{210}Pb ($t_{\frac{1}{2}}$ = 22.6 years) and ^{137}Cs ($t_{\frac{1}{2}}$ = 30.3 years) are present in the Peterstone 1 and 2, Barry Island and Sudbrook cores (Figures 4.14, 4.15 and 4.16). ^{241}Am ($t_{\frac{1}{2}}$ = 432.2 years) is also present in Peterstone 1 core sediments (Figure 4.14). ^{210}Pb is a naturally occurring radionuclide, which in sediments is derived from two sources: 'supported' ^{210}Pb is produced in situ in the sediments by radioactive decay of the long-lived radionuclide ^{226}Ra; and 'excess' ^{210}Pb results from the atmospheric deposition of ^{210}Pb onto the sediment surface (Appleby and Oldfield, 1992). In contrast, ^{137}Cs and ^{241}Am are anthropogenic radionuclides. The sources of these radionuclides are further discussed in Section 4.4.3.

In the Peterstone 1 core, both total and excess ^{210}Pb activities are relatively constant

with depth (Figure 4.14). The total sediment ^{210}Pb activities are dominated by the supported ^{210}Pb activities, with excess ^{210}Pb activities lower than 10 Bq/kg in most samples. There are two peaks in ^{137}Cs activity, at 22 and 29 cm depth (Figure 4.14), and then a gradual decrease to base of the core. There is also a peak in ^{241}Am activities at 27 cm depth.

Total ^{210}Pb activities are also relatively constant with depth in the Peterstone 2 core, however excess ^{210}Pb activity concentrations have not been measured (Figure 4.14). The ^{137}Cs profile is variable, with activities varying between 10 and 20 Bq/kg down to 24 cm depth, and two sharp peaks at 28 and 32 cm.

In the Barry Island core, total ^{210}Pb activities vary between 40 and 60 Bq/kg to 17 cm depth before decreasing to ∼10 Bq/kg, apart from peaks at 22 - 23 cm and 32 cm depth (Figure 4.15). ^{137}Cs activities follow a similar trend. There are strong correlations between ^{137}Cs activities and Rb concentrations ($r^2 = 0.92$) and between ^{210}Pb activities and Pb concentrations ($r^2 = 0.82$) (Figure 4.15).

Although excess ^{210}Pb has not been measured, total ^{210}Pb activities remain relatively constant (at around 50 Bq/kg) in the Sudbrook core, apart from peaks at 2, 11, 19, 21 and 28 cm depth (Figure 4.16). ^{137}Cs activities are highest at the surface and variable with depth, with peaks at 5, 8, 16, 21, 24 and 26 cm. There is also a correlation between ^{137}Cs activities and Rb concentration ($r^2 = 0.67$) (Figure 4.16).

4.3.4 Tritium activities

All core sediment $^{3}H_{total}$ activities were decay corrected to the date of sampling. Sediment $^{3}H_{total}$ activities tend to decrease with depth in the Peterstone 1 core to below limit of detection levels (0.02 Bq/g dry weight) by 25 cm depth, except for a broad peak centred at 20 cm (Figure 4.17). In the Peterstone 2 core, sediment $^{3}H_{total}$ activities tend to be relatively constant (∼0.2 Bq/g dry weight) with depth, except for two broad peaks centred at 8 and 33 cm. Sediment $^{3}H_{total}$ activities are lower than limit of detection levels at the surface (1 cm depth) and below 19 cm depth in the Barry Island core; from 3 to 16 cm $^{3}H_{total}$ activities tend to be relatively constant (∼0.2 Bq/g dry weight). In the Sudbrook core, sediment $^{3}H_{total}$ activities tend to decrease with depth, apart from sharp peaks at 15, 25 and 28 cm depth, but activities are above limit of detection levels throughout the entire core.

4.4 Discussion

4.4.1 Sediment composition and depositional environments

Fine sediments The elements Al, K and Rb have been used as proxies for fine sediment in other studies (e.g. Allen and Rae, 1986; Zwolsman *et al*, 1993). Rb, a trace element that is a constituent of clay particles, has been found to correlate strongly with the <10 μm grain size fraction of salt marsh sediments from Tites Point in the Severn estuary (Allen, 1987c). As the fine sediment fraction in the estuary is relatively uniform (Section 3.3.4),

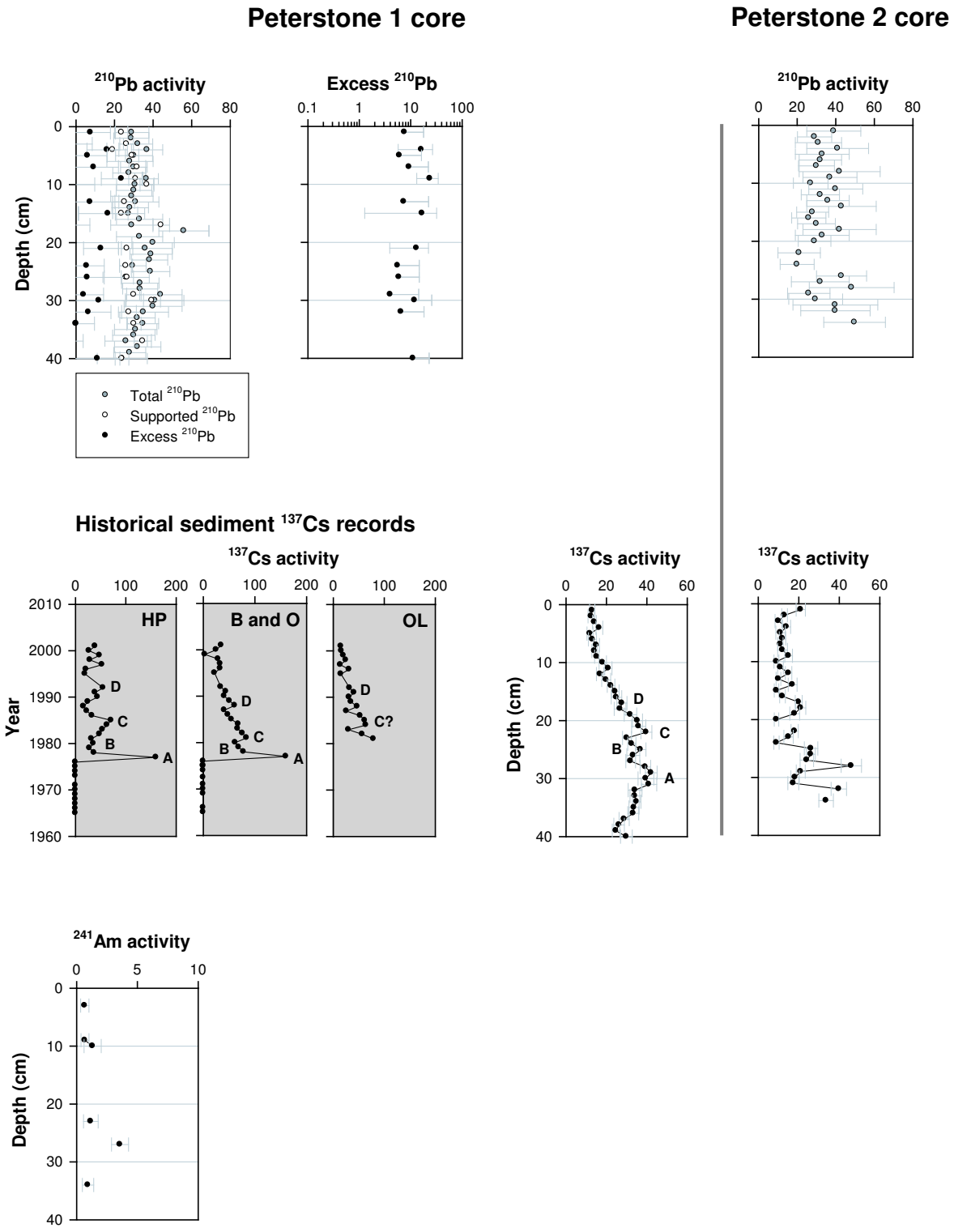

Figure 4.14: Variation in ^{210}Pb, ^{137}Cs and ^{241}Am activities (in Bq/kg dry weight) with depth in the Peterstone 1 and 2 cores. Error bars show counting statistical uncertainties to the 95 % confidence level (2σ). The Peterstone 1 core ^{137}Cs profile is compared with historical ^{137}Cs activities obtained from the environmental monitoring of sediments in the Severn estuary at Hinkley Point (HP), Berkeley and Oldbury (B and O) and Orchard Ledges (OL) (Camplin, 1992-5; FSA and SEPA, 1994-2001; Hunt, 1979-89; Mitchell, 1968-78). The rationale for identifying peaks A to D from the historical records in the Peterstone 1 core is justified in Section 4.4.3.

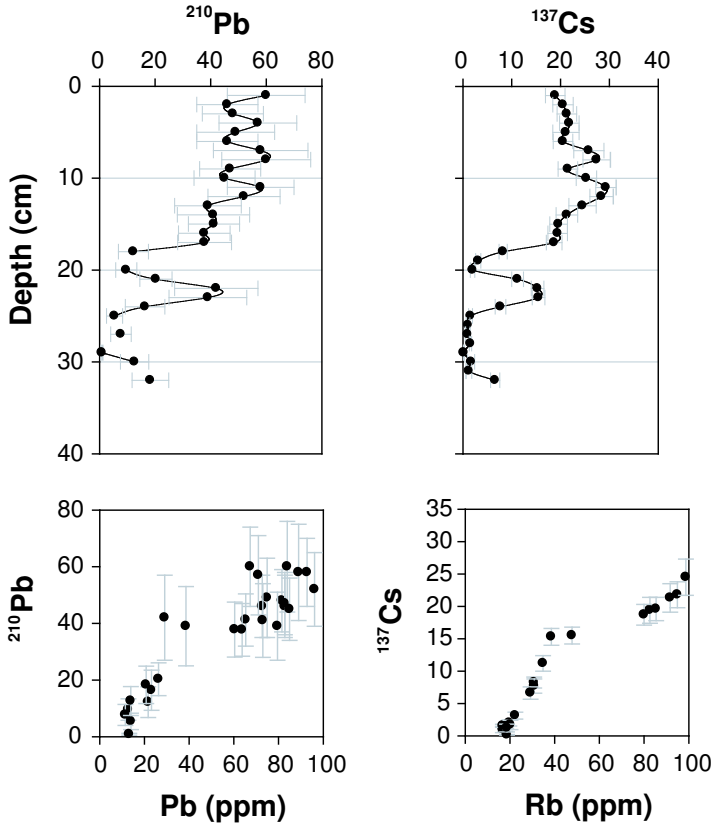

Figure 4.15: Variation in ^{210}Pb and ^{137}Cs activities (Bq/kg dry weight) with depth in the Barry Island core. Error bars show counting statistical uncertainties to the 95 % confidence level (2σ).

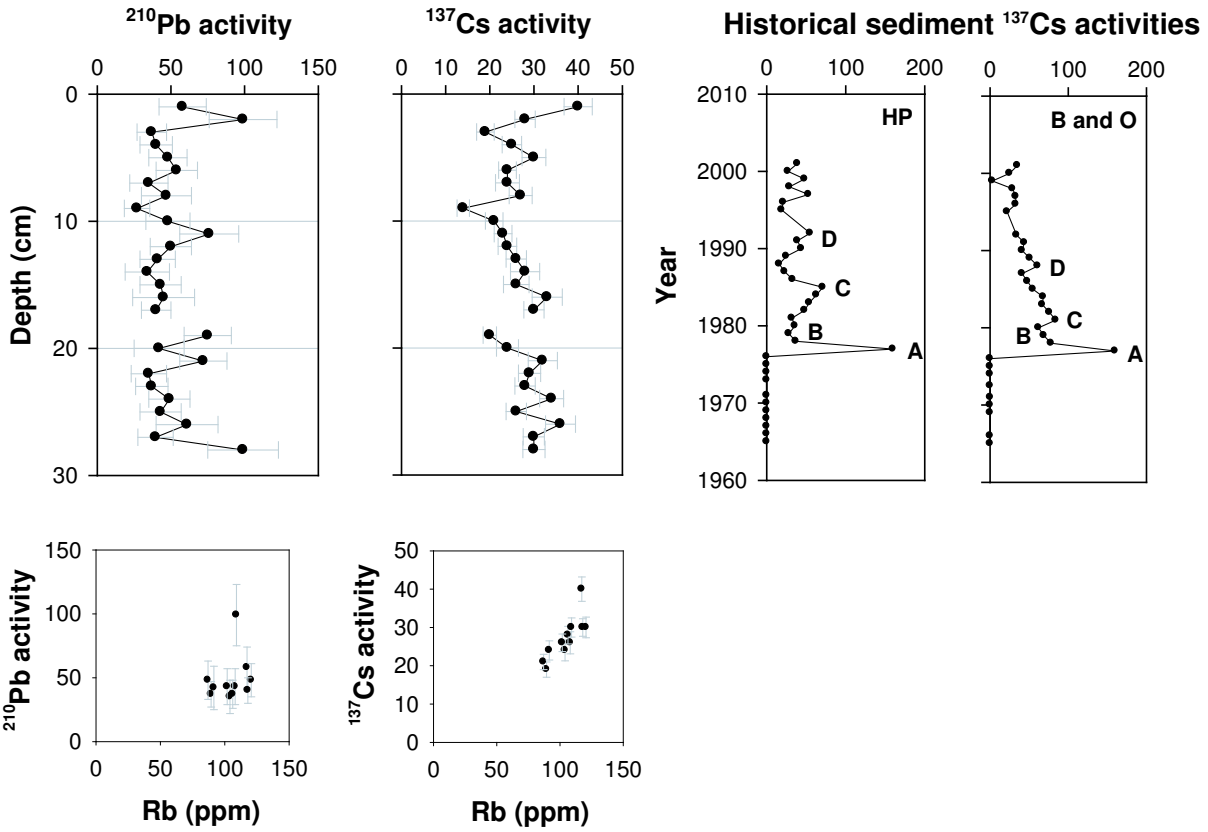

Figure 4.16: Variation in ^{210}Pb and ^{137}Cs activities with depth (Bq/kg dry weight) in the Sudbrook core. Error bars show counting statistical uncertainties to the 95 % confidence level (2 σ). The Sudbrook core ^{137}Cs profile is compared with historical ^{137}Cs activities obtained from the environmental monitoring of sediments in the Severn estuary at Hinkley Point (HP) and Berkeley and Oldbury (B and O) (Camplin, 1992-1995; FSA and SEPA, 1994-2001; Hunt, 1979-1989; Mitchell, 1968-1978).

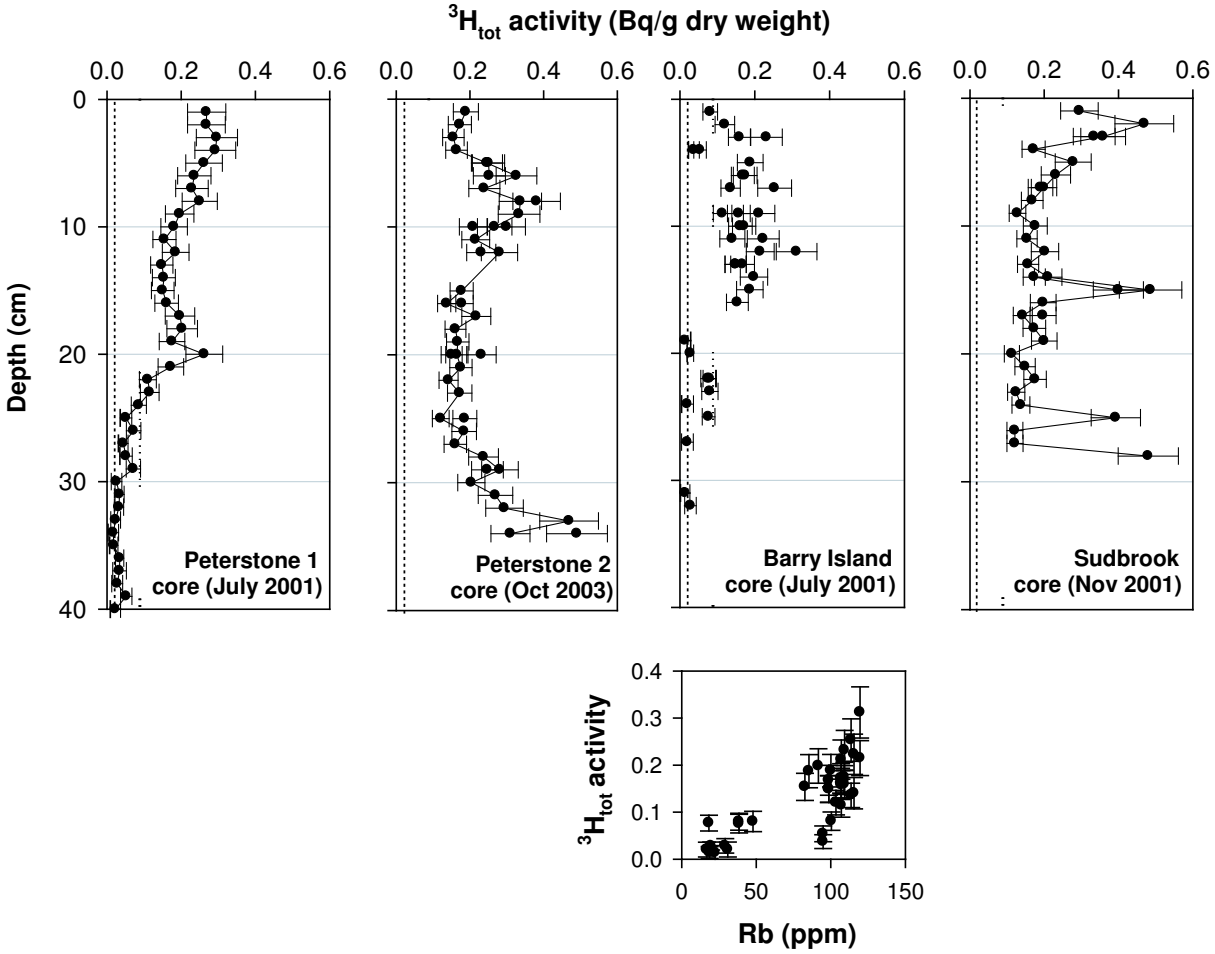

Figure 4.17: Sediment $^3H_{total}$ profiles for the Peterstone 1 and 2, Barry Island and Sudbrook cores. Sediment $^3H_{total}$ activities are decay corrected to the date of sampling and total (method and counting statistical) uncertainties have been calculated to the 95 % confidence level (2σ).

Rb can justifiably be used as a grain size proxy in the present study.

Rb profiles indicate that the proportion of fine sediment gradually increases with depth in the Peterstone 1 core (Figure 4.5). A change in depositional environment from mud flat to salt marsh has been inferred, from textural and compositional changes in the sediments, at 20 cm depth in the Peterstone 1 core and at 30 cm depth in the Peterstone 2 core. The Peterstone 2 core contains relatively homogeneous cohesive mud flat sediments down to 30 cm depth, where an irregular boundary probably marks an erosional surface, formed when mud flat sediments were scoured by tidal currents. Above this surface, crumbly non-consolidated sediments containing shells and abundant plant roots, have been deposited onto a developing salt marsh. Mixing or resuspension was probably restricted to sediments close to the surface, as there is no evidence for the physical mixing of the sediments by bioturbation or grazing.

In the Barry Island core, the transition from sand flat to salt marsh at 18 cm depth is inferred from Rb concentrations and field observations (Figures 4.10 and 4.11). A discrete layer of muddy sand, located at 20 - 25 cm depth may be a relict of an earlier patch of marsh, or a consolidated mud flat that developed on top of the sand flat and was later covered by it, prior to the formation of the present salt marsh. This layer contains high concentrations of salts (probably halite, as this has been identified in mud flat sediments from the estuary; Section 3.3.4), which reduces the concentrations of the other major elements.

In the Sudbrook core, sediments have been deposited entirely in a salt marsh environment, as they contain frequent small roots and have a crumbly, non-consolidated texture with a relatively constant proportion of fine sediment (Figures 4.4 and 4.12). Infrequent coarsening upwards sequences within the predominantly silty mud sediments are probably storm deposits (Figure 4.4). The preservation of these horizontal sandy layers indicates that the core sediments are not physically mixed by bioturbation or grazing. This variation in grain size was not, however, apparent in the Rb profile because it occurs over sub-cm scales and samples were only analysed for sediment composition at 5 cm intervals.

Trace metals Trace metals correlate well with Rb in sediments from the Peterstone 1, Barry Island and Sudbrook salt marshes, indicating that they are mainly associated with the fine sediment fraction (the adsorption of metals to sediments is a function of surface area; Jickells and Rae, 1997). Pb/Rb and Zn/Rb ratios are also elevated in all of the core sediments relative to the standard shale (Figures 4.6, 4.8, 4.11 and 4.13), as a result of either mineralisation associated with the Carboniferous South Wales coal field (Allen and Rae, 1986; Allen, 1987a; Waters and Lawrence, 1987) or anthropogenic inputs related to Zn smelting (EA, 2002; Hamilton *et al*, 1979).

Organic, inorganic and elemental carbon In the Peterstone 1 and 2 cores, the most prominent geochemical indicator of the transition between mud flat and salt marsh is the change in carbonate content of the sediments, as inferred from IC and CaO concentrations. Layers of intact shells in the Peterstone 2 core sediments, which seem to correlate with

peaks in CaO content, appear to be the main source of carbonate, although carbonates from rocks, sediments and soils in the catchment area are likely to be a minor component (Section 1.4.1). These shells all appear to be of the same species, indicating a low diversity population, and those in each layer are of a similar size (1 - 2 cm across), which probably indicates physical sorting prior to deposition. This is consistent with their emplacement as washover deposits during storms (similar to those observed by Allen and Pye (1992) in the Blackwater estuary, Essex). The discontinuous spatial distribution of these washover deposits could also explain the differences between the CaO profiles of the Peterstone 1 and 2 cores. Large but irregular inputs of carbonate from 31 cm depth are replaced above 17 cm depth by more regular inputs of carbonates inter-bedded with fine sediments. This may be due to the redeposition of eroded salt marsh sediments containing shelly material.

Thicker shell deposits are inferred in the Peterstone 2 core compared to the Peterstone 1 core, implying that sediment accumulation was non-continuous, because storm deposits accrete rapidly in comparison to the settling out of muddy sediments. The Peterstone 2 core may therefore have had a higher average accumulation rate than the Peterstone 1 core. This would explain both the deeper position of the transition from mud flat to salt marsh in the Peterstone 2 core (which was also collected 2 years later; Table 4.1) and the presence of above detection limit $^{3}H_{total}$ activities at a greater depth than in the Peterstone 1 core. However, it is not possible to assume that this transition from mud flat to salt marsh occurred synchronously in the two cores, and this boundary cannot therefore be used as a 'marker horizon' to date the Peterstone 2 core.

In the Barry Island core, CaO and Sr concentrations indicate that the carbonate content of sediments is relatively constant with depth, apart from a decrease between 20 and 25 cm depth. This decrease is an artefact of the increased salt content of the sediments in this muddy layer (known as the closed sum effect; Rollinson, 1993). The IC content of the sediments in the Sudbrook core is similar in magnitude to those at the bottom of the Peterstone 1 and 2 cores; however, no whole shells are observed in the core sediments, indicating that the sources of these carbonates are probably shell fragments and eroded limestones from rocks, soil and sediments in the catchment area. As the inorganic carbon content was only determined at 5 to 10 cm intervals, just limited interpretation is possible.

In contrast to the exponential decrease in TOC with depth generally observed in salt marsh sediments due to organic matter degradation (Allen, 2000), the TOC content of the Peterstone 1 core increases with depth, and appears to correlate with the elemental carbon (coal) content of sediments. This indicates that the measured TOC content is predominantly controlled by coal content, which may increase with depth due to historically higher inputs of coal, from mining and industrial activity, into the estuary. Therefore, TOC is not a reliable indicator of the unlithified carbon content of sediments from the Severn estuary. In contrast, surface TOC values of 2 - 3 %, falling gradually with depth, have been measured in Severn estuary salt marsh sediments (Rae and Allen, 1993), using a method for TOC determination that did not include elemental carbon (Gaudette *et al*, 1974).

In the Peterstone 2 core, peaks in TOC concentration at 8, 23 and 30 cm depth may

have been produced by woody roots (seen in the top 12 cm of the core) or large coal fragments (observed at 20, 25 and 32 cm depth) (Figure 4.3), however, minor roots and particulate coal are abundant throughout the Peterstone 2 core. The TOC content of Peterstone 2 core sediments is reasonably constant, at around 5 %, in the rest of the core; this may be produced by particulate coal and minor roots.

In the Sudbrook core, the TOC content is lower and less variable than in either of the Peterstone cores (Figure 4.9), probably because only thin plant roots and particulate coal are observed (Figure 4.4). However, samples were only measured for TOC at 5 cm intervals.

4.4.2 Post-depositional changes

The composition of sediments can also be affected by post-depositional changes, including redox-related mobilisation and reprecipitation of elements and organic matter biodegradation and related mobilisation of organic-phase metals (Rae and Allen, 1993) and other elements.

In the Peterstone 1 core, concentrations of the redox-sensitive elements Fe, Mn and S decrease slightly from the surface to 18 cm depth; this decrease becomes more pronounced after the elements are normalised to Rb to remove grain size effects. Below 18 cm depth, these concentrations are relatively constant, indicating that the Peterstone core is oxic throughout and contains no redox boundaries. The Sudbrook core also contains no variation in normalised Fe_2O_3, MnO and S concentrations, and no changes in depositional environment or sediment colour are apparent in Figure 4.4. This core is therefore oxic, with no remobilisation of redox-sensitive elements or trace metals. In contrast, there are sharp peaks in the Fe_2O_3/Rb, MnO/Rb and S/Rb profiles at 24 and 30 cm depth in the Peterstone 2 core (Figure 4.7). These peaks may have been produced by the change in depositional conditions at 30 cm depth (Figure 4.3). If this were the case, different Fe_2O_3, MnO and S concentrations would be expected in the salt marsh and mud flat sediments, following normalisation to Rb to remove the effect of any differences in grain size. Instead of this, clear peaks in the concentrations of redox-sensitive elements are observed at and above the boundary. This distinction would not be expected because the fine sediment population of the estuary has a consistent composition that reflects the composition of source rocks, soils and sediments from the estuary catchment (Hamilton *et al*, 1979) and is well mixed (Section 3.3.4).

The transition from mud flat to salt marsh is also accompanied by a change in the texture of the sediments, from consolidated muddy sediments to crumbly sediments containing abundant shells and roots, and desiccation cracks which may allow exchange between the sediments and either water or air (Allen and Duffy, 1988a; Jickells and Rae, 1997; Rae and Allen, 1993). This transition may therefore have led to a change in redox conditions; the accompanying colour change of the sediments, from red-brown to grey, at 30 cm depth (Figure 4.3), may therefore be due to the production of sulphides in a reducing environment (e.g. Lee and Cundy, 2001). Another peak in the Fe_2O_3/Rb, MnO/Rb and S/Rb profiles at 24 cm depth, which is within sediments deposited in a

salt marsh environment, may represent the top of a sub-oxic zone, or the top of a zone of oscillating redox conditions, with oxic conditions above this depth. This suboxic zone may be produced by a decrease in abundance of roots, especially the thicker woody roots which can produce channels that allow air and water to penetrate the sediments, below 20 cm depth.

Trace metals are also susceptible to early diagenetic remobilisation and precipitation at redox boundaries, and Cu, Ni, Pb and Zn concentrations all peak at 24 and 30 cm depth when normalised to Rb. These elements have mainly been supplied from regional sources, including industrial discharges and mineralisation associated with the Carboniferous South Wales coalfield; however, the presence of this remobilisation implies that trace metal concentrations in this core will not provide a reliable record of historical inputs into the estuary.

In the Barry Island core, there are sharp peaks in the S/Rb profile at 18 and 27 cm depth, in the MnO/Rb profile at 3 and 14 cm depth, and a sharp decrease in the normalised Fe_2O_3, MnO and S profiles at 23 cm depth. A decrease in Rb concentration at 17 cm depth marks the transition from a sand flat to a salt marsh depositional environment, representing a significant change in sediment composition. The sharp peaks at varying depths for MnO and S indicate that there has been redox-related remobilisation and redeposition of these elements in this core as well. However, the element distributions are more complex than in the Peterstone 2 core, probably as a result of the compositional change from mud to sand.

Organic matter degradation can also produce post-depositional changes in sediment composition; however, it has not been possible to determine its effects on the core sediments discussed above because the unlithified organic matter content of the sediments was not measured in the present study.

4.4.3 Dating the salt marsh cores

In previous studies, ^{210}Pb, ^{137}Cs and ^{241}Am (with half-lives of 22.6 years, 30.3 years and 432.2 years, respectively (Mills *et al*, 1988)) have been used to determine sediment accumulation rates in salt marshes (e.g. Delaune *et al*, 1978; French *et al*, 1994; Plater and Appleby, 2004).

^{137}Cs was released into the atmosphere in the northern hemisphere by nuclear weapons testing that peaked in 1963, and by the Chernobyl accident in 1986. It has also been discharged into the marine environment from the nuclear fuel reprocessing plants in Cumbria and La Hague, and the nuclear power stations at Hinkley Point, Berkeley and Oldbury (Figure 4.1). There are, therefore, a number of potential sources of ^{137}Cs into the Severn estuary, which range widely in both magnitude and transport distance, making it difficult to accurately reconstruct the historical inputs into the sediments. However, annual environmental monitoring records of surface sediment ^{137}Cs activities are available, from 1966 to the present day, for two sites in the estuary (Camplin, 1992-95; FSA and SEPA, 1994-2001; Hunt, 1979-89; Mitchell, 1968-78); these data provide an accurate historical record for comparison with the salt marsh core ^{137}Cs profiles (Figure 4.14 and 4.16).

The radionuclide ^{241}Pu ($t_{\frac{1}{2}} = 14.4$ years) was released by atmospheric weapons testing, which peaked in 1963, and both ^{241}Pu and the daughter radionuclide ^{241}Am are released directly by the nuclear fuel reprocessing plants at Sellafield and La Hague (where ^{241}Am discharges peaked in 1974 and 1986, respectively; Gray *et al*, 1995).

Peterstone 1 core Total, supported and excess ^{210}Pb activities are relatively constant with depth in the Peterstone 1 core and, because the core is oxic, the profile is not affected by migration as a result of redox changes (Figure 4.14). Several models for dating recent sediment cores using ^{210}Pb have been developed by Appleby and Oldfield (1992), and applied to salt marshes in the Severn estuary by French *et al* (1994) and Allen (1991). However, as these models for dating sediment cores using ^{210}Pb explicitly assume decreasing concentrations of excess ^{210}Pb with depth (Appleby and Oldfield, 1992), they are not applicable to the Peterstone 1 core.

Supported ^{210}Pb activities dominate the total sediment ^{210}Pb activities in the Peterstone 1 core, with excess ^{210}Pb activities below 10 Bq/kg in most samples (Figure 4.14). The low excess ^{210}Pb activities may be produced by the relatively high influx of suspended sediments onto the marsh, compared to atmospheric or biogenic deposition. As the estuary is a well-mixed, dynamic system with a high suspended sediment load (Section 1.4.2), and the suspended sediments are derived from both fresh and resuspended sources with a range of ^{210}Pb activities, the mixture of sediments deposited onto the marsh surface will have low excess ^{210}Pb activities. Relatively consistent trace metal concentrations throughout the core are a further indication that the sediments are well mixed prior to deposition. In contrast, the peaks in ^{137}Cs and ^{3}H profiles (which both have time-varying inputs into the estuary), and the structured Ca and Sr profiles, imply that the core has not been physically mixed after deposition.

Both the Peterstone 1 core and the historical sediment ^{137}Cs profiles exhibit two broad peaks, followed by a decline in ^{137}Cs activities to the surface or present day (Figure 4.14). Whereas in the historical records ^{137}Cs peaked sharply at A, the decrease in ^{137}Cs activities below A in core sediments is much more gradual. However, above peak A, core ^{137}Cs activities are similar in magnitude to the historical sediment record. This indicates downward diffusion of ^{137}Cs from peak A in core sediments, rather than sediment mixing, because the peak is reduced in magnitude but is still well-defined. Because the Peterstone 1 core has remained oxic at depth there cannot have been any redox-induced mobilisation of ^{137}Cs (Comans *et al*, 1989; Milan *et al*, 1995). In the historical record, the first peak (A) in 1977 was produced by the delayed arrival of a significant peak in discharges from Sellafield in 1973, in comparison to which the releases from local nuclear power stations were relatively minor (Figure 4.18). Prandle (1984) modelled ^{137}Cs dispersion from Sellafield (then Windscale) and La Hague; discharges from both sites reached the Severn Estuary after a transport time of 3.5 years. This produces a lag in the sediment ^{137}Cs activity profiles in the Severn estuary compared with the discharge profile from Sellafield (Figure 4.18); ^{137}Cs activities reaching the Severn estuary will also be lower in magnitude than those discharged as a result of dispersion into the North Sea and Irish Sea. Fallout

^{137}Cs activities from Chernobyl onto South Wales were relatively low (0.1 - 1 kBq/m^2, Clark and Smith, 1988). Therefore the second peak (C), which occurred between 1981 and 1985 depending on the location of the monitoring site, is probably related to discharges from the local nuclear power stations at Hinkley Point, Berkeley and Oldbury (Baxter and Camplin, 1993; Figure 4.18).

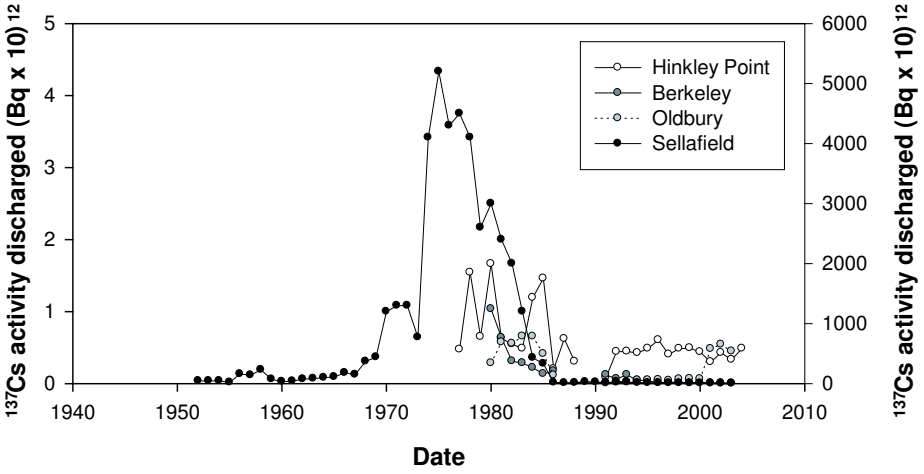

Figure 4.18: Variations in the magnitude of ^{137}Cs activities (in Bq x 10^{12}) with time from Sellafield, Hinkley Point, Berkeley and Oldbury (compiled from Baxter and Camplin, 1993; Camplin, 1992-1995; FSA and SEPA, 1996-2004; Gray *et al*, 1995).

The peaks in the historical sediment record have been used to ascribe dates to the corresponding peaks in the Peterstone 1 core (Table 4.2). These dates imply an average sediment accumulation rate of 1.3 cm/year, which is comparable with accumulation rates for salt marshes in the Severn estuary calculated by other workers, using a range of dating methods (e.g. 0.4 cm/year for the Wentlooge Formation (Figure 1.10) at sites in the Inner estuary, 20 km downstream from Gloucester, from Allen, 1991; 1.1 cm/year (for the Northwick Formation, from French, 1996).

The peak in ^{241}Am activities at 27 cm depth in the Peterstone 1 core may be linked to the maximum discharges into the environment from atmospheric weapons testing, Sellafield or La Hague. As Am is trivalent under both reducing and oxidising conditions, it is unlikely to be affected by post-depositional mobility (Appleby *et al*, 1991); therefore if the origin of the ^{241}Am peak could be identified and a date established, then it could be used to support the ^{137}Cs-derived chronology. Unfortunately, environmental ^{241}Am activities in Severn estuary sediments have not been monitored, and although the source of the peak could be identified by Pu isotopic analysis (weapons fallout and fuel reprocessing Pu have different ^{240}Pu/^{239}Pu isotope ratios; Warneke *et al*, 2002), this was beyond the scope of the present study. As transport times for ^{137}Cs from both Sellafield and La Hague are $\sim$ 3.5 years (Prandle, 1984), the peak in ^{241}Am activities may correspond to either 1978 or 1989 respectively. A date of 1978 would be in reasonable agreement with the chronology obtained from the ^{137}Cs profile; however, the source of ^{241}Am to the Severn estuary needs to be identified in order to confirm this chronology.

Table 4.2: Comparison of the age of features in the ^{137}Cs environmental monitoring record with the Peterstone 1 core ^{137}Cs profile (Figure 4.14), including equivalent dates for the features from the core.

Code	Description of feature	Site	Date/depth	Equivalent date
A	Initial peak in discharges	Hinkley Point	1977	
		Berkeley and Oldbury	1977	
		Peterstone 1 core	30 cm	1977
B	Trough following initial peak	Hinkley Point	1979 - 1981	
		Berkeley and Oldbury	1980	
		Peterstone 1 core	23 - 27 cm	1979-81
C	Second major peak	Hinkley Point	1985	
		Berkeley and Oldbury	1981	
		Cardiff	1981?	
		Peterstone 1 core	22 cm	1981-1985
D	Decline in activities to present day	Hinkley Point	1992	
		Berkeley and Oldbury	1988	
		Cardiff	1990	
		Peterstone 1 core	18 cm	1988-1992?

Peterstone 2 core In the Peterstone 2 core, although there are large uncertainties associated with the total ^{210}Pb activity concentrations, they tend to stay relatively constant with depth (Figure 4.14). Therefore, although the excess ^{210}Pb profile was not measured, it probably would not satisfy the requirements for ^{210}Pb dating (Appleby and Oldfield, 1992). In contrast, there are sharp peaks in ^{137}Cs activity concentrations at 28 and 32 cm depth as Cs is mobile in anoxic conditions (Benoit and Hemond, 1991; Comans *et al*, 1989), these peaks may have been produced by early diagenetic remobilisation and re-precipitation around the anoxic/sub-oxic zone boundary at 30 cm depth, rather than reflecting historical variations in ^{137}Cs activities. These uncertainties mean that it is not possible to establish a chronology for the Peterstone 2 core using radiometric dating.

Barry Island core In the Barry Island core, ^{210}Pb and ^{137}Cs activities are significantly lower in the sandy sediments than in the clay rich sediments. ^{210}Pb activities and Pb concentrations determined by XRF are related (Figure 4.15), as are ^{137}Cs activities and Rb concentrations ($r^2 = 0.93$). Although the correlations are not linear, they do indicate that the concentrations of γ-emitting radionuclides are compositionally controlled and, therefore cannot be used to date the Barry Island core.

Sudbrook core In the Sudbrook core, total ^{210}Pb activities are higher than in the Peterstone or Barry Island cores, and do not correlate with Rb concentrations ($r^2 = 0.10$). However, the total ^{210}Pb profile is still relatively constant with depth and, although excess

^{210}Pb was not measured, the sediment composition, and therefore the supported ^{210}Pb activities, do not vary significantly in this core. Therefore, the assumptions of the dating model were not met and the ^{210}Pb profile could not be used to date the core

There is, however, an apparent correlation between the ^{137}Cs activity profile of the Sudbrook core and the historical sediment ^{137}Cs record from the Berkeley and Oldbury site (Figure 4.16). This would date the base of the core (at 28 cm) as approximately 1980, and the peak in ^{137}Cs activity at 16 cm depth (labelled D) as 1988. However, there is also a correlation between the ^{137}Cs activities and Rb concentrations of the sediments (where measured, $r^2 = 0.67$), indicating that there may be some compositional control on ^{137}Cs activities; therefore, without independent confirmation the ^{137}Cs activity profile cannot be used to establish a chronology for the Sudbrook core.

4.4.4 Factors controlling tritium accumulation in salt marsh sediments

Changes in inputs of organically bound tritium, sediment composition or changes in depositional and post-depositional environments may affect the accumulation of tritium in the salt marsh sediments.

Organically bound tritium discharges from Amersham plc Using the chronology established for the Peterstone 1 core from the ^{137}Cs profile (Section 4.4.3), the dated sediment $^{3}H_{total}$ activity profile can be compared with the decay-corrected Amersham plc organically bound tritium discharge record (Williams, 2003, Figure 4.19).

1. Amersham plc began discharging organic ^{3}H in 1981, and $^{3}H_{total}$ activities are around limit of detection levels (0.02 Bq/g dry weight) in sediments deposited before 1982. This may indicate that there has been limited diffusion of ^{3}H down the core.

2. A rapid increase in the magnitude of organic ^{3}H discharges from Amersham plc up to 1985 corresponds with a rapid increase in sediment $^{3}H_{total}$ activities from 1981 to 1985.

3. The peak in $^{3}H_{total}$ activities in sediments deposited in 1985 correlates with the peak in Amersham plc discharges from 1984 to 1986.

4. Organic ^{3}H activities from Amersham plc decreased to a low in 1990. Sediment $^{3}H_{total}$ activities also correspondingly decrease.

5. Later increases in sediment $^{3}H_{total}$ activities (from 1997 to 2000) corresponds with an increase in Amersham plc OBT discharges in 1998. Following this, both Amersham plc OBT discharges and Peterstone 1 core $^{3}H_{total}$ activities declined.

In the Peterstone 1 core, the correlation between the sediment $^{3}H_{total}$ profile and the decay-corrected Amersham plc organically bound tritium discharge record indicates that there has been little post-depositional remobilisation of ^{3}H in the core sediments. However, measurable ^{3}H activities in sediments deposited before 1982 may be the result of limited diffusion of ^{3}H at depth. As the core has not been physically mixed (Section

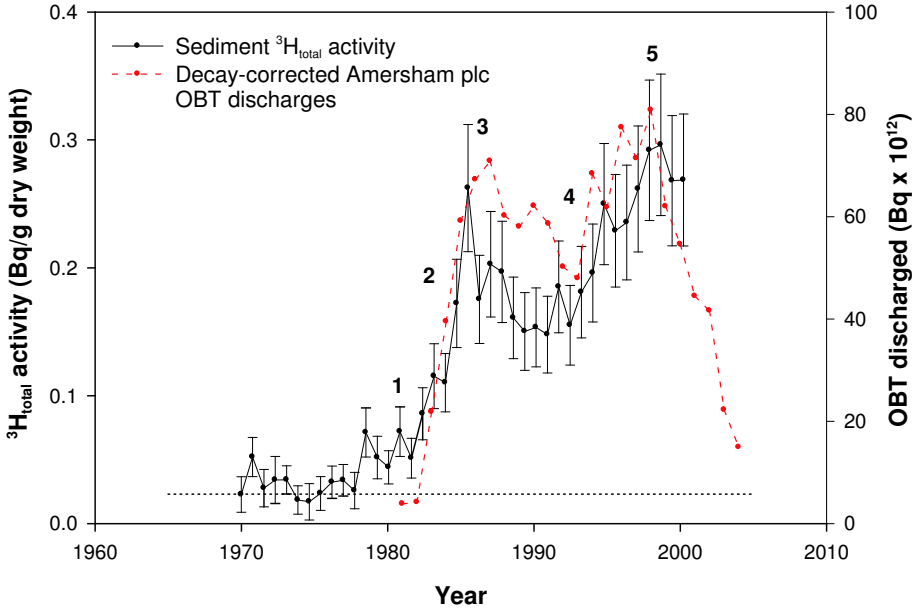

Figure 4.19: Comparison between sediment $^3H_{total}$ activities in the Peterstone 1 core, dated using the ^{137}Cs profile (Section 4.4.3) and the decay corrected organic tritium discharge record from Amersham plc. Sediment $^3H_{total}$ activities are decay corrected to the date of sampling and total uncertainties were calculated to the 95 % confidence level (2σ). The dotted line indicates the limit of detection of the tritium analysis method. The numbers correspond to points in the interpretation above (on page 147).

4.4.3), this diffusion may be the result of limited post-depositional remobilisation of ^3H by organic matter degradation in older sediments.

In the Peterstone 2 core, there are high $^3H_{total}$ activities in sediments throughout the core (Figure 4.17). Although it has not been possible to date this core, which was collected 2 years after the Peterstone 1 core (Table 4.1), because the ^{210}Pb and ^{137}Cs profiles have probably been affected by post-depositional remobilisation, the presence of above limit of detection $^3H_{total}$ activities throughout the core implies that the sediments at its base were deposited after 1981. This would imply that the Peterstone 2 core has a higher average sediment accumulation rate than the Peterstone 1 core, which could result from the emplacement of thicker, and possibly more regular, storm overwash deposits compared to the Peterstone 1 core. Currently, however, the stability of sediment-bound tritium has yet to be established under anoxic conditions.

Sediment composition and depositional environments The poor correlation between sediment $^3H_{total}$ activities and Rb and CaO concentrations in both the Peterstone 1 and 2 cores indicates that there is no relationship between the $^3H_{total}$ activities and either the clay or carbonate content of the sediments. Although some of the organically bound tritium may be associated with organic matter in the sediments, it was not possible to confirm this because the unlithified organic carbon content of the sediments was not measured.

The peak in sediment $^3H_{total}$ activities centred at 20 cm depth in the Peterstone

1 core is concurrent with the peak in CaO concentrations that indicates the boundary between salt marsh and mud flat environments. However, the peak in $^3H_{total}$ activities at 20 cm depth is relatively broad, whereas the transition from mud flat to salt marsh is relatively sharp, suggesting that the $^3H_{total}$ activity peak is not a direct response to the change in depositional environment. There is also no relationship between the $^3H_{total}$ activity profile and the transition from mud flat to salt marsh in the Peterstone 2 core. The gradually declining $^3H_{total}$ activities below 20 cm depth may have been produced by either the accumulation and consolidation of sediments with increasing $^3H_{total}$ activities onto the mud flat surface, or by the mixing of sediments in the more dynamic mud flat environment, which may have produced the gradual decline in activities with depth below 20 cm.

The accumulation of tritium will be affected by any changes in sediment deposition or erosion. Sediment is deposited and eroded regularly on mud flats (depending on wind and tides) because there is no vegetation to trap or bind the particles, whereas the salt marsh surface is more stable; it is inundated less frequently so less sediment is deposited but less is also eroded. This generally leads to a steadier accumulation rate, although irregular storm deposits, such as those observed in the Peterstone 2 core sediments, can dominate sedimentation on some salt marshes (Nyman *et al*, 1995).

In the Barry Island core, sediment $^3H_{total}$ activities correlate strongly with Rb concentrations, which are higher in muddy salt marsh sediments and lower in sandy sediments (Figure 4.17); therefore, the tritium profile in the Barry Island core is predominantly controlled by the sediment composition. A similar effect is observed in the surface sediments at Site 2, where coarser sediments result in significantly lower $^3H_{total}$ activities (Figure 3.4). The record of OBT discharges from Amersham plc would consequently only be preserved in the salt marsh sediments. Lower sediment $^3H_{total}$ activities in the top 4 cm of the Barry Island core may be related to the recent decrease in magnitude of Amersham plc discharges, as this decrease is also observed at the top of the Peterstone 1 core, which was collected at the same time.

In the Sudbrook core there was no change in depositional environment with depth.

Post-depositional changes Peterstone 1 core sediments that were deposited before the discharges started in 1981 (Figure 4.17) have $^3H_{total}$ activities that are around the limit of detection (0.02 Bq/g dry weight), indicating that there is limited diffusion of tritium at depth by organic matter degradation, and therefore that redox changes are not significant factors controlling the $^3H_{total}$ activity profiles in the Peterstone 1 and 2 cores. However, more work is required to determine both the types of OBT present and the degree to which organic matter degradation has affected $^3H_{total}$ activities in these sediments.

The effect on the sediment $^3H_{total}$ activity profile of a change from oxidising to reducing conditions depends on whether this change accelerates the degradation of the tritiated organic molecules, producing soluble or gaseous compounds. The observed change in oxidation state in the Peterstone 2 core would be accompanied by a switch from aerobic to

anaerobic bacteria, which metabolise different terminal electron acceptors . In general, aerobic bacteria are better at breaking down large, complex and refractory organic molecules because oxygen also acts as a catalyst (Kristensen *et al*, 1995), so a change to a reducing environment may actually retard degradation of OBT. However, in fluctuating redox conditions, which are common in intertidal sediments due to alternating wet and dry conditions, there is an increase in the decomposition potential of benthic microbial communities compared with stable oxic or anoxic conditions (Aller, 1994). This can encourage the decomposition of refractory organic carbon that is resistant to degradation under stable conditions.

Sediment composition is the predominant control on sediment $^{3}H_{total}$ activities in the Barry Island core, there are no apparent effects on the sediment $^{3}H_{total}$ profile from the complex redox potential changes or organic matter degradation.

When the ^{137}Cs activity profile for the Sudbrook core is compared with historical environmental monitoring ^{137}Cs records, the base of the core is dated to approximately 1980. However, this comparison is probably invalid because ^{137}Cs activities are compositionally controlled. Assuming that tritiated sediments are not mobilised after deposition, the presence of above limit of detection $^{3}H_{total}$ activities throughout the core confirms that all of the sediments in this core were deposited after Amersham plc began discharging organic ^{3}H in 1981.

The sediment $^{3}H_{total}$ activity profile of the Sudbrook core do not resemble those of the Peterstone cores. Although in the Peterstone 1 core and Sudbrook cores there is a general decline in $^{3}H_{total}$ activities with depth, the peaks in the Sudbrook core profile are sharper. As the dominant direction of transport of labelled sediments from the Amersham plc discharge point was to the west, it is possible that periods of rapid sediment accumulation, such as storm deposits, on the Sudbrook salt marsh coincided with higher suspended sediment $^{3}H_{total}$ activities, producing discrete peaks in the $^{3}H_{total}$ profile.

4.5 Summary

The Peterstone salt marsh accreted over the underlying mud flat, and this transition of sedimentary environments is observed in both the Peterstone 1 and 2 cores. The most prominent indicator is the increase in CaO concentrations in the salt marsh sediments, produced by storm overwash deposits. These deposits are not spatially or temporally synchronous across the marsh, and the Peterstone 2 site contained much thicker and more frequent deposits than at the Peterstone 1 site.

The Peterstone 1 core has been dated using ^{137}Cs activities, by comparison with historical records of sediment ^{137}Cs activities. However, this is not possible for the Peterstone 2 core because redox potential changes have mobilised and re-precipitated ^{137}Cs, along with other redox sensitive elements such as S, Mn, Fe, P and trace metals.

The dated Peterstone 1 core correlates well with the organic ^{3}H discharge record from Amersham plc, apart from the most recent peak in 1998, which may have been produced by the deposition of tritium-labelled reworked sediments. The effect of changes in sediment

composition, depositional and post-depositional environments on the ^{3}H profile in this core are likely to be minimal.

Salt marsh cores were also collected from Barry Island and Sudbrook (approximately 20 km to the west and east of Peterstone salt marsh respectively) to investigate ^{3}H accumulation with depth at more distal sites from the Amersham plc discharge point.

The Barry Island core sediments were deposited during a sand flat salt marsh transition. This strong compositional change controls the ^{3}H, ^{137}Cs and ^{210}Pb activity profiles. However, sediment $^{3}H_{total}$ activities are above limit of detection levels in the salt marsh sediments, indicating that sediment labelled with organic tritium released by Amersham plc is accumulated at depth in salt marsh sediments located approximately 20 km from the Amersham plc discharge point.

The Sudbrook core sediments were also deposited in a salt marsh environment that is oxic to the base of the core. It is not possible to determine a definite chronology for this core because the ^{137}Cs activity concentrations are potentially compositionally controlled; sediment $^{3}H_{total}$ activities are present at above limit of detection levels to the base of the core. These cores indicate that tritium-labelled sediments have been stored immobile in salt marshes approximately 20 km to the west of the Amersham plc discharge point and Peterstone salt marsh.

Sediments from Peterstone, Barry Island and Sudbrook salt marshes all accumulated organic tritium discharges from Amersham plc. Sediment-bound tritium is apparently resistant to biodegradation, even in anoxic conditions. The Peterstone 1 core sediment $^{3}H_{total}$ activity profile correlates well with the organic ^{3}H discharge record from Amersham plc, implying that ^{3}H is immobile in sediments. As in the mud flat sediments (Chapter 3), sediment composition is a secondary control on salt marsh sediment $^{3}H_{total}$ activities, such as in the Barry Island core.

Chapter 5

Characterisation of non-aqueous tritium in sediments from the Severn estuary

5.1 Introduction

Organically bound tritium (OBT) discharges from Amersham plc into the Severn estuary accumulate in mud flat sediments (Chapter 3), salt marsh sediments (Chapter 4) and biota (McCubbin *et al*, 2001) from the estuary. Biota are hypothesised to accumulate ^{3}H through the consumption of 'sediment-dwelling microbes and meiofauna' (McCubbin *et al*, 2001), indicating that similar types of OBT may accumulate in both biota and sediment.

As the speciation of OBT in sediments is unknown, a series of simple extraction experiments were conducted on a dried, homogeneous, in-house reference sediment to observe how the sediment-bound OBT behaves with water, methanol, toluene, dichloromethane, aqueous and glacial acetic acid, 6M hydrochloric acid and 6M sodium hydroxide. The different properties of these solvents will allow a number of groups of tritiated organic compounds that may accumulate in surface and salt marsh sediments to be distinguished, or allow other groups to be ruled out, informing further, more detailed, investigations.

5.2 Methods

The methods used for measuring total and water-extractable tritium activities in sediments are described in Chapter 2, but procedures specific to this chapter are detailed below.

5.2.1 Preparation of an in-house reference sediment

Approximately nine litres of fine-grained surface sediment was collected from the mud flat at Orchard Ledges (Figure 3.1, Site 3) in January 2004 (taken from a surface area of 2 m^2 to a depth of 1 cm). This sample was wet sieved to obtain the < 63 μm fraction, which was air dried, then ground using tungsten grinding barrels in a TEMA mechanical grinding unit. The resulting material was homogenised and stored in an airtight container.

5.2.2 Extraction of sediment with water

Aliquots of between 2 and 9 g of the dried in-house reference sediment were accurately weighed into 50 ml plastic centrifuge tubes and high purity Milli-Q water (10 to 20 ml, giving a range of sediment: water ratios from 1:2 to 1:5) was added using a pipette. These were mixed, either by a mixing wheel for 1 hour or by an ultrasonic bath for 2 hours, to allow the equilibration of the water-extractable tritium between the sediment and water phases. The samples were centrifuged at 2500 rpm and the extracts were then filtered through 0.45 μm cellulose nitrate filters and weighed into 22 ml polythene scintillation vials. These were made up to 20 ml with Goldstar scintillation cocktail, dark-adapted overnight to minimise chemiluminescence and counted for 2 hours on a Wallac Quantulus 1220 Liquid Scintillation Counter (LSC).

5.2.3 Soxhlet extraction of sediments

Approximately 20 g of sediment was accurately weighed into a permeable extraction thimble, then placed into the Soxhlet apparatus (Figure 5.1) above a round-bottomed flask containing approximately 350 ml of solvent. The solvents methanol, toluene, dichloromethane and glacial acetic acid were used in separate extractions. The solvent was heated with a heating mantle until it evaporated into the condenser, where it cooled to a liquid and filled the extraction thimble. The solvent then filtered through the sediment into the Soxhlet vessel until it reached the top of the siphon tube, drained through the siphon and returned to the flask. This cycle was repeated every 5 to 10 minutes, with the extractions lasting from 4 to 6 hours.

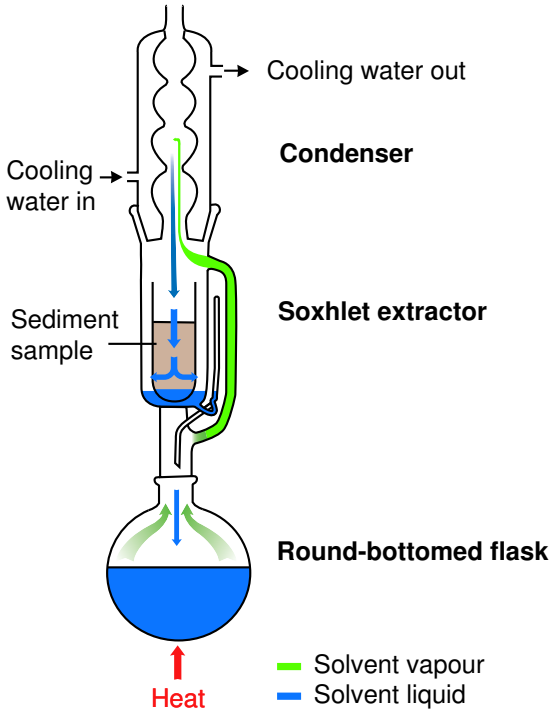

Figure 5.1: Design of the Soxhlet extraction apparatus, showing the movement of solvent liquid and vapour through the system during a cycle of solvent evaporation and condensation. This cycle was repeated every 5 to 10 minutes and the extraction lasted from 4 to 6 hours.

The solvent was evaporated onto SiO_2 under vacuum using a rotary evaporator. The SiO_2 was then weighed into a quartz sample boat and analysed for total tritium using a modified combustion method in a purpose-built furnace (Figure 2.1). The sample zone of the furnace was heated from 50 °C to 500 °C over 3 hours. The catalyst zone was initially held at 100 °C to minimise the risk of explosion if traces of solvent remained in the sample, then gradually increased to 700 °C. The compressed air flow through the furnace was not enriched with O_2 until the sample zone reached 500 °C. An aliquot of the bubbler solution was mixed with Goldstar scintillation cocktail and counted on the LSC for 2 hours, as in the original method.

5.2.4 Ultrasonic extraction of sediments

Approximately 3 g of the in-house reference sediment was accurately weighed with 10 ml of solvent into 40 ml glass tubes. The solvents used were methanol, toluene, dichloromethane (DCM), 6M hydrochloric acid, 20 % (v/v) aqueous acetic acid, glacial acetic acid and 6M sodium hydroxide. These were hand-shaken to disperse the sediment and placed in a water-filled ultrasonic bath at 30 °C (this rose to ∼50 °C by the end of the extraction because of the ultrasonic energy) for 2 hours. For extractions with the volatile solvent DCM, 20 ml of solvent was used and ice was added to the water in the ultrasonic bath to minimise evaporation.

Following extraction, the samples were decanted into centrifuge tubes and spun at 2500 rpm for 5 minutes. The supernatants were filtered using glass fibre (GF/A or GF/C) filters. The methanol and toluene extracts were then mixed directly with Goldstar scintillation cocktail in 22 ml polythene scintillation vials, dark-adapted overnight and counted on the LSC. However, many extracts could not be analysed directly: the dichloromethane and 6M HCl extracts because Cl is a strong chemical quenching agent; the NaOH extract because it is basic and produced high chemiluminescence which is recorded in the same channels as tritium, preventing accurate measurement; and the acetic acid extracts because they were strongly coloured and absorbed the light emitted by the scintillant fluors (L'Annunziata, 2003). Therefore, these extracts were placed in beakers on a hot plate at 60 °C and evaporated onto SiO_2. The SiO_2 was analysed for total tritium using the modified combustion furnace method described above to convert the tritiated organic molecules to HTO and CO_2. The residues were dried by placing the tubes in a water bath heated to 60 °C, and analysed for total tritium using the combustion furnace method.

Calibration of the liquid scintillation counter for the measurement of methanol and toluene The counting efficiency of the liquid scintillation counter can be calculated for any mixture of solvent and scintillation cocktail by measuring the activity and the Spectral Quench Parameter of the External Standard (SQP(E)) of a number of samples of known activity on the Wallac 1220 ultra-low-level liquid scintillation counter. Goldstar scintillation cocktail was added to a range of volumes of methanol and toluene to make a constant volume of 20 ml in a 22 ml polythene scintillation vial. These samples were spiked with known activities of tritiated water (diluted from a certified source obtained from Amersham plc, Cardiff), dark-adapted overnight and measured on the LSC.

Toluene is an aromatic solvent, with a chemically similar composition to ingredients in the scintillation cocktail. As it does not cause quenching, the calibration curve is approximately linear (Figure 5.2), with an average efficiency of 33 %. However, methanol is a mild quencher (diluter), so the counting efficiency varies with the amount of solvent (from 30 % at 2 ml to 23 % at 8 ml) added to the scintillation cocktail.

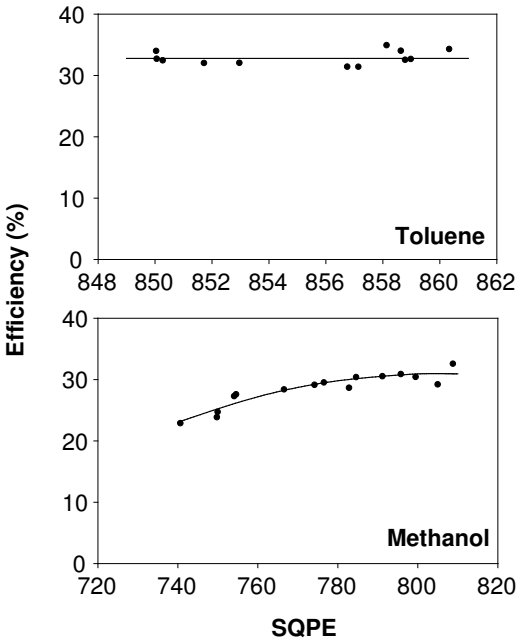

Figure 5.2: Spectral Quench Parameter of the External Standard (SQP(E)) calibration curves for samples composed of methanol or toluene mixed with Goldstar scintillation cocktail in 22 ml polythene scintillation vials.

5.2.5 Microwave digestion of sediments

Approximately 5 g of the in-house reference sediment and 10 ml of 6M NaOH solution were accurately weighed into high-pressure PTFE digestion vessels, which were sealed and microwaved in a CEM MDS 2000 Microwave Digestion System for 30 minutes at 20 psi, with a target vapour pressure of 10 psi. The temperature was not measured during the extraction. The residues were rinsed several times with MilliQ water, centrifuged at 2500 rpm and dried by placing the tubes in a water bath heated to (60 °C), before being analysed for tritium in the combustion furnace. The extract could not be analysed because it produced high chemiluminescence when mixed with the scintillation cocktail.

5.3 Results

5.3.1 Characterisation of the in-house reference sediment

Aliquots of the in-house reference sediment were analysed for $^{3}H_{total}$ activity (Figure 5.3). The average $^{3}H_{total}$ activity was 0.19 ± 0.03 Bq/g dry weight to the 95 % confidence level (2σ). This reproducibility implies that the in-house reference sediment is homogeneous; therefore, replicate results from subsequent extractions are comparable.

Significant tritium activities (above the limit of detection) were not extracted from the in-house reference sediment with water using the ultrasonic or microwave methods (Table 5.1), implying that tritium activity in the sediments is predominantly present as non-aqueous tritium (NAT).

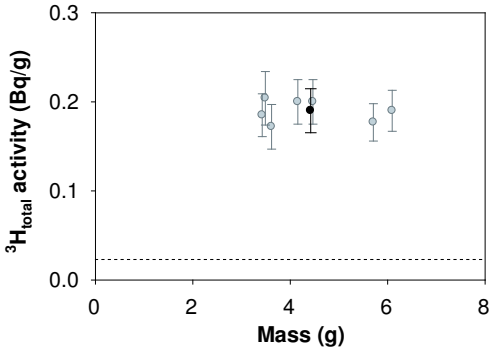

Figure 5.3: Comparison of $^3H_{total}$ activities (in Bq/g dry weight) for replicate samples of the in-house reference sediment. The replicate and mean $^3H_{total}$ activities are shown in grey and black respectively, with method uncertainties propagated to the 95 % confidence interval (2σ). The limit of detection of the technique is shown as a dotted line.

5.3.2 Extractions from the in-house reference sediment with organic solvents

Methanol, toluene, dichloromethane (DCM) and 20 % acetic acid did not extract significant $^3H_{total}$ activities from the in-house reference sediment (Figure 5.4). Methanol extracted <25 % of the $^3H_{total}$ activity using the Soxhlet methods, and an average of 91 ± 20 % of the $^3H_{total}$ activity remained in the sediment residue following the ultrasonic extractions. Toluene extracted $^3H_{total}$ activities below the limit of detection using the Soxhlet method. With the ultrasonic method, toluene had a low instrument blank and detection limit (4 % of the sediment $^3H_{total}$ activity), but this method still extracted <10 % of the $^3H_{total}$ from the sediment. Dichloromethane extracted $^3H_{total}$ activities lower than the limit of detection using both the ultrasonic (<37 %) and Soxhlet (<47 %) methods. These detection limits were high, possibly because some chlorinated organic compounds (chlorine is a strong quenching agent) passed through the furnace into the water trap, significantly affecting the detection of low energy β-emitting radionuclides, such as tritium (Section 2.2.3; L'Annunziata, 2003a). Following ultrasonic extraction with 20 % acetic acid, >90 % of the $^3H_{total}$ activity remained in the sediment residue (Table 5.1). One residue sample had an anomalously high sediment ^3H activity after this extraction, which may be attributed to an inhomogeneous sample or system contamination. Soxhlet extractions with methanol, toluene and DCM are from a dried bulk sediment, rather than the ground, homogeneous and well-characterised in-house reference sediment used for all other extractions (Table 5.1).

In contrast, glacial acetic acid, 6M HCl and 6M NaOH did extract significant $^3H_{total}$ activities from the in-house reference sediment (Figure 5.4). Glacial acetic acid extracted an average of 18 ± 10 % of the $^3H_{total}$ activity, with 94 ± 18 % remaining in the residue after the ultrasonic extractions (Table 5.1). Following the Soxhlet extractions, however, the residue reproducibly contained 37 ± 7 % of the $^3H_{total}$ activity, indicating that 56 to 70 % of the $^3H_{total}$ activity in the sediment was extracted, even though only 13 to 32 % of this activity was measured in the extract. Further work is required to determine

how and where the $^{3}H_{total}$ activity was lost. An average of 80 ± 16 % of the $^{3}H_{total}$ activity remained in the residue following ultrasonic extraction with 6M HCl (Table 5.1). Although the solvent extracts could not be analysed, these results imply that ∼ 20 % of the $^{3}H_{total}$ activity was extracted by 6M HCl from the sediment. After extraction with 6M NaOH using the ultrasonic and microwave methods, an average of 49 ± 10 % and 43 ± 9 % of the $^{3}H_{total}$ activity respectively, remained in the residue (Table 5.1). Although the solvent extract was not analysed, this indicates that 6M NaOH extracted at least 40 % of the $^{3}H_{total}$ activity from the sediment.

Table 5.1: Summary of extraction results (average ^{3}H activity is 0.19 ± 0.03 Bq/g dry weight) with water and a range of organic and reactive solvents. Method uncertanties are propagated to the 95 % confidence limit (2σ).

Solvent	**Mass of sediment (g)**	**Uncertainty (2σ)**	**Fraction**	**Activity in each fraction (%)**	**Uncertainty (%, to 2σ)**	**Measured total activity (%)**	**Uncertainty (2σ)**	**Is this a significant and positive result?**
Soxhlet extractions								
Methanol[1]	18.06	0.18	Extract			21	4	No[2]
	19.68	0.20	Extract			< 21		
Toluene[1]	17.87	0.18	Extract			< 36		No
DCM[1]	18.38	0.18	Extract			< 47		No
	17.62	0.18	Extract			< 47		
	17.02	0.17	Extract			< 47		
GAA	21.07	0.21	Extract	27	5			Yes[3]
			Residue	37	7	64	9	
	23.41	0.23	Extract	16	3			
			Residue	37	7	53	7	
Ultrasonic extractions								
Water	4.06	0.04	Extract			< 11		No
	2.95	0.03	Extract			< 11		
	1.90	0.02	Extract			< 11		
	4.74	0.05	Extract			< 11		
	9.04	0.09	Extract			< 11		
Methanol	2.94	0.03	1st Extract	< 10				No
			2nd Extract	< 10				
			Residue	93	19	93	19	
	3.00	0.03	1st Extract	< 10				
			2nd Extract	< 10				
			Residue	83	17	83	17	
	3.06	0.03	1st Extract	14	6			
			2nd Extract	< 10				
			Residue	93	21	107	23	
	2.97	0.03	1st Extract	< 10				
			2nd Extract	< 10				
			Residue	94	20	94	20	
Toluene	1.99	0.02	Extract			7	3	No
	2.79	0.03	Extract			4	2	

Solvent	**Mass of sediment (g)**	**Uncertainty (2σ)**	**Fraction**	**Activity in each fraction (%)**	**Uncertainty (%, to 2σ)**	**Measured total activity (%)**	**Uncertainty (2σ)**	**Is this a significant and positive result?**
	3.14	0.03	Extract			< 3		
DCM	3.96	0.04	Extract			< 37		No
	6.51	0.07	Extract			< 37		
6M HCl	5.02	0.05	Residue			77	15	Yes
	5.05	0.05	Residue			75	15	
	4.97	0.05	Residue			86	17	
	4.94	0.05	Residue			82	16	
20 % AA	3.11	0.03	Extract	< 15				No
			Residue	153	30	153[4]	30	
	3.02	0.03	Extract	< 15				
			Residue	103	21	103	21	
	3.01	0.03	Extract	< 15				
			Residue	96	20	96	20	
GAA	2.95	0.03	Extract	26	11			No
			Residue	94	18	121	21	
	3.10	0.03	Extract	14	9			
			Residue	94	18	108	20	
	2.98	0.03	Extract	14	10			
			Residue	96	18	110	21	
NaOH	4.98	0.05	Residue			48	10	Yes
	4.96	0.05	Residue			49	10	
Microwave digestion								
NaOH	5.09	0.05	Residue			35	7	Yes
	4.96	0.05	Residue			42	9	
	4.99	0.05	Residue			50	10	
	5.04	0.05	Residue			45	9	
Water	5.01	0.05	Residue			81	15	No
	4.99	0.05	Residue			72	13	

[1] - Extraction carried out on a bulk unground sediment with a $^{3}H_{total}$ activity of 0.19 ± 0.02 Bq/g dry weight. [2] - Discussed in Section 5.3.2. Detection limits ($<$ values) are calculated according to Currie (1968). [3] - Significant $^{3}H_{total}$ activity is lost during this extraction. [4] - This result is anomalously high, for reasons that are currently unclear.

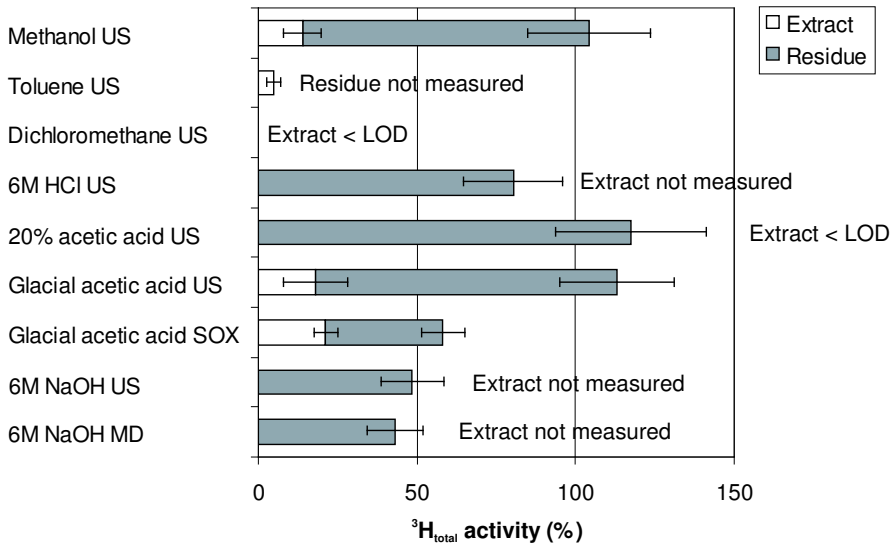

Figure 5.4: Proportion of the total tritium activity in the in-house reference sediment extracted by organic solvents (methanol, toluene, dichloromethane, 6M HCl, 20 % acetic acid, glacial acetic acid and 6M NaOH) using three methods: ultrasonic extraction with an ultrasonic bath for two hours (US); Soxhlet extraction for four to six hours (SOX); and microwave digestion at up to 20 psi for 30 minutes (MD). Uncertainties are propagated (method and counting statistics) to the 95 % confidence level (2σ). Limits of detection are calculated according to Currie (1968). If only one replicate extracted measurable tritium activities, this has been included; otherwise the mean tritium activity in the extract or remaining in the residue is plotted.

5.4 Discussion

5.4.1 Choice of solvents and methods

A variety of solvents, ranging in polarity from toluene to water, were used to extract the in-house reference sediment. Each was selected to extract specific groups of compounds from the sediment (Figure 5.5). The reactive solvents 6M HCl, 6M NaOH and glacial acetic acid were also used, in an attempt to lyse large biomolecules and cells (Figure 5.6).

In Soxhlet extraction, hot solvent percolates repeatedly through the sediment, leaching the soluble fraction. Higher temperatures increase the speed of reactions and the length of the Soxhlet extraction, up to 6 hours in the present study, also allows more time for

Solvent (dielectric constant)	Polarity	Type of molecules dissolved	Substances dissolving by reaction
Water (80)		Tritiated water Polar organic molecules - amino acids - nucleic acids - carboxylic acids - alcohols	
6M HCl			Hydrolysis of peptide links in proteins (Fig 5.6 a) Hydrolysis of lipids (Fig 5.6 c)
6M NaOH			Saponification of lipids (Fig 5.6 b) Hydrolysis of peptide links in proteins (Fig 5.6 a)
20 % Acetic acid 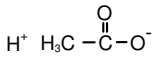			
Methanol (33) 	Polar		Hydrogen exchange on -OH group
Dichloromethane (9.08) 		Lipids Benzene Polycyclic aromatic hydrocarbons (PAHs)	
Glacial acetic acid (6.15) 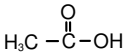		Fatty acids Polar organic molecules	Transesterification (substitution) of fatty acids (Fig 5.6 d)
Toluene (2.04) 	Non-polar	Aliphatic hydrocarbons Benzene and PAHs	

Figure 5.5: The types of molecules that dissolve or react with various solvents used in the extraction experiments (Clayden *et al*, 2001).

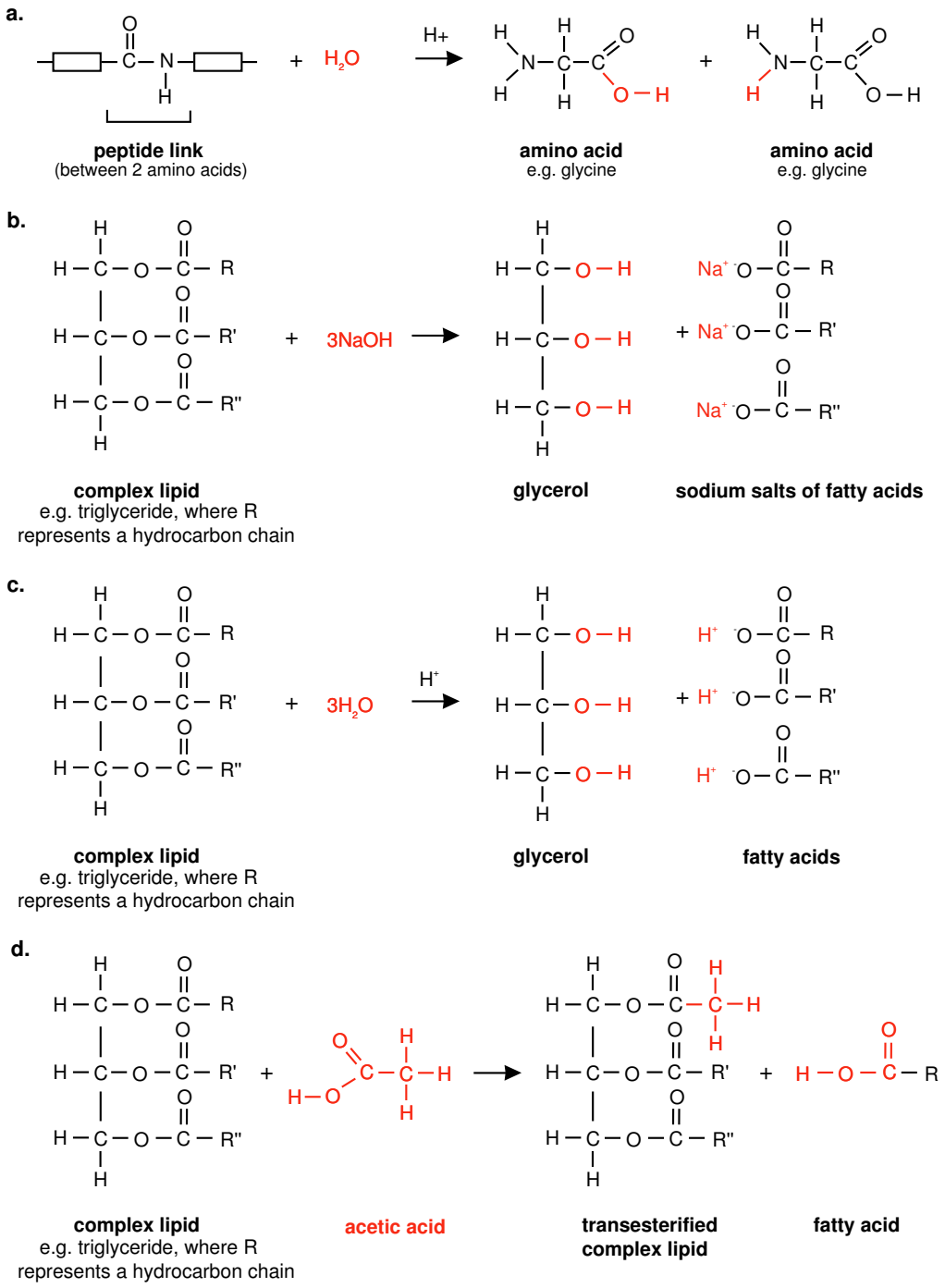

Figure 5.6: Potential reactions between proteins, lipids and reactive solvents: a. Acid hydrolysis of peptide links in proteins with 6M HCl; b. saponification of lipids with 6M NaOH; c. acid hydrolysis of lipids with 6M HCl; d. transesterification of fatty acids with glacial acetic acid (Clayden *et al*, 2001).

hydrogen-tritium exchange. However, solvents can be channelled through the sediment (Radke *et al*, 1978), resulting in solvent-sediment interactions over a smaller surface area, and potentially incomplete leaching of the soluble fraction.

In ultrasonic extraction, the ultrasound disrupts particles and divides flocs, which increases the surface area of sediment available for reaction with the solvent. It also encourages cavitation (the formation of microbubbles), which may act as a catalyst in reactions (Doulah, 1977; Wang, 1998). The efficiency of the reaction is enhanced as the temperature increases up to 50 °C; however, as the temperature approaches the boiling point of the solvents, surface tension is disrupted and sonication becomes ineffective (Filgueiras *et al*, 2000). The ultrasonic energy lengthens the settling time of the sediment particles, but the tubes are also shaken by hand at regular intervals (every 30 minutes) during the extraction to resuspend the sediments. A higher energy ultrasonic probe, used instead of the ultrasonic bath, would increase the disruption to sediment particles, and possibly improve the efficiency of the extraction. However, the ultrasonic bath allows replicate samples to be analysed under identical experimental conditions.

In microwave digestion, the combined solvent and sediment phases are placed under increased pressure and temperature conditions for 30 minutes. The increased pressure speeds up the diffusion of solvents into the pores of the matrix, reducing the necessary extraction time; overall extraction efficiency is similar to the Soxhlet extraction method (Ferrera *et al*, 2004). Microwave energy can also lyse cell walls, releasing the molecules within into solution.

Physical conditions, such as temperature and pressure, vary between the three methods discussed above. This may change the efficiency of the reaction by altering the type and/or extent of the reaction between solvent and sediment. This can be tested by comparing different methods where the same solvent has been used. Ultrasonic and microwave extractions with sodium hydroxide as the solvent leaves 58 ± 12 % and 43 ± 9 % of the $^{3}H_{total}$ activity in the residue, respectively (the solvent was not analysed). There are, therefore, no statistically significant differences between the results produced by these different methods. It appears that similar interactions occur between the sediment and solvent in all of the methods, so the extraction results for different solvents using a range of methods can be directly compared.

5.4.2 Extraction of tritiated species associated with sediments into solvents of different polarity

Less than 15 % of the total ^{3}H activity was extracted with water from the freeze-dried in-house reference sediment. Measurable ^{3}H activities were also not extracted with water from over 100 other fresh sediment samples using the mixing-wheel method (Section 3.3.1), indicating that there was little water-extractable ^{3}H in Severn estuary sediments, and >85 % is non-aqueous tritium. In comparison, McCubbin *et al* (2001) measured a loss on drying of 9 % of the total ^{3}H for a sediment sample from the Severn estuary, implying that 91 % of the total ^{3}H in Severn estuary sediments is in the form of OBT (defined as that remaining in sediment after drying to a constant weight at 40 °C). It has been established

that HTO is not responsible for the accumulation of tritium in Severn estuary sediments (Section 1.2.4). Polar organic solvents did not extract measurable ^{3}H activities from the in-house reference sediment (Figure 5.4). However, methanol has a high detection limit (20 % of the total tritium activity). During a study of OBT accumulation in fish (Williams, 2005), <20 % of the total ^{3}H activity was extracted from fish fillets with methanol using a sequential Soxhlet extraction method.

The polar aprotic solvent dichloromethane (DCM) extracts <37 % of the total tritium (Figure 5.4), but because the strong quenching effect of Cl produces a high detection limit (L'Annunziata, 2003a), this experiment does not yield useful results. However, when dichloromethane was used in Soxhlet extractions of fish fillets (Williams, 2005), it also failed to extract measurable tritium activities (< 2 %). Toluene extracts 7 ± 3 % of the total tritium (Figure 5.4).

Hydrophobic, non-polar tritiated organic molecules will tend to associate with colloids, organic matter or sediments, but their availability for extraction may be dependent on the type and location of binding sites of the tritium atoms and/or tritiated molecules. Sedimentary particles, such as clays and coal particles, have large and reactive surfaces that contain a range of potential binding sites (Yariv and Cross, 1979). For example, Ghosh *et al* (2000) measured significant concentrations of polycyclic aromatic hydrocarbons (PAHs) on coal from a coarse-grained harbour sediment. However, as ultrasonic extraction with toluene, dichloromethane and water all failed to extract measurable tritium activities, it is unlikely that a significant proportion of the tritiated organic molecules are sorbed onto mineral or organic surfaces, because ultrasonic vibrations speed up solvent diffusion into substrate pores, and should therefore efficiently extract organic molecules of a similar polarity to the solvent.

Tritiated organic molecules may also be physically or chemically trapped within aggregates, flocs, cells or other large molecules (Baumgartner and Donhaerl, 2004; Droppo, 2004) and, therefore, are not easily extracted. Ultrasonic extraction should release tritiated molecules trapped in flocs or aggregates by shaking them apart, but in the present study this technique, using solvents with a range of polarities, consistently failed to extract significant tritium activities. It can therefore be inferred that most (>75 %) of the tritium activity in sediments from the Severn estuary was contained within cells or large molecules that were insoluble in the polar and non-polar solvents used, but may be extractable with reactive solvents.

5.4.3 Extraction of tritiated organic molecules into reactive solvents

McCubbin *et al* (2001) state that tritium in 'sediment-dwelling microbes and meiofauna' may be the primary source of tritium bioaccumulation in benthic organisms (lugworms, shrimps, crabs, cockles and mussels) because periwinkles, which feed predominantly on seaweed, accumulate much lower levels of tritium. In the Severn estuary up to 50 % of the bacterial population is associated with sediments (Joint and Pomroy, 1982). Bacteria contain proteins and amide-bound lipids (lipopolysaccharides), which are lysed into monomers and short chain polymers by acid hydrolysis (Buchanan and Longbottom, 1970;

Goosens *et al*, 1989). However, if tritiated organic molecules are located inside cells, then the cell walls must be lysed using strong acids or bases before they can be extracted.

6M hydrochloric acid extracted up to 40 % of the total tritium (calculated from the activity remaining in the residue; Figure 5.4), probably by acid hydrolysis of proteins and lipids (Figure 5.6); glacial acetic acid, which can transesterify fatty acids from lipids (Figure 5.6), extracted 15 to 37 % of the total tritium (Figure 5.4). Both acids can also extract tritiated water and polar organic molecules from the sediment, but this has been shown to represent <20 % of the total tritium (page 164). Sodium hydroxide (NaOH) extracted 30 to 66 % of the total tritium from the in-house reference sediment, probably by the hydrolysis of proteins and the saponification of lipids (Figure 5.6). These results indicate that a significant fraction of the total tritium, up to 66 %, is contained within larger molecules, such as lipids and proteins, and is only released into solution by the lysing of these molecules with reactive solvents.

As only reactive solvents successfully extracted measurable tritium activities from the in-house reference sediment, the tritium appears to be either non-exchangeably bound to soluble monomers (e.g. amino acids), or exchangeably bound at sites that, before lysing, are inaccessible due to the physical structure (coiling and folding) of large molecules (Baumgartner and Donhaerl, 2004). The solvents therefore probably extracted tritium as tritium-labelled fragments and monomers from lysed proteins, lipids, hydrocarbons, carbohydrates or humic compounds. Consequently, the tritiated organic molecules in solution will not be in the same form as they were within the sediment.

The tritiated biomolecules that constitute up to 66 % of the total tritium in the sediment may be discharged directly from Amersham plc (Williams, 2003), produced by microbes (in either the sewage system or sediment) that consumed and metabolised other tritiated organic molecules (Libes, 1992), or released by the degradation of tritiated organic matter. The results above suggest that the interaction of tritiated organic molecules with bacteria is an important factor determining the fate of tritium in sediments. The biodegradation of the non-aqueous tritium is very slow, as tritium is not released from the sediment in soluble form over twenty years (Chapter 4), indicating that at least some of the tritium activity is associated with a refractory fraction of organic carbon, such as humic matter (Filip and Alberts, 1994).

5.5 Further work

Further work should focus on answering three important questions:

- What is the speciation of the tritiated organic molecules present in the sediment?
- How bioavailable are they?
- What fractions of the sediment are they associated with?

Speciation of tritiated molecules The identity of broad groups of compounds can be inferred from the solvent extraction experiments discussed above. An important mod-

ification to many of the experiments will be increasing the sample size to produce lower detection limits. As discussed in Section 2.2.2, further investigation and development of the method used to determine water-extractable tritium from sediments is necessary. This may focus on achieving a total mass balance for the extractions, including the filtered fraction, and could also have ramifications for the solvent extraction methods that are developed. Characterisation of the lysed tritiated molecules extracted from the sediment with NaOH would reduce the number of groups of potential precursors. Following extraction, the NaOH solution could be acidified and extracted with hexane for analysis by thin layer chromatography (TLC) to identify the organic fractions, and tritium could be detected directly by solid scintillation fluorography (Prydz *et al*, 1973). Willsch *et al* (1997) used chromatography columns to separate organic matter in solution into fractions based on their polarity and aromaticity; this method would provide more information on the chemical composition of the extract, and the resulting fractions could be analysed for tritium or characterised further.

Improvement of non-polar extraction methods and assessment of bioavailability The results of the extractions with reactive solvents suggest that tritium might be present in lipids and proteins. As dichloromethane is an effective solvent for lipids, lowering the detection limit for this method may allow the measurable extraction of any lipids not contained within large molecules or cells. This could be achieved by increasing the sample size, and therefore the amount of activity, or by liquid-liquid extraction to transfer the extracted tritiated molecules to a non-chlorinated solvent before analysis by liquid scintillation counting. Using an ultrasonic probe to increase the ultrasonic energy used to combine the sediment and solvent phases would break cell walls, releasing any lipids within, and would also increase the speed of the extraction, although a cooling system would be required to prevent the evaporation of DCM (which has a boiling point of 40 °C (US EPA, 1994)) during the extraction and to allow time for hydrogen-tritium exchange.

An alternative method for extracting lipids and PAHs, microwave-assisted cloud point extraction with detergents (non-ionic surfactants), is attractive because detergents are available which are miscible with scintillation cocktails, and hence allow direct determination of tritium activity (L'Annunziata, 2003a), and are also suitable for use with a high-pressure liquid chromatography (HPLC) system for characterisation of the extracted organic molecules (Ferrera *et al*, 2004). McCubbin *et al* (2001) inferred that the ingestion of sediment may contribute to the bioaccumulation of tritium in benthic organisms if ^{3}H is subsequently released by acids and enzymes in the animal's gut. Although the composition of gut fluids varies between species (some are surfactant-rich while others contain hydrophobic regions to increase solubility of more hydrophobic compounds), they are complex mixtures, containing a range of proteins and lipids, with a low pH (Voparil *et al*, 2003). Therefore, extraction of the sediment with a combination of acids, detergents and enzymes may allow the total bioavailibility of tritium in sediments to be assessed.

Association of tritium with separate fractions of the sediment The behaviour of tritiated organic molecules not only depends upon their speciation, but also upon the fraction of the sediment they associate with. Determination of the tritium activities of separate fractions of the sediment would allow this behaviour to be better predicted. Various forms of organic carbon are present in sediments: bacteria and other biota; humic matter particles and humic coatings on mineral surfaces; detrital debris; vegetative debris; coal; wood; and combustion products (Allen, 1987a; Hamilton *et al*, 1979). As discussed previously, the association of tritium with inorganic flocs is unlikely because ultrasonic extraction disintegrates flocs and speeds up diffusion of solvents into pore spaces.

Bacteria in the Severn estuary are thought to bioaccumulate tritium (McCubbin *et al*, 2001), and around 50 % are associated with sediments (Joint and Pomroy, 1982). Bacteria and microbes are at the bottom of the food chain containing benthic organisms and demersal fish, which are also known to bioaccumulate tritium (McCubbin *et al*, 2001). Bacteria can be separated from sediments by repeatedly extracting the bulk sample with a 0.1 % peptone solution in an ultrasonic bath (Craig *et al*, 2002); Epstein *et al* (1997) have confirmed the quantitative recovery of bacteria from sandy sediments using ^{3}H and ^{14}C labelled bacteria, demonstrating that it would be possible to extract, and measure tritium activities in, bacteria within the sediment.

Tritium may also be covalently bonded to humic compounds, large compounds with complex structures and high molecular weights (Filip and Alberts, 1994), that occur in sediments as discrete particles or as coatings on other sediment grains. This fraction tends to be refractory, which would explain the observed slow degradation rates of tritiated organic matter, which have resulted in little mobility in the sediment over 20 years (Chapter 4). Humic matter is unlikely to have been released or lysed by the solvent extractions used in the present study, and may therefore contain the remainder of the tritium activity in the in-house reference sediment (at least 34 % was not extracted by any method in the present study). This remainding activity could potentially be extracted by some bacteria and enzymes.

5.6 Summary

A dry, homogeneous in-house reference sediment with an average total tritium activity of 0.19 ± 0.03 Bq/g dry weight to 2 σ) was prepared, characterised and used in Soxhlet, ultrasonic and microwave extractions with water, 6M HCl and 6M NaOH, and the organic solvents toluene, dichloromethane, methanol, glacial acetic acid, 20 % acetic acid. Less than 25 % of the total tritium was extractable with the polar solvents water, 20 % acetic acid and methanol. Results from extractions with dichloromethane were inconclusive, and toluene extracted < 10 % of the total tritium. However, the reactive solvents hydrochloric acid, glacial acetic acid and sodium hydroxide were more successful, extracting up to 40 %, 37 % and 66 %, respectively, of the total tritium.

It is inferred that a small proportion (<25 %) of the total tritium is adsorbed to the surfaces of clays and organic particles, and is therefore easily released into solution. A

larger proportion of the total tritium (∼40 – 60 %) may be contained within macromolecules such as lipids and proteins, which would be lysed by the reactive solvents to release exchangeable tritium or tritiated soluble fragments (such as amino acids). Up to 30 % of the $^{3}H_{total}$ activity was not extracted by any of the solvents or methods used in the present study. Sediment-bound tritiated organic molecules in salt marsh cores from the Severn estuary are immobile over a period of 25 years (Chapter 4), indicating that this fraction is likely to be refractory organic matter, possibly humic substances, as these are most resistant to biodegradation. Potential further work would involve characterising this fraction, as well as identifying the extraction products and making improvements to the DCM extraction method.

Chapter 6

Summary and implications

6.1 Summary

6.1.1 Factors controlling ^{3}H activities in sediments

Organically bound tritium (OBT), discharged by Amersham plc into the Severn estuary, associates with sediments, whereas tritiated water (HTO) remains in the aqueous phase. OBT is transported with fine sediment in suspension, acting as a non-conservative tracer, and accumulates in mud flats, salt marshes and subtidal sediment sinks (Appendix 5). Sediment $^3H_{total}$ activities are affected by a number of variables, including the distance of the site from the Amersham plc discharge point, changes to the OBT component of discharges from Amersham plc and sediment composition.

Distance from Amersham plc

Measurable ^{3}H activities (>0.02 Bq/g dry weight) are detected in mud flat sediments over 40 km to the east of the Amersham discharge point. The highest sediment $^3H_{total}$ activities are found at sites closest to the Amersham plc discharge point, and tend to decrease in magnitude with distance from the discharge point, probably as a result of dilution by unlabelled suspended sediment.

Temporal variations in discharges from Amersham plc

The temporal variability of sediment $^3H_{total}$ activities is predominantly controlled by variations in the magnitude, composition and treatment of tritiated discharges from Amersham plc. Decreasing OBT discharges from 2000 to 2004 have resulted in decreasing sediment $^3H_{total}$ activities at all mud flat sites monitored during this period. The treatment of discharges by a waste water treatment plant from January 2002 (Williams, 2003), and a decrease in the discharge of 'high impact' tritiated organic compounds such as hydrocarbons, proteins, nucleotides and lipids, from April 2003 (Williams, 2005), has led to further stepped decreases in sediment $^3H_{total}$ activities.

Shallow sediment cores collected from salt marshes at Barry Island, Peterstone and Sudbrook, on the northern shore of the Severn estuary, preserve evidence of historical OBT inputs. Sediment $^3H_{total}$ activities vary with depth in the cores. Maximum $^3H_{total}$ activities recorded in the Peterstone 1 core correspond to maximum discharges from Amersham plc in 1986; although the Peterstone 2 core has not been dated, it contains a similar sediment $^3H_{total}$ profile, with a broad peak close to the surface and a sharper peak at depth. The Barry Island core $^3H_{total}$ profile, however, is strongly influenced by variations in sediment composition.

Sediment composition

Organically bound tritium (OBT) predominantly, but not exclusively, associates with the <63 μm (clay and silt) fraction. A change in composition from mud to sand in the Barry Island core corresponds with a significant decrease in sediment $^3H_{total}$ activities, and surface sediments of coarse sand and gravel composition, collected from Site 2, have

anomalously low $^{3}H_{total}$ activities. However, there are generally poor correlations between sediment $^{3}H_{total}$ activities and compositional indicators such as Rb and TOC (including coal content), implying that these proxies do not exclusively represent the specific fraction(s) of the sediment that OBT associated with.

6.1.2 Persistence of OBT in sediments

There is a correlation ($r^2 = 0.63$) between Peterstone 1 core sediment $^{3}H_{total}$ activities and Amersham plc organic ^{3}H discharges, implying that OBT has remained fixed in the sediment since deposition. In sediments dated as pre-1980, before Amersham plc discharges began, sediment $^{3}H_{total}$ activities approached limit of detection levels, indicating only limited downward diffusion of tritium. OBT in sediments is, therefore, largely resistant to biodegradation over a period of 25 years. Similar sediment $^{3}H_{total}$ activity profiles are found in two subtidal sediment cores from Newport Deep (Appendix 5; Warwick and Croudace, 2005); therefore the magnitude, treatment and composition of OBT discharges from Amersham plc is the predominant control on sediment $^{3}H_{total}$ activities in both intertidal and subtidal deposits.

The persistence of OBT in sediments indicates that sediment-bound OBT is hydrophobic and refractory. Furthermore, extraction experiments have found that non-reactive organic solvents and water extract <20 % of the total tritium from sediments, whereas reactive solvents (strong acids and bases) lyse sediment-bound OBT and release ~60 % of the total tritium as exchangeable tritium or tritiated soluble fragments (such as amino acids). Therefore, tritiated organic compounds in sediments may include large, complex macromolecules, such as lipids, carbohydrates, hydrocarbons and humic compounds.

6.2 Implications

6.2.1 Tritium activities in sediments

Salt marsh, mud flat and subtidal sediments all accumulate organic ^{3}H. By measuring the activities of these sediments and estimating the amount of labelled sediment in each compartment, the total ^{3}H accumulation in Severn estuary sediments can be estimated, allowing the significance of this accumulation relative to the magnitude of organic ^{3}H discharges from Amersham plc over the past 25 years to be assessed. There are large uncertainties on the estimates of the size of each compartment, and insufficient data are available to make a precise estimate of the tritium activities of the subtidal and suspended sediment compartments; however, order of magnitude estimates have been made to enable a model to be constructed (Figure 6.1). The assumptions made in this model are detailed in Figure 6.1 and Appendix 6, it was also assumed that a quarter of the suspended sediment population of the estuary was labelled, and that average depths of labelled sediments in intertidal mud flats, salt marshes and Newport Deep were 10, 40 and 20 cm respectively (from sampling observations and the analysis of sediment cores). Newport Deep was assumed to be the only subtidal area where tritiated sediments accumulate, as

low sediment $^3H_{total}$ activities have been recorded near Bridgwater Bay on the southern shore of the estuary (Figure 3.4).

Although past OBT discharges have measurably accumulated in sediments, it is apparent that this only represents a small proportion (<2 %) of the organic ^3H discharged from Amersham plc (Figure 6.1). The rest of the discharges either remain in solution within the estuary or are flushed into the Bristol Channel. These model results, together with the reduction in sediment $^3H_{total}$ activities after the introduction of the waste water treatment process in March 2002 and the removal of 80 % of the high impact fraction in April 2003 (Table 1.1; Williams, 2003), indicate that a specific tritiated species, which comprises a small proportion of the total discharges, is responsible for a large proportion of the accumulation reported by this study. The resistance of the sediment-bound tritium to biodegradation in salt marsh sediment cores indicates that this fraction of the discharges must be both hydrophobic and refractory.

As sediment $^3H_{total}$ activities have in the past depended primarily on the magnitude, composition and treatment of organic ^3H discharges from Amersham plc, these factors will also influence future sediment $^3H_{total}$ activities. The magnitude of organic ^3H discharges from Amersham plc (Figure 1.4) decreased significantly in 1998, and will cease completely in 2007 when a tritium recovery plant is commissioned (EA, 2003). It can be predicted that this cessation of ^3H discharges into the estuary will result in decreasing surface sediment $^3H_{total}$ activities in the future. However, ^3H in different compartments have different residence times in the estuary. Tritium in salt marshes or the subtidal mud patches could either be eroded and resuspended, or removed by radioactive decay (with a residence time of 10 half-lives or 123 years). In contrast, suspended sediments, which can be removed from the estuary by flushing into the Bristol Channel, have an average residence time of 10 years (Warwick and Croudace, 2005), which would result in below detection limit activities after $\sim$ 20 years unless ^3H-labelled sediments from the salt marshes or subtidal mud flats were resuspended. The estimated ^3H inventory for the subtidal sediments in Newport Deep is similar in magnitude to the estimated suspended sediment inventory, whereas the estimated ^3H inventory for the salt marshes is much lower, implying that the release of ^3H-labelled sediments from the subtidal sediment sinks could significantly increase suspended sediment ^3H activities in the future.

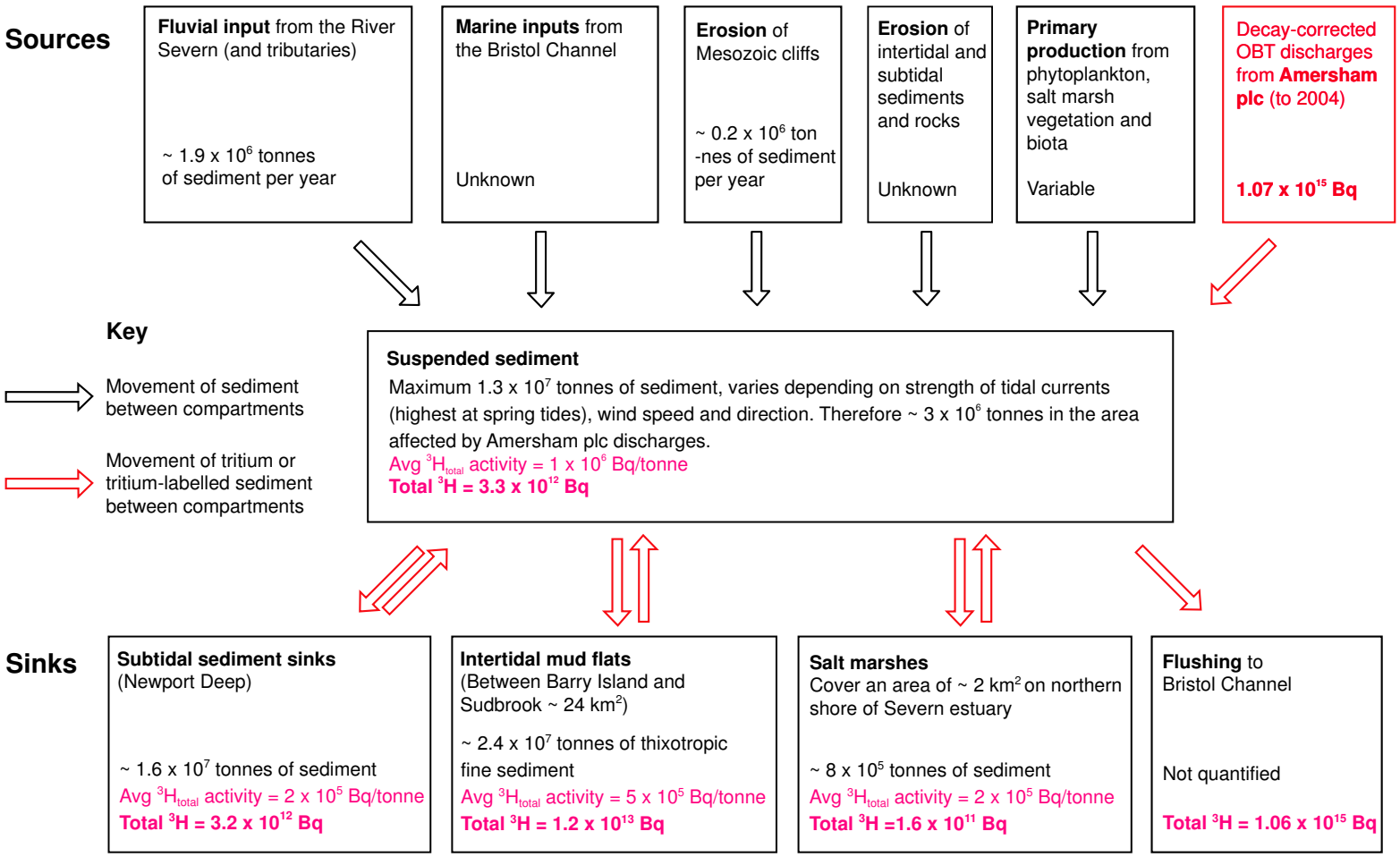

Figure 6.1: An assessment of the significance of OBT accumulation in Severn estuary sediments, calculated by combining the Severn estuary fine sediment inventory (data from Allen, 1987; Allen, 1992; Collins, 1987; Kirby, 1994; Parker and Kirby; 1982) with average $^3H_{total}$ measurements for sediments from each compartment and the decay-corrected total organic ^3H discharges from Amersham plc (Williams, 2004; 2005).

6.2.2 Tritium activities in biota

In the past, $^{3}H_{total}$ activities in both fish and sediments have followed similar trends to OBT discharges from Amersham plc (Figure 1.5 and 3.6). The correlation between fish and sediment $^{3}H_{total}$ activities is poor ($r^2 = 0.2$), perhaps because despite the daily variability of magnitude and composition of tritiated discharges from Amersham plc, sampling frequencies were limited to monthly for sediments and bi-monthly or less for fish in the studies compared (EA, EHS, FSA and SEPA, 2003 - 2005; FSA and SEPA, 1998 - 2002; Williams, 2002), and results were then averaged over the year. Therefore, data from the present study tentatively supports the hypothesis of McCubbin *et al* (2001) that ^{3}H bioaccumulation occurs primarily by feeding upon OBT-contaminated sediment dwelling microbes and meiofauna.

It is expected that the activities in flounder, and therefore the dose received by the critical group of seafood consumers, will decrease once tritiated discharges from Amersham plc into the Severn estuary cease. The release of tritiated sediments into suspension by erosion may increase suspended sediment ^{3}H activities, but this sediment would be rapidly diluted by the high suspended sediment load in the estuary. The current dose coefficient of OBT from Severn estuary flounder is 6 x 10^{-11} Sv Bq^{-1} for an average adult (Hodgson *et al*, 2005)(compared with 4.2 x 10^{-11} Sv Bq^{-1} and 1.8 x 10^{-11} Sv Bq^{-1} respectively for OBT and HTO; ICRP, 1993; Lambert, 2001). This results in an estimated dose of $\sim$60 μSv (Hodgson *et al*, 2005), which is not significant compared to the ICRP annual limit of exposure to an adult member of the public of 1 mSv/yr.

6.2.3 Tritium accumulation at other sites

OBT is also discharged under authorisation from hospitals, research institutes and pharmaceutical companies, who are end-users of the tritiated organic compounds produced by Amersham plc. Rowe *et al* (2001) studied the impact of discharges from a number of hospitals, research institutes and other pharmaceutical companies that use ^{3}H-labelled organic molecules produced by Amersham plc, on the Thames and Cam rivers. Elevated levels of tritium in biota relative to water were only observed near the outfall for UKAEA Harwell into the Thames; total ^{3}H activities in pike were higher than expected (201 Bq/kg and 129 Bq/kg in April 1999 and October 2000 respectively) and elevated OBT activities (240 Bq/kg) were also measured in pike collected in March 2000 (Rowe *et al*, 2001), although Rowe *et al* (2001) have recommended further sampling and analysis to confirm these results. Tritiated effluents from Harwell have significantly lower activities than Amersham plc, with a mean total ^{3}H activity concentration of 4400 Bq/l and a maximum of 14 600 Bq/l (FSA and SEPA, 2001).

Bioaccumulation of OBT in the environment is uncommon, but nevertheless it is possible wherever OBT is discharged, even at relatively low activities. It is important, therefore, that non-aqueous ^{3}H activities of sediments and biota are measured near all sites that discharge tritiated effluents containing OBT, especially if there are a number of smaller institutes located close together, as cumulatively they may have a larger effect.

References

Alexander, R., Kagi, R. I. and Larcher, A. V., 1982. Clay catalysis of aromatic hydrogen-exchange reactions. *Geochimica et Cosmochimica Acta*, **46**, 219-222.

Alexander, R., Kagi, R. I. and Larcher, A. V., 1984. Clay catalysis of alkyl hydrogen exchange reactions - reaction mechanisms. *Organic Geochemistry*, **6**, 755-760.

Allen, J. R. L., 1987. Coal dust in the Severn estuary, southwestern UK. *Marine Pollution Bulletin*, **18**, 169-174.

Allen, J. R. L., 1987. Reworking of muddy intertidal sediments in the Severn estuary, southwestern UK - a preliminary survey. *Sedimentary Geology*, **50**, 1-23.

Allen, J. R. L., 1987. Towards a quantitative chemostratigraphic model for sediments of Late Flandrian age in the Severn estuary, UK. *Sedimentary Geology*, **53**, 73-100.

Allen, J. R. L., 1988. Modern-period muddy sediments in the Severn estuary (southwestern UK): a pollutant-based model for dating and correlation. *Sedimentary Geology*, **58**, 1-21.

Allen, J. R. L., 1990. The Severn estuary in southwest Britain: its retreat under marine transgression, and fine-sediment regime. *Sedimentary Geology*, **66**, 13-28.

Allen, J. R. L., 1991. Salt-marsh accretion and sea-level movement in the Inner Severn Estuary, southwest Britain - the archaeological and historical contribution. *Journal of the Geological Society*, **148**, 485-494.

Allen, J. R. L., 1992. Tidally influenced marshes in the Severn estuary, southwest Britain. In *Saltmarshes: morphodynamics, conservation and engineering significance* (Edited by J. R. L. Allen and K. Pye), Cambridge University Press, Cambridge.

Allen, J. R. L., 2000. Morphodynamics of Holocene salt marshes: a review sketch from the Atlantic and Southern North Sea coasts of Europe. *Quaternary Science Reviews*, **19**, 1155-1231.

Allen, J. R. L. and Duffy, M. J., 1998. Medium-term sedimentation on high intertidal mud-

flats and salt marshes in the Severn Estuary, SW Britain: the role of wind and tide. *Marine Geology*, **150**, 1-27.

Allen, J. R. L. and Duffy, M. J., 1998. Temporal and spatial depositional patterns in the Severn estuary, SW Britain: intertidal studies at spring-neap and seasonal scales, 1991-3. *Marine Geology*, **146**, 147-171.

Allen, J. R. L. and Pye, K., 1992. *Saltmarshes: morphodynamics, conservation and engineering significance*. Cambridge University Press, Cambridge.

Allen, J. R. L. and Rae, J. E., 1986. Time sequence of metal pollution, Severn estuary, southwestern UK. *Marine Pollution Bulletin*, **17**, 427-431.

Allen, J. R. L., Rae, J. E., Longworth, G., Hasler, S. E. and Ivanovich, M., 1993. A comparison of the Pb-210 dating technique with 3 other independent dating methods in an oxic estuarine salt marsh sequence. *Estuaries*, **16**, 670-677.

Allen, J. R. L., Rae, J. E. and Zanin, P. E., 1990. Metal speciation (Cu, Zn, Pb) and organic matter in an oxic salt marsh, Severn estuary, southwest Britain. *Marine Pollution Bulletin*, **21**, 574-580.

Aller, R. C., 1994. Bioturbation and remineralisation of sedimentary organic matter: effect of redox oscillation. *Chemical Geology*, **114**, 331-345.

Appleby, P. G. and Oldfield, F., 1992. Application of lead-210 to sedimentation studies. In *Uranium-series disequilibrium: applications to earth, marine and environmental sciences* (Edited by M. Ivanovich and R. S. Harmon), 731-778. Clarendon Press, Oxford.

Appleby, P. G., Richardson, N. and Nolan, P. J., 1991. ^{241}Am dating of lake sediments. *Hydrobiologia*, **214**, 35-42.

Artemyev, V. E., 1996. *Geochemistry of organic matter in river-sea systems*. Kluwer Academic Publishers, Dordrecht.

Baumgartner, F. and Donhaerl, W., 2004. Non-exchangeable organically bound tritium (OBT): its real nature. *Analytical and Bioanalalytical Chemistry*, **379**, 204-209.

Baxter, A. J. and Camplin, W. C., 1993. *Measures of dispersion from discharge pipelines at nuclear sites in the UK using caesium-137 in sea water data. Fisheries Research Data Report Number 34*. MAFF Directorate of Fisheries Research, Lowestoft.

Beeftink, W. G. and Rozema, J., 1998. The nature and functioning of salt marshes. In *Pollution of the North Sea: an assessment* (Edited by W. Salomans, B. L. Bayne, E. K. Duursma and U. Forstner), 59-87. Springer, Berlin.

Begemann, F. and Libby, W. F., 1957. Continental water balance, ground water inventory and storage times, surface ocean mixing rates and world-wide water circulation patterns from cosmic-ray and bomb tritium. *Geochimica et Cosmochimica Acta*, **12**, 277-296.

Benoit, G. and Hemond, H. F., 1991. Evidence for diffusive redistribution of Pb-210 in lake sediments. *Geochimica et Cosmochimica Acta*, **55**, 1963-1975.

Blaylock, B. G., Hoffman, F. O. and Frank, M. L., 1986. Tritium in the aquatic environment. *Radiation Protection Dosimetry*, **16**, 65-71.

Bogen, D. C., Henkel, C. A., White, C. G. C. and Welford, A., 1973. A method for the determination of tritium distribution in environmental and biological samples. *Journal of Radioanalytical Chemistry*, **13**, 335-341.

Bryant, R. and Williams, D. J. A., 1983. Characteristics of suspended cohesive sediment of the Severn estuary, UK. *Canadian Journal of Fisheries and Aquatic Sciences*, **40 (Suppl. 1)**, 96-101.

Buchanan, J. B. and Longbottom, M. R., 1970. The determination of organic matter in marine muds: the effect of the presence of coal and the routine determination of protein. *Journal of Experimental Marine Biology and Ecology*, **5**, 158-169.

Burd, F., 1989. *The saltmarsh survey of Great Britain. An inventory of British saltmarshes.* Nature Conservancy Council, Peterborough.

Camplin, W. C., 1992 to 1995. *Radioactivity in surface and coastal waters of the British Isles, 1990 to 1994 (Annual reports).* MAFF Directorate of Fisheries Research, Lowestoft.

Clark, M. J. and Smith, F. B., 1988. Wet and dry deposition of Chernobyl releases. *Nature*, **332**,

Clarke, W. B., Jenkins, W. J. and Top, Z., 1976. Determination of tritium by mass spectrometric measurement of 3He. *International Journal of Applied Radiation and Isotopes*, **27**, 515-522.

Clayden, J., Greeves, N., Warren, S. and Wothers, P., 2001. *Organic Chemistry.* Oxford University Press, Oxford.

COGEMA, 2004. Webmaster. pers. comm.

Collins, M., 1983. Supply, distribution and transport of suspended sediment in a macrotidal environment: Bristol Channel, UK. *Canadian Journal of Fisheries and Aquatic Sciences*, **40(Suppl. 1)**, 44-59.

Collins, M., 1987. Sediment transport in the Bristol Channel: a review. *Proceedings of the Geological Association*, **98**, 367-383.

Comans, R. N. J., Middelburg, J. J., Zonderhuis, J., Woittiez, J. R. W., De Lange, G. J., Das, H. A. and Van Der Weijden, C. H., 1989. Mobilization of radiocaesium in pore water of lake sediments. *Nature*, **339**, 367-369.

Cooper, L. H. N., 1966. English Channel. In *The Encyclopedia of Oceanography* (Edited by

R. W. Fairbridge), Reinhold Publishing Corporation, New York.

Craig, D. L., Fallowfield, H. J. and Cromar, N. J., 2002. Enumeration of faecal coliforms from recreational coastal sites: evaluation of techniques for the separation of bacteria from sediments. *Journal of Applied Microbiology*, **93**, 557-565.

Craig, H. and Lal, D., 1961. The production rate of natural tritium. *Tellus*, **13**, 85.

Croudace, I. W., 1998. *Interpretation of geochemical data, laboratory practical handout.* Geosciences Advisory Unit, Southampton.

Culver, S. J., 1980. Differential two-way sediment transport in the Bristol Channel and Severn estuary, UK. *Marine Geology*, **34**, M39-M43.

Currie, L. A., 1968. Limits for qualitative detection and quantitative determination: application to radiochemistry. *Analytical chemistry*, **40**, 586-593.

DeLaune, R. D., Patrick, W. H. and Buresh, R. J., 1978. Sedimentation rates determined by ^{137}Cs dating in a rapidly accreting salt marsh. *Nature*, **275**, 532-533.

Diabete, S. and Strack, S., 1993. Organically bound tritium. *Health Physics*, **65**, 698-712.

Doulah, M. S., 1977. Mechanism of disintegration of biological cells in ultrasonic cavitation. *Biotechnology and Bioengineering*, **19**, 649-660.

Droppo, I. G., 2001. Rethinking what constitutes suspended sediment. *Hydrological Processes*, **15**, 1551-1564.

Dyer, A., 1974. *An introduction to liquid scintillation counting.* Heyden and Son Ltd, London.

Dyer, K. R., 1984. Sedimentation processes in the Bristol Channel/Severn estuary. *Marine Pollution Bulletin*, **15**, 53-57.

Dyer, K. R., 1997. *Estuaries, a physical introduction.* John Wiley Sons, Chichester.

EA, 2002. *Industry in Avonmouth: A public guide to pollution management.* Environment Agency South West Region, Exeter.

EA, 2003. *Radioactive Substances Act 1993. Proposed decision document on the application made by Amersham plc for a variation to the authorisation to dispose of radioactive wastes from its premises at: The Maynard Centre, Forest Farm, Whitchurch, Cardiff. Reference AB1363/BK3328..* Environment Agency Wales, Cardiff.

EA, EHS, FSA and SEPA, 2003. *Radioactivity in food and the environment, 2002. RIFE Report 8.* Environment Agency, Environment and Heritage Service, Food Standards Agency and Scottish Environment Protection Agency, Preston, Belfast, London and Stirling.

EA, EHS, FSA and SEPA, 2004. *Radioactivity in food and the environment, 2003. RIFE Re-*

port 9. Environment Agency, Environment and Heritage Service, Food Standards Agency and Scottish Environment Protection Agency, Preston, Belfast, London and Stirling.

Eisma, D., 1993. *Suspended matter in the aquatic environment.* Springer-Verlag, Berlin.

Epstein, S. S., Alexander, A., Cosman, K., Dompe, A., Gallagher, S., Jarsobski, J., Laning, E., Martinez, R., Panasik, G., Peluso, C., Runde, R. and Timmer, E., 1997. Enumeration of sandy sediment bacteria: are the counts quantitative or relative? *Marine Ecology Progress Series*, **151**, 11-16.

Ferrera, Z. S., Sanz, C. P., Santana, C. M. and Rodriguez, J. J. S., 2004. The use of micellar systems in the extraction and pre- concentration of organic pollutants in environmental samples. *Trac-Trends in Analytical Chemistry*, **23**, 469-479.

Fettweis, P. F., Verplancke, J., Venkataraman, R., Young, B. M. and Schwenn, H., 2003. Semiconductor detectors. In *Handbook of radioactivity analysis* (Edited by M. F. L'Annunziata), 239-347. Academic Press, San Diego.

Filgueiras, A. V., Capelo, J. L., Lavilla, I. and Bendicho, C., 2000. Comparison of ultrasound-assisted extraction and microwave-assisted digestion for determination of magnesium, manganese and zinc in plant samples by flame atomic absorption spectrometry. *Talanta*, **53**, 433-441.

Filip, Z. and Alberts, J. J., 1994. Microbial utilization resulting in early diagenesis of salt marsh humic acids. *Science of the Total Environment*, **144**, 121-135.

Fitton, G., 1997. X-ray fluorescence spectrometry. In *Modern Analytical Geochemistry: An introduction to quantitative chemical analysis techniques for earth, environmental and materials scientists* (Edited by R. Gill), 87-115. Longman, Singapore.

French, P. W., 1996. Implications of a saltmarsh chronology for the Severn estuary based on independent lines of dating evidence. *Marine Geology*, **135**, 115-125.

French, P. W., 1998. The impact of coal production on the sediment record of the Severn estuary. *Environmental Pollution*, **103**, 37-43.

French, P. W., Allen, J. R. L. and Appleby, P. G., 1994. 210-Lead dating of a modern period salt marsh deposit from the Severn estuary (southwest Britain), and its implications. *Marine Geology*, **118**, 327-334.

Froelich, P. N., 1980. Analysis of organic carbon in marine sediments. *Limnology and Oceanography*, **25**, 564-572.

FSA, 2005. *Provisional Radioactivity Surveillance Results - 2004.* Food Standards Agency, London.

FSA and SEPA, 1994-2001. *Radioactivity in Food and the Environment, 1994-2001. RIFE Reports 1-7.* FSA and SEPA, London.

FSA and SEPA, 1996. *Radioactivity in food and the environment, 1995. RIFE Report 1.* Food

Standards Agency and Scottish Environment Protection Agency, London and Stirling.

FSA and SEPA, 1997. *Radioactivity in food and the environment, 1996. RIFE Report 2.* Food Standards Agency and Scottish Environment Protection Agency, London and Stirling.

FSA and SEPA, 1998. *Radioactivity in food and the environment, 1997. RIFE Report 3.* Food Standards Agency and Scottish Environment Protection Agency, London and Stirling.

FSA and SEPA, 1999. *Radioactivity in food and the environment, 1998. RIFE Report 4.* Food Standards Agency and Scottish Environment Protection Agency, London and Stirling.

FSA and SEPA, 2000. *Radioactivity in food and the environment, 1999. RIFE Report 5.* Food Standards Agency and Scottish Environment Protection Agency, London and Stirling.

FSA and SEPA, 2001. *Radioactivity in food and the environment, 2000. RIFE Report 6.* Food Standards Agency and Scottish Environment Protection Agency, London and Stirling.

FSA and SEPA, 2002. *Radioactivity in food and the environment, 2001. RIFE Report 7.* Food Standards Agency and Scottish Environment Protection Agency, London and Stirling.

GAU, 2005. *Southern England radiation monitoring programme annual report: November 2003 to October 2004.* Geosciences Advisory Unit, Southampton.

Gaudette, H. E., Flight, W. R., Toner, L. and Folger, D. W., 1974. An inexpensive titration method for the determination of inorganic carbon in recent sediments. *Journal of Sedimentary Petrology*, **44**, 249-253.

Geonex, 1991. Aerial photographic print 046 (160 91), Scale 1:5000, taken on 01/07/1991. Obtained from the Central Register of Air Photography for Wales, The National Assembly for Wales, Cathays Park, Cardiff.

Ghosh, U., Gillette, J. S., Luthy, R. G. and Zare, R. N., 2000. Microscale location, characterisation and association of polycyclic aromatic hydrocarbons on narbor sediment particles. *Environmental Science Technology*, **34**, 1729-1736.

Goosens, H., de Leeuw, J. W., Rijpstra, W. I. C., Meyburg, G. C. and Schenck, P. A., 1989. Lipids and their mode of occurrence in bacteria and sediments - 1. A methodological study of the lipid composition of *Acinetobacter calcoaceticus* LMD 79-41. *Organic Geochemistry*, **14**, 15-25.

Gray, J., Jones, S. R. and Smith, A. D., 1995. Discharges to the environment from the Sellafield site 1951 - 1992. *Journal of Radiological Protection* , **15**, 99-131.

Green, G. A. and Welch, F. B. A., 1965. *Geology of the country around Wells and Cheddar. (Sheet 280).* HMSO, London.

Hamilton, E. I., Watson, P. G., Clearly, J. J. and Clifton, R. J., 1979. The geochemistry of recent sediments of the Bristol Channel - Severn estuary system. *Marine Geology*, **31**, 139-182.

Harrison, F. L. and Koranda, J. J., 1971. Tritiation of aquatic animals in an experimental fresh-

water pool. CONF-710501-P1 Proceedings of the Third National Symposium on Radioecology, Oak Ridge, Tennessee

Harrison, F. L., Koranda, J. J. and Tucker, J. S., 1973. Tritiation of aquatic animals in experimental marine pool. In *Tritium* (Edited by A. A. Moghissi and M. W. Carter), p. 363. Messenger Graphics, Phoenix, AZ.

Hill, R. L. and Johnson, J. R., 1993. Metabolism and dosimetry of tritium. *Health Physics*, **65**, 628-647.

Hodgson, A., Scott, J. E., Fell, T. P. and Harrison, J. D., 2005. Doses from the consumption of Cardiff Bay flounder containing organically bound tritium. *Journal of Radiological Protection*, **25**, 149-159.

Hosken, D., 2002. Captain of survey vessel New Ross I. pers. comm.

Howarth, M. J., 2001. North Sea Circulation. In *Encyclopedia of Ocean Sciences* (Edited by J. H. Steele, K. K. Turekian and S. A. Thorpe), 1917. Academic Press, London, San Diego.

Hunt, G. J., 1979 to 1989. *Radioactivity in surface and coastal waters of the British Isles, 1977 to 1988 (Annual reports).* MAFF Directorate of Fisheries Research, Lowestoft.

ICRP, 1993. *Age-dependent doses to members of the public from intakes of radionuclides: Part 2. Ingestion dose coefficients (publication 67).* International Commision on Radiological Protection, Oxford.

Jenkins, W. J., 2001. Tritium-helium dating. In *Encyclopedia of Ocean Sciences* (Edited by J. H. Steele, S. A. Thorpe and K. K. Turekian), 3048-3056. Academic Press, London.

Jenkins, W. J. and Rhines, P. B., 1980. Tritium in the deep North Atlantic Ocean. *Nature*, **286**, 877-880.

Jickells, T. D. and Rae, J. E., 1997. Biogeochemistry of intertidal sediments. In *Biogeochemistry of intertidal sediments* (Edited by T. D. Jickells and J. E. Rae), Cambridge University Press, Cambridge.

Joint, I. R. and Pomroy, A. J., 1982. Aspects of microbial heterotrophic production in a highly turbid estuary. *Journal of Experimental Marine Biology and Ecology*, **58**, 33-46.

Kallman, H., 1950. Scintillation counting with solutions. *Physics Reviews*, **78**, 621-622.

Kaufman, S. and Libby, W. F., 1954. The natural distribution of tritium. *Physics Reviews*, **93**, 1337-1344.

Kellaway, G. A. and Welch, F. B. A., 1993. *Geology of the Bristol District. Memoir for the 1:63 360 geological special sheet.* HMSO, London.

Kim, C. K., Cho, Y. W., Han, M. J. and Pak, C. K., 1992. Tritium distribution in some en-

vironmental sample - rice, Chinese cabbage and pine needles in Korea. *Journal of the Korean Association of Radiation Protection*, **17**, 25-35.

Kim, C. K. and Han, M. J., 1999. Dose assessment and behavior of tritium in environmental samples around Wolsong nuclear power plant. *Applied Radiation and Isotopes*, **50**, 783-791.

Kim, M. A. and Baumgartner, F., 1991. Tritium fractionation in biological systems and in analytical procedures. *Radiochmica Acta*, **54**, 121-128.

King, P., Kennedy, H., Newton, P. P., Jickells, T. D., Brand, T., Calvert, S., Cauwet, G., Etcheber, H., Head, B., Khripounoff, A., Manighetti, B. and Miquel, J. C., 1998. Analysis of total and organic carbon and total nitrogen in settling oceanic particles and a marine sediment: an interlaboratory comparison. *Marine Chemistry*, **60**, 203-216.

Kirby, R., 1986. *Suspended fine cohesive sediment in the Severn estuary and Inner Bristol Channel, UK*. Ravensrodd Consultants Ltd., Taunton, Somerset.

Kirby, R., 1994. The evolution of the fine sediment regime of the Severn estuary and Bristol Channel. *Biological Journal of the Linnean Society*, **51**, 37-44.

Kirby, R. and Parker, W. R., 1983. Distribution and behaviour of fine sediment in the Severn estuary and Inner Bristol Channel, UK. *Canadian Journal of Fisheries and Aquatic Sciences*, **40 (Suppl. 1)**, 83-95.

Kirchmann, R., Bonotto, S., Soman, S. D., Krishnamoorthy, T. M., Iyengar, T. S. and Moghissi, A. A., 1979. Transfer and incorporation of tritium in aquatic organisms. In *Behaviour of tritium in the environment* (Edited by IAEA, Vienna, Austria.

Knoll, G. F., 1979. *Radiation detection and measurement*. John Wiley and Sons, New York.

Krishnamurthy, R. V., Syrup, K. A., Baskaran, M. and Long, A., 1995. Late glacial climate record of Midwestern United States from the hydrogen isotope record of lake organic matter. *Science*, **269**, 1565-1567.

Krishnan, V. V., Sukumar, M., Gierasch, L. M. and Cosman, M., 2000. Dynamics of cellular retinoic acid binding protein I on multiple time scales with implications for ligand binding. *Biochemistry*, **39**, 9119-9129.

Kristensen, E., Ahmed, S. I. and Devol, A. H., 1995. Aerobic and anaerobic decomposition of organic matter in marine sediments: which is fastest? *Limnology and oceanography*, **40**, 1430-1437.

L'Annunziata, M. F., 2003. Liquid scintillation analysis: principles and practice. In *Handbook of radioactivity analysis* (Edited by M. F. L'Annunziata), 348-537. Academic Press, San Diego.

L'Annunziata, M. F., 2003. Nuclear radiation, its interaction with matter and radioisotope decay. In *Handbook of radioactivity analysis* (Edited by M. F. L'Annunziata), 1-122. Academic Press, San Diego.

Lambert, B., 2001. Invited editorial: Welsh tritium. *Journal of Radiological Protection*, **21**, 333-335.

Langston, W. J., Chesman, B. S., Burt, G. R., Hawkins, S. J., Readman, J. and Worsfold, P., 2003. *The Severn estuary.* Marine Biological Association, Plymouth.

Lee, S. V. and Cundy, A. B., 2001. Heavy metal contamination and mixing processes in sediments from the Humber estuary, eastern England. *Estuarine, Coastal and Shelf Science*, **53**, 619-636.

Libes, S. M., 1992. *An introduction to marine biogeochemistry.* John Wiley and Sons, Inc., New York.

Loring, D. H., 1990. Lithium - a new approach for the granulometric normalization of trace metal data. *Marine Chemistry*, **29**, 155-168.

Lucas, L. L. and Unterweger, M. P., 2000. Comprehensive review and critical evaluation of the half-life of tritium. *Journal of Research of the National Institute of Standards and Technology*, **105**, 541-549.

Mareque-Rivas, J. C., Prabaharan, R. and Parsons, S., 2004. Quantifying the relative contribution of hydrogen bonding and hydrophobic environments, and coordinating groups, in the zinc(II)-water acidity by synthetic modelling chemistry. *Dalton Transactions*, 1648-1655.

McCubbin, D., Leonard, K. S., Bailey, T. A., Williams, J. and Tossell, P., 2001. Incorporation of organic tritium (^{3}H) by marine organisms and sediment in the Severn estuary/Bristol Channel (UK). *Marine Pollution Bulletin*, **42**, 852-863.

Milan, C. S., Swenson, E. M., Turner, R. E. and Lee, J. M., 1995. Assessment of the ^{137}Cs method for estimating sediment accumulation rates: Louisiana salt marshes. *Journal of Coastal Research*, **11**, 296-307.

Mills, G. L. and Quinn, J. G., 1979. Determination of organic carbon in marine sediments by persulfate oxidation. *Chemical Geology*, **25**, 155-162.

Mills, I., Cvitas, T., Homann, K., Kallay, N. and Kuchitsu, K., 1988. *Quantities, units and symbols in physical chemistry.* Blackwell Scientific Publications, Oxford.

Mitchell, N. T., 1968-1978. *Radioactivity in surface and coastal waters of the British Isles, 1967 to 1978 (Annual reports).* MAFF Directorate of Fisheries Research, Lowestoft.

Moghissi, A. A., Bretthauer, E. W. and Compton, E. H., 1973. Separation of water from biological and environmental samples for tritium analysis. *Analytical chemistry*, **45**, 1565-1566.

Moghissi, A. A., Bretthauer, E. W., Whittaker, E. L. and McNelis, D. N., 1975. Oxygen bomb combustion of environmental and biological samples for tritium analysis. *International Journal of Applied Radiation and Isotopes*, **26**, 339-342.

Momoshima, N., Tjahaja, P. I., Okai, T. and Takashima, Y., 1994. Measurement of tritium in forest soil. G. T. Cook, D. D. Harkness, A. B. MacKenzie, B. F. Miller and E. M. Scott Liquid Scintillation Spectrometry 1994,

Moore, D. M. and Reynolds, R. C., 2003. *X-ray diffraction and the identification and analysis of clay minerals.*. Oxford University Press, Oxford.

Murray, J. W. and Hawkins, A. B., 1976. Sediment transport in the Severn estuary during the past 8000 to 9000 years. *Journal of the Geological Society, London*, **132**, 385-398.

NCRP, 1979. *Tritium in the environment*. National Council on Radiation Protection and Measurement, Bethesda, Maryland.

NCRP, 1985. *A handbook of radioactive measurements procedures*. National Council on Radiation Protection and Measurement, Bethesda, Maryland.

Nyman, J. A., Delaune, R. D., Pezeshki, S. R. and Patrick, W. H., 1995. Organic-matter fluxes and marsh stability in a rapidly submerging estuarine marsh. *Estuaries*, **18**, 207-218.

Okada, S. and Momoshima, N., 1993. Overview of tritium: characteristics, sources and problems. *Health Physics*, **65**, 595-609.

OS, 1978. Aerial photographic prints 19-20 (OS 78 134), Scale 1:7500, taken on 03/09/1978. Obtained from the Central Register of Air Photography for Wales, The National Assembly for Wales, Cathays Park, Cardiff.
OS, 1985. Aerial photographic prints 9-11 (OS 85 087), various scales, taken on 31/05/1985. Obtained from the Central Register of Air Photography for Wales, The National Assembly for Wales, Cathays Park, Cardiff.
Panel, S. E. S. a. S., 1977. *First report to the Technical Working Party of the Severn Estuary Joint Committee*.

Parker, W. R. and Kirby, R., 1982. *Sources and transport patterns of sediment in the inner Bristol Channel and Severn Estuary*. Thomas Telford, London.

Pernetta, J., 1994. *Philip's Atlas of the Oceans*. Reed International Books Ltd, London.

Plater, A. J. and Appleby, P. G., 2004. Tidal sedimentation in the Tees estuary during the 20th century: radionuclide and magnetic evidence of pollution and sedimentary response. *Estuarine Coastal and Shelf Science*, **60**, 179-192.

Pointurier, F., Baglan, N., Alanic, G. and Chiappini, R., 2003. Determination of organically bound tritium background level in biological samples from a wide area in the south-west of France. *Journal of Environmental Radioactivity*, **68**, 171-189.

Potts, P. J., 1993. Laboratory methods of analysis. In *Analysis of geological materials* (Edited by C. Riddle), 123-221. Marcel Dekker, Inc., New York.

Prandle, D., 1984. A modelling study of the mixing of ^{137}Cs in the seas of the European conti-

nental shelf. *Philosophical Transactions of the Royal Society of London A*, **310**, 407-436.

Prandle, D. and Beechey, J., 1991. The dispersal of ^{137}Cs from Sellafield and Chernobyl in the NWE European shelf seas. In *Radionuclides in the study of marine processes.* (Edited by P. J. Kershaw and D. S. Woodhead), 84-93. Elsevier Applied Sciences, London.

Prydz, S., Melo, T. B. and Koren, J. F., 1973. Low-temperature solid scintillation fluorography applied to radiochromatography with weak beta-emitters. *Analytical chemistry*, **45**, 2106-2111.

Radke, M., Sittardt, H. G. and Welte, D. H., 1978. Removal of soluble organic matter from rock samples with a flow-through extraction cell. *Analytical chemistry*, **50**, 663-665.

Rae, J. E. and Allen, J. R. L., 1993. The significance of organic matter degradation in the interpretation of historical pollution trends in depth profiles of estuarine sediment. *Estuaries*, **16**, 678-682.

RAF, 1947. Aerial photographic prints 5127-8 (CPE UK 2258), Scale 1:29100, taken on 25/08/1947. Obtained from the Central Register of Air Photography for Wales, The National Assembly for Wales, Cathays Park, Cardiff.
RAF, 1950. Aerial photographic prints 4122-3 (541 RAF 527), Scale 1:10000, taken on 14/05/1950. Obtained from the Central Register of Air Photography for Wales, The National Assembly for Wales, Cathays Park, Cardiff.
Reynolds, G. T., Harrison, F. B. and Salvini, G., 1950. Liquid scintillation counters. *Physics Reviews*, **78**, 488.

Rodgers, D. W., 1986. Tritium dynamics in juvenile rainbow trout. *Health Physics*, **50**, 89-98.

Rollinson, H., 1993. *Using geochemical data: evaluation, presentation, interpretation.* Longman, Harlow.

Rowe, J., James, A. and Allot, R., 2001. *Potential for bio-accumulation of organically bound tritium in the environment: review of monitoring data.* NCAS, Lancaster.

Rudran, K., 1988. Significance of *in vivo* organic binding of tritium following intake of tritiated water. *Radiation Protection Dosimetry*, **25**, 5-13.

Sessions, A. L., Sylva, S. P., Summons, R. E. and Hayes, J. M., 2004. Isotopic exchange of carbon-bound hydrogen over geologic timescales. *Geochimica et Cosmochimica Acta*, **68**, 1545-1559.

Sollas, W. J., 1883. The estuaries of the Severn and its tributaries; an inquiry into the nature and origin of their tidal sediments and alluvial flats. *Quarterly Journal of the Geological Society of London*, **39**, 611-626.

Strack, S. and Koenig, L. A., 1981. *Determination of organically bound tritium in environmental samples by application of the oxidising plasma technique. Report KfK 3294.* Kernforschungszentrum, Karlsruhe.

Tertian, R. and Claisse, F., 1982. *Principles of quantitative X-ray fluorescence analysis.* Heyden and Son Ltd., London.

Toole, J., 2001. *Intercomparison exercise: measurement of total tritium in dried sediment. Report NCAS/TR/2001/010.* Environment Agency, Lancaster.

Turekian, K. K. and Wederpohl, K. H., 1961. Distribution of the elements in some major units of the Earth's crust. *Geological Society of America Bulletin*, **72**, 175-192.

UIC Inc., 2005. *Application note 1: carbon dioxide coulometer.* UIC Inc., Joilet, IL.

Uncles, R. J., 1984. Hydrodynamics of the Bristol Channel. *Marine Pollution Bulletin*, **15**, 47-53.

Underwood, G. J. C. and Paterson, D. M., 1993. Seasonal changes in diatom biomass, sediment stability and biogenic stabilisation in the Severn estuary. *Journal of the Marine Biological Association UK*, **73**, 871-887.

UNSCEAR, 1977. *Sources and effects of ionising radiation. Report to the General Assembly by the United Nations Scientific Committee on the Effects of Atomic Radiation.* United Nations, Vienna.

UNSCEAR, 1993. *Sources and effects of ionising radiation. Report to the General Assembly by the United Nations Scientific Committee on the Effects of Atomic Radiation.* United Nations, Vienna.

UNSCEAR, 2000. *Sources and effects of ionising radiation. United Nations Scientific Committee on the Effects of Atomic Radiation. Report to the General Assembly, Volume 1: Sources.* United Nations, Vienna.

US EPA., 1994. *Material Safety Data Sheet for Methylene Chloride.* United States Environmental Protection Agency.

Verrall, K. E. and Odell, K. J., 2002. Measurement of organically bound tritium in environmental and effluent samples. Poster presented at. the 9th International Symposium on Environmental Radiochemical Analysis, Maidstone, UK.

Voparil, I. M., Mayer, L. M. and Place, A. R., 2003. Interactions among contaminants and nutritional lipids during mobilization by digestive fluids of marine invertebrates. *Environmental Science Technology*, **37**, 3117-3122.

Vre, R. M. and Binet, J., 1984. Molecular aspects of tritiated water and natural water in radiation biology. *Progress in Biophysics and Molecular Biology* , **43**, 61-193.

Waneke, T., Croudace, I. W., Warwick, P. E. and Taylor, R. N., 2002. A new ground-level fallout record of uranium and plutonium isotopes for northern temperate latitudes. *Earth and Planetary Science Letters*, **203**, 1047-1057.

Wang, B. C., Yoshikoshi, A. and Sakanishi, A., 1998. Carrot cell growth response in a stimulated ultrasonic environment. *Colloids and Surfaces B-Biointerfaces*, **12**, 89-95.

Ware, A. and Allot, R. W., 1999. *Review of methods for the analysis of total tritium and organically bound tritium. Report no. NCAS/TR/99/003.* National Compliance and Assessment Service, Environment Agency, Lancaster.

Warwick, P. E. and Croudace, I. W., 2005. *Organically bound tritium (OBT) dispersion and accumulation in Severn estuary sediments (RO1034). Report on extension to study.* Geosciences Advisory Unit, Southampton.

Warwick, P. E., Croudace, I. W. and Howard, A. G., 1999. Improved technique for the routine determination of tritiated water in aqueous samples. *Analytica Chimica Acta*, **382**, 225-231.

Warwick, P. E., Croudace, I. W., Howard, A. G., Cundy, A. B., Morris, J. E. and Doucette, K., 2003. Spatial and temporal variation of tritium activities in coastal marine sediments of the Severn estuary, UK. In *Environmental Radiochemical Analysis 2. Special Publication No. 291.* (Edited by P. Warwick), 192-197. Royal Society of Chemistry, Cambridge.

Water, D. C. W., 2002. *Annual report of the quality and environment committee, 2002.* Dwr Cymru/Welsh Water, Treharris.

Waters, R. A. and Lawrence, D. J. D., 1987. *Geology of the South Wales Coalfield, part III, the country around Cardiff. Memoir for 1:50 000 geological sheet 263 (England and Wales).* British Geological Survey, HM Staitionery Office, London.

Welch, F. B. A. and Trotter, F. M., 1961. *Geology of the country around Monmouth and Chepstow (Sheets 233 and 250).* HMSO, London.

Wickenden, D. A., 1993. Determination of tritiated water in biological matrices. *The Science of the Total Environment*, **130/131**, 121-128.

Williams, J. L., 2002. pers. comm. Amersham plc.

Williams, J. L., 2003. pers. comm. Amersham plc.

Williams, J. L., 2004. pers. comm. Amersham plc.

Williams, J. L., 2005. pers. comm. Amersham plc.

Williams, J. L., Russ, R. M., McCubbin, D. and Knowles, J. F., 2001. An overview of tritium behaviour in the Severn estuary (UK). *Journal of Radiological Protection*, **21**, 337-344.

Willsch, H., Clegg, H., Horsfield, B., Radke, M. and Wilkes, H., 1997. Liquid chromatographic separation of sediment, rock and coal extracts and crude oil into compound classes. *Analytical chemistry*, **69**, 4203-4209.

Yariv, S. and Cross, H., 1979. *Geochemistry of colloid systems for earth scientists.* Springer-Verlag, Berlin.

Zwolsman, J. J. G., Berger, G. W. and Van Eck, G. T. M., 1993. Sediment accumulation rates,

historical input, postdepositional mobility and retention of major elements and trace metals in salt marsh sediments of the Scheldt estuary, SW Netherlands. *Marine Chemistry*, **44**, 73-94.

Appendices

Appendix 1: Record of fieldwork

Appendix 2: Summary of all surface sediment data (Chapter 3)

Appendix 3: All data for the Peterstone 1, Peterstone 2, Barry Island and Sudbrook cores (Chapter 4)

Appendix 4: Raw data and calculations for the extraction experiments (Chapter 5)

Appendix 5: Results from the Newport Deep study of subtidal sediments and suspended sediment samples (Chapter 6)

Appendix 6: Calculations and assumptions made when constructing a model to assess the significance of OBT accumulations in Severn estuary sediments (Figure 6.1; Chapter 6)

Appendix 1: Record of fieldwork

Table A.1: Samples collected and observations made during sampling.

Date	Site	Type of sample	Sample description	Sample size (cm)	Notes
20/01/00	2	SS	Thin layer of soft sed with biofilm, overlying lt grey eroded sm surface	36 x 36 x 0.3	Erosion surface extends 100 m into estuary from sea wall
24/02/00	1 to 7	SS		25 x 25 x 1	
21/03/00	1 to 7 5	SS CORE	 mud	25 x 25 x 1 10 diameter x 40 length?	
17/05/00	1 2 3 4 5 6 7	SS SS SS SS SS SS SS	mud mud and gravel sand and gravel mud mud mud mud	25 x 25 x 1 25 x 25 x 1 25 x 25 x 1 25 x 25 x 1 25 x 25 x 1 25 x 25 x 1 25 x 25 x 1	
15/06/00	1 2 3 4 5 6 7	SS SS SS SS SS SS SS		25 x 25 x 1 25 x 25 x 1 25 x 25 x 1 25 x 25 x 1 25 x 25 x 1 25 x 25 x 1 25 x 25 x 1	 scouring erosion erosion visible surface sediments compacted
31/07/00	1 to 7 4	SS SS		25 x 25 x 1 25 x 25 x 1	 4 replicate samples (1-4) collected at 10 m intervals along a line perpendicular to the shore to check sampling homogeneity
25/09/00	1 to 7	SS		25 x 25 x 1	
25/10/00	1 2 3 4 5 6 7	SS SS SS SS SS SS SS		25 x 25 x 1 25 x 25 x 1 25 x 25 x 1 25 x 25 x 1 25 x 25 x 1 25 x 25 x 1 25 x 25 x 1	 eroded, only thin veneer present no mud, eroded marsh substrate
08/12/00	1 2 3 4 5 6 7	SS SS SS SS SS SS SS	sandy mud sand	25 x 25 x 1 25 x 25 x 1 25 x 25 x 1 25 x 25 x 1 25 x 25 x 1 25 x 25 x 1 25 x 25 x 1	 storms emplaced 3 cm of coarse sand on top of mud flat no mud, eroded marsh substrate eroded, no mud some mud eroded, no mud
06/02/01	1 to 5	SS		25 x 25 x 1	
26/04/01	1 2 3 4 6 7	SS SS SS - - SS	mud mud mud mud	25 x 25 x 1 25 x 25 x 1 25 x 25 x 1 25 x 25 x 1 25 x 25 x 1 25 x 25 x 1	 no access due to foot and mouth no access due to foot and mouth

Date	Site	Type of sample	Sample description	Sample size (cm)	Notes
04/07/01	1	SS	mud	25 x 25 x 1	sampling after v. heavy rain, sediments diluted
	1	CORE	mud/sand	10 diameter x 30 depth	*Spartina* marsh
	2	SS		25 x 25 x 1	
	3	SS		25 x 25 x 1	
	4	SS		25 x 25 x 1	
	4	CORE		10 diameter x 40 depth	taken from higher terrace of salt marsh
	6	SS		25 x 25 x 1	
30/08/01	1	SS		25 x 25 x 1	
	2	SS		25 x 25 x 1	
	2	BULK		100 x 50 x 1	
	3	SS		25 x 25 x 1	5 replicate samples collected at 5 m intervals to check sampling homogeneity
	3	BULK		100 x 50 x 1	
	4	SS		25 x 25 x 1	
	4	CORE		10 diameter x 5 depth	
	5	SS		25 x 25 x 1	
	6	SS		25 x 25 x 1	
02/10/01	1 to 6	SS		25 x 25 x 1	
05/11/01	J	SS	mud	25 x 25 x 1	
	H	SS	mud	25 x 25 x 1	
	H	CORE	mud	10 diameter x 40 depth	
	G	SS	mud	25 x 25 x 1	
	7	SS		25 x 25 x 1	
29/11/01	1	SS	mud	25 x 25 x 1	
	2	SS	sand	25 x 25 x 1	
	3	SS	muddy sand	25 x 25 x 1	
	4	SS	mud	40 x 25 x 0.5	
	5	SS		25 x 25 x 1	
	6	SS	mud	25 x 25 x 2	deployed sediment traps
	7	SS		25 x 25 x 1	
13/12/01	6	SS		25 x 25 x 1	
	6	ST	mud		trap sediments
	F	SS	muddy sand	30 x 10 x 0.3	mud bank behind sand dune
	1	SS	mud	25 x 25 x 1	
10/04/02	1	SS	mud	25 x 25 x 1	
	2	SS	fine sand	25 x 25 x 1	
	3	SS	muddy sand	40 x 10 x 1	
	4	SS	mud	25 x 25 x 1	
	5	SS	mud	25 x 25 x 1	massive marsh retreat since last visit
	6	SS	mud	25 x 25 x 1	
	7	SS	mud	25 x 25 x 1	
28/05/02	1	SS	mud	25 x 25 x 2	
	2	SS	muddy sand	25 x 25 x 1	
	3	SS	muddy sand	25 x 25 x 1	
	4	SS	mud	30 x 20 x 1	
	5	SS	mud	25 x 25 x 1	marsh ridge and furrow system completely eroded
	6	SS	mud	25 x 25 x 1	
	7	SS	mud	25 x 25 x 1	
12/07/02	1	SS	mud	25 x 25 x 2	
	2	SS	muddy sand	25 x 25 x 0.5	
	3	SS	mud	20 x 40 x 1	
	4	SS		25 x 25 x 1	
	5	SS	mud	25 x 25 x 1	
	6	SS	mud	30 x 30 x 0.5	
	7	SS	mud	25 x 25 x 1	

Date	Site	Type of sample	Sample description	Sample size (cm)	Notes
12/08/02	1	SS	mud	25 x 25 x 1	
	1	CORE		25 x 25 x 1	sandy fraction subsampled
	2	SS	mud	25 x 25 x 1	
	3	SS	mud	25 x 25 x 1	
	4	SS	mud	25 x 25 x 1	
	5	SS	mud	25 x 25 x 1	*Aster* on high marsh and *Salicornia* on low marsh - inundated more often
	6	SS		25 x 25 x 1	
	7	SS		25 x 25 x 1	
09/09/02	1	SS	mud	25 x 30 x 1	
	2	SS	sand	25 x 25 x 1	
	3	SS	mud	25 x 25 x 1	
	3	BULK		40 x 40 x 6	mud and sandy substrate
	4	SS	mud	25 x 25 x 1	
	5	SS	mud	40 x 40 x 0.5	
	6	SS	mud	25 x 25 x 1	
	7	SS	mud	25 x 40 x 1	
08/10/02	1	SS		25 x 25 x 1	
	2	SS	sand	10 x 15 x 2	
	3	SS	mud	25 x 25 x 1	mud patch developing over shingle
	4	SS	mud	15 x 20 x 1	
	5	SS	mud	15 x 20 x 1	well-developed ridge and furrows
	6	SS	mud	15 x 15 x 1	
	7	SS	mud	20 x 20 x 1	
29/10/02	NPD	CORES 2 to 7	mud to sand	10 diameter x 112 to 53 depth	
30/10/02	NPD	GRABS 24 to 1	mud to sand/gravel	From top 5 cm of sediment	
	NPD	WATER	water/suspended sediment samples	500 ml at 4m and 8 m depth	
31/10/02	NPD	CORES 8 to 10	mud	10 diameter x 115 to 44 depth	
01/11/02	1	SS	mud	30 x 20 x 1	
	2	SS	gritty sand	30 x 20 x 1	
	3	SS	mud	20 x 20 x 1	
	4	SS	mud	20 x 40 x 0.5	
	6	SS	mud	20 x 40 x 0.5	
	7	SS	mud	40 x 40 x 0.5	
18/12/02	1	SS	mud	25 x 25 x 1	
	2	SS	muddy sand	10 x 15 x 2	
	3	SS	sand	25 x 25 x 1	no mud
	4	SS	mud	40 x 20 x 1	fresh mud eroded
	5	SS	mud	50 x 20 x 1	grazing, ridge and furrows retreated further, little mud
	6	SS	sandy mud	20 x 30 x 1	
03/02/03	1	SS	mud	25 x 20 x 1	
	2	SS	sandy mud	25 x 20 x 1	
	3	SS	mud	25 x 20 x 1	
	4	SS	grey sticky mud	40 x 10 x 0.5	scouring, sample consisted of muddy substrate
	5	SS	grey sticky mud	50 x 20 x 0.5	little fresh mud, sample included muddy substrate
	6	SS	mud	15 x 20 x 1	v little fresh mud
	7	SS	mud	15 x 15 x 1	
21/02/03	1	SS	mud	30 x 40 x 1	
	2	SS	sandy mud	20 x 40 x 1	
	3	SS	mud	25 x 25 x 1	
	5	SS	mud	20 x 20 x 1	salt marsh still retreating
	6	SS	mud	30 x 25 x 1	diatom-rich algal bloom (a.b.) on mud flat surface

Date	Site	Type of sample	Sample description	Sample size (cm)	Notes
18/03/03	Q	SS	sandy mud	25 x 25 x 1	
	Q	CORE	mud	10 diameter x 40? cm depth	from creek bank
	N	SS	mud	20 x 20 x 1	
	M	CORE	mud	10 diameter x 30 cm depth	Atlantic high marsh (*Phragmites*)
	L	SS	muddy sand	60 x 30 x 0.5	
19/03/03	K	SS	mud	50 x 30 x 0.5	
	J	SS	mud	25 x 25 x 1	
	H	SS	mud	25 x 25 x 1	
	G	SS	mud	25 x 25 x 1	a.b.
	7	SS	mud	25 x 25 x 1	a.b.
	6	SS	mud	25 x 25 x 1	a.b.
	5	SS	mud	25 x 25 x 1	high marsh recently inundated
	4	SS	mud	25 x 25 x 1	
	1	SS	mud	25 x 25 x 1	
20/03/03	A	SS	mud	50 x 30 x 0.5	
	C	SS	sandy mud	25 x 25 x 1	
	D	SS	mud and sand	20 x 20 x 1	
	E	SS	mud and sand	25 x 30 x 1	
	F	SS	muddy sand	25 x 25 x 1	
07/05/03	1	SS	mud	30 x 15 x 1	
	6	SS	mud	25 x 25 x 1	
	5	SS	mud	20 x 20 x 1.5	
	4	SS	mud	20 x 20 x 1	
	3	SS	muddy sand	30 x 15 x 0.5	
	2	SS	mud	15 x 20 x 1	
02/06/03	1	SS	mud	15 x 20 x 1	
	2	SS	gravelly sand	35 x 30 x 0.5	
	4	SS	mud	30 x 30 x 1	
	5	SS	mud	60 x 30 x 1	marsh retreated further
	6	SS	sticky mud	30 x 30 x 1	
	7	SS	mud	30 x 30 x 1	
01/07/03	7	SS	mud	25 x 25 x 1	
	1	SS	mud	35 x 25 x 1	a.b.
	A	SS	mud	25 x 25 x 1	
02/07/03	B	SS	mud	20 x 40 x 1	anoxic mud from base of creek
	B	CORE	mud	10 cm diameter x 52 cm depth	Marsh vegetated by *Salicornia*
	2	SS	muddy sand	25 x 40 x 1	
	3	SS	mud	25 x 25 x 1	
	4	SS	mud	25 x 40 x 1	thin veneer wet mud
	5	SS	mud	20 x 40 x 1	marsh retreating, mud cracks developed
	6	SS	mud	25 x 25 x 1	
13/08/03	1	SS	mud	30 x 20 x 1	
	1	BULK	mud	50 x 50 x 2	
	2	SS	mud	30 x 30 x 1	surface veneer of mud
	2	BULK	mud	50 x 50 x 1	
	3	SS	mud	20 x 20 x 1	
	3	BULK	mud	50 x 50 x 1	
	4	SS	mud	25 x 25 x 1	
	4	BULK	mud	50 x 50 x 1	
	5	SS	mud	20 x 30 x 1	*Salicornia* regrowing on ridges
	5	BULK	mud	50 x 50 x 1	
	6	SS	mud	25 x 30 x 2	
	6	BULK	mud	50 x 50 x 2	
	7	SS	mud	25 x 25 x 1	
	7	BULK	mud	50 x 50 x 1	
11/09/03	1	SS	mud	25 x 25 x 1	
	2	SS	sandy mud	20 x 20 x 2	sediment trap deployed
	3	SS	mud	20 x 20 x 1	sediment trap deployed
	4	SS	mud	25 x 25 x 1	
	5	SS	mud	20 x 20 x 1	marsh sparsely recolonised by *Salicornia*
	6	SS	mud	25 x 25 x 1	
	7	SS	mud	20 x 25 x 1	

Date	Site	Type of sample	Sample description	Sample size (cm)	Notes
30/09/03	1	SS	mud	25 x 25 x 1	
	6	SS	mud	25 x 25 x 1	sediment trap deployed
	5	SS	mud	25 x 25 x 1	sediment trap deployed
	4	SS	mud	25 x 20 x 2	sediment trap deployed
	2	SS	mud	25 x 25 x 1	
	2	ST	mud		trap sediments collected
	3	SS	mud	25 x 25 x 1	no sample in sediment trap

Date	Site	Type of sample	Sample description	Sample size (cm)	Notes
28/10/03	1	SS	mud	25 x 25 x 1	
	2	SS	sandy mud	20 x 20 x 1-2	collected from ripples
	2	ST	mud		trap sediments collected
	3	SS	muddy gravel	25 x 25 x 1	sediment trap fell over
	4	SS	mud	25 x 25 x 1	a.b.
	4	ST	mud		trap sediments collected
	5	SS	mud	25 x 25 x 1	
	5	ST	mud		trap sediments collected
	5	CORE	mud	10 cm diameter x 45 cm depth	core collected from edge of creek on high marsh, front of marsh eroded further with no vegetation on ridges
	6	SS	mud	25 x 25 x 1	
	6	ST	mud		trap sediments collected
	7	SS	mud	25 x 25 x 1	sediment trap deployed
25/11/03	1	SS	mud	25 x 25 x 1	wet sediment, recent heavy rain
	2	SS	gravel	25 x 25 x 1	
	2	ST	mud		trap sediments collected
	3	SS	mud	25 x 25 x 1	erosion of mud patch
	4	SS	mud	25 x 25 x 1	no sample in sediment trap
	4	BULK	mud	50 x 50 x 1	
	5	SS	mud	25 x 25 x 1	a.b., cows grazing on marsh
	5	ST	mud		trap sediments collected
	5	BULK	mud	100 x 50 x 2	
	6	SS	sandy mud	25 x 25 x 1	
	6	ST	mud		trap sediments collected
	7	SS	sandy mud	25 x 25 x 1	
	7	ST	mud		trap sediments collected
11/12/03	1	SS	mud	25 x 25 x 1	
	2	SS	gravel	25 x 25 x 1	mud flat scoured
	2	ST	sandy mud		trap sediments collected
	3	SS	mud	25 x 45 x 0.5	mud patch eroded further
	4	SS	mud	30 x 40 x 0.5	mud flat scoured except for 1 or 2 patches
	4	ST	mud		trap sediments collected
	5	SS	mud	25 x 25 x 1	
	5	ST	mud		trap sediments collected
	6	SS	mud	25 x 25 x 1	no sample in sediment trap
22/01/04	2	SS	gravel	25 x 25 x 1	heavy rain that morning resuspended fine sediment
	3	SS	mud	20 x 25 x 1	
	3	BULK	mud	200 x 100 x 1	$\sim$ 9 litres of sediment collected
	4	SS	mud	20 x 25 x 1	sediments runny due to rains
	4	ST	mud		trap sediments collected
	5	SS	mud	25 x 25 x 1	sediments runny due to rains
	5	ST	mud		trap sediments collected
	6	SS	mud	20 x 40 x 1	
	6	ST	mud		trap sediments collected
	7	SS	mud	25 x 25 x 1	
	7	ST	mud		trap sediments collected
20/02/04	1	SS	mud	25 x 25 x 1	
	2	SS	sand	25 x 25 x 2	
	2	ST	sandy mud		trap sediments collected
	3	SS	gravelly mud	25 x 25 x 1	wind/wave-emplaced gravels on top of mud flat
	4	SS	mud	25 x 25 x 1	
	4	ST	mud		trap sediments collected
	5	SS	mud	25 x 25 x 1	marsh erosion increased at transition from high to low marsh, lots of shells
	5	ST	mud		trap sediments collected
	6	SS	sandy mud	25 x 25 x 1	coarse sand/gravel on top of mud
	6	ST	mud		trap sediments collected

Date	Site	Type of sample	Sample description	Sample size (cm)	Notes
18/03/04	1	SS	mud	20 x 25 x 1	
	2	SS	mud	20 x 20 x 1	
	2	ST	mud		trap sediments collected
	3	SS	mud	20 x 20 x 1	
	6	SS	mud	20 x 30 x 1	no sample in sediment trap
	7	SS	mud	20 x 30 x 1	no sample in sediment trap
04/05/04	1	SS	mud	25 x 25 x 1	
	2	SS	mud	20 x 20 x 1	
	3	SS	gravel	20 x 20 x 1	
	4	SS	mud	20 x 20 x 1	
	5	SS	mud	20 x 20 x 1	shells deposited on marsh surface - storm overwash deposits?
	6	SS	sandy mud	20 x 20 x 1.5 cm	

Notes:

SS - Surface sample
ST - Sediment trap
CS - Core sample
Grid references and descriptions of each sampling site are detailed in Table 3.1.

Appendix 2: Summary of all surface sediment data

Table A.2: Results from the analysis of surface sediment samples for total and water-extractable tritium and γ-emitting radionuclides. Total and water-extractable tritium activities were compiled from measurements by J. Morris, K. Doucette, Dr F.M. Dyer, Dr P. Teasdale and Dr J. Oh.

Sample ID	Sampling site	Sampling date	Water-extractable ^{3}H activity (Bq/g dry weight)	Uncertainty (2σ)	Total ^{3}H activity (Bq/g dry weight)	Uncertainty (2σ)	Duplicate total ^{3}H activity (Bq/g dry weight)	Uncertainty (2σ)	Triplicate total ^{3}H activity (Bq/g dry weight)	Uncertainty (2σ)	^{137}Cs activity (Bq/g)	Uncertainty (2σ)	^{210}Pb activity (Bq/g)	Uncertainty (2σ)
MT 16	1	24/02/2000	< 0.019		0.18	0.03					0.0041	0.00097	0.0199	0.0056
MT 17	3	24/02/2000	0.046	0.012	0.91	0.16					0.0203	0.0028	0.074	0.017
MT 18	2	24/02/2000	0.006	0.011	0.59	0.11					0.0167	0.0013	0.0599	0.0083
MT 19	4	24/02/2000	0.015	0.011	1.84	0.33					0.0307	0.0026	0.07	0.016
MT 20	5	24/02/2000	0.050	0.013	1.65	0.30					0.0382	0.005	0.081	0.027
MT 21	6	24/02/2000	0.047	0.013	1.01	0.18					0.0232	0.004	0.088	0.022
MT 22	7	24/02/2000	0.031	0.010	0.62	0.11					0.028	0.0039	0.068	0.021
MT 23	1	21/03/2000	< 0.053		0.21	0.04					0.004	0.0007	0.011	0.0053
MT 24	3	21/03/2000	0.024	0.033	1.15	0.21	0.89	0.16			0.012	0.0011	0.029	0.007
MT 25	2	21/03/2000	0.010	0.030	0.29	0.05					0.005	0.0008	0.022	0.0065
MT 26	5	21/03/2000	0.020	0.029	2.82	0.51					0.036	0.0033	0.068	0.018
MT 27	4	21/03/2000			1.78	0.32					0.041	0.0035	0.092	0.022
MT 28	6	21/03/2000	0.047	0.034	1.73	0.31					0.038	0.0031	0.074	0.018
MT 29	7	21/03/2000	0.006	0.031	1.19	0.21					0.08	0.0059	0.064	0.015
MT 30	1	17/05/2000	0.001	0.025	0.65	0.12					0.028	0.0028	0.077	0.019
MT 31	3	17/05/2000	0.031	0.027	1.18	0.21	0.59	0.11			0.019	0.0023	0.051	0.016
MT 32	2	17/05/2000	< 0.020		0.47	0.09					0.007	0.001	0.031	0.008
MT 33	5	17/05/2000	< 0.039		2.15	0.39					0.029	0.0023	0.066	0.015
MT 34	4	17/05/2000	0.017	0.020	1.56	0.28	1.49	0.27	1.66	0.30	0.03	0.0028	0.066	0.016
MT 35	6	17/05/2000	< 0.037		2.50	0.45					0.034	0.0044	0.052	0.019

Sample ID	Sampling site	Sampling date	Water-extractable ^{3}H activity (Bq/g dry weight)	Uncertainty (2σ)	Total ^{3}H activity (Bq/g dry weight)	Uncertainty (2σ)	Duplicate total ^{3}H activity (Bq/g dry weight)	Uncertainty (2σ)	Triplicate total ^{3}H activity (Bq/g dry weight)	Uncertainty (2σ)	^{137}Cs activity (Bq/g)	Uncertainty (2σ)	^{210}Pb activity (Bq/g)	Uncertainty (2σ)
MT 36	7	17/05/2000	< 0.033		0.98	0.18					0.034	0.0038	0.06	0.018
MT 37	1	15/06/2000	< 0.034		0.96	0.17					0.023	0.002	0.069	0.015
MT 38	3	15/06/2000	< 0.034		0.84	0.15					0.016	0.0022	0.041	0.012
MT 39	2	15/06/2000	0.006	0.027	0.48	0.09					0.005	0.001	0.023	0.0076
MT 40	4	15/06/2000	< 0.032		1.10	0.20					0.031	0.0032	0.06	0.017
MT 41	5	15/06/2000	0.010	0.031	1.21	0.22					0.027	0.0027	0.061	0.015
MT 42	6	15/06/2000	< 0.035		0.78	0.14					0.028	0.0033	0.047	0.016
MT 43	7	15/06/2000	< 0.035		0.68	0.12					0.027	0.0024	0.055	0.013
MT 44	1	31/07/2000	< 0.037		0.45	0.08					0.023	0.0032	0.079	0.022
MT 45	3	31/07/2000	< 0.034		0.44	0.08					0.01	0.0015	0.023	0.0092
MT 46	2	31/07/2000	< 0.037		0.26	0.05					0.003	0.0012	0.037	0.0097
MT 47	4	31/07/2000	< 0.031		3.22	0.58	2.87	0.51			0.029	0.0037	0.081	0.023
MT 48	4 (1)	31/07/2000	< 0.032		2.38	0.43					0.032	0.0037	0.062	0.02
MT 49	4 (2)	31/07/2000	< 0.033		2.45	0.44					0.033	0.0032	0.066	0.02
MT 50	4 (3)	31/07/2000	< 0.037		2.09	0.38					0.033	0.005	0.089	0.031
MT 51	4 (4)	31/07/2000	< 0.028		2.19	0.39					0.03	0.0041	0.064	0.022
MT 52	5	31/07/2000	< 0.032		1.60	0.29	1.56	0.28			0.024	0.0026	0.049	0.014
MT 53	6	31/07/2000	< 0.032		0.82	0.15					0.026	0.0026	0.071	0.018
MT 54	7	31/07/2000	< 0.036		0.77	0.14					0.033	0.0041	0.079	0.023
MT 55	1	25/09/2000	< 0.036		0.37	0.07					0.019	0.0025	0.062	0.017
MT 56	3	25/09/2000	< 0.014		0.41	0.08					0.011	0.0016	0.042	0.0091
MT 57	2	25/09/2000	0.011	0.027	0.16	0.03					0.005	0.0005		
MT 58	4	25/09/2000	< 0.030		0.97	0.17					0.025	0.0026	0.058	0.016
MT 59	5	25/09/2000	0.029	0.023	1.87	0.34					0.022	0.0018	0.042	0.013
MT 60	6	25/09/2000	0.037	0.029	0.33	0.06					0.028	0.003	0.054	0.017
MT 61	1	25/10/2000	< 0.041		0.42	0.08					0.018	0.0019	0.083	0.013

Sample ID	Sampling site	Sampling date	Water-extractable ^{3}H activity (Bq/g dry weight)	Uncertainty (2σ)	Total ^{3}H activity (Bq/g dry weight)	Uncertainty (2σ)	Duplicate total ^{3}H activity (Bq/g dry weight)	Uncertainty (2σ)	Triplicate total ^{3}H activity (Bq/g dry weight)	Uncertainty (2σ)	^{137}Cs activity (Bq/g)	Uncertainty (2σ)	^{210}Pb activity (Bq/g)	Uncertainty (2σ)
MT 62	3	25/10/2000	< 0.045		0.63	0.11					0.014	0.0013	0.039	0.0088
MT 63	2	25/10/2000	< 0.048		0.20	0.04					0.004	0.0006	0.026	0.0079
MT 64	4	25/10/2000	< 0.034		1.38	0.25					0.031	0.0022	0.069	0.014
MT 65	5	25/10/2000	0.001	0.019	0.86	0.16					0.031	0.0028	0.066	0.017
MT 66	6	25/10/2000	< 0.039		0.59	0.11					0.023	0.0025	0.069	0.013
MT 67	7	25/10/2000	< 0.030		0.46	0.08					0.032	0.0028	0.067	0.017
MT 73	1	08/12/2000	< 0.035		0.17	0.04					0.014	0.0019	0.048	0.014
MT 74	3	08/12/2000	0.001	0.023	0.42	0.08					0.007	0.0018	0.033	0.011
MT 75	2	08/12/2000	< 0.023		0.15	0.03					0.004	0.0007	0.022	0.0064
MT 76	4	08/12/2000	< 0.028		0.41	0.08					0.003	0.0005	0.018	0.0049
MT 77	6	08/12/2000	< 0.036		0.67	0.12					0.035	0.0024	0.063	0.014
MT 78	1	06/02/2001	< 0.040		0.23	0.05					0.023	0.0032	0.093	0.022
MT 79	3	06/02/2001	< 0.041		0.94	0.17					0.027	0.0035	0.063	0.021
MT 80	2	06/02/2001	< 0.040		0.11	0.02					0.004	0.0009	0.034	0.0073
MT 81	4	06/02/2001	< 0.031		0.36	0.07					0.006	0.0012	0.026	0.0098
MT 82	5	06/02/2001	0.041	0.013	0.37	0.07					0.007	0.0014	0.021	0.011
MT 83	6	06/02/2001	0.028	0.024	0.74	0.14					0.025	0.0039	0.042	0.023
MT 84	7	06/02/2001	< 0.043		0.04	0.02					0.031	0.0031	0.075	0.018
MT 89	6	30/08/2001			1.04	0.19					0.0312	0.0022	0.054	0.014
MT 90	5	30/08/2001			0.03	0.01								
MT 91	1	30/08/2001			0.16	0.04								
MT 92	4	30/08/2001			1.02	0.18								
MT 94	2	30/08/2001			0.18	0.04								
MT 95	2	30/08/2001			0.21	0.04					0.00396	0.00043	0.018	0.0043
MT 96	3	30/08/2001			0.87	0.16					0.0231	0.002	0.045	0.011
MT 97	3 (1)	30/08/2001			1.05	0.19								

Sample ID	Sampling site	Sampling date	Water-extractable ^{3}H activity (Bq/g dry weight)	Uncertainty (2σ)	Total ^{3}H activity (Bq/g dry weight)	Uncertainty (2σ)	Duplicate total ^{3}H activity (Bq/g dry weight)	Uncertainty (2σ)	Triplicate total ^{3}H activity (Bq/g dry weight)	Uncertainty (2σ)	^{137}Cs activity (Bq/g)	Uncertainty (2σ)	^{210}Pb activity (Bq/g)	Uncertainty (2σ)
MT 98	3 (2)	30/08/2001			0.59	0.11								
MT 99	3 (3)	30/08/2001			0.52	0.10								
MT 100	3 (4)	30/08/2001			1.15	0.21					0.0291	0.0024	0.053	0.011
MT 101	3 (5)	30/08/2001			0.49	0.09					0.0173	0.0014	0.044	0.012
MT 102	2	04/07/2001			0.28	0.05								
MT 103	3	04/07/2001			0.63	0.12								
MT 104	5	04/07/2001			0.81	0.15								
MT 105	1	04/07/2001			0.26	0.05					0.0136	0.0012	0.064	0.021
MT 106	6	04/07/2001			0.52	0.10								
MT 107	5	03/10/2001			0.38	0.07					0.024	0.0024	0.048	0.013
MT 109	2	03/10/2001			0.20	0.04	0.21	0.05			0.006	0.0009	0.019	0.0066
MT 110	1	03/10/2001			0.06	0.02					0.016	0.0018	0.045	0.012
MT 111	4	03/10/2001			0.17	0.04					0.026	0.0037	0.075	0.017
MT 112	6	03/10/2001			0.12	0.03					0.026	0.0029	0.068	0.013
MT 113	P	03/11/2001			0.11	0.03					0.016	0.002	0.039	0.012
MT 114	4	05/11/2001			6.65	1.19	8.19	1.47			0.043	0.0035	0.071	0.018
MT 115	J	05/11/2001			0.42	0.08	1.04	0.19			0.048	0.0047	0.073	0.023
MT 116	H	05/11/2001			0.15	0.03					0.04	0.0034	0.051	0.013
MT 117	G	05/11/2001			0.31	0.06					0.029	0.0026	0.048	0.013
MT 119	5	17/05/2000			1.23	0.22	0.29	0.05			0.027	0.0032	0.049	0.016
MT 120	3	26/04/2001			0.33	0.06					0.015	0.0017	0.034	0.0099
MT 121	4	26/04/2001			0.43	0.08					0.03	0.0036	0.062	0.021
MT 122	7	26/04/2001			0.55	0.10	0.73	0.13			0.028	0.0034	0.073	0.021
MT 123	2	26/04/2001			0.20	0.04					0.011	0.0016	0.031	0.012
MT 124	6	29/11/2001			0.49	0.09					0.03	0.0043	0.074	0.02
MT 125	1	29/11/2001			0.49	0.09					0.017	0.0015	0.04	0.0095

Sample ID	Sampling site	Sampling date	Water-extractable ^{3}H activity (Bq/g dry weight)	Uncertainty (2σ)	Total ^{3}H activity (Bq/g dry weight)	Uncertainty (2σ)	Duplicate total ^{3}H activity (Bq/g dry weight)	Uncertainty (2σ)	Triplicate total ^{3}H activity (Bq/g dry weight)	Uncertainty (2σ)	^{137}Cs activity (Bq/g)	Uncertainty (2σ)	^{210}Pb activity (Bq/g)	Uncertainty (2σ)
MT 126	4	29/11/2001			0.90	0.16								
MT 127	3	29/11/2001			0.36	0.07	0.40	0.07	0.44	0.08				
MT 128	2	29/11/2001			0.47	0.09	0.20	0.04						
MT 129	7	29/11/2001			0.01	0.00					0.038	0.0027	0.058	0.013
MT 130	5	29/11/2001			0.32	0.06								
MT 134	1	13/12/2001			0.27	0.05	0.18	0.04						
MT 135	F (1)	13/12/2001			0.19	0.04								
MT 136	F (2)	13/12/2001			0.34	0.06	0.17	0.04			0.002	0.0006	0.012	0.0049
MT 137	4	10/04/2002			1.08	0.20	1.10	0.20						
MT 138	2	10/04/2002	< 0.006		0.19	0.04					0.007	0.0011	0.021	0.0097
MT 139	3	10/04/2002			0.31	0.06					0.014	0.0014	0.022	0.0069
MT 140	1	10/04/2002			0.10	0.02								
MT 143	5	10/04/2002	0.035	0.007	0.33	0.06								
MT 144	2	27/05/2002	0.005	0.002	0.04	0.02								
MT 145	5	27/05/2002			0.26	0.05					0.035	0.0028	0.05	0.013
MT 146	4	27/05/2002									0.031	0.0027	0.053	0.012
MT 147	3	27/05/2002	< 0.006		0.08	0.02								
MT 148	6	27/05/2002									0.023	0.0023	0.04	0.012
MT 149	1	27/05/2002			0.04	0.01					0.016	0.0019	0.045	0.012
MT 153	1	12/07/2002	< 0.006		0.11	0.02					0.015	0.0011	0.044	0.0082
MT 155	6	12/07/2002			0.01	0.00					0.004	0.0008	0.01	0.0054
MT 156	2	12/07/2002	< 0.006											
MT 157	5	12/07/2002			0.32	0.06					0.03	0.0029	0.054	0.018
MT 158	4	12/07/2002			0.52	0.10					0.032	0.0038	0.071	0.02
MT 159	7	12/07/2002			0.29	0.05					0.032	0.0023	0.052	0.012
MT 160	1	01/11/2002			0.15	0.03								

Sample ID	Sampling site	Sampling date	Water-extractable ^{3}H activity (Bq/g dry weight)	Uncertainty (2σ)	Total ^{3}H activity (Bq/g dry weight)	Uncertainty (2σ)	Duplicate total ^{3}H activity (Bq/g dry weight)	Uncertainty (2σ)	Triplicate total ^{3}H activity (Bq/g dry weight)	Uncertainty (2σ)	^{137}Cs activity (Bq/g)	Uncertainty (2σ)	^{210}Pb activity (Bq/g)	Uncertainty (2σ)
MT 161	6	01/11/2002			0.27	0.05					0.033	0.0029	0.056	0.014
MT 162	1	03/02/2003			0.11	0.02					0.015	0.0016	0.042	0.015
MT 163	5	09/09/2002			0.48	0.09					0.039	0.0039	0.069	0.018
MT 164	5	08/10/2002			0.32	0.06					0.041	0.0033	0.064	0.015
MT 165	5	03/02/2003			0.09	0.02					0.005	0.0012	0.019	0.0095
MT 166	6	03/02/2003			0.25	0.05					0.02	0.0025	0.035	0.014
MT 167	4	03/02/2003			0.41	0.08					0.004	0.0013	0.033	0.014
MT 168	4	08/10/2002			1.00	0.19					0.02	0.0028	0.05	0.015
MT 169	3	21/02/2003			0.90	0.18	0.52	0.10						
MT 170	3	08/10/2002			0.32	0.06					0.034	0.0027	0.053	0.012
MT 171	2	12/08/2002			0.30	0.06					0.031	0.0028	0.082	0.014
MT 172	5	19/03/2003	0.010	0.004	0.53	0.10	0.35	0.06			0.042	0.0047	0.055	0.023
MT 173	N	18/03/2003			0.17	0.03	0.27	0.05			0.047	0.0039	0.058	0.022
MT 174	2	20/03/2003	0.007	0.004	0.16	0.03	0.21	0.04			0.007	0.0011	0.024	0.0067
MT 175	D	20/03/2003			0.00	0.00	0.02	0.01			0.001	0.0006	0.013	0.0052
MT 176	C	20/03/2003			0.04	0.01					0.016	0.0017	0.073	0.015
MT 177	F	20/03/2003			0.01	0.00	0.01	0.00			0.003	0.0007	0.015	0.0055
MT 178	E	20/03/2003			0.02	0.00	0.02	0.00			0.003	0.0009	0.015	0.007
MT 179	4	19/03/2003			0.69	0.12	0.99	0.18			0.038	0.0045	0.089	0.023
MT 180	3	20/03/2003			0.28	0.05	0.48	0.09	0.45	0.08	0.032	0.0029	0.071	0.017
MT 181	G	19/03/2003			0.44	0.08	0.40	0.07			0.045	0.0045	0.05	0.02
MT 182	7	08/10/2002			0.29	0.05					0.034	0.0035	0.056	0.017
MT 183	3	12/08/2002			0.22	0.04								
MT 184	3	01/11/2002			0.30	0.06					0.034	0.0034	0.054	0.016
MT 185	6	09/09/2002			0.20	0.04					0.031	0.0029	0.048	0.012
MT 186	7	01/11/2002			0.25	0.05					0.034	0.0028	0.06	0.017

Sample ID	Sampling site	Sampling date	Water-extractable ^{3}H activity (Bq/g dry weight)	Uncertainty (2σ)	Total ^{3}H activity (Bq/g dry weight)	Uncertainty (2σ)	Duplicate total ^{3}H activity (Bq/g dry weight)	Uncertainty (2σ)	Triplicate total ^{3}H activity (Bq/g dry weight)	Uncertainty (2σ)	^{137}Cs activity (Bq/g)	Uncertainty (2σ)	^{210}Pb activity (Bq/g)	Uncertainty (2σ)
MT 187	1	12/08/2002			0.12	0.02					0.015	0.0022	0.049	0.02
MT 188	5	21/02/2003			0.67	0.12					0.041	0.0038	0.062	0.017
MT 189	6	08/10/2002			0.36	0.07					0.04	0.0041	0.059	0.018
MT 190	1	09/09/2002			0.13	0.02					0.016	0.002	0.052	0.014
MT 191	4	12/08/2002	0.057	0.008	1.22	0.22					0.034	0.0031	0.055	0.016
MT 192	2	01/11/2002	< 0.007		0.11	0.02					0.011	0.0011	0.035	0.0078
MT 193	6	12/08/2002			0.34	0.06					0.029	0.0036	0.05	0.018
MT 194	2	08/10/2002			0.18	0.03					0.014	0.0018	0.042	0.012
MT 195	4	01/11/2002	0.029	0.006	0.82	0.15					0.034	0.0031	0.069	0.015
MT 196	3	12/07/2002			0.22	0.04					0.009	0.0013	0.022	0.0085
MT 197	5	12/08/2002			0.37	0.07					0.034	0.0027	0.054	0.013
MT 198	3	18/12/2002			0.21	0.04					0.01	0.0009	0.016	0.005
MT 199	1	18/12/2002	< 0.007		0.05	0.01					0.018	0.0022	0.046	0.014
MT 200	2	21/02/2003			0.26	0.05					0.005	0.0009	0.023	0.0071
MT 201	4	09/09/2002			0.72	0.13					0.038	0.005	0.063	0.019
MT 202	6	18/12/2002			0.13	0.03					0.008	0.0008	0.014	0.0055
MT 203	2	18/12/2002			0.22	0.04					0.009	0.0014	0.025	0.0081
MT 204	6	21/02/2003			0.52	0.10					0.043	0.0044	0.062	0.02
MT 205	1	21/02/2003	0.006	0.003	0.44	0.08					0.022	0.0031	0.047	0.017
MT 206	5	18/12/2002			0.51	0.09					0.029	0.0028	0.037	0.015
MT 207	7	27/05/2002			0.30	0.06					0.03	0.0033	0.049	0.015
MT 208	6	19/03/2003			0.34	0.06	0.41	0.07			0.037	0.0035	0.047	0.018
MT 209	1	19/03/2003			0.11	0.02	0.13	0.02			0.015	0.0023	0.042	0.014
MT 210	L	18/03/2003			0.06	0.01	0.06	0.01			0.012	0.0014	0.022	0.0086
MT 211	Q	18/03/2003	0.008	0.004	0.03	0.01	0.04	0.01			0.011	0.0011	0.019	0.006
MT 212	7	19/03/2003			0.36	0.07	0.32	0.06						

Sample ID	Sampling site	Sampling date	Water-extractable ^{3}H activity (Bq/g dry weight)	Uncertainty (2σ)	Total ^{3}H activity (Bq/g dry weight)	Uncertainty (2σ)	Duplicate total ^{3}H activity (Bq/g dry weight)	Uncertainty (2σ)	Triplicate total ^{3}H activity (Bq/g dry weight)	Uncertainty (2σ)	^{137}Cs activity (Bq/g)	Uncertainty (2σ)	^{210}Pb activity (Bq/g)	Uncertainty (2σ)
MT 213	A	20/03/2003	0.006	0.004	0.02	0.01	0.02	0.00			0.01	0.0026	0.084	0.018
MT 214	J	19/03/2003			0.31	0.06	0.22	0.04			0.047	0.0037	0.051	0.015
MT 215	K	19/03/2003			0.21	0.04					0.029	0.0027	0.047	0.014
MT 216	H	19/03/2003			0.14	0.03								
MT 217	2	03/02/2003			0.37	0.07					0.015	0.0017	0.027	0.0089
MT 218	7	03/02/2003			0.16	0.03					0.029	0.0019	0.053	0.0096
MT 219	7	09/09/2002									0.043	0.0043	0.067	0.018
MT 220	3	03/02/2003			0.67	0.12					0.024	0.0029	0.039	0.013
MT 221	7	12/08/2002			0.23	0.04					0.031	0.003	0.059	0.014
MT 223	1	07/05/2003			0.07	0.02					0.017	0.0019	0.03	0.013
MT 224	5	07/05/2003			0.25	0.05					0.035	0.0031	0.063	0.018
MT 225	4	07/05/2003			0.49	0.09					0.038	0.0038	0.067	0.019
MT 226	3	07/05/2003			0.33	0.06					0.027	0.0027	0.071	0.015
MT 227	2	07/05/2003			0.24	0.04					0.017	0.0018	0.042	0.0094
MT 228	6	07/05/2003			1.19	0.21					0.038	0.0044	0.051	0.02
MT 229	4	18/12/2002									0.033	0.0033	0.059	0.021
MT 230	1	02/06/2003			0.18	0.03					0.024	0.0028	0.068	0.017
MT 231	2	02/06/2003			0.10	0.03								
MT 232	4	02/06/2003			0.52	0.09					0.037	0.004	0.077	0.023
MT 233	5	02/06/2003	< 0.007		0.28	0.05					0.037	0.0035	0.065	0.017
MT 234	6	02/06/2003			0.39	0.07								
MT 235	1	01/07/2003	0.003	0.004	0.42	0.08								
MT 236	7	01/07/2003			0.15	0.03					0.023	0.0034	0.032	0.016
MT 237	A	01/07/2003	< 0.006		0.01	0.00					0.003	0.0013	0.02	0.01
MT 238	B	02/07/2003			0.01	0.00					0.027	0.0026	0.044	0.013
MT 239	2	02/07/2003			0.14	0.03					0.012	0.0016	0.035	0.0095

Sample ID	Sampling site	Sampling date	Water-extractable ^{3}H activity (Bq/g dry weight)	Uncertainty (2σ)	Total ^{3}H activity (Bq/g dry weight)	Uncertainty (2σ)	Duplicate total ^{3}H activity (Bq/g dry weight)	Uncertainty (2σ)	Triplicate total ^{3}H activity (Bq/g dry weight)	Uncertainty (2σ)	^{137}Cs activity (Bq/g)	Uncertainty (2σ)	^{210}Pb activity (Bq/g)	Uncertainty (2σ)
MT 240	3	02/07/2003			0.33	0.06					0.033	0.003	0.065	0.016
MT 241	5	02/07/2003			0.30	0.06	0.28	0.05			0.03	0.0033	0.062	0.016
MT 242	4	02/07/2003			0.23	0.04	0.39	0.07			0.035	0.004	0.063	0.021
MT 243	6	02/07/2003			0.09	0.02	0.15	0.03						
MT 244	1	13/08/2003			0.07	0.02	0.05	0.01						
MT 245	3	13/08/2003			0.26	0.05	0.24	0.04			0.034	0.0029	0.071	0.015
MT 246	2	13/08/2003			0.02	0.01	0.09	0.02			0.005	0.0008	0.021	0.0062
MT 247	4	13/08/2003			0.26	0.05					0.034	0.0042	0.056	0.017
MT 248	5	13/08/2003			0.18	0.04					0.038	0.0036	0.071	0.017
MT 249	6	13/08/2003			0.31	0.06					0.032	0.0029	0.044	0.014
MT 250	7	13/08/2003	0.002	0.002	0.17	0.03					0.038	0.0031	0.058	0.016
MT 251	7	13/08/2003			0.19	0.04								
MT 252	5	13/08/2003			0.26	0.05								
MT 253	2	13/08/2003			0.13	0.02								
MT 254	1	13/08/2003			0.08	0.02								
MT 255	6	13/08/2003			0.21	0.04								
MT 256	3	13/08/2003			0.26	0.05								
MT 257	4	13/08/2003			0.16	0.03								
MT 258	2	09/09/2002	0.023	0.025	0.19	0.04							0.032	0.0077
MT 259	3	09/09/2002									0.033	0.0039	0.07	0.018
MT 260	1	11/09/2003			0.08	0.02					0.018	0.0025	0.043	0.017
MT 261	3	11/09/2003			0.14	0.03					0.022	0.0019	0.044	0.01
MT 262	2	11/09/2003			0.09	0.02					0.006	0.0014	0.029	0.008
MT 263	4	11/09/2003			0.12	0.02					0.04	0.0037	0.069	0.017
MT 264	5	11/09/2003			0.27	0.05					0.044	0.0044	0.031	0.0039
MT 265	6	11/09/2003	< 0.006		0.97	0.18	0.23	0.05			0.037	0.0034	0.06	0.017

Sample ID	Sampling site	Sampling date	Water-extractable ^{3}H activity (Bq/g dry weight)	Uncertainty (2σ)	Total ^{3}H activity (Bq/g dry weight)	Uncertainty (2σ)	Duplicate total ^{3}H activity (Bq/g dry weight)	Uncertainty (2σ)	Triplicate total ^{3}H activity (Bq/g dry weight)	Uncertainty (2σ)	^{137}Cs activity (Bq/g)	Uncertainty (2σ)	^{210}Pb activity (Bq/g)	Uncertainty (2σ)
MT 266	1	08/10/2002	< 0.006		0.17	0.03	0.30	0.19			0.039	0.0032	0.064	0.021
MT 267	5	30/09/2003			0.02	0.01					0.038	0.003	0.058	0.015
MT 268	4	30/09/2003			0.15	0.03					0.039	0.0037	0.065	0.017
MT 269	1	30/09/2003			0.02	0.01					0.012	0.0014	0.03	0.0079
MT 270	2	30/09/2003	0.003	0.003	0.11	0.02	0.10	0.02			0.006	0.0011	0.028	0.0075
MT 271	3	30/09/2003			0.10	0.02					0.029	0.0022	0.047	0.011
MT 272	6	30/09/2003	< 0.003		0.30	0.06	0.27	0.05			0.035	0.0036	0.058	0.018
MT 273	2	30/09/2003			0.13	0.03								
MT 274	5	28/10/2003			0.11	0.02					0.04	0.0035	0.074	0.019
MT 275	7	28/10/2003			0.19	0.04					0.034	0.0031	0.05	0.015
MT 276	2	28/10/2003			0.09	0.02					0.005	0.0011	0.026	0.0081
MT 277	4	28/10/2003	< 0.005		0.26	0.05					0.044	0.0039	0.058	0.018
MT 278	3	28/10/2003			0.07	0.02								
MT 279	1	28/10/2003	0.005	0.005	0.05	0.02					0.021	0.0023	0.061	0.014
MT 280	6	28/10/2003			0.22	0.04					0.038	0.0034	0.057	0.015
MT 281	2	28/10/2003			0.09	0.02								
MT 282	4	28/10/2003			0.13	0.03								
MT 283	5	28/10/2003			0.10	0.02					0.04	0.004	0.078	0.018
MT 284	6	28/10/2003			0.21	0.04	0.21	0.04			0.034	0.0034	0.054	0.015
MT 285	5	25/11/2003	0.003	0.001	0.21	0.04	0.31	0.06			0.04	0.0033	0.056	0.015
MT 286	4	25/11/2003			0.33	0.06								
MT 287	3	25/11/2003	< 0.006		0.28	0.05					0.031	0.0025	0.057	0.013
MT 288	7	25/11/2003			0.18	0.04	0.19	0.04			0.034	0.0028	0.052	0.014
MT 289	6	25/11/2003	0.003	0.002	0.16	0.03					0.036	0.0035	0.057	0.019
MT 290	2	25/11/2003			0.07	0.02					0.006	0.0008	0.023	0.0063
MT 291	1	25/11/2003			0.14	0.03					0.023	0.0023	0.052	0.014

Sample ID	Sampling site	Sampling date	Water-extractable ^{3}H activity (Bq/g dry weight)	Uncertainty (2σ)	Total ^{3}H activity (Bq/g dry weight)	Uncertainty (2σ)	Duplicate total ^{3}H activity (Bq/g dry weight)	Uncertainty (2σ)	Triplicate total ^{3}H activity (Bq/g dry weight)	Uncertainty (2σ)	^{137}Cs activity (Bq/g)	Uncertainty (2σ)	^{210}Pb activity (Bq/g)	Uncertainty (2σ)
MT 292	6	25/11/2003			0.06	0.01								
MT 293	5	25/11/2003			0.07	0.02								
MT 295	7	25/11/2003			0.08	0.02								
MT 296	4	25/11/2003			0.35	0.07	0.65	0.12			0.04	0.0041	0.061	0.018
MT 297	5	25/11/2003			0.23	0.04	0.23	0.04						
MT 298	1	11/12/2003			0.22	0.04	0.14	0.03			0.023	0.0031	0.067	0.017
MT 299	2	11/12/2003			0.08	0.02	0.08	0.02			0.005	0.0009	0.025	0.0081
MT 300	3	11/12/2003			0.19	0.04	0.24	0.04			0.026	0.0023	0.05	0.012
MT 301	5	11/12/2003			0.12	0.03					0.027	0.0032	0.055	0.017
MT 303	6	11/12/2003			0.20	0.04					0.031	0.0029	0.058	0.015
MT 304	4	11/12/2003			0.05	0.02	0.07	0.02						
MT 305	5	11/12/2003			0.06	0.01	0.04	0.01			0.03	0.0028	0.06	0.016
MT 306	2	11/12/2003			0.09	0.02								
MT 307	3	22/01/2004			0.18	0.04					0.029	0.0025	0.049	0.012
MT 308	5	22/01/2004			0.10	0.03								
MT 309	7	22/01/2004	0.002	0.002	0.10	0.02	0.12	0.02			0.031	0.0035	0.06	0.02
MT 310	2	22/01/2004			0.05	0.01					0.006	0.0014	0.02	0.008
MT 311	4	22/01/2004			0.20	0.04					0.039	0.0037	0.061	0.019
MT 312	6	22/01/2004			0.08	0.02	0.25	0.05			0.026	0.0024	0.046	0.012
MT 313	3	22/01/2004	0.030	0.004	0.19	0.03	0.23	0.04			0.037	0.0028	0.058	0.014
MT 314	7	22/01/2004			0.06	0.01					0.036	0.003	0.057	0.013
MT 315	4	22/01/2004			0.11	0.02					0.032	0.003	0.063	0.015
MT 316	6	22/01/2004			0.13	0.03					0.018	0.0017	0.033	0.0082
MT 317	2	22/01/2004			0.17	0.03					0.024	0.0022	0.044	0.011
MT 318	5	22/01/2004			0.12	0.02					0.028	0.0026	0.058	0.014
MT 319	5	20/02/2004	< 0.004		0.22	0.04					0.041	0.0033	0.077	0.018

Sample ID	Sampling site	Sampling date	Water-extractable ^{3}H activity (Bq/g dry weight)	Uncertainty (2σ)	Total ^{3}H activity (Bq/g dry weight)	Uncertainty (2σ)	Duplicate total ^{3}H activity (Bq/g dry weight)	Uncertainty (2σ)	Triplicate total ^{3}H activity (Bq/g dry weight)	Uncertainty (2σ)	^{137}Cs activity (Bq/g)	Uncertainty (2σ)	^{210}Pb activity (Bq/g)	Uncertainty (2σ)
MT 320	4	20/02/2004	< 0.006		0.19	0.04					0.043	0.0032	0.074	0.015
MT 321	3	20/02/2004	< 0.005		0.21	0.04					0.041	0.003	0.069	0.015
MT 322	6	20/02/2004	< 0.005		0.08	0.02	0.18	0.03			0.029	0.0032	0.047	0.015
MT 323	1	20/02/2004			0.08	0.02	0.11	0.02			0.02	0.0023	0.063	0.016
MT 324	2	20/02/2004	< 0.004		0.07	0.02					0.008	0.0012	0.019	0.0076
MT 325	4	20/02/2004			0.22	0.04	0.12	0.02			0.041	0.0042	0.078	0.024
MT 326	6	20/02/2004			0.13	0.02	0.15	0.03	0.16	0.03	0.023	0.0022	0.044	0.012
MT 327	2	20/02/2004			0.19	0.03	0.19	0.04			0.023	0.0027	0.047	0.014
MT 328	5	20/02/2004	0.005	0.002	0.20	0.04	0.06	0.02			0.034	0.0032	0.066	0.016
MT 329	1	18/03/2004			0.11	0.02					0.018	0.002	0.049	0.014
MT 331	3	18/03/2004			0.25	0.05								
MT 332	6	18/03/2004			0.23	0.04					0.0402	0.0032	0.055	0.015
MT 334	7	04/05/2004			0.18	0.03					0.038	0.0034	0.058	0.016
MT 335	3	04/05/2004			0.18	0.03					0.037	0.0035	0.063	0.02
MT 336	6	04/05/2004			0.23	0.04					0.036	0.0037	0.057	0.02
MT 337	2	04/05/2004			0.08	0.02								
MT 338	4	04/05/2004			0.28	0.05					0.038	0.0038	0.076	0.019
MT 339	1	04/05/2004			0.08	0.02					0.019	0.0018	0.047	0.012
MT 340	5	04/05/2004			0.17	0.03								
MT 341	2	18/03/2004			0.21	0.04					0.03	0.0033	0.049	0.019

Table A.3: Results from the analysis of surface sediment samples for elemental composition by XRF analysis.

Sample ID	**SiO_2** (%)	**TiO_2** (%)	**Al_2O_3** (%)	**Fe_2O_3** (%)	**MnO** (%)	**MgO** (%)	**CaO** (%)	**K_2O** (%)	**Na_2O** (%)	**P_2O_5** (%)	**Rb** (ppm)	**Cu** (ppm)	**Pb** (ppm)	**Zn** (ppm)	**Ni** (ppm)	**Sn** (ppm)	**Sr** (ppm)	**Br** (ppm)	**I** (ppm)	**S** (ppm)	**Cl** (%)
MT 1	46.58	0.79	15.60	6.78	0.15	2.93	7.13	3.32	2.66	0.24	138	40	95	274	45	46	255	157	73	3110	3.10
MT 3	48.55	0.80	15.47	6.71	0.13	2.49	7.22	3.06	1.77	0.23	123	57	100	322	45	49	254	71	45	3355	1.38
MT 4	48.88	0.80	15.40	6.94	0.15	2.54	7.07	3.09	1.61	0.20	125	62	101	304	44	76	244	56	39	3564	1.11
MT 5	48.80	0.81	15.21	6.84	0.15	2.64	7.61	3.14	1.48	0.19	129	55	90	238	42	79	253	63	44	3483	1.00
MT 7	48.28	0.73	13.65	5.72	0.11	2.18	6.70	2.76	1.92	0.18	100	44	66	202	41	32	240	47	24	6934	1.34
MT 9	51.46	0.71	12.65	5.19	0.12	2.29	8.61	2.54	1.65	0.16	85	24	32	107	31	18	280	36	17	5221	0.96
MT 10	51.30	0.75	13.24	5.25	0.14	2.53	9.61	2.70	1.52	0.16	94	20	28	103	32	16	306	42	16	4667	0.89
MT 11	50.78	0.77	13.83	5.44	0.12	2.61	9.36	2.83	1.57	0.16	103	30	46	151	35	44	310	50	27	4626	0.99
MT 12	50.55	0.74	13.20	5.36	0.12	2.53	9.70	2.72	1.47	0.16	99	20	31	111	34	15	331	43	18	6524	0.82
MT 14	49.61	0.74	12.80	5.25	0.13	2.63	11.44	2.72	1.58	0.19	100	15	20	90	34	4	398	37	13	3983	0.83
MT 15	46.01	0.77	15.32	7.66	0.15	3.04	6.99	3.23	3.37	0.24	132	42	94	265	47	43	255	198	72	5589	4.23
MT 17	50.63	0.73	16.95	12.02	0.21	2.23	5.86	2.80	2.26	0.26	109	108	221	607	68	88	245	56	45	5046	1.51
MT 18	52.57	0.65	14.94	8.98	0.13	2.06	5.19	2.56	1.74	0.24	94	61	151	341	56	51	270	45	29	4510	1.15
MT 19	48.64	0.80	13.94	5.90	0.13	2.82	8.04	2.86	3.37	0.22	113	34	74	220	40	52	252	144	63	3565	3.50
MT 20	48.08	0.80	14.83	6.41	0.14	2.76	7.69	3.08	3.18	0.23	125	38	84	247	42	49	254	131	72	2899	2.86
MT 21	50.44	0.80	13.82	5.72	0.13	2.65	8.31	2.78	2.25	0.23	111	35	71	214	39	53	257	104	64	2749	1.98
MT 22	50.77	0.79	13.26	5.36	0.12	2.54	8.65	2.61	2.35	0.22	100	31	66	197	36	51	252	88	59	2680	1.87
MT 24	51.65	0.69	18.79	11.00	0.24	1.81	4.81	2.77	1.49	0.28	105	142	219	777	68	93	240	38	36	3950	0.90
MT 26	45.88	0.77	15.14	6.56	0.15	2.97	7.38	3.21	4.87	0.23	132	41	90	261	44	39	264	191	63	3671	4.39
MT 27	45.43	0.77	15.04	6.46	0.14	3.08	7.15	3.23	3.57	0.23	131	39	90	258	43	44	255	218	70	3906	4.48
MT 28	46.75	0.79	15.09	6.52	0.14	2.95	7.56	3.18	2.89	0.23	130	41	89	257	43	45	262	170	70	3376	3.38
MT 29	48.09	0.80	14.44	6.11	0.13	2.88	7.94	2.97	2.95	0.23	119	37	82	237	41	50	257	151	71	3108	3.09
MT 30	46.61	0.76	14.00	5.83	0.15	2.71	8.83	2.90	3.37	0.22	114	34	74	210	39	51	282	160	64	3448	3.54
MT 31	48.56	0.73	16.25	7.70	0.20	2.18	6.60	2.84	3.11	0.25	109	67	137	414	48	47	275	78	36	3875	2.38
MT 32	59.45	0.54	14.74	5.50	0.11	1.44	3.14	2.21	1.33	0.24	77	54	107	218	45	34	289	23	14	4237	0.84
MT 33	48.38	0.77	14.68	6.54	0.12	2.74	7.72	3.07	2.35	0.24	117	36	82	230	41	41	255	117	54	3944	2.41
MT 34	49.23	0.80	14.81	7.42	0.12	2.73	7.66	3.04	2.13	0.24	122	39	85	247	44	49	250	114	61	4587	1.98

Sample ID	**SiO_2** (%)	**TiO_2** (%)	**Al_2O_3** (%)	**Fe_2O_3** (%)	**MnO** (%)	**MgO** (%)	**CaO** (%)	**K_2O** (%)	**Na_2O** (%)	**P_2O_5** (%)	**Rb** (ppm)	**Cu** (ppm)	**Pb** (ppm)	**Zn** (ppm)	**Ni** (ppm)	**Sn** (ppm)	**Sr** (ppm)	**Br** (ppm)	**I** (ppm)	**S** (ppm)	**Cl** (%)
MT 35	48.61	0.80	15.01	6.49	0.14	2.79	7.52	3.14	2.13	0.24	127	38	87	250	43	54	251	126	67	2941	2.16
MT 36	48.79	0.81	14.79	6.35	0.14	2.77	7.76	3.04	2.37	0.23	124	38	85	245	41	53	254	120	68	2785	2.27
MT 37	47.72	0.75	13.72	5.64	0.15	2.68	9.13	2.80	4.24	0.22	107	32	70	197	37	49	275	151	66	3475	3.83
MT 38	48.26	0.70	15.96	7.83	0.21	2.03	7.58	2.70	2.44	0.24	103	74	124	396	50	45	312	56	32	4868	1.80
MT 39	57.26	0.58	14.85	5.38	0.11	1.55	4.11	2.30	1.37	0.24	82	48	96	205	50	18	359	28	14	4760	0.87
MT 40	48.94	0.80	14.96	7.30	0.12	2.83	7.65	3.10	2.15	0.23	126	40	86	248	48	47	253	115	60	5045	2.14
MT 41	49.41	0.76	14.25	6.35	0.12	2.65	7.75	2.95	2.97	0.24	115	35	78	221	41	43	251	109	53	3901	2.61
MT 42	49.95	0.79	14.26	6.07	0.13	2.68	7.74	2.91	2.67	0.23	112	33	76	219	39	48	242	104	60	2974	2.41
MT 43	49.53	0.81	14.80	6.38	0.14	2.71	7.99	3.04	1.89	0.23	123	38	83	241	42	50	253	92	68	2525	1.49
MT 47	45.83	0.79	14.72	6.37	0.15	3.07	7.53	3.10	6.31	0.22	125	38	83	243	43	45	259	205	58	4297	5.45
MT 48	46.48	0.79	14.95	6.46	0.14	3.01	7.46	3.14	5.53	0.23	128	38	83	245	43	43	258	181	55	4306	4.67
MT 49	47.56	0.80	15.22	6.88	0.12	2.83	7.43	3.21	2.98	0.24	133	39	88	252	45	45	254	132	61	4009	2.90
MT 50	47.32	0.79	14.74	6.38	0.13	2.96	7.66	3.07	5.37	0.22	124	37	81	236	42	48	256	166	60	4085	4.44
MT 51	47.58	0.81	14.79	6.40	0.16	2.92	7.52	3.08	4.72	0.23	126	36	83	240	42	46	250	154	56	3605	3.95
MT 52	49.54	0.73	13.82	6.10	0.10	2.60	8.22	2.85	3.30	0.24	105	32	73	197	37	34	255	97	43	4801	2.79
MT 53	49.87	0.76	14.35	6.17	0.13	2.66	7.51	2.93	2.83	0.24	111	34	77	220	38	47	235	99	54	3086	2.57
MT 54	47.72	0.81	14.86	6.41	0.16	2.85	7.71	3.08	2.89	0.24	126	37	86	249	42	51	254	131	62	2983	2.97
MT 55	49.31	0.71	12.74	5.14	0.10	2.48	9.87	2.53	4.38	0.23	94	30	63	180	34	47	271	113	52	2943	3.21
MT 56	48.93	0.70	17.42	13.24	0.26	1.90	5.52	2.57	1.32	0.26	97	117	209	621	73	73	252	30	31	6392	0.68
MT 57	58.95	0.56	14.83	5.25	0.11	1.53	3.61	2.25	1.35	0.24	80	45	96	187	49	11	364	24	8	2774	0.89
MT 58	50.46	0.83	14.54	6.64	0.12	2.68	7.95	2.97	2.22	0.22	119	33	74	217	42	44	248	84	47	4340	1.78
MT 59	50.46	0.81	14.11	5.86	0.11	2.57	8.58	2.87	2.15	0.23	112	31	69	201	38	44	261	70	46	2890	1.58
MT 60	50.40	0.80	14.54	6.23	0.10	2.59	7.81	2.96	2.07	0.24	113	34	78	223	39	47	239	73	52	2789	1.52
MT 61	49.93	0.72	12.49	5.00	0.11	2.43	10.12	2.47	3.38	0.23	89	29	60	171	32	47	273	103	53	2825	2.78
MT 62	49.41	0.72	17.43	13.15	0.22	1.97	5.31	2.65	1.68	0.24	100	129	244	611	74	81	253	39	35	6494	1.00
MT 64	49.11	0.82	14.68	6.59	0.13	2.72	7.85	3.01	2.94	0.23	122	38	81	236	43	46	251	105	59	3410	2.49
MT 65	48.66	0.81	14.74	6.33	0.12	2.73	7.84	3.05	3.03	0.23	124	37	81	236	43	45	254	115	54	2883	2.70
MT 66	51.47	0.77	13.71	5.85	0.11	2.52	8.10	2.73	2.42	0.22	101	32	68	197	37	53	238	70	42	3470	1.83
MT 67	49.79	0.81	14.44	6.02	0.10	2.64	8.17	2.95	2.33	0.21	116	35	78	227	40	52	253	85	52	2703	1.87

Sample ID	**SiO_2** (%)	**TiO_2** (%)	**Al_2O_3** (%)	**Fe_2O_3** (%)	**MnO** (%)	**MgO** (%)	**CaO** (%)	**K_2O** (%)	**Na_2O** (%)	**P_2O_5** (%)	**Rb** (ppm)	**Cu** (ppm)	**Pb** (ppm)	**Zn** (ppm)	**Ni** (ppm)	**Sn** (ppm)	**Sr** (ppm)	**Br** (ppm)	**I** (ppm)	**S** (ppm)	**Cl** (%)
MT 73	50.31	0.71	11.74	4.55	0.09	2.24	11.26	2.27	2.39	0.22	79	26	53	150	30	48	278	72	49	2442	1.71
MT 74	36.77	0.70	16.27	9.68	0.23	1.30	4.54	2.63	0.97	0.34	84	102	166	530	54	59	306	34	21	11298	0.67
MT 75	58.36	0.53	14.38	5.69	0.12	1.45	3.51	2.17	0.99	0.25	72	44	123	210	45	16	337	15	7	2858	0.50
MT 77	49.66	0.81	15.28	6.80	0.12	2.59	7.48	3.18	1.53	0.22	130	39	91	259	44	49	245	64	58	2738	0.91
MT 78	48.63	0.76	13.34	5.41	0.12	2.45	9.79	2.68	2.96	0.21	102	32	64	179	36	53	293	127	83	2823	2.60
MT 80	56.54	0.59	15.94	5.12	0.11	1.47	3.52	2.43	1.24	0.27	84	52	107	204	50	11	390	22	7	2965	0.77
MT 82	53.82	0.72	11.64	4.95	0.11	2.20	10.11	2.35	1.58	0.18	86	20	37	116	32	22	301	45	26	3880	0.84
MT 83	49.53	0.80	14.44	6.31	0.12	2.57	7.05	2.97	2.41	0.22	117	33	70	211	41	47	235	101	55	5650	1.96
MT 84	49.27	0.82	14.66	6.29	0.14	2.65	7.85	2.96	2.32	0.23	121	37	81	231	41	50	255	93	72	2436	1.79
MT 89	48.99	0.82	14.90	6.44	0.14	2.68	7.84	3.06	2.26	0.24	126	37	82	239	42	51	256	93	66	2418	1.83
MT 92	48.45	0.82	15.36	6.82	0.15	2.81	7.46	3.22	1.96	0.24	135	39	89	256	44	46	258	119	62	2924	1.93
MT 94	60.34	0.53	13.55	5.08	0.11	1.31	3.52	2.01	1.15	0.23	71	46	95	169	51	13	387	18	5	4190	0.68
MT 95	58.31	0.55	14.80	5.08	0.11	1.49	3.46	2.22	1.03	0.26	78	48	91	195	48	13	370	25	9	2844	0.70
MT 96	48.62	0.80	15.68	7.39	0.19	2.53	7.24	3.04	2.32	0.25	126	55	115	340	48	49	267	69	42	2852	1.84
MT 97	47.19	0.78	15.29	7.89	0.15	2.55	7.79	3.02	2.78	0.24	121	59	122	349	49	54	278	94	55	3531	2.30
MT 98	48.88	0.79	18.34	6.61	0.21	1.96	6.06	3.06	1.89	0.25	120	66	105	363	47	36	282	55	29	2960	1.33
MT 99	51.46	0.70	17.38	13.35	0.28	2.00	5.17	2.63	2.04	0.29	109	138	221	760	74	96	243	41	44	5323	1.16
MT 100	48.86	0.81	15.25	6.83	0.15	2.67	7.72	3.14	1.85	0.24	129	42	94	262	44	49	259	101	61	2691	1.41
MT 101	46.78	0.74	15.78	8.61	0.18	2.21	9.41	2.73	2.14	0.23	103	74	133	387	53	54	376	54	34	4538	1.47
MT 102	50.81	0.65	16.54	5.53	0.11	1.52	3.90	2.61	1.36	0.26	91	55	105	208	52	13	407	30	8	5176	0.90
MT 103	48.39	0.77	15.24	7.90	0.14	2.59	7.57	3.01	2.81	0.23	120	58	116	338	50	61	262	96	52	3239	2.18
MT 104	50.80	0.82	14.14	5.89	0.11	2.55	8.50	2.83	2.00	0.23	112	32	70	207	38	48	264	77	50	2720	1.37
MT 105	50.52	0.74	12.95	5.01	0.12	2.35	10.56	2.51	1.66	0.22	90	27	54	158	32	49	294	82	67	2450	1.21
MT 106	49.84	0.82	14.53	6.18	0.10	2.63	7.96	2.98	2.14	0.23	122	35	79	224	41	51	254	97	56	2722	1.74
MT 107	50.84	0.82	14.42	6.16	0.10	2.52	8.16	2.93	1.82	0.23	115	32	75	212	39	49	252	69	49	2630	1.19
MT 109	49.48	0.61	15.39	6.13	0.11	1.60	3.98	2.56	1.30	0.25	80	51	145	206	46	17	353	29	10	5345	0.87
MT 110	50.95	0.74	12.54	4.99	0.12	2.30	10.62	2.43	1.96	0.22	87	27	54	159	31	52	288	82	67	2380	1.36
MT 111	50.54	0.82	14.89	6.59	0.11	2.58	8.07	3.04	1.35	0.22	123	36	80	229	42	52	260	77	55	3712	0.81
MT 112	50.48	0.80	14.33	6.00	0.10	2.57	8.00	2.92	1.80	0.23	110	33	73	212	38	45	245	80	50	2720	1.42

Sample ID	**SiO_2** (%)	**TiO_2** (%)	**Al_2O_3** (%)	**Fe_2O_3** (%)	**MnO** (%)	**MgO** (%)	**CaO** (%)	**K_2O** (%)	**Na_2O** (%)	**P_2O_5** (%)	**Rb** (ppm)	**Cu** (ppm)	**Pb** (ppm)	**Zn** (ppm)	**Ni** (ppm)	**Sn** (ppm)	**Sr** (ppm)	**Br** (ppm)	**I** (ppm)	**S** (ppm)	**Cl** (%)
MT 113	58.09	0.52	9.89	3.99	0.09	1.89	8.68	2.10	1.97	0.18	72	20	49	131	26	23	257	45	29	1881	1.32
MT 114	47.46	0.81	15.68	7.11	0.15	2.72	7.37	3.34	2.16	0.27	140	43	94	274	46	43	265	106	73	2413	1.85
MT 115	48.97	0.82	14.69	6.33	0.14	2.69	7.98	2.96	2.47	0.24	121	42	87	263	42	54	256	97	74	2281	1.95
MT 116	49.93	0.80	14.26	6.06	0.13	2.64	8.19	2.88	1.80	0.22	117	36	79	233	40	50	258	97	72	2473	1.54
MT 117	51.71	0.81	14.23	5.75	0.10	2.56	8.27	2.82	1.54	0.23	110	33	71	209	38	54	250	70	54	2119	1.01
MT 119	49.38	0.79	15.19	6.79	0.11	2.62	7.62	3.17	1.97	0.25	125	39	86	246	42	43	254	83	58	3298	1.46
MT 121	49.09	0.82	15.20	6.66	0.15	2.68	7.71	3.16	1.89	0.23	131	37	84	245	43	53	264	105	75	2453	1.60
MT 122	50.10	0.81	14.27	6.02	0.13	2.61	8.11	2.87	1.94	0.22	116	35	74	217	40	49	260	95	66	2516	1.64
MT 123	48.62	0.67	15.39	6.89	0.14	1.76	5.36	2.63	1.55	0.25	93	54	128	277	47	32	311	41	23	5711	1.02
MT 124	50.40	0.82	14.81	6.29	0.11	2.54	7.96	3.03	1.84	0.22	123	35	79	228	41	52	255	68	60	2575	1.11
MT 126	49.42	0.81	15.59	7.64	0.13	2.68	7.73	3.24	1.75	0.24	134	44	102	267	49	44	267	79	64	3689	1.23
MT 127	49.51	0.70	17.63	10.00	0.57	1.91	6.35	2.70	1.17	0.25	101	95	176	464	62	64	294	26	27	5174	0.52
MT 128	54.70	0.64	16.77	5.26	0.11	1.47	3.80	2.58	1.29	0.25	95	56	111	224	56	31	433	24	14	4308	0.77
MT 129	49.87	0.82	14.93	6.43	0.13	2.64	7.94	3.05	2.05	0.23	126	37	83	241	42	53	259	82	67	2254	1.46
MT 130	50.30	0.81	14.62	6.32	0.11	2.54	8.08	2.97	1.79	0.24	118	35	76	218	41	49	260	66	53	2703	1.15
MT 134	50.41	0.69	12.36	4.77	0.10	2.34	10.34	2.44	2.10	0.21	88	28	56	160	31	43	283	97	60	2645	2.05
MT 135	48.52	0.65	11.96	4.75	0.10	2.16	11.49	2.39	2.52	0.19	86	28	56	160	32	40	302	110	67	3193	1.86
MT 136	66.38	0.21	2.77	1.27	0.06	0.56	13.33	0.56	0.78	0.10	12	4	11	33	9	4	223	18	6	1055	0.61

Table A.4: Results from the analysis of surface sediment samples for organic, inorganic and elemental carbon.

Sample ID	LOI 450 (%)	TC (%)	IC (%)	OC (%)	TC (%)	IC (%)	OC (%)
MT 31	12.6	5.60	0.83	4.77			
MT 47	14.2	4.20	1.15	3.05		1.05	
MT 59	10.0	3.14	1.52	1.62			
MT 74	24.6	17.96	0.53	17.43	23.18		
MT 82	6.7	2.76	1.82	0.93			
MT 89	11.3						
MT 90	10.1						
MT 91	4.4						
MT 92	12.3						
MT 94	8.1						
MT 95	7.1						
MT 96	10.4						
MT 97	11.7						
MT 98	10.9						
MT 99	7.8						
MT 100	11.1						
MT 101	10.0						
MT 102	9.1						
MT 103	11.6						
MT 104	9.6						
MT 105	7.6						
MT 106	11.3						
MT 112	9.7	3.39	1.30	2.09			
MT 121	12.3	3.42	1.33	2.08	4.51		
MT 125	10.7	3.97	1.72	2.25			
MT 126	11.0	3.43	1.32	2.11			
MT 128	11.1	6.69	0.48	6.22			
MT 169	13.5	6.91	1.14	5.77			
MT 251	10.5	1.30	1.00	0.30			
MT 252	11.2	3.28	1.25	2.03			
MT 253	8.5	5.84	0.71	5.13			
MT 254	6.4	2.89	0.84	2.05			
MT 255	10.4	4.78	1.25	3.53			
MT 256	12.3	4.49	1.18	3.31	5.75	1.07	4.68
MT 257	11.9	3.36	1.14	2.22			

Appendix 3: All data for cores

Table A.5: Results from the analysis of Peterstone 1 core sediments for total tritium, total, organic and inorganic carbon and γ-emitting radionuclides. Tritium activities were compiled from measurements by K. Doucette.

Sample ID	Depth (cm)	Wet/ dry ratio	Total ^{3}H activity (Bq/g dry weight)	Uncert-ainty (2σ)	Total organic carbon (%)	Dupl-icate TOC (%)	Inorganic carbon (%)	Dupl-icate IC (%)	LOI 450 °C (%)	Coal (%)	^{137}Cs activity (Bq/kg dry weight)	Uncert-ainty (2σ)	^{210}Pb activity (Bq/kg dry weight)	Uncert-ainty (2σ)
Pet 01	1	1.5	0.27	0.05	3.72		1.63		7		13.0		31	10
Pet 02	2	1.5	0.27	0.05	2.03		1.70		7					
Pet 03	3	1.5	0.30	0.06					8		14.2	1.6	25	9
Pet 04	4	1.5	0.29	0.05					8		15	1.6	35	10
Pet 05	5	1.5	0.26	0.05	2.83		0.32		9		14.7	1.6	35	10
Pet 06	6	1.5	0.24	0.04					8					
Pet 07	7	1.5	0.23	0.04	4.70	3.86	0.74	0.57	8		21.9	2.1	41	12
Pet 08	8	1.5	0.25	0.05					9					
Pet 09	9	1.5	0.20	0.04					10		15	1.7	55	10
Pet 10	10	1.5	0.18	0.04	4.09	4.45	1.11	0.81	11		19.5	1.7	36	10
Pet 11	11	1.6	0.16	0.03					13					
Pet 12	12	1.6	0.19	0.04	7.88		1.15		13					
Pet 13	13	1.6	0.15	0.03					13		22	2.4	33	14
Pet 14	14	1.6	0.15	0.03					14					
Pet 15	15	1.6	0.15	0.03	5.08	5.25	0.76	0.68	13		24	2	40	15
Pet 16	16	1.6	0.16	0.03	4.60		0.79		11					
Pet 17	17	1.6	0.20	0.04	4.40		0.79		12		34.5	2.4	40	11
Pet 18	18	1.5	0.20	0.04	4.27		0.73		11					
Pet 19	19	1.5	0.18	0.03	4.80		0.20		11					
Pet 20	20	1.6	0.26	0.05	4.45		0.36		12					
Pet 21	21	1.6	0.17	0.03	5.63		0.36		13		40.8	2.5	40	9
Pet 22	22	1.6	0.11	0.02	5.10		0.29		13					

Sample ID	**Depth (cm)**	**Wet/ dry ratio**	**Total ^{3}H activity (Bq/g dry weight)**	**Uncert-ainty (2σ)**	**Total organic carbon (%)**	**Dupl-icate TOC (%)**	**Inorganic carbon (%)**	**Dupl-icate IC (%)**	**LOI 450 °C (%)**	**Coal (%)**	**^{137}Cs activity (Bq/kg dry weight)**	**Uncert-ainty (2σ)**	**^{210}Pb activity (Bq/kg dry weight)**	**Uncert-ainty (2σ)**
Pet 23	23	1.6	0.12	0.03					12					
Pet 24	24	1.5	0.09	0.02					11		34.3	2.4	32	8
Pet 25	25	1.6	0.05	0.02	4.67		0.23		13					
Pet 26	26	1.6	0.07	0.02					13		38	2.4	33	8
Pet 27	27	1.6	0.04	0.01					12					
Pet 28	28	1.6	0.05	0.02	6.03		0.16		13					
Pet 29	29	1.6	0.07	0.02					13		41	2.9	34	10
Pet 30	30	1.6	0.03	0.01	5.58		0.20		13		50.3	3.4	51	13
Pet 31	31	1.6	0.03	0.01					13					
Pet 32	32	1.6	0.03	0.01					13		37	2.7	34	11
Pet 33	33	1.7	0.02	0.01	5.70		0.31		13					
Pet 34	34	1.7	0.02	0.01					14		35	2.4	30	9
Pet 35	35	1.7	0.02	0.01	7.33		0.00		14					
Pet 36	36	1.7	0.03	0.01					15					
Pet 37	37	1.7	0.03	0.02	8.58		0.07		16		29	2.9	27	11
Pet 38	38	1.6	0.03	0.01					15					
Pet 39	39	1.6	0.05	0.02					14					
Pet 40	40	1.7	0.02	0.01	8.21		0.21		15		30.6	2.4	35	11

Table A.6: Results from the analysis of Peterstone 1 core sediments for elemental composition by XRf analysis.

Sample ID	**SiO_2** (%)	**TiO_2** (%)	**Al_2O_3** (%)	**Fe_2O_3** (%)	**MnO** (%)	**MgO** (%)	**CaO** (%)	**K_2O** (%)	**Na_2O** (%)	**P_2O_5** (%)	**Rb** (ppm)	**Cu** (ppm)	**Pb** (ppm)	**Zn** (ppm)	**Ni** (ppm)	**Sn** (ppm)	**Sr** (ppm)	**Br** (ppm)	**I** (ppm)	**S** (ppm)	**Cl** (%)
Pet 01	53.85	0.68	12.04	7.39	0.19	2.15	7.68	2.33	1.14	0.36	63	25	69	171	32	34	218	53	31	4601	0.31
Pet 02	53.97	0.71	12.49	7.88	0.20	2.19	7.13	2.45	1.27	0.35	68	28	80	188	34	33	201	60	34	4292	0.41
Pet 03	54.51	0.74	12.82	7.39	0.17	2.24	6.71	2.52	1.47	0.30	75	36	73	185	34	42	182	75	40	3960	0.60
Pet 04	54.55	0.74	12.51	7.54	0.17	2.22	6.60	2.45	1.71	0.33	74	30	78	189	34	54	172	81	43	4240	0.76
Pet 05	53.05	0.74	12.56	8.35	0.20	2.23	6.79	2.48	1.63	0.37	75	32	98	208	37	44	189	85	41	4412	0.78
Pet 06	52.80	0.73	12.43	8.14	0.19	2.21	7.23	2.43	1.75	0.35	74	32	90	202	36	48	199	82	44	4131	1.09
Pet 07	53.60	0.74	12.54	7.98	0.18	2.23	6.89	2.45	1.75	0.32	75	31	90	201	36	50	187	87	42	4130	1.11
Pet 09	53.52	0.76	12.22	7.44	0.17	2.19	7.05	2.37	1.89	0.32	75	34	89	202	35	53	190	93	42	3436	1.26
Pet 10	52.84	0.80	12.48	7.13	0.18	2.22	7.45	2.44	1.88	0.31	83	35	87	206	38	54	208	105	45	3118	1.23
Pet 11	49.69	0.77	12.23	7.26	0.19	2.15	8.22	2.44	1.81	0.30	86	37	98	219	38	51	235	138	57	3520	1.27
Pet 13	51.52	0.79	12.50	7.16	0.18	2.20	7.10	2.45	1.85	0.31	83	38	92	211	37	50	201	152	57	3300	1.32
Pet 14	51.78	0.80	12.44	6.62	0.15	2.20	6.37	2.47	1.97	0.27	85	36	83	199	36	56	177	165	58	3577	1.46
Pet 15	53.80	0.80	13.01	6.40	0.16	2.27	5.89	2.55	1.87	0.25	90	34	82	200	37	53	159	142	55	2903	1.28
Pet 16	53.13	0.81	13.34	6.33	0.16	2.31	5.79	2.63	1.88	0.25	93	36	83	206	38	55	159	134	57	2903	1.29
Pet 17	55.39	0.84	13.18	6.01	0.15	2.30	5.77	2.59	1.97	0.22	96	34	79	201	37	58	156	125	50	2575	1.04
Pet 18	56.74	0.86	13.37	5.83	0.14	2.31	5.53	2.59	1.88	0.22	99	35	78	201	38	70	152	121	56	2267	1.11
Pet 19	57.34	0.88	13.44	5.73	0.12	2.33	5.54	2.60	1.75	0.20	101	34	78	198	38	74	152	110	54	2052	0.94
Pet 20	57.01	0.87	14.06	6.43	0.15	2.37	3.80	2.76	2.00	0.24	107	39	93	228	41	68	134	129	62	2499	0.94
Pet 21	56.58	0.84	14.48	6.72	0.16	2.41	3.58	2.82	1.65	0.27	105	38	98	232	40	61	133	121	61	2536	0.92
Pet 22	56.64	0.82	14.31	6.55	0.17	2.38	3.10	2.83	1.81	0.26	107	39	98	234	40	56	129	139	63	2829	1.15
Pet 23	56.04	0.87	15.84	7.31	0.11	2.47	3.03	3.12	1.35	0.28	128	52	130	300	45	72	137	122	59	2355	0.53
Pet 24	59.23	0.86	13.47	5.93	0.15	2.33	3.44	2.61	1.87	0.24	98	35	86	209	38	71	127	120	60	2486	1.07
Pet 25	57.20	0.86	14.70	6.68	0.17	2.46	2.94	2.88	1.93	0.27	111	42	100	246	43	65	128	130	67	2517	1.10
Pet 26	58.85	0.84	14.00	6.34	0.12	2.39	2.68	2.72	1.98	0.27	102	41	94	219	37	64	122	123	59	2531	1.14
Pet 27	57.59	0.83	13.88	6.45	0.12	2.36	2.49	2.74	1.79	0.29	102	41	99	225	37	59	119	136	59	2934	1.05
Pet 28	56.05	0.83	14.35	6.77	0.11	2.54	2.38	2.90	2.04	0.30	109	44	103	247	39	63	120	159	63	2720	1.48
Pet 29	57.36	0.85	14.92	6.71	0.10	2.55	2.58	2.96	1.89	0.30	113	45	107	245	39	66	123	122	57	2524	1.01

Sample ID	**SiO_2** (%)	**TiO_2** (%)	**Al_2O_3** (%)	**Fe_2O_3** (%)	**MnO** (%)	**MgO** (%)	**CaO** (%)	**K_2O** (%)	**Na_2O** (%)	**P_2O_5** (%)	**Rb** (ppm)	**Cu** (ppm)	**Pb** (ppm)	**Zn** (ppm)	**Ni** (ppm)	**Sn** (ppm)	**Sr** (ppm)	**Br** (ppm)	**I** (ppm)	**S** (ppm)	**Cl** (%)
Pet 30	55.52	0.85	15.57	6.64	0.09	2.63	2.63	3.16	1.38	0.26	123	50	112	252	42	64	124	141	53	2356	0.62
Pet 31	56.30	0.86	15.71	6.87	0.09	2.67	2.80	3.20	1.52	0.26	127	47	115	266	43	67	127	144	57	2485	0.76
Pet 32	55.03	0.86	15.15	6.90	0.10	2.59	2.92	3.05	1.70	0.27	121	46	113	273	42	65	130	149	53	2512	1.17
Pet 33	54.24	0.86	15.93	7.23	0.11	2.46	2.98	3.15	1.33	0.27	129	55	130	316	46	68	139	121	57	2256	0.54
Pet 34	55.24	0.87	16.15	7.06	0.10	2.47	3.07	3.16	1.41	0.25	129	55	131	304	44	68	139	132	54	2485	0.60
Pet 35	55.13	0.86	15.85	6.95	0.09	2.43	3.13	3.13	1.54	0.25	126	53	130	299	43	66	138	139	55	2744	0.73
Pet 36	51.74	0.85	15.51	7.69	0.18	2.48	2.94	3.12	2.07	0.29	125	56	135	353	48	63	141	167	63	2753	1.49
Pet 37	52.93	0.83	14.61	7.09	0.14	2.24	3.21	2.89	1.48	0.28	113	48	123	295	42	61	140	135	62	3861	0.76
Pet 38	52.13	0.83	14.64	6.85	0.11	2.25	4.24	2.89	1.49	0.26	112	50	122	307	42	60	154	132	54	3227	0.75
Pet 39	53.39	0.80	14.02	6.35	0.09	2.17	4.34	2.74	1.53	0.26	105	43	103	268	38	50	150	109	44	2974	0.75
Pet 40	51.61	0.85	15.15	7.19	0.09	2.45	3.96	3.05	1.95	0.25	123	51	119	309	43	63	150	138	50	2597	1.25

Table A.7: Results from the analysis of Peterstone 2 core sediments for total tritium, organic and inorganic carbon and γ-emitting radionuclides.

Sample ID	Depth (cm)	Wet/dry ratio	Total ^{3}H activity (Bq/g dry weight)	Uncertainty (2σ)	Duplicate ^{3}H activity (Bq/g dry weight)	Uncertainty (2σ)	Triplicate ^{3}H activity (Bq/g dry weight)	Uncertainty (2σ)	Total organic carbon (%)	Duplicate TOC (%)	Inorganic carbon (%)	Duplicate IC (%)	^{137}Cs activity (Bq/kg dry weight)	Uncertainty (2σ)	^{210}Pb activity (Bq/kg dry weight)	Uncertainty (2σ)
PET 2.1	1	1.81	0.19	0.034					5.73		1.53		21	2.3	39	14
PET 2.2	2	1.44	0.17	0.031									13	1.4	29	8.9
PET 2.3	3	1.43	0.16	0.029					4.47		1.06		10	1.7	31	12
PET 2.4	4	1.47	0.16	0.030									14	2	41	16
PET 2.5	5	1.54	0.25	0.042	0.25	0.044			5.18		1.34		11	2.3	33	14
PET 2.6	6	1.53	0.33	0.055	0.25	0.044							12	1.6	32	11
PET 2.7	7	1.55	0.24	0.042									11	1.3	30	9.3
PET 2.8	8	1.56	0.34	0.057	0.38	0.064			13.78	14.06	1.05	0.95	12	2.4	42	21
PET 2.9	9	1.64	0.33	0.057									15	1.9	37	14
PET 2.10	10	1.52	0.27	0.047	0.21	0.038	0.30	0.051	9.21		0.90		9	1.2	27	9
PET 2.11	11	1.62	0.22	0.038									11	1.4	40	14
PET 2.12	12	1.61	0.28	0.049	0.23	0.040			5.24		1.00		15	1.6	32	9.9
PET 2.13	13	1.48							4.74		2.26		10	1.2	36	11
PET 2.14	14	1.68											17	2.2	43	18
PET 2.15	15	1.55	0.18	0.031					4.76		1.49		9	1.1	28	8.3
PET 2.16	16	1.50	0.14	0.025	0.18	0.030							12	1.4	26	8.9
PET 2.17	17	1.62	0.22	0.039					4.88		1.06		20	1.7	30	9.8
PET 2.18	18	1.57	0.16	0.028									21	2.5	42	19
PET 2.19	19	1.56	0.17	0.030									18	2.4	33	14
PET 2.20	20	1.64	0.16	0.030	0.23	0.040	0.15	0.028	9.37		0.63		9	1.1	29	8.5
PET 2.21	21	1.63	0.18	0.030												
PET 2.22	22	1.63	0.14	0.026									18	1.8	21	11
PET 2.23	23	1.57	0.17	0.033					13.42		0.39		15	2.3	0	0
PET 2.24	24	1.57											9	1.3	20	8.8
PET 2.25	25	1.82	0.12	0.023	0.19	0.032			9.33	9.44	0.75	0.77	26.1	3.3	0	0

Sample ID	Depth (cm)	Wet/ dry ratio	Total ^{3}H activity (Bq/g dry weight)	Uncertainty (2σ)	Duplicate ^{3}H activity (Bq/g dry weight)	Uncertainty (2σ)	Triplicate ^{3}H activity (Bq/g dry weight)	Uncertainty (2σ)	Total organic carbon (%)	Duplicate TOC (%)	Inorganic carbon (%)	Duplicate IC (%)	^{137}Cs activity (Bq/kg dry weight)	Uncertainty (2σ)	^{210}Pb activity (Bq/kg dry weight)	Uncertainty (2σ)
PET 2.26	26	1.68	0.18	0.033									26	2.2	43	13
PET 2.27	27	1.83	0.16	0.030					6.99		0.90		24	3.3	32	15
PET 2.28	28	1.87	0.24	0.040									46.0	5	48.3	22
PET 2.29	29	1.73	0.28	0.050	0.25	0.043			15.36		1.01		21	2.2	26.0	11
PET 2.30	30	1.75	0.20	0.037					25.19		0.24		18.2	2.1	29.6	14
PET 2.31	31	1.77	0.27	0.047									17.3	2.7	39.8	22
PET 2.32	32	1.87	0.29	0.051									39.8	3.8	39.8	18
PET 2.33	33	1.91	0.47	0.080												
PET 2.34	34	1.95	0.31	0.053	0.49	0.083							33.5	3.6	49.8	16

Table A.8: Results from the analysis of Peterstone 2 core sediments for elemental composition by XRF analysis.

Sample ID	SiO_2 (%)	TiO_2 (%)	Al_2O_3 (%)	Fe_2O_3 (%)	MnO (%)	MgO (%)	CaO (%)	K_2O (%)	Na_2O (%)	P_2O_5 (%)	Rb (ppm)	Cu (ppm)	Pb (ppm)	Zn (ppm)	Ni (ppm)	Sn (ppm)	Sr (ppm)	Br (ppm)	I (ppm)	S (ppm)	Cl (%)
PET 2.1	47.36	0.69	10.76	6.46	0.16	2.16	10.32	2.31	2.28	0.35	77	29	61	181	30	49	307	109	37	4114	1.86
PET 2.2	48.09	0.56	8.52	7.20	0.22	1.65	13.58	1.68	1.60	0.47	54	29	77	166	29	27	412	65	22	5516	1.04
PET 2.3	50.61	0.52	8.27	7.41	0.23	1.58	12.00	1.62	1.55	0.49	51	27	73	175	29	27	365	68	23	6234	0.96
PET 2.4	49.18	0.62	9.80	7.11	0.20	1.86	11.22	1.95	1.94	0.43	64	33	71	174	32	39	348	95	30	5021	1.22
PET 2.5	45.79	0.53	8.85	8.10	0.25	1.64	13.34	1.78	1.82	0.57	58	32	93	188	32	23	409	95	30	6616	1.17
PET 2.6	45.78	0.54	8.57	8.28	0.21	1.69	12.15	1.79	1.90	0.54	57	31	86	183	32	24	374	95	30	6732	1.32
PET 2.7	50.83	0.62	9.70	7.95	0.21	1.87	9.97	1.97	1.90	0.44	67	34	84	192	33	35	310	93	37	5598	1.19
PET 2.8	36.44	0.59	8.31	8.75	0.22	1.61	14.78	1.79	1.90	0.63	53	34	86	201	30	29	437	117	38	7604	1.48
PET 2.9	38.86	0.67	10.58	6.99	0.20	1.97	15.88	2.21	2.08	0.40	74	34	75	198	33	36	485	128	43	4547	1.50
PET 2.10	42.51	0.57	8.17	8.48	0.23	1.53	14.26	1.70	1.77	0.57	55	33	92	207	33	38	433	92	32	5932	1.23
PET 2.11	36.48	0.66	8.52	7.54	0.19	1.62	16.68	1.81	1.74	0.51	55	33	83	191	31	27	470	115	32	6029	1.41
PET 2.12	48.87	0.69	10.78	6.91	0.17	2.02	10.47	2.21	2.08	0.36	80	34	79	200	35	46	317	109	46	3531	1.37
PET 2.13	48.12	0.55	7.87	7.54	0.21	1.52	13.21	1.64	1.69	0.49	56	36	86	193	33	29	404	83	33	4789	1.09

Sample ID	**SiO_2** (%)	**TiO_2** (%)	**Al_2O_3** (%)	**Fe_2O_3** (%)	**MnO** (%)	**MgO** (%)	**CaO** (%)	**K_2O** (%)	**Na_2O** (%)	**P_2O_5** (%)	**Rb** (ppm)	**Cu** (ppm)	**Pb** (ppm)	**Zn** (ppm)	**Ni** (ppm)	**Sn** (ppm)	**Sr** (ppm)	**Br** (ppm)	**I** (ppm)	**S** (ppm)	**Cl** (%)
PET 2.14	47.20	0.71	10.45	7.16	0.18	1.98	10.18	2.14	2.20	0.39	74	33	87	199	34	42	312	122	39	3862	1.63
PET 2.15	47.29	0.58	8.64	7.65	0.20	1.62	13.01	1.77	1.85	0.49	60	31	91	195	32	42	391	82	35	4325	1.22
PET 2.16	51.88	0.62	9.48	7.38	0.17	1.80	9.89	1.91	1.79	0.41	66	31	80	185	34	38	305	78	34	4190	1.10
PET 2.17	49.39	0.76	11.81	6.41	0.15	2.16	10.23	2.45	1.62	0.29	92	35	75	201	37	53	307	100	44	2619	1.04
PET 2.18	49.47	0.79	11.38	6.06	0.14	2.14	10.40	2.31	1.79	0.29	85	30	68	184	352	56	300	101	43	2371	1.12
PET 2.19	47.19	0.75	11.12	6.29	0.18	2.07	11.68	2.26	2.13	0.35	82	36	73	191	35	59	351	98	45	2601	1.37
PET 2.20	45.67	0.75	10.62	6.69	0.14	1.96	11.39	2.24	1.98	0.35	80	34	77	194	34	53	333	105	42	3416	1.31
PET 2.21	39.63	0.71	10.64	5.69	0.13	1.95	14.99	2.26	2.07	0.29	76	35	80	176	34	42	422	117	43	3666	1.57
PET 2.22	38.17	0.69	9.89	5.54	0.14	1.84	16.53	2.11	1.92	0.29	66	33	66	166	34	41	478	113	41	4126	1.49
PET 2.23	36.41	0.60	9.12	5.35	0.14	1.69	19.49	1.89	1.83	0.40	59	35	64	165	28	32	530	91	34	4020	1.33
PET 2.24	31.55	0.61	7.91	5.36	0.15	1.53	19.07	1.74	2.06	0.49	48	41	58	168	25	26	493	142	31	9700	1.70
PET 2.25	44.49	0.78	11.09	6.05	0.15	2.09	10.68	2.38	2.45	0.27	82	37	71	210	35	47	299	151	50	4444	1.87
PET 2.26	48.32	0.80	12.22	5.52	0.14	2.24	10.16	2.50	2.32	0.22	92	34	69	210	36	61	293	133	47	2797	1.60
PET 2.27	49.41	0.79	11.71	5.90	0.14	2.22	7.74	2.48	2.50	0.23	88	36	70	200	35	59	214	161	56	3615	1.85
PET 2.28	46.21	0.78	12.87	6.46	0.10	2.29	8.09	2.72	2.44	0.26	102	41	84	226	37	49	240	165	60	3383	1.91
PET 2.29	37.59	0.71	10.08	6.89	0.10	1.78	13.28	2.20	1.96	0.31	72	34	60	189	29	36	373	127	45	4901	1.70
PET 2.30	31.48	0.62	8.78	8.37	0.12	1.52	12.08	1.88	1.74	0.48	50	36	94	280	24	22	319	125	35	9440	1.78
PET 2.31	32.01	0.64	9.05	6.87	0.09	1.60	11.81	1.97	2.28	0.70	53	41	76	220	24	23	347	136	36	8641	2.21
PET 2.33	46.44	0.75	11.38	4.52	0.08	2.09	9.59	2.39	2.21	0.17	78	35	73	217	32	43	243	91	36	7425	1.60
PET 2.35	48.85	0.81	12.40	5.15	0.08	2.24	6.11	2.61	2.07	0.16	90	58	77	214	33	55	170	90	35	7510	1.41
PET 2.36	50.85	0.81	12.91	5.12	0.08	2.28	6.66	2.68	2.00	0.17	97	53	125	234	38	54	188	89	33	5718	1.30
PET 2.37	48.70	0.77	12.46	4.98	0.08	2.21	6.98	2.60	2.00	0.18	89	39	99	230	35	45	192	96	34	7397	1.46
PET 2.38	49.39	0.80	12.79	5.32	0.08	2.25	6.22	2.74	2.20	0.17	99	79	92	243	38	42	177	103	34	7158	1.60
PET 2.39	49.17	0.81	13.18	5.53	0.08	2.27	6.31	2.79	1.98	0.18	99	66	82	228	37	50	170	99	39	7692	1.35
PET 2.40	50.20	0.82	13.62	5.84	0.09	2.36	6.15	2.82	1.96	0.19	106	48	86	240	40	54	201	100	43	7391	1.38

Table A.9: Results from the analysis of Barry Island core sediments for total tritium and γ-emitting radionuclides.

Sample ID	Depth (cm)	Wet/ dry ratio	Total ^{3}H activity (Bq/g dry weight)	Uncertainty (2σ)	Duplicate total ^{3}H activity (Bq/g dry weight)	Uncertainty (2σ)	Triplicate total ^{3}H activity (Bq/g dry weight)	Uncertainty (2σ)	^{137}Cs activity (Bq/g dry weight)	Uncertainty (2σ)	^{210}Pb activity (Bq/kg dry weight)	Uncertainty (2σ)
BI 1	1	2.0	0.08	0.02					18.9	2.0	60.0	14.0
BI 2	2	1.7	0.12	0.03	3.48	0.57			20.5	2.1	46.0	11.0
BI 3	3	1.8	0.23	0.04	0.16	0.03			21.3	2.0	48.0	11.0
BI 4	4	1.8	0.04	0.01	0.05	0.02			21.8	2.0	57.0	14.0
BI 5	5	1.7	0.19	0.03					21.1	2.7	49.0	14.0
BI 6	6	1.8	0.17	0.03	0.17	0.03			20.5	2.0	46.0	11.0
BI 7	7	1.9	0.25	0.05	0.14	0.03			25.8	3.1	58.0	17.0
BI 8	8	1.8							27.4	2.8	60.0	16.0
BI 9	9	1.8	0.11	0.02	0.16	0.03	0.21	0.04	21.5	2.0	47.0	11.0
BI 10	10	1.8	0.16	0.03	0.17	0.03			25.3	2.1	45.0	11.0
BI 11	11	2.0	0.14	0.03	0.22	0.04			29.3	2.1	58.0	12.0
BI 12	12	1.9	0.31	0.05	0.21	0.04			28.4	2.4	52.0	13.0
BI 13	13	1.7	0.15	0.03	0.15	0.03	0.17	0.03	24.5	2.8	39.0	12.0
BI 14	14	1.7	0.20	0.04					21.3	2.2	41.0	13.0
BI 15	15	1.6	0.19	0.04					19.6	1.8	41.2	9.2
BI 16	16	1.5	0.15	0.03					19.4	2.0	37.7	9.3
BI 17	17	1.5							18.7	1.6	37.8	9.7
BI 18	18	1.3							8.2	0.8	12.2	5.4
BI 19	19	1.3	0.01	0.02					3.1	0.5		
BI 20	20	1.2	0.03	0.01					2.0	0.5	9.6	3.8
BI 21	21	1.3							11.2	1.2	20.3	5.8
BI 22	22	1.4	0.08	0.02	0.08	0.02			15.3	1.3	42.0	15.0
BI 23	23	1.4	0.08	0.02					15.5	1.3	39.0	14.0
BI 24	24	1.2	0.02	0.02					7.7	1.1	16.4	7.1
BI 25	25	1.2	0.08	0.02					1.6	0.4	5.4	2.9

Sample ID	Depth (cm)	Wet/ dry ratio	Total ^{3}H activity (Bq/g dry weight)	Uncert-ainty (2σ)	Duplicate total ^{3}H activity (Bq/g dry weight)	Uncert-ainty (2σ)	Triplicate total ^{3}H activity (Bq/g dry weight)	Uncert-ainty (2σ)	^{137}Cs activity (Bq/g dry weight)	Uncert-ainty (2σ)	^{210}Pb activity (Bq/kg dry weight)	Uncert-ainty (2σ)
BI 26	26	1.2							1.1	0.4		
BI 27	27	1.2	0.02	0.02					1.0	0.5	7.7	3.7
BI 28	28	1.2							1.6	0.2		
BI 29	29	1.2							0.2	0.0	0.9	0.3
BI 30	30	1.2							1.7	0.7	12.6	5.1
BI 31	31	1.2	0.01	0.01					1.2	0.6		
BI 32	32	1.3	0.03	0.02					6.6	1.0	18.3	6.6

Table A.10: Results from the analysis of Barry Island core sediments for elemental composition by XRF analysis.

Sample ID	**SiO_2** (%)	**TiO_2** (%)	**Al_2O_3** (%)	**Fe_2O_3** (%)	**MnO** (%)	**MgO** (%)	**CaO** (%)	**K_2O** (%)	**Na_2O** (%)	**P_2O_5** (%)	**Rb** (ppm)	**Cu** (ppm)	**Pb** (ppm)	**Zn** (ppm)	**Ni** (ppm)	**Sn** (ppm)	**Sr** (ppm)	**Br** (ppm)	**I** (ppm)	**S** (ppm)	**Cl** (%)
BI 1	52.55	0.73	13.40	5.59	0.11	3.00	10.36	2.72	1.84	0.26	100	30	67	185	33	51	341	151	67	2300	2.45
BI 2	55.95	0.78	14.20	5.69	0.09	3.02	8.82	2.77	1.78	0.24	104	31	73	191	33	51	215	116	67	1460	1.94
BI 3	55.64	0.77	14.34	6.11	0.12	3.07	7.93	2.81	1.84	0.27	109	34	82	211	37	51	197	139	70	1460	2.08
BI 4	56.00	0.76	13.88	5.75	0.14	3.01	8.71	2.69	1.56	0.28	95	31	71	186	33	46	204	135	68	1530	1.76
BI 5	56.11	0.75	13.92	5.48	0.11	2.99	8.44	2.68	1.79	0.25	100	32	75	192	33	51	196	118	68	1400	1.97
BI 6	55.34	0.79	14.35	6.16	0.12	3.13	7.98	2.82	1.44	0.27	109	35	83	220	36	54	195	122	68	1640	1.65
BI 7	55.25	0.79	14.61	6.74	0.13	3.18	7.61	2.90	1.56	0.29	114	36	89	227	38	54	201	144	67	1660	1.90
BI 8	55.32	0.80	14.55	6.07	0.12	3.13	8.59	2.87	1.54	0.24	112	34	84	219	38	57	218	119	76	1770	1.76
BI 9	54.54	0.77	14.14	5.88	0.13	3.04	9.08	2.77	1.80	0.24	107	34	83	211	37	52	228	108	66	1680	2.06
BI 10	55.09	0.78	14.21	5.94	0.14	3.15	9.00	2.80	1.78	0.24	107	36	85	224	37	53	223	109	60	2370	2.07
BI 11	53.82	0.80	14.45	6.87	0.14	3.20	8.05	2.91	1.88	0.25	116	37	93	244	41	53	216	132	63	3280	2.34
BI 12	55.14	0.82	14.97	6.46	0.13	3.27	7.97	3.01	1.48	0.26	120	37	96	250	42	56	214	123	69	1980	1.74
BI 13	54.98	0.78	14.27	5.68	0.09	3.11	9.70	2.83	1.53	0.24	99	33	80	208	34	49	244	84	53	1760	1.70
BI 14	56.14	0.69	13.31	5.45	0.17	2.89	9.66	2.56	1.72	0.25	92	31	73	187	32	46	223	86	67	1450	1.94
BI 15	56.86	0.70	13.36	5.19	0.10	2.88	9.35	2.56	1.68	0.25	85	28	65	169	29	44	201	76	52	1500	1.82
BI 16	57.01	0.66	12.82	4.77	0.08	2.79	10.33	2.44	1.59	0.19	83	27	64	167	28	44	219	61	44	2000	1.61
BI 17	56.09	0.73	13.40	5.04	0.08	2.93	9.94	2.60	1.55	0.21	80	28	60	170	28	42	219	72	43	2150	1.60
BI 18	64.20	0.18	5.66	1.51	0.03	1.32	9.17	0.87	7.27	0.09	31	13	22	50	9	14	180	42	8	5080	9.16
BI 19	76.72	0.12	4.62	1.15	0.02	0.95	8.37	0.70	3.65	0.07	22	12	17	33	9	7	162	26	3	1130	4.96
BI 20	73.03	0.10	4.11	1.01	0.02	0.83	10.09	0.64	4.93	0.06	20	11	13	26	6	6	188	33	1	1120	6.37
BI 21	46.96	0.19	6.03	1.48	0.02	1.28	7.48	0.82	22.51	0.07	35	14	26	58	9	16	191	52	10	2350	24.30
BI 22	50.78	0.17	5.61	1.53	0.02	1.06	7.05	0.73	24.73	0.07	39	16	29	67	12	17	204	46	13	1720	25.31
BI 23	22.03	0.14	4.46	1.42	0.02	0.43	3.78	0.41	46.22	0.04	48	16	39	82	12	27	218	37	22	1670	47.24
BI 24	62.24	0.16	5.28	1.46	0.02	1.07	9.35	0.77	13.10	0.08	31	15	23	52	10	14	215	38	7	1940	14.22
BI 25	65.72	0.09	3.95	1.01	0.02	0.82	11.32	0.58	7.57	0.06	18	11	14	29	6	7	218	32		1420	9.64
BI 26	66.50	0.09	4.03	1.01	0.02	0.81	11.50	0.61	6.51	0.07	18	18	14	29	6	7	217	33		1370	8.72
BI 27	69.23	0.08	3.72	0.90	0.02	0.77	10.82	0.55	5.55	0.06	17	10	12	26	6	4	215	35		2240	8.18

Sample ID	SiO_2 (%)	TiO_2 (%)	Al_2O_3 (%)	Fe_2O_3 (%)	MnO (%)	MgO (%)	CaO (%)	K_2O (%)	Na_2O (%)	P_2O_5 (%)	Rb (ppm)	Cu (ppm)	Pb (ppm)	Zn (ppm)	Ni (ppm)	Sn (ppm)	Sr (ppm)	Br (ppm)	I (ppm)	S (ppm)	Cl (%)
BI 28	68.84	0.08	3.70	0.87	0.02	0.76	10.63	0.54	6.26	0.06	17	10	11	23	6	5	218	33		1540	8.74
BI 29	65.83	0.09	3.91	0.95	0.02	0.76	10.03	0.56	8.87	0.06	19	11	13	27	6	6	215	35		1750	11.59
BI 30	72.73	0.10	4.10	1.03	0.02	0.78	9.48	0.65	4.80	0.06	20	10	14	30	7	5	194	32		1740	6.81
BI 31	73.87	0.08	3.81	0.97	0.02	0.71	9.48	0.65	4.24	0.06	19	12	12	25	9	7	216	31		1070	7.48
BI 32	51.50	0.17	5.52	1.53	0.03	1.37	10.07	0.81	16.48	0.08	29	15	21	55	8	11	224	67	8	2440	19.16

Table A.11: Results from the analysis of Sudbrook core sediments for total tritium, organic and inorganic carbon and γ-emitting radionuclides.

Sample ID	Depth (cm)	Wet/dry ratio	Total ^3H activity (Bq/g dry weight)	Uncertainty (2σ)	Duplicate total ^3H activity (Bq/g dry weight)	Uncertainty (2σ)	Triplicate total ^3H activity (Bq/g dry weight)	Uncertainty (2σ)	Total organic carbon (%)	Uncertainty (2σ)	Duplicate TOC (%)	Uncertainty (2σ)	Inorganic carbon (%)	Uncertainty (2σ)	Duplicate IC (%)	Uncertainty (2σ)	^{137}Cs activity (Bq/g dry weight)	Uncertainty (2σ)	^{210}Pb activity (Bq/kg dry weight)	Uncertainty (2σ)
SUD 1	1	1.78	0.29	0.05					3.4	1.0	3.8	1.1	1.6	0.14	1.28	0.35	40	3.2	58	16
SUD 2	2	1.67	0.47	0.08													28	2.3	99	23
SUD 3	3	1.55	0.36	0.06	0.33	0.06											19	2	37	10
SUD 4	4	1.60	0.17	0.03													25	2.2	40	11
SUD 5	5	1.66	0.28	0.05					3.0	0.8			1.42	0.13	1.48	0.41	30	2.7	48	13
SUD 6	6	1.56	0.23	0.04													24	2	54	14
SUD 7	7	1.57	0.20	0.03	0.19	0.03											24	2.7	35	13
SUD 8	8	1.60	0.17	0.03													27	2.6	47	17
SUD 9	9	1.51	0.13	0.02													14	1.4	27	9
SUD 10	10	1.52	0.18	0.03					2.1	0.6	3.3	0.9	1.58	0.14	1.12	0.31	21	2	48	15
SUD 11	11	1.62	0.15	0.03													23	2	76	20
SUD 12	12	1.54	0.20	0.04													24	2.1	50	14
SUD 13	13	1.57	0.16	0.03													26	2.3	41	12
SUD 14	14	1.61	0.21	0.04	0.17	0.03											28	3.3	34	15
SUD 15	15	1.60	0.23	0.04	0.49	0.08	0.40	0.07									26	2.9	43	14

Sample ID	Depth (cm)	Wet/dry ratio	Total ^{3}H activity (Bq/g dry weight)	Uncertainty (2σ)	Duplicate total ^{3}H activity (Bq/g dry weight)	Uncertainty (2σ)	Triplicate total ^{3}H activity (Bq/g dry weight)	Uncertainty (2σ)	Total organic carbon (%)	Uncertainty (2σ)	Duplicate TOC (%)	Uncertainty (2σ)	Inorganic carbon (%)	Uncertainty (2σ)	Duplicate IC (%)	Uncertainty (2σ)	^{137}Cs activity (Bq/g dry weight)	Uncertainty (2σ)	^{210}Pb activity (Bq/kg dry weight)	Uncertainty (2σ)
SUD 16	16	1.65	0.20	0.03													33	3.4	45	21
SUD 17	17	1.63	0.14	0.03	0.20	0.03											30	2.3	40	10
SUD 18	18	1.66	0.17	0.03																
SUD 19	19	1.54	0.04	0.01	0.20	0.03											20	1.5	75	16
SUD 20	20	1.56	0.11	0.02					3.2	0.9	3.0	0.8	1.4	0.13	1.53	0.42	24	2.5	42	17
SUD 21	21	1.67	0.15	0.03													32	3.3	72	16
SUD 22	22	1.71	0.18	0.03													29	2.5	35	12
SUD 23	23	1.66	0.12	0.02													28	2.3	37	11
SUD 24	24	1.71	0.14	0.02													34	2.7	49	14
SUD 25	25	1.65	0.22	0.04	0.39	0.07											26	2.3	43	14
SUD 26	26	1.66	0.12	0.02													36	3.4	61	21
SUD 27	27	1.61	0.12	0.02													30	2.4	40	12
SUD 28	28	1.71	0.27	0.05	0.48	0.08			4.9	1.4	4.1	1.1	0.54	0.05	1.31	0.36	30	2.5	99	24

Table A.12: Results from the analysis of Sudbrook core sediments for elemental composition by XRF analysis.

Sample ID	**SiO_2** (%)	**TiO_2** (%)	**Al_2O_3** (%)	**Fe_2O_3** (%)	**MnO** (%)	**MgO** (%)	**CaO** (%)	**K_2O** (%)	**Na_2O** (%)	**P_2O_5** (%)	**Rb** (ppm)	**Cu** (ppm)	**Pb** (ppm)	**Zn** (ppm)	**Ni** (ppm)	**Sn** (ppm)	**Sr** (ppm)	**Br** (ppm)	**I** (ppm)	**S** (ppm)	**Cl** (%)
SUD 1	49.92	0.82	14.21	6.19	0.13	2.57	8.16	2.90	1.56	0.23	117	39	77	239	40	57	252	87	73	2103	0.77
SUD 3	53.40	0.80	12.18	5.01	0.11	2.32	8.58	2.39	1.55	0.21	89	29	57	174	33	60	233	63	56	1924	0.61
SUD 5	49.96	0.84	14.58	6.38	0.15	2.56	7.70	2.96	1.47	0.23	121	40	86	251	42	61	232	73	78	1772	0.61
SUD 7	52.31	0.82	13.66	5.61	0.13	2.45	7.99	2.69	1.50	0.23	104	33	70	211	36	57	224	70	65	1889	0.58
SUD 10	53.98	0.83	12.18	4.94	0.11	2.32	8.40	2.38	1.53	0.20	87	31	58	177	33	67	219	55	57	1693	0.57
SUD 15	51.97	0.83	14.02	5.84	0.13	2.51	7.76	2.77	1.51	0.22	108	37	79	229	38	59	218	69	68	1811	0.59
SUD 17	51.05	0.84	14.69	6.26	0.15	2.57	7.43	2.94	1.49	0.23	118	40	88	254	41	63	219	72	70	1725	0.59
SUD 20	53.20	0.82	12.82	5.11	0.12	2.41	8.08	2.48	1.58	0.21	92	31	64	189	33	68	200	68	57	1801	0.62
SUD 23	51.89	0.83	13.84	5.77	0.14	2.49	7.34	2.75	1.57	0.22	106	39	77	225	37	66	199	90	70	1901	0.68
SUD 25	52.87	0.85	13.46	5.55	0.12	2.45	7.35	2.66	1.59	0.21	102	35	71	210	36	72	192	82	62	1756	0.67
SUD 28	51.86	0.83	14.03	5.86	0.12	2.51	6.87	2.83	1.57	0.22	109	37	77	229	38	63	186	88	61	1859	0.70

Appendix 4: Raw data and calculations for the extraction experiments

Table A.13: Results and calculations for extraction experiments (summarised in Table 5.1). The average ^{3}H activity of the in-house reference sediment used for the extractions (except those indicated otherwise[1]) is 0.19 ± 0.03 Bq/g dry weight; this activity is used to calculate the total activity present in the sample[2], and method uncertainties are propagated to the 95 % confidence limit (2σ).

Solvent	Mass of sediment (g)	Uncertainty (2σ)	Calculated total activity (Bq)[2]	Uncertainty (2σ)	Fraction	Mass analysed (g)	Uncertainty (2σ)	Activity in fraction (Bq/g)	Uncertainty (2σ)	Measured activity in fraction (Bq)	Uncertainty (2σ)	Activity in fraction (%)	Uncertainty (2σ)	Total measured activity (%)	Uncertainty (2σ)
Soxhlet extractions															
Methanol	18.06	0.18	3.45	0.29	Extract	1.04	0.01	0.69	0.12	0.72	0.12	21	4.0		
	19.68	0.20	3.76	0.32	Extract	0.99	0.01	0.75	0.12	0.74	0.12	< 21[3]			
Toluene	17.87	0.18	3.41	0.29	Extract	0.99	0.01	0.22	0.07	0.21	0.07	< 36[3]			
DCM	18.38	0.18	3.51	0.30	Extract	0.75	0.01	0.29	0.08	0.22	0.06	< 47[3]			
	17.62	0.18	3.36	0.28	Extract	0.89	0.01	0.33	0.08	0.29	0.07	< 47[3]			
	17.02	0.17	3.25	0.27	Extract	0.64	0.01	0.40	0.09	0.25	0.06	< 47[3]			
	18.29	0.18	3.49	0.30	Extract	0.86	0.01	0.30	0.08	0.26	0.07	< 47[3]			
	16.94	0.17	3.23	0.27	Extract	0.82	0.01	0.39	0.09	0.32	0.07	< 47[3]			
GAA	21.065	0.21	4.00	0.53	Extract	5.967	0.06	0.18	0.02	1.07	0.12	27	4.6		
					Residue	7.192	0.07	0.06	0.01						
					Residue	10.814	0.11	0.08	0.01						
					Total residue	21.065	0.21	0.07	0.01	1.47	0.21	37	7.2	64	8.5
	23.411	0.23	4.45	0.59	Extract	4.243	0.04	0.04	0.01						
					Extract	2.037	0.02	0.26	0.04						
					Total extract	6.28	0.05			0.70	0.09	16	2.8		
					Residue	9.687	0.10	0.08	0.01						
					Residue	4.392	0.04	0.03	0.01						
					Residue	6.445	0.06	0.16	0.02						
					Total residue	23.411	0.23			1.66	0.19	37	6.6	53	6.6
Ultrasonic extractions															
Water	4.059	0.04	0.77	0.10	Extract	4.059	0.04	0.016	0.02	0.06	0.081	< 11[3]			
	2.954	0.03	0.56	0.07	Extract	2.954	0.03	0.015	0.02	0.04	0.059	< 11[3]			
	1.9	0.02	0.36	0.05	Extract	1.9	0.02	0.006	0.02	0.01	0.038	< 11[3]			
	4.744	0.05	0.90	0.12	Extract	4.744	0.05	0.008	0.02	0.04	0.095	< 11[3]			

Solvent	Mass of sediment (g)	Uncertainty (2σ)	Calculated total activity (Bq)[2]	Uncertainty (2σ)	Fraction	Mass analysed (g)	Uncertainty (2σ)	Activity in fraction (Bq/g)	Uncertainty (2σ)	Measured activity in fraction (Bq)	Uncertainty (2σ)	Activity in fraction (%)	Uncertainty (2σ)	Total measured activity (%)	Uncertainty (2σ)
	9.043	0.09	1.72	0.23	Extract	9.043	0.09	0.007	0.02	0.06	0.181	< 11			
Methanol	2.94	0.029	0.56	0.074	1st extract	2.939	0.029	0.009	0.010	0.026	0.029	$< 10^3$			
					2nd extract	2.939	0.029	0.007	0.010	0.021	0.029	$< 10^3$			
					Residue	2.921	0.029	0.177	0.027	0.517	0.079	93	18.7	93	18.7
	2.996	0.030	0.57	0.075	1st extract	2.996	0.030	0.009	0.010	0.027	0.030	$< 10^3$			
					2nd extract	2.996	0.030	0.011	0.010	0.033	0.030	$< 10^3$			
					Residue	2.962	0.030	0.157	0.025	0.465	0.074	83	17.1	83	17.1
	3.064	0.031	0.58	0.077	1st extract	3.064	0.031	0.027	0.010	0.083	0.031	14	5		
					2nd extract	3.064	0.031	0.006	0.010	0.018	0.031	$< 10^3$			
					Residue	2.957	0.030	0.176	0.033	0.520	0.098	93	21.3	107	22.6
	2.973	0.030	0.56	0.075	1st extract	2.973	0.030	0.013	0.010	0.039	0.030	$< 10^3$			
					2nd extract	2.973	0.030	0.008	0.010	0.024	0.030	$< 10^3$			
					Residue	2.965	0.030	0.178	0.031	0.528	0.092	94	20.5	94	20.5
Toluene	1.99	0.02	0.38	0.05	Extract	1.99	0.02	0.013	0.01	0.027	0.01	7	3.1		
	2.79	0.03	0.53	0.07	Extract	2.79	0.03	0.008	0.00	0.021	0.01	4	2.1		
	3.14	0.03	0.60	0.08	Extract	3.14	0.03	0.006	0.00	0.020	0.01	3	1.8		
DCM	3.96	0.04	0.752	0.10	Extract	1.219	0.01	< 0.057		< 0.069		$< 37^3$			
	6.51	0.07	1.237	0.16	Extract	0.945	0.01	< 0.070		< 0.066		$< 37^3$			
6M HCl	5.023	0.05	0.95	0.13	Residue	4.681	0.05	0.16	0.02	0.74	0.11	78	15.3		
	5.046	0.05	0.96	0.13	Residue	4.866	0.05	0.15	0.02	0.72	0.11	75	15.0		
	4.968	0.05	0.94	0.12	Residue	4.78	0.05	0.17	0.03	0.81	0.12	86	17.0		
	4.944	0.05	0.94	0.12	Residue	4.582	0.05	0.17	0.02	0.77	0.11	82	16.0		
20 % AA	3.11	0.03	0.59	0.08	Extract	1.777	0.02	< 0.05		< 0.09		$< 15^3$			
					Residue	3.203	0.03	0.28	0.04	0.91	0.13	153^5	29.7	153	29.7
	3.02	0.03	0.57	0.08	Extract	1.985	0.02	< 0.04		< 0.08		$< 15^3$			
					Residue	2.782	0.03	0.21	0.03	0.59	0.09	103	21.4	103	21.4
	3.01	0.03	0.57	0.08	Extract	1.992	0.02	< 0.04		< 0.07		$< 15^3$			
					Residue	2.823	0.03	0.19	0.03	0.55	0.09	96	19.9	96	19.9
GAA	2.95	0.03	0.56	0.07	Extract	1.448	0.01	0.10	0.04	0.15	0.06	26	10.9		
					Residue	3.079	0.03	0.17	0.02	0.53	0.08	94	18.4	121	21.4
	3.10	0.03	0.59	0.08	Extract	1.313	0.01	0.06	0.04	0.08	0.05	14	9.4		
					Residue	3.285	0.03	0.17	0.02	0.55	0.07	94	17.7	108	20.0
	2.98	0.03	0.57	0.07	Extract	1.052	0.01	0.07	0.05	0.08	0.05	13	9.9		
					Residue	3.151	0.03	0.17	0.02	0.55	0.07	96	18.0	110	20.5
NaOH	4.98	0.05	0.95	0.12	Residue	4.98	0.05	0.09	0.02	0.45	0.07	47.89	10.12		
	4.96	0.05	0.94	0.12	Residue	4.96	0.05	0.09	0.02	0.47	0.07	49.26	10.21		

Solvent	Mass of sediment (g)	Uncertainty (2σ)	Calculated total activity (Bq)[2]	Uncertainty (2σ)	Fraction	Mass analysed (g)	Uncertainty (2σ)	Activity in fraction (Bq/g)	Uncertainty (2σ)	Measured activity in fraction (Bq)	Uncertainty (2σ)	Activity in fraction (%)	Uncertainty (2σ)	Total measured activity (%)	Uncertainty (2σ)
Microwave digestion															
NaOH	5.09	0.05	0.97	0.13	Residue	4.335	0.04	0.07	0.01	0.34[6]	0.06	35	7.5		
	4.96	0.05	0.94	0.12	Residue	4.836	0.05	0.08	0.01	0.40[6]	0.06	42	8.8		
	4.99	0.05	0.95	0.13	Residue	4.806	0.05	0.10	0.01	0.47[6]	0.07	50	9.5		
	5.04	0.05	0.96	0.13	Residue	5.023	0.05	0.09	0.01	0.43[6]	0.07	45	9.1		
Water	5.01	0.05	0.95	0.13	Residue	4.906	0.05	0.15	0.02	0.77[6]	0.10	81	15.1		
	4.99	0.05	0.95	0.13	Residue	4.822	0.05	0.14	0.02	0.68[6]	0.08	72	12.8		

[1] - Extraction carried out on a bulk unground sediment with a $^{3}H_{total}$ activity of 0.19 ± 0.02 Bq/g dry weight.

[2] - Calculated total activity obtained by multiplying the mass and $^{3}H_{total}$ activity of the sediment.

[3] - Detection limit values are calculated according to Currie (1968).

[4] - A significant proportion of the $^{3}H_{total}$ activity present in the sediment is unaccounted for after this extraction.

[5] - This result is anomalously high, however no reason has been identified to explain it.

[6] - Measured activity (Bq) is corrected for the difference in mass between the sample digested and the residue measured.

Appendix 5: Results from a study of tritium activities in subtidal sediments from Newport Deep

A study of tritium activities in sediments from Newport Deep was commissioned by Amersham plc in parallel with the present study, which was funded by the Food Standards Agency, to investigate a potential subtidal sink for OBT in the Severn estuary. Water and suspended sediment samples, surface grab samples and shallow sediment cores were collected from Newport Deep in the Severn estuary from 29-31 October 2002 on the New Ross 1 (Captain D. Hosken), by Dr J. Taylor (Compass Hydrographics, Southend on Sea, Essex, UK.), Dr P. Teasdale, Dr F.M. Dyer and J.E. Morris.

Table A.14: Results from the $^{3}H_{total}$ analysis of suspended sediment samples from Newport Deep.

Sample ID	**Water depth (m)**	**Volume of water filtered (l)**	**Mass of particulate fraction (g)**	**Particulate loading (mg/l)**	**$^{3}H_{total}$ activity (Bq/g dry sediment)**	**Uncertainty (2σ)**	**$^{3}H_{total}$ activity (Bq/l from particulate)**	**Uncertainty (2σ)**
WS 2	4	0.6	0.025	45	427.1	7.3	19.2	0.3
WS 3	4	0.6	0.015	27	488.4	8.7	12.9	0.2
WS 4a	4	0.6	0.02	36	22.2	1.8	0.8	0.1
WS 4b	4	0.6	0.024	43	¡ 2.3		0.1	0.0
WS 5	4	0.6	0.022	39	439.0	7.0	17.2	0.3
WS 6	4	0.6	0.017	31	372.4	7.9	11.4	0.2
WS 6	8	0.6	0.031	56	4.6	1.2	0.3	0.1
WS 7	4	0.6	0.026	46	6.8	1.4	0.3	0.1
WS 8	4	0.5	0.012	25	3.1	1.6	0.1	0.0
WS 10	4	0.5	0.025	51	¡ 1.5		0.1	0.0
WS 11	4	0.5	0.027	57	¡ 1.3		0.1	0.0
WS 12a	4	0.5	0.026	54	1.4	0.7	0.1	0.0
WS 12b	4	0.5	0.032	67	¡ 1.1		0.1	0.0
WS 16	4	0.4	0.092	229	0.8	0.4	0.1	0.1

Table A.15: Results from the $^{3}H_{total}$ analysis of grab samples of subtidal surface sediment from Newport Deep. These data were compiled from measurements performed by **Dr J. Oh?**

Sample ID	**Wet/ dry ratio**	**$^{3}H_{total}$ activity (Bq/g dry weight)**	**Uncert-ainty (2σ)**
GRAB 1	2.0	0.34	0.04
GRAB 2	2.1	0.23	0.03
GRAB 3	2.2	0.16	0.02
GRAB 4	1.4	0.07	0.01
GRAB 5	1.3	0.05	0.01
GRAB 6	2.3	0.14	0.02
GRAB 7	2.0	0.18	0.02
GRAB 8	2.3	0.23	0.03
GRAB 10	2.0	0.07	0.01
GRAB 11	1.3	0.05	0.01
GRAB 12	2.2	0.18	0.02
GRAB 16	1.2	0.00	0.00
GRAB 22	1.9	0.02	0.01
GRAB 23	2.0	0.20	0.02

Table A.16: Results from the $^3H_{total}$ analysis of core sediments from Newport Deep. These data were compiled from measurements performed by Dr P. Teadale, Dr J. Oh, Dr F.M. Dyer, J.E. Morris and P. Ferrer.

Sample ID	Depth (cm)	Wet/ dry ratio	$^3H_{total}$ activity (Bq/g dry weight)	Uncertainty (2σ)
CORE 7.1	1	1.87	0.44	0.03
CORE 7.2	2	1.87	0.36	0.02
CORE 7.3	3	1.97	0.38	0.02
CORE 7.4	4	1.90	0.31	0.02
CORE 7.5	5	1.87	0.23	0.02
CORE 7.6	6	2.00	0.23	0.02
CORE 7.7	7	1.79	0.18	0.01
CORE 7.8	8	1.86	0.21	0.02
CORE 7.9	9	1.90	0.26	0.02
CORE 7.10	10	1.89	0.23	0.02
CORE 7.11	11	1.93	0.19	0.02
CORE 7.12	12	1.83	0.16	0.01
CORE 7.13	13	1.95	0.62	0.07
CORE 7.14	14	1.80	0.23	0.02
CORE 7.15	15	1.88	0.19	0.02
CORE 7.16	16	1.92	0.11	0.01
CORE 7.17	17	1.87	0.14	0.02
CORE 7.18	18	1.97	0.24	0.02
CORE 7.19	19	2.03	0.34	0.02
CORE 7.20	20	1.96	0.10	0.01
CORE 7.21	21	2.53	0.23	0.01
CORE 7.22	22	1.95	0.18	0.02
CORE 7.23	23	2.02	0.13	0.01
CORE 7.24	24	1.95	0.15	0.01
CORE 7.25	25	1.88	0.16	0.01
CORE 7.26	26	1.81	0.29	0.02
CORE 7.27	27	1.85	0.10	0.01
CORE 7.28	28	1.77	0.20	0.02
CORE 7.29	29	1.76	0.09	0.02
CORE 7.30	30	1.78	0.05	0.01
CORE 7.31	31	1.89	0.15	0.01
CORE 7.32	32	1.89	0.10	0.01
CORE 7.33	33	1.88	0.05	0.01
CORE 7.34	34	1.97	0.06	0.01
CORE 7.35	35	1.93	0.06	0.01
CORE 7.36	36	2.03	0.09	0.01
CORE 7.37	37	1.92	0.13	0.01
CORE 7.38	38	1.71	0.05	0.01
CORE 7.39	39	1.78	0.03	0.01
CORE 7.40	40	1.99	0.12	0.01
CORE 7.45	45	1.87	0.20	0.02
CORE 7.50	50	1.85	0.09	0.02
CORE 7.55	55	1.84	0.01	0.006
CORE 7.60	60	1.79	0.02	0.008
CORE 7.65	65	1.77	0.03	0.008

CORE 7.70	70	1.69	< 0.06	
CORE 8.1	1	1.76	0.10	0.02
CORE 8.2	2	1.68	0.10	0.02
CORE 8.3	3	1.76	0.07	0.02
CORE 8.4	4	1.89	0.11	0.02
CORE 8.5	5	1.80	0.07	0.02
CORE 8.6	6	1.79	0.12	0.02
CORE 8.7	7	1.81	0.16	0.03
CORE 8.8	8	1.84	0.20	0.03
CORE 8.9	9	1.69	0.15	0.02
CORE 8.10	10	1.58	0.07	0.02

Appendix 6: Calculations and assumptions made in the construction of a model to assess the significance of OBT discharges (Figure 6.1)

Each of the subsections below corresponds with a box in the tritium budget model (Figure 6.1)

Decay corrected total OBT discharged from Amersham plc (to 2004)
Decay corrected total OBT = 1.72 x 10^{15} Bq

Suspended sediment
Average $^{3}H_{total}$ activity of suspended sediment = $\sim$ 1 Bq/g = 1 x 10^{6} Bq/tonne
Estimated mass of labelled suspended sediment = 13000000 (maximum suspended sediment load)/4 = 3 x 10^{6} tonnes

Total ^{3}H = 3.3 x 10^{12} Bq

Subtidal sediment from Newport Deep (Appendix 5)
Average $^{3}H_{total}$ activity of NPD grab samples = 0.14 Bq/g dry weight
Average $^{3}H_{total}$ activity of NPD core sediments = 0.2 Bq/g dry weight $\equiv$ 2 x 10^{5} Bq/tonne
Estimated mass of labelled subtidal sediment:
Area of NPD $\approx$ 5 km^2
Depth of labelled sediment $\approx$ 20 cm $\equiv$ 0.002 km
Volume $\approx$ 0.01 km^3
Density of sediment = 1.6 g/cm^3 $\equiv$ 1.6 x 10^{9} tonnes/km^3 (Warwick and Croudace, 2005)
Therefore, the mass of labelled subtidal sediment $\approx$ 16000000 tonnes

Total ^{3}H = Average $^{3}H_{total}$ activity of NPD core sediments x mass of labelled sediment = 3.2 x 10^{12} Bq

Salt marshes
Average $^{3}H_{total}$ activity of Peterstone 1 core sediments = 0.19 Bq/g dry weight to 40 cm depth
Average $^{3}H_{total}$ activity of Peterstone 2 core sediments = 0.22 Bq/g dry weight to 34 cm depth
Average $^{3}H_{total}$ activity of Sudbrook core sediments = 0.19 Bq/g dry weight to 28 cm depth
Therefore, the average $^{3}H_{total}$ activity of salt marsh sediments = 200000 Bq/tonne

Estimated mass of labelled salt marsh sediment:
Area of salt marshes $\approx$ 2 km^2
Depth of labelled sediment $\approx$ 40 cm $\equiv$ 0.004 km
Volume $\approx$ 0.008 km^3
Density of sediment = 1 g/cm^3 $\equiv$ 1 x 10^{9} tonnes /km^3
Therefore, the mass of labelled salt marsh sediment $\approx$ 8000000 tonnes

Total ^{3}H = Average $^{3}H_{total}$ activity of salt marsh sediments x mass of labelled sediment = 1.6 x 10^{12} Bq

Intertidal sediments
Average $^{3}H_{total}$ activity of surface sediments = 0.5 Bq/g dry weight $\equiv$ 5 x 10^{5} Bq/tonne
Area of intertidal sediments estimated from a map of depositional environments (Figure 1.9) for the area between Barry Island and Sudbrook $\approx$ 24 km^2 Depth of labelled sediment is highly variable (Appendix 1), estimated to be 10 cm $\equiv$ 0.001 km
Volume $\approx$ 0.02 km^3
Density =1 x 10^{9} tonnes/km^3
Therefore, the mass of labelled intertidal sediment $\approx$ 24000000 tonnes

Total ^{3}H = Average $^{3}H_{total}$ activity of intertidal sediments x mass of labelled sediment = 1.2 x 10^{13} Bq

Calculation of amount of total OBT lost by flushing
OBT lost by flushing = 1.07×10^{15} - ($3.3 \times 10^{12} + 3.2 \times 10^{12} + 1.2 \times 10^{13} + 1.6 \times 10^{12} = 1.05 \times 10^{15}$ Bq